



ADVANCES IN CHEMICAL ENGINEERING

Volume 5

Thomas B. Drew

ADVANCES IN CHEMICAL ENGINEERING

Volume 5

CONTRIBUTORS TO THIS VOLUME

S. G. BANKOFF
GEORGE D. FULFORD
K. RIETEMA
J. H. SINFELT
J. F. WEHNER

Advances in

CHEMICAL ENGINEERING

Edited by

THOMAS B. DREW

*Department of Chemical Engineering
Columbia University
New York, New York*

JOHN W. HOOPES, JR.

*Atlas Chemical Industries, Inc.
Wilmington, Delaware*

THEODORE VERMEULEN

*Department of Chemical Engineering
University of California
Berkeley, California*

Assistant Editor

Giles R. Cokelet

*Division of Chemistry and Chemical Engineering
California Institute of Technology
Pasadena, California*

VOLUME 5



Academic Press · New York and London · 1964

COPYRIGHT © 1964, BY ACADEMIC PRESS INC.

ALL RIGHTS RESERVED

NO PART OF THIS BOOK MAY BE REPRODUCED IN ANY FORM,
BY PHOTOSTAT, MICROFILM, OR ANY OTHER MEANS,
WITHOUT WRITTEN PERMISSION FROM THE PUBLISHERS.

ACADEMIC PRESS INC.
111 FIFTH AVENUE
New York, New York 10003

United Kingdom Edition
Published by
ACADEMIC PRESS INC. (LONDON) LTD.
Berkeley Square House
London W.1

Library of Congress Catalog Card Number: 56-6600

PRINTED IN THE UNITED STATES OF AMERICA

CONTRIBUTORS TO VOLUME 5

S. G. BANKOFF, *Department of Chemical Engineering, Northwestern University, Evanston, Illinois*

GEORGE D. FULFORD,* *Department of Chemical Engineering, University of Birmingham, Birmingham, England*

K. RIETEMA, *Department of Chemical Engineering, Technical University, Eindhoven, Netherlands*

J. H. SINFELT, *Esso Research and Engineering Company, Linden, New Jersey*

J. F. WEHNER, *Department of Chemical Engineering, University of Notre Dame, Notre Dame, Indiana*

* Present address: E. I. du Pont de Nemours & Company, Inc., Photo Products Department, Research Division, Parlin, New Jersey.

This Page Intentionally Left Blank

PREFACE

This 1964 volume of *Advances* provides a new group of submitted and solicited reviews, authoritative and timely, in areas where the need has been recognized to evaluate the significance of recent chemical engineering research and to forecast the nature of future studies.

Two of this year's articles discuss the fluid-mechanical aspects of systems where material transfer may occur, accompanied by chemical reaction or heat transfer. Fulford analyzes thin-film flow in terms of the flow regimes and of surface disturbances, and relates recent experimental findings to the theoretical framework. Rietema discusses segregation phenomena in heterogeneous reactions, in relation to conditions of flow and of mass transfer.

Bankoff provides a comprehensive analysis of representative practical cases of simultaneous heat and mass transfer at phase boundaries. This is to be followed in a forthcoming volume by a review of evaporation and condensation at bubble boundaries.

The remaining two reviews treat active topics in applied chemical kinetics. Wehner provides a unified treatment of the theory of flames, including the role of intermediates and the problems of flammability limits and ignition conditions. Sinfelt discusses the near-simultaneous conduct of successive reactions needed, for instance, in the reforming of petroleum fractions, as produced by intimate mixtures of metallic and acidic catalysts.

The editors express their appreciation to Giles R. Cokelet of the California Institute of Technology, who has also participated in manuscript review as the assistant editor for this volume; to Michel Boudart, for his review of the chapter by J. H. Sinfelt; and to the staff of Academic Press, for help in expediting publication.

November 1964

THOMAS B. DREW
JOHN W. HOOPES, JR.
THEODORE VERMEULEN

This Page Intentionally Left Blank

CONTENTS

CONTRIBUTORS TO VOLUME 5	v
PREFACE	vii

Flame Processes—Theoretical and Experimental

J. F. WEHNER

I. Introduction	1
II. Structure of One-Dimensional Laminar Flames	4
III. Stabilization of Flames	16
IV. Burning of Solid Propellants	24
V. Chemical Synthesis in Flames	28
Nomenclature	32
References	33

Bifunctional Catalysts

J. H. SINFELT

I. Introduction	37
II. Nature of Bifunctional Reforming Catalysis	38
III. Nature of Reactions Occurring over Bifunctional Catalysis	42
IV. Kinetics and Mechanism of Individual Hydrocarbon Reactions	49
V. Conclusion	71
Nomenclature	71
References	73

Heat Conduction or Diffusion with Change of Phase

S. G. BANKOFF

I. Introduction	75
II. Exact Solutions	78
III. Analytic Approximation Methods	105
IV. Analog and Digital Computer Solutions	132
V. Concluding Remarks	142
Nomenclature	143
References	146

The Flow of Liquids in Thin Films

GEORGE D. FULFORD

I. Introduction	151
II. Description of Film Flow	153
III. Theoretical Treatments of Film Flow	155
IV. Experimental Results and Comparison with Theory	176

V. Conclusions	207
Nomenclature	209
Appendix. Brief Chronological Résumé of Papers on Film Flow and Related Topics	210
References	228

Segregation in Liquid-Liquid Dispersions and Its Effect on Chemical Reactions

K. RIETEMA

I. Introduction	237
II. The Effect of Segregation on the Kinetics of a Liquid-Liquid Two-Phase Chemical Reaction	243
III. Partial Segregation. Theory of Finite Interaction Rate. Models for Interaction in the Dispersed Phase	270
IV. Measurements of the Interaction Rate	283
V. Discussion about the Interaction Rate	291
VI. Concluding Remarks	299
Nomenclature	299
References	301
Author Index	303
Subject Index	314

FLAME PROCESSES—THEORETICAL AND EXPERIMENTAL

J. F. Wehner

Department of Chemical Engineering
University of Notre Dame
Notre Dame, Indiana

I. Introduction	1
II. Structure of One-Dimensional Laminar Flames	4
A. Theoretical Description by Exact and Approximate Methods	4
B. Experimental Determination of Temperature and Composition Profiles and Significant Chemical Kinetics	12
C. Uncertainties of Present Knowledge of Flame Structure	16
III. Stabilization of Flames	16
A. Composition Limitations—Flammability	16
B. Spatial Aspect—Hydrodynamical and Quenching	18
C. Ignition	19
D. Transition to Detonation	21
IV. Burning of Solid Propellants	24
V. Chemical Synthesis in Flames	28
A. Various Chemical Systems Capable of Sustaining a Stable Flame	28
B. The Flame as a Reactor	31
Nomenclature	32
References	33

I. Introduction

Flames are usually studied for one of two reasons. The engineer is interested in utilizing the understanding of flame processes in the design of combustion chambers. The scientist is interested in the flame as a device for studying high temperature chemical kinetics. The literature of combustion contains studies which embrace practically a continuum of combinations of these two justifications. A subsidiary interest in combustion processes exists for some chemical engineers who see in flames possible new ways to chemical synthesis. This review is undertaken with the latter viewpoint in mind, although it is hoped that it will be of value to people with other interests in combustion as well.

A flame may be defined as a zone of chemical reaction accompanied by heat release which propagates into a combustible mixture until a steady state is reached or until the mixture is entirely burned. In the steady state the flame zone is a region of rapidly varying temperature and composition, which separates the burned from the unburned gases and which is stationary in a suitable frame of reference. It may or may not be distinguished by the emission of visible light. The combustible mixture may be homogeneous or consist of two or more phases. A flame may propagate within a combustible mixture prepared ahead of time or it may be associated with a zone of mixing—premixed or diffusion flames. The flame zone may be laminar or turbulent, and the flow may be subsonic or supersonic. Gases, liquids, and solids may be involved in a variety of combinations as fuel or product. The size and diversity of the field of combustion may be seen in a review article written for the years 1951–1952, which included some 600 references (L6). Few reviews since that time have attempted to be so all-inclusive, although excellent summaries of the field have appeared from time to time (F9, P6).

The study of flame processes is a good example of the interplay between experiment and theory and between practical and fundamental approaches to a problem. For example, as the knowledge of the field has grown, the attitude of researchers towards the study of burning velocity has undergone quite a change. Since burning velocity determines heat release, the design of a burner depends on knowledge of this parameter. Much early effort was expended on the definition and measurement of burning velocity.¹ The variation of burning velocity with pressure and temperature was used to derive parameters in various correlating theories in order to predict velocities of new mixtures. Since the approximate theories available were so crude, little useful information was obtained in this way. The goal of the research was then changed, and measured flame velocities were used as experimental verification of the postulates of the theories of flame propagation. The various theories involve either integration of a set of differential equations or their approximate solution. Therefore, the details of the theories are submerged, and it has been shown that trends in variation of flame velocities are not adequate verification of such theories (S2). At the present time flame theory is so highly developed that composition and temperature profiles can be determined for a system with fairly complicated kinetics, and even more complex kinetics might be analyzed in the future (H1). In the verification of this kind of a theory, prediction of burning velocity is a necessary, but not sufficient, requirement; the profiles must also be predicted. Since independent measurements

¹ See Jost (J5) for a description of the early flame velocity studies.

of the kinetics of a flame system are usually not possible, present day flame theory may be considered as a tool for deriving kinetics from experimental profiles, although it may be used to generate theoretical profiles if sufficient kinetic information is available.

The involved interaction between thermal, diffusional, and chemical kinetic processes which make up a theory of flame propagation prevents the development of a simple method for the estimation of a burning velocity. The danger involved in trying to develop an empirical method from even experimental kinetics may be seen by considering the strong effect of chemical additives on the burning velocity. It has been shown that substances added in amounts too small to change the mixture's thermal conductivity or adiabatic flame temperature may change the burning velocity appreciably (L3). This effect may be attributed to a direct modification of the kinetics of the reactions.

This relatively advanced stage of understanding of flame processes has been attained only for laminar premixed flames in which curvature of the flame front is not large. The bulk of the material in this paper is developed from our knowledge of this area with the understanding that extrapolations are often involved. The validity of such extrapolations into the field of turbulent flames is largely unknown, although there is some evidence which supports the idea that turbulent flame zones consist of wrinkled laminar flames as one limiting case and that turbulent transport processes completely govern in another limiting case (F4). Most industrially important flames are turbulent and are not necessarily premixed. The fields of turbulent combustion and diffusion flames are not reviewed in this paper, since little progress toward the understanding of the fundamental aspects of these problems has been achieved recently. There are excellent surveys of these fields in the combustion symposia and other standard works.

If we restrict ourselves to laminar flames, it appears possible to understand quantitatively how the concentration of all species present is distributed throughout the flame zone and how this distribution varies with temperature and additives. This possibility makes it attractive to consider ways in which intermediates may be withdrawn from the flame zone or to attempt to produce species which do not reach equilibrium within the flame zone. It is, of course, still practical to produce useful substances by combustion to a favorable equilibrium, but this type of synthesis does not require much knowledge of the flame zone. It is useful however to use a flame in synthesis in this way in order to prevent contact with surfaces or to regulate the coagulation of solid products.

II. Structure of One-Dimensional Laminar Flames

A. THEORETICAL DESCRIPTION BY EXACT AND APPROXIMATE METHODS

A complete set of conservation equations which govern any fluid dynamical system in which chemical reaction occurs with heat release may be written for the general time-dependent situation. These equations consist of the application of the conservation of mass, Newton's second law, thermodynamics, the transport phenomena of heat and mass transfer, and chemical kinetics to a multicomponent system. Tracing the development of these equations is a difficult task and would amount to a complete survey of physics (with the exception of nuclear phenomena) from the time of Newton to modern times. The historical highlights of the successful application of the conservation equations to flames occur at three times. Shortly before the turn of the century it was realized that conservation equations governed flame speeds (M3, M6). In the 1930's Lewis and von Elbe (L5) and Zeldovich (Z1) made the first reasonably satisfactory application of the theory to experimental observations. In the late 1940's, Hirschfelder and his colleagues were the first to generalize the equations so that multicomponent diffusion could be handled in the conservation equations. They have written the flame equations in such a convenient and general notation (H1) that almost all investigators now derive their equations by simplification from this form rather than by using first principles or the classical method of reference to the earliest literature. A modified system of notation, which minimizes the use of molal units, proposed by von Kármán and Penner, is used by aerodynamicists (V3).

The general equations are simplified for a one-dimensional laminar flame in the steady state (H1).

Conservation of individual chemical species is given by the following equation:

$$\frac{dG_i}{dz} = \frac{m_i K_i}{M} \quad (1)$$

The mass fraction G_i of the mass velocity M differs from the mass fraction of the local mixture when diffusion is taking place. K_i is the ordinary reaction rate of chemical kinetics, expressed as mole/unit volume/unit time, which is measured in a static experiment as a function of temperature and composition if the flame is in local thermal equilibrium. If not, this equation serves only as a measure of the nonequilibrium local reaction rate.

The energy balance is given by

$$\frac{\lambda}{M} \frac{dT}{dz} = \sum_{i=1}^s [G_i \hat{H}_i - (G_i \hat{H}_i)_\infty] \quad (2)$$

This equation has been written so that the boundary condition in the hot gases (∞) is satisfied as far as the temperature gradient is concerned. Radiation losses and kinetic energy changes have been ignored, as they are usually negligible. The diffusion thermal effect has also been ignored. The concept of local thermodynamic equilibrium is applied so that the thermal conductivity may be calculated using the appropriate mixing laws and the specific enthalpy may be defined.

The diffusion equation is given as follows:

$$\frac{dx_i}{dz} = \frac{M}{n} \sum_j \left(\frac{x_i m_i G_j - x_j m_j G_i}{m_i m_j D_{ij}} \right) \quad (3)$$

These equations contain a number of assumptions. First of all, they are a result of a dilute gas approximation in which binary diffusion coefficients, which may be assumed independent of composition, are used. Secondly, thermal diffusion has been neglected although this assumption should be verified for the system under investigation. It appears that the flux due to thermal diffusion could be a substantial fraction of the ordinary diffusion flux for some systems (F6).

The assumption has been made that the pressure drop across a flame is so small that the momentum equation may be ignored. The steady-state restriction in the ordinary continuity equation ensures that the mass flux M is constant throughout. The mass flux is converted to the interesting parameter, burning velocity, by use of the cold gas density.

In spite of the many approximations used in deriving this set of equations, the mathematics of solving them is formidable. The set of equations is $2s + 1$ in number, where s is the number of species that occur within the flame. Of these, $s + r - 1$ equations ($r < s$) form a set of independent equations since the quantities x_i and G_i are fractions such that $\sum_i x_i = 1$ and $\sum_i G_i = 1$, and stoichiometry reduces the number of independent species by some number ($s - r$), (H3). Part of the mathematical complexity is due to the presence of intermediate species whose concentrations are low in the hot and cold gases but which may pass through a maximum within the flame zone. Since the rates of appearance and disappearance must be comparable for this to occur, it is approximately true near the maximum that $K_i = 0$ for these species. This fact results in an indeterminacy of the system of equations, although, at the same time, it provides a method which permits an approximate solution to be obtained.

Before a discussion of the solution of these equations, complications

due to the boundary conditions should be mentioned. The equations have been formulated in such a way as to introduce the proper boundary conditions in the hot gases.² In the cold gases, there are two difficulties. The reaction rates are not identically zero according to the laws of chemical kinetics and, properly speaking, no solution exists to the problem. This difficulty is removed either by (1) assuming a finite heat flux

$$q_0 = -\lambda \left(\frac{dT}{dz} \right)_0$$

at the cold boundary which occurs at a fixed point taken as zero of distance, in which case it can be shown that a range of small values of q_0 does not change the solution obtained or (2) by recognizing that the rates K_i are negligibly small at the cold boundary and redefining the reaction rate so that it disappears completely in the cold gases which may then extend indefinitely in the negative direction. Diffusion occurs right up to the cold boundary fixed in space, so that the x_i 's cannot be fixed there, but must be permitted to assume the values determined by the conservation equations. Since the x_i 's are determined in the mixing chamber, some artifice must be used to permit a discontinuity to be sustained at the cold boundary. A fictitious semipermeable membrane is used if a heat sink is assumed at the cold boundary (H1), but is not necessary when the reaction rate goes to zero in the cold gases. If, in the latter case, a flame is stabilized near a heat sink, the membrane is also required. The diffusion at the flame holder is demonstrated most vividly in the H_2 - Br_2 flame where the large difference in molecular weights causes the Br_2 concentration to be considerably higher near the flame holder than in the premixed gases (C3, F6). After the proper assignment of the boundary conditions, it is apparent that the problem is overspecified and is therefore an eigenvalue problem. For the $s + r - 1$ independent 1st-order equations, we have $s + 2r - 1$ boundary conditions or a multiple eigenvalue problem in r parameters.³ One of these eigenvalues is trivial (C4), since the distance coordinate may be removed by dividing the continuity and diffusion equations by the energy equation, which introduces temperature instead of distance as the independent variable. The trivial eigenvalue is the arbitrary origin of the z coordinate which appears in the integration of the energy equation after the $2r - 2$ equations in x_i , G_i , and T have been solved. The number of important eigenvalues ($r - 1$) is equal to the number of independent x_{i0} 's

² All derivatives are zero in the hot gases. The concentration of all species in the hot gases may be calculated when sufficient thermodynamic data are available. Many procedures for performing this calculation are available in the literature (F1, P5, L11).

³ T , x_i , G_i have zero derivatives in the hot gases, T and x_i may be specified in the premixed gases, $G_i = (n/\rho)x_i$ in the cold gases and thus is not independent there.

(alternately, G_{i0}). For an initial mixture of fuel and oxidizer this number will be equal to the number of independent intermediate species plus one. A flame without intermediates is a single eigenvalue problem. This eigenvalue is the mass velocity M which has only a single value for each composition of fuel and oxidizer. A flame with intermediates is also reduced to a single eigenvalue problem when the chemical kinetic steady-state approximation ($K_i = 0$) may be made for these species since their G_i is not then determined by a differential equation. Almost all flame theories in an integrated form are based on this approximation. A complete mathematical discussion of the existence of solutions to the single eigenvalue problem has recently been presented (J1, J3).

The solution of the flame equations when the intermediates do not exist in their steady-state concentrations is an imposing task which is somewhat less forbidding after the simpler equations are studied. The single reaction flame where no intermediates are involved is still a substantial problem, but is quite tractable when the most ordinary of digital computers is available. After elimination of distance, as previously discussed, this set of two ordinary nonlinear 1st-order differential equations is obtained:

$$\frac{dG_i}{dT} = \frac{\lambda m_i K_i}{M^2 \sum_j [G_j \hat{H}_j - (G_i \hat{H}_i)_\infty]} \quad (4)$$

$$\frac{dx_i}{dT} = \frac{n}{M^2 \sum_j [G_j \hat{H}_j - (G_i \hat{H}_i)_\infty]} \sum_j \left(\frac{x_i G_j}{m_j D_{ij}} - \frac{x_j G_i}{m_i D_{ij}} \right) \quad (5)$$

Only a single G_i and x_i are independent, and all thermodynamic and transport properties are presumed known. A functional form of $K_i(T, x_i)$ is assumed. This is usually a simple first- or second-order relationship. The solution of the problem consists of the two profiles $G_i(T)$ and $x_i(T)$, along with the eigenvalue M which permits the boundary conditions to be satisfied.

A numerical method for finding these profiles may be outlined briefly. First of all, the value of K_i in the cold gases will be so low that, as far as the computer is concerned, it may be considered zero, and the previously mentioned difficulty at the cold boundary is circumvented. The derivatives are thus zero in the cold gases, and it can be shown that, although they are indeterminate in the hot gases, l'Hospital's rule may be used to evaluate them at this limit in terms of the unknown eigenvalue M . After assuming a value for M , a Taylor series expansion about the hot boundary will provide starting values for continuation of the integration towards the cold boundary by the use of numerical integration such as the Milne or

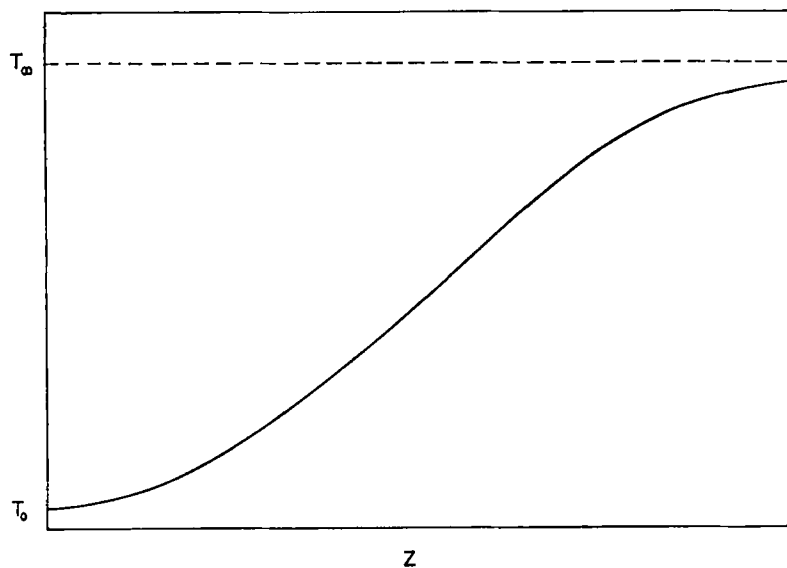


FIG. 1. Temperature profile for a flame zone. The slope of the curve at T_0 is assumed to have a small nonzero value.

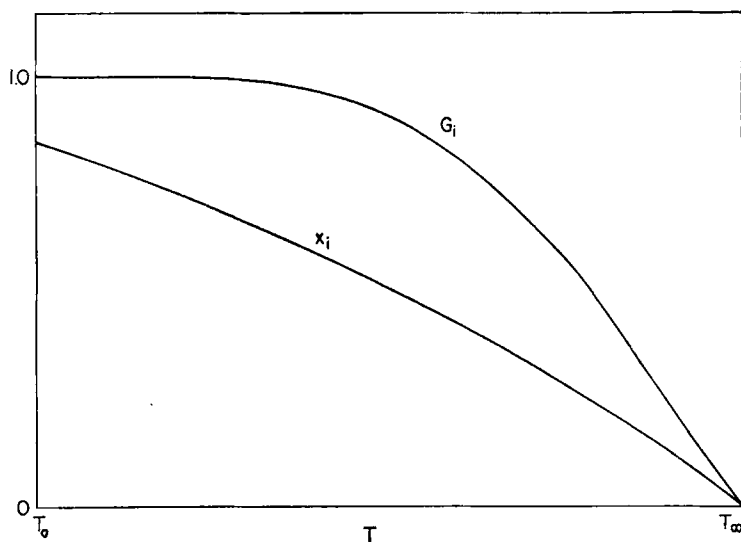


FIG. 2. Flux fractions G_i and mole fractions x_i of either reactant as a function of temperature through a flame zone. Two portions of the G_i curve are approximately straight lines. For a constant enthalpy flame, $x_i(T)$ would be a straight line.

Runge-Kutta procedures. Repeated applications of this method are performed until a value of M is found which allows the cold boundary conditions to be satisfied. Figures 1 and 2 are schematic diagrams representing the solutions of the above problem.

No complication is introduced into this method of solution by the introduction of additional independent species as far as machine computation is concerned unless the additional species is close to the chemical kinetic steady-state condition. In the latter case, machine integration is extremely unstable, so that the algebraic equation $K_i = 0$ must be used to determine the variation of the component i in at least some regions of the independent variable. At the same time, the additional eigenvalue is introduced. The physical significance of this eigenvalue in terms of propagation limits is currently under investigation (C4, W1). The profiles for temperature and fuel or oxidizer concentration are not changed qualitatively from those of the previous problem. The profiles for an intermediate species is represented by Fig. 3. The excess of the intermediate species over its equilibrium value is a quantity which was overlooked in the older theories of flame propagation. The maximum has been observed

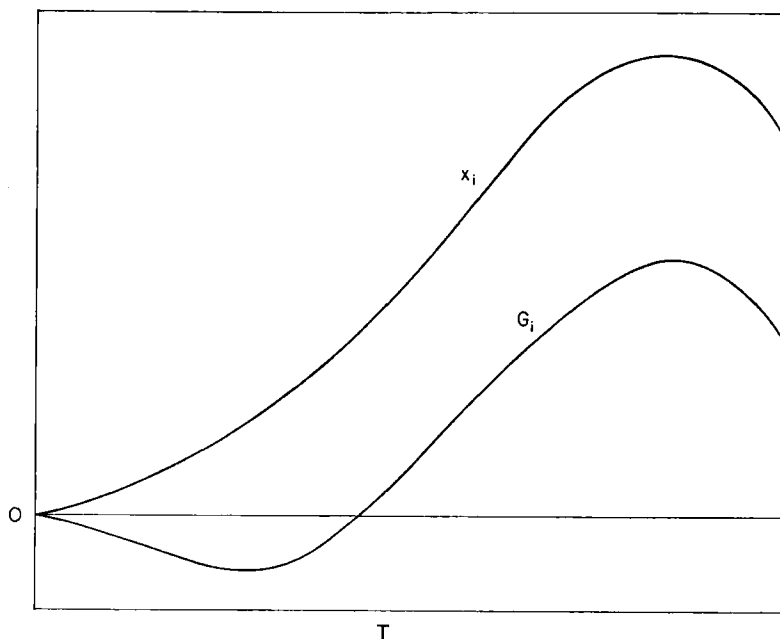


FIG. 3. Intermediate species curve. The negative portion of the G_i curve represents a net flux of the species towards the cold gases. For the constant enthalpy single-reaction flame, the curve for G_i cuts across that for x_i at the maximum point of x_i .

for a number of substances (B6, F3), although its necessity within the theory of flame propagation has not been discussed. It may be significant in theories of ignition.

In order to develop an intuition for the theory of flames it is helpful to be able to obtain analytical solutions to the flame equations. With such solutions, it is possible to show trends in the behavior of flame velocity and the profiles when activation energy, flame temperature, diffusion coefficients, or other parameters are varied. This is possible if one simplifies the kinetics so that an exact solution of the equation is obtained or if an approximate solution to the complete equations is determined. In recent years Boys and Corner (B4), Adams (A1), Wilde (W5), von Kármán and Penner (V3), Spalding (S4), Hirschfelder (H2), de Sendagorta (D1), and Rosen (R1) have developed methods for approximating the solution to a single reaction flame. The approximations are usually based on the simplification of the set of two equations [(4) and (5)] into one equation by setting all of the diffusion coefficients equal to $\lambda/c_p\rho$. In this model, x_i becomes a linear function of temperature (the constant enthalpy case), and the following equation is obtained:

$$\frac{dG_i}{dT} = \frac{\lambda m_i}{M^2} \frac{K_i(T)}{\sum_j [G_j \hat{H}_j - (G_j \hat{H}_j)_\infty]} \quad (6)$$

If the specific heat of the components may be approximated by an average value, the summation in the denominator may be replaced by

$$\bar{c}_p(T - T_\infty) + \sum_j (G_j - G_{j\infty}) \hat{H}_{j\infty} \quad (7)$$

An integration by parts after multiplying through by the denominator gives an expression which contains the integral

$$\int_{T_0}^T G_i(T) dT \quad (8)$$

as the only unknown quantity. As reference to Fig. 2 will indicate, an approximate function for G_i is easy to devise. The choice of an analytical form of G_i is the principal feature of the various approximations proposed by the above list of authors. Hirschfelder (H2) has compared several of these approximate solutions with the exact solutions of a set of flames based on this model. Penner and Williams have written a comprehensive review of recent work on the single reaction flame (P8).

De Sendagorta (D1) has extended the approximation to the case where $D_{ij} \neq \lambda/c_p\rho$. Very good flame velocities are obtained by this latest work, although it is difficult to see how it would be possible to develop such good approximations without the benefit of the exact solutions

which have been obtained by numerical integration. There is no assurance that the approximations are valid for a very wide range of parameters outside the range in which they were developed, since they could be considered to be an analytical fit to the exact solutions. Nevertheless the availability of an analytical solution is valuable for the compact representation of results and as a starting point for more exact calculations.

A most successful application of the approximate theory has been performed for the ozone decomposition flame, where the flame velocity has been estimated over the entire O_2 - O_3 composition range in which the flame is propagated (V2). A comparison of the calculated flame velocities and the experimental values is made in Fig. 4.

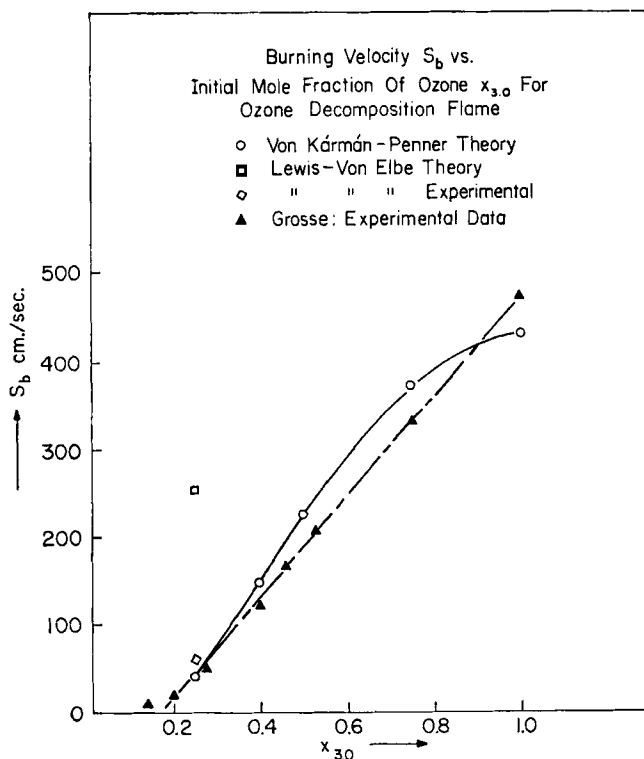


FIG. 4. The ozone dissociation; comparison between compiled and measured values of the burning velocity. From von Kármán (V2) with the permission of the Combustion Institute.

The most general flame problem has been formulated by Klein in such a way that a successive approximation technique may usually be used to

find a solution if one is willing to make the investment in time, effort, and money involved (K5).

B. EXPERIMENTAL DETERMINATION OF TEMPERATURE AND COMPOSITION PROFILES AND SIGNIFICANT CHEMICAL KINETICS

Temperature measurements and chemical analysis within a flame zone are difficult because of the small distance through the zone. For typical hydrocarbon-air flames, the region over which temperature and composition have most of their variation is a fraction of a millimeter thick at one atmosphere. Most of this distance is due to conduction and diffusion. The primary reaction zone, which corresponds roughly to the zone of visible radiation and where most of the heat is released, is often less than one-fifth of the total flame thickness. It may often appear thicker due to optical effects (W2). This information has been determined, in the case of low pressure flames, only in recent years, primarily by careful traversing with fine thermocouples and small sampling probes. Pressure scaling permits extrapolation of the flame structure to higher pressures under some circumstances. Much information on heat release and the reaction zone has been obtained over a long period of time by inference from flame velocity variation and a variety of well-chosen techniques (G1, G2, W2), which usually have been of the optical variety. Experimentation within flame zones has resulted in an understanding of reactions in hydrocarbon flames which could not have been predicted a few years ago. A survey of the literature through 1960 has recently been published (M8). The monograph by Weinberg (W2) on flame optics contains an up-to-date discussion of flame processes. A monograph by Fristrom and Westenberg (F13) on flame structure covering all pertinent techniques is in press.

The methods used for accurate probe measurements have been developed since the work of Kläukens and Wölfhard (K4), who showed that fine thermocouples could be used to measure temperature profiles meaningfully. Friedman (F7) used even smaller thermocouples and showed that catalytic effects could be eliminated by coating the wires. Friedman and Cyphers (F8) later showed by means of a fine quartz sampling probe, used earlier by Prescott *et al.* (P11), that hydrocarbon oxidation proceeds in two stages. First, the hydrocarbon is converted rapidly into carbon monoxide and water and then the monoxide is more slowly converted into the dioxide. Fenimore and Jones (F2) have written a series of papers in which they have analyzed composition profiles in the second stage of the burning process to obtain the rate laws of a number of the reactions which occur there. They have also traced initial decompositions by isotope studies and oxygen atom detection techniques. Sugden (B6) and his co-workers have estimated the concentration of radical species in the later

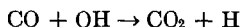
stages of combustion. Fristrom, Westenberg, and co-workers (F11, F14, W4) have made complete traverses of the stable species within several hydrocarbon flames and, with the help of accurate transport coefficients, have been able to delineate rather completely the regions in which the various stages of reaction occur. They have also been able to deduce a plausible scheme of reaction kinetics throughout the flame and estimate some of the kinetic constants. The work of Fristrom and Westenberg and Fenimore and Jones, as described most recently in the Ninth Symposium on Combustion (F2, F11), provides a rather complete discussion of the reactions, diffusion, and heat release occurring in hydrocarbon flames, although some details have not been completely resolved. Dixon-Lewis and Williams (D2) have carried out the analysis of the hydrogen-oxygen flame system to nearly the same point of understanding. The assumption has been made in these studies that species which are highly excited and ionic species do not play an important role in determining reaction rates, even though they are observed in flames. This topic will be discussed in a later section.

The internal structure of a flame may be summarized as consisting of three zones: the region of transport, the reaction zone, and the final region of equilibration, although the separation is not quite complete. In the transport region, thermal conduction from the reaction zone increases the temperature of the incoming gases, so that reaction rates become rapid enough to consume the reactants in the small time interval (about 100 μ sec) that they remain in the reaction zone. Fuel and oxidizer disappear in the transport region by diffusion ahead of the main flow of gases into the reaction zone which effectively acts as a sink for these constituents.⁴ The transport zone therefore contains some product gases, while the less reactive intermediates may also diffuse back into this region. The dilution by product is a process which limits the heat release somewhat with respect to a flame model in which no diffusion occurs. It is fully predicted in the flame model with unit Lewis number. Within the reaction zone, active intermediates attack either the fuel or oxidizer as a controlling step, whereupon a rapid chain of reactions leads to heat release. The reaction sequence, which almost surely occurs in most flames, is the consumption of an active intermediate at the forward part of the reaction zone which serves to generate some other active species. The second species sub-

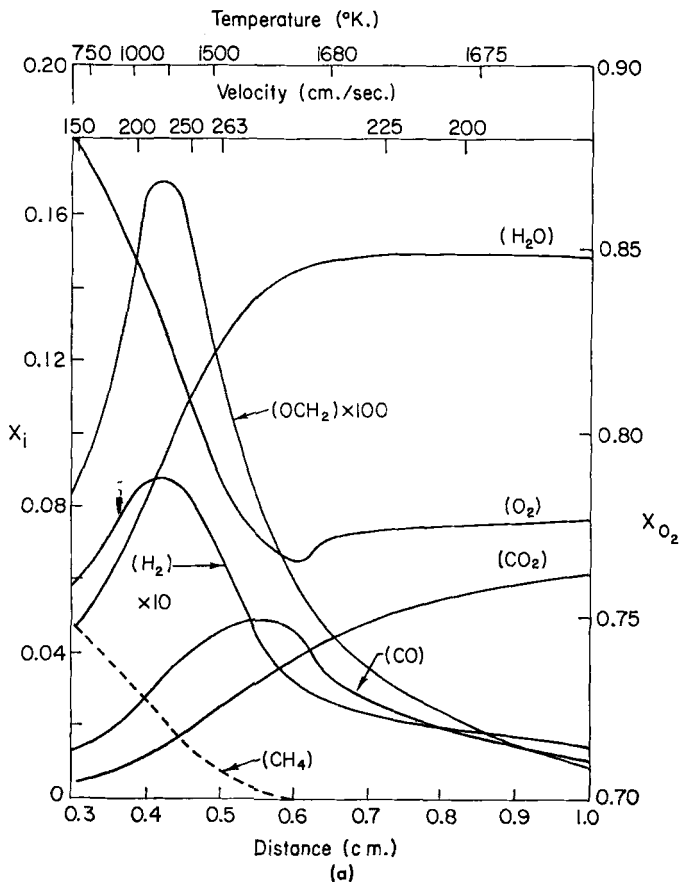
⁴It can only be ascertained that the transport region is free of chemical reaction if accurate diffusion coefficients as a function of temperature and composition are available, since if diffusion is ignored the disappearance of the fuel and oxidizer would be interpreted as slow reaction which is accelerated as the temperature is increased until the reactants are completely consumed. A posteriori, it seems most logical that diffusion and reaction could not possibly compete over such a wide range of temperature and composition and that regions in which each controls should occur.

sequently reacts with a stable molecule to regenerate the active intermediate further along in the hot gases. The intermediates rise above their equilibrium concentration such that they diffuse in both directions while at the same time disappearing by reaction.

The methane flame may be used as an example of the present state of knowledge of a flame system. In the reaction zone of this flame, the attack of hydroxyl radical on methane is followed rapidly by the further decomposition of the methyl radical into carbon monoxide and active species. CO is oxidized slowly in an equilibration zone by the reaction



Hydrogen atoms are responsible for the disappearance of oxygen by the reaction $\text{H} + \text{O}_2 \rightarrow \text{OH} + \text{O}$. Oxygen atoms are in excess in the methane-oxygen flame, and they probably play a part in the reactions of



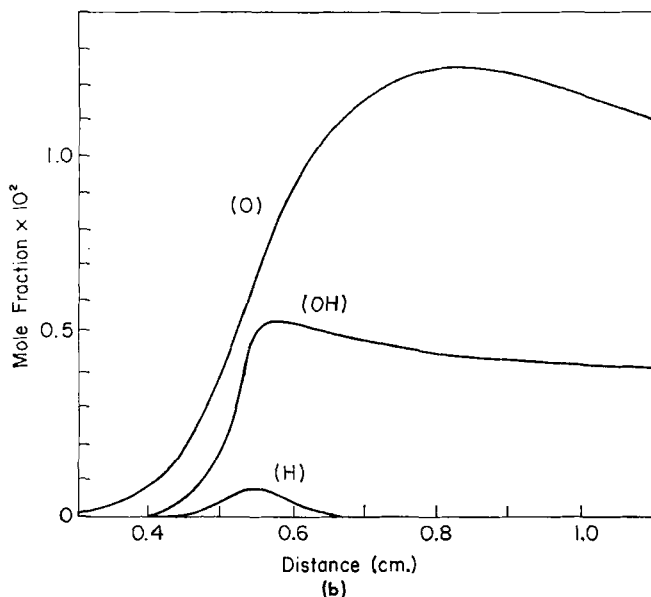


FIG. 5. Characteristics of a spherical flame: $(x_{\text{CH}_4})_0 = 0.078$, $(x_{\text{O}_2})_0 = 0.92$, pressure = 0.05 atm. (a) Stable species mole fraction versus distance from sphere surface, temperature, and velocity. (b) Radical species (mole fraction versus distance). From Fristrom (F11).

the intermediates although they are less reactive towards CH_4 and CO than OH . The reaction removing CH_3 has not been definitely established. Its reaction with O_2 or O -producing formaldehyde and OH or H has been suggested by the different groups of workers in the field (F2, F11). The first reaction has been suggested by work on the flame with oxygen, while the second is proposed from work on air flames where reaction with O_2 is less probable since its concentration is greatly reduced by diffusion. Whether either reaction completely controls this step in either flame can only be established by further work. Formaldehyde reacts with H , O , and OH , and it is suspected that all three reactions are important in this stage, although formaldehyde disappears so rapidly that the stage is not important as a governing step. Profiles of the principal stable species throughout this flame, showing the separations of the processes into regions, are shown in Fig. 5(a). Estimates of likely intermediate distributions are shown in Fig. 5(b).

These profiles, which can be obtained only for low pressure flames, will scale inversely with pressure as long as all of the controlling reactions are bimolecular because of the pressure dependence of the transport

phenomena and bimolecular collisions (H3). Since radical recombination reactions, which occur to reduce the radical concentrations to their equilibrium values, are termolecular, the equilibration zone will not have a profile that can be scaled with pressure. However this region is not of primary importance for flame stabilization, so that a measure of control of the lifetime of active species is afforded.

C. UNCERTAINTIES OF PRESENT KNOWLEDGE OF FLAME STRUCTURE

The concentration of free radicals is a difficult property to measure directly, although the first results are being reported on methods for scavenging radicals quantitatively (F12). The indirect methods, which depend on emission of light by the radicals themselves or by added species which are excited selectively by reaction with radicals, are reliable in the equilibration region where temperature equilibrium prevails. In the reaction zone, the radicals may not be in complete thermal equilibrium as far as vibration and rotational degrees of freedom are concerned, so that spectroscopic measurements of these properties are difficult to interpret. Good estimates of radical concentration in the reaction zone are obtained from the rate of reaction of a stable species when it is known that the radical can only be involved in this one reaction. Examples are difficult to find, although OH and O have been measured by this method (F3, K1).

In sampling with probes where only stable species can be determined, radicals will affect the analysis if their concentration is comparable to any stable species. In the methane flame, the formaldehyde measured by a mass spectrometer is partially due to methyl radical (F11).

Two very distinguishing features of flames are the emission of visible radiation and the presence of an abnormal number of ions in the reaction zone (C1, G1). Both of these features appear to be kinetic by-products, which are completely unnecessary for flame propagation.⁵ The radical CH is responsible for much radiation and now also appears to be the precursor of many of the ions observed in flames (C2). Enhancement of CH or other radical or ion concentration in flames could result in any number of applications if an understanding of their formation made such control possible.

III. Stabilization of Flames

A. COMPOSITION LIMITATIONS—FLAMMABILITY

One of the most characteristic features of flame propagation is the existence of flammability limits. For any given fuel-oxidizer mixture, there exists a range of compositions, which usually centers about the

⁵ The hydrogen flame is almost invisible and contains a normal ion concentration.

stoichiometric, within which a flame will propagate. Outside these composition limits, where the mixture is nearly pure fuel or pure oxidizer, it is impossible to stabilize a propagating flame regardless of the strength of the ignition source. Figure 6 shows schematically the experimental variation of burning velocity. As shown by the broken lines, these curves extrapolate to zero velocity at finite compositions. At these compositions the adiabatic flame temperature is often 1500°C . for the common hydrocarbon-air flame. The limits will depend strongly upon pressure and at low pressures will be quite dependent on the dimensions of the equipment used to determine the limits. In this latter case, the loss of energy and active species to the surfaces of the equipment is the physical mechanism responsible for the failure of a flame to propagate.

At higher pressures, the composition limit appears to be experimentally independent of the dimensions of the equipment and has been widely considered to be a property of an adiabatically propagating mixture (B1). This type of limit has been referred to as a fundamental limit. The demonstration of the existence of such a limit is an exceedingly difficult task. Since all flames radiate some of their thermal energy, it is impossible to stabilize a flame without losses to the surroundings. However, most flame gases are very poor radiators, and, since the residence time of the gases in the reaction zone of a flame is quite small, flames have been observed which come quite close to the adiabatic flame temperature (F14).

A theory of flammability limits based on a nonadiabatic model of flame propagation has been developed by Spalding (S5) and Mayer (M4). In this model, two possible burning velocities arise for each combustible mixture. The second velocity is shown as the dotted line of Fig. 6. As the heat loss parameter in the theory changes in the direction of increasing heat loss, the two burning velocities approach each other. With a further change in the parameter, the flame velocity becomes imaginary. This situation corresponds to a composition limit, since the heat loss parameter may be changed by a variation in flame temperature, which is in turn due to a variation in composition. Of the two flame velocities, the higher one is usually observed. The lower velocity appears to be unstable but apparently has been observed under special circumstances by Botha and Spalding (B3). The experimental observation of increasing flame thickness with decreasing flame temperature provides for an increasing residence time of the gases as the mixture strength approaches the limiting compositions. At this limit, therefore, flames have a tendency to be nonadiabatic. The heat loss theory is likely to be a valid description of flammability limits. It is, however, based on a flame model with ultra-simplified chemical kinetics. There is no possibility of predicting the limit composition with such a model. Another explanation of the limit lies in the observation

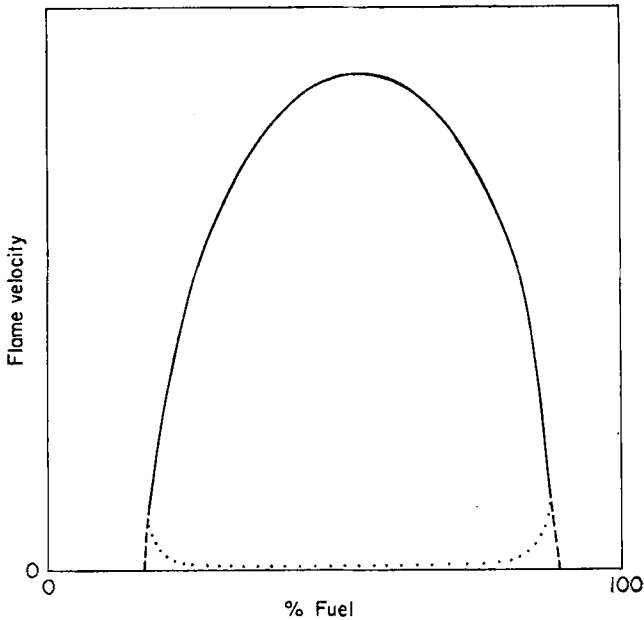


FIG. 6. A plot of flame velocity versus composition for a typical combustible. The solid lines represent an experimentally observed variation. See text for an explanation of the broken and dotted lines.

that natural convection is quite important at the lowest flame velocities which have been observed (L12). It has also been proposed that the steady-state solution to the flame equations is not necessarily stable (L8). Recently, the author (W1) has suggested a basis for a theory of fundamental limits for an adiabatic flame which arises from the eigenvalue nature of the flame equations. It is conceivable that each of the theories proposed for the limit may be valid depending upon the particular flame and equipment used to obtain the limit. It would appear that the natural convection limit could easily mask a heat loss or other fundamental limit. Practically, one can always increase the range of flammability of a given mixture by preheating the unburned mixture.

B. SPATIAL ASPECTS—HYDRODYNAMICAL AND QUENCHING

A flame will remain stationary only if the flow velocity perpendicular to the flame front is exactly equal to the burning velocity. However, this condition needs to be met only for a limited region over a flame front. For other regions it is possible for the flame front to be inclined to the flow at an angle such that the component of the velocity perpendicular to the front is equal to the flow velocity. The limited region over which the

exact matching takes place is generally met by reducing the velocity to zero at a wall, so that, at some point near the wall, a streamline with a velocity equal to the flame velocity is found. In general, bringing a flame front near a wall will reduce the burning velocity by heat losses and/or diffusion of reactive species to the wall, and this reduction also plays a part in stabilization. If the velocity gradient near the wall is too extreme the flow velocity will not be reduced as rapidly as the burning velocity, and stabilization will not be possible. A complete account of flame stabilization on burner tubes is given in the work of Lewis and von Elbe (L7). An excellent review of the quenching of flames by solid surfaces has recently been given by Potter (P9).

Recent work on spatial stabilization has been directed towards the production of one-dimensional flames (F11, P10). These may be either flat, cylindrical, or spherical. The primary purpose of such flames has been to measure velocities accurately and to provide a flame that can be described by a one-dimensional theory. The measurement of temperature and composition profiles is meaningful, of course, only in a flame in which the geometry is known. One-dimensional geometry greatly reduces the labor required to analyze such profiles in order to study kinetics.

C. IGNITION

Any practical flame system must be ignited in an efficient and safe manner. The design of suitable techniques for ignition depends largely on the accumulated experience of many practitioners of the art, as a clear-cut theory of ignition is lacking. There is however a wealth of information on ignition in the literature, which can serve as a guide to the uninitiated. Résumés of standard techniques along with discussions of theory may be found in references (B1, L9, P7).

Common methods of ignition include electric sparks, hot wires, and pilot flames of easily ignited substances. Spontaneous ignition (P7) and the burning of hypergolic fluids (K2, M1) are topics of interest closely related to ignition which, however, ordinarily imply the application of an external stimulus. Almost any intense source of energy may be used for the purpose of ignition. The exploding wire has been used in the ignition of accelerating flames (L1). The author is not aware of any work in which the popular laser has been used in ignition studies. It would be expected that information on the ignition process might be revealed in such studies.

It is thought by some workers in the field that the principles underlying ignition processes could be understood if the complete time-dependent equations governing flames could be solved. This point of view has originated from the standardized ignition techniques, which are aimed at the determination of the minimum energy requirements for ignition. The

object of a theory is to calculate this energy from first principles. In practice the physical and chemical parameters needed for such a theory are never available. Since a steady-state flame profile is independent of the previous history of the gases, a number of routes that lead to ignition are possible. It is obvious that, theoretically, a purely thermal source of energy may be used to initiate the reaction necessary to establish a steady flame. A sufficiently high temperature will accelerate reactions, so that chemical equilibrium can be rapidly approached in a region. The profile can then decay to the steady-state profile. A more efficient method of ignition is based on the idea that the active intermediates (free radicals) previously mentioned (see Fig. 3) are necessary for flame propagation and that most radical reactions are not temperature sensitive. In this case, introduction of the active intermediate at room temperature will accelerate the reactions, release heat, and thus generate the steady-state profile. No method presently exists for the production and introduction of such radicals in an efficient way. Moreover, electric spark ignition, in which both heat and active species are generated, has been analyzed almost entirely from the thermal point of view.

The thermal theory of ignition, which was pioneered by Semenov and Frank-Kamenetski (F5), is based on a model which is nonadiabatic for stationary systems and which may or may not be nonadiabatic for flowing systems. For stationary systems an energy balance is written for heat generated by the system and heat lost to the surroundings. Since chemical reactions accelerate more rapidly with temperature than heat losses, at high enough temperatures heat is accumulated so that a "thermal explosion" results. This process is presumed to lead to ignition. Since chemical reaction rates are always finite at temperatures above absolute zero, it is necessary that a nonadiabatic model be used. Otherwise all combustion mixtures must be considered to ignite spontaneously. For the case of flowing systems, the finite reaction rate results in the cold boundary difficulty discussed in Section II, A. If a theory based on the steady-state profiles is valid for ignition, an adiabatic model in which the cold boundary condition is resolved should be sufficient. On the other hand, when the heat losses are important as far as flame propagation is concerned, as in the theory of Spalding (S5) and Mayer (M4) for limiting conditions, they must also be included in a model for ignition. One should distinguish carefully the difference between ignition and flame stabilization. Practical ignition must involve ignition in the region of a flame holder and thus includes stabilization. It would appear that the minimum energy requirement in this case would be related to the establishment of the steady-state profile. In the case of the ignition of a traveling flame, some part of the energy necessary to establish the steady-state profile may be accumulated

during the nonsteady period. The minimum ignition energy in this case is just sufficient to balance the heat losses so that chemical reaction can accelerate. The flame profile will then become steady after an induction period and will not necessarily be stabilized near the igniting element.

Little work has been done on the theory of ignition in the past several years. Yang (Y1), however, has calculated the minimum ignition energies required to initiate the development of the steady-state profiles of a single-reaction flame from plane, line, and point sources. His minimum ignition energies are defined as the energy necessary to give a net heat release within a region in which some losses occur. They are not the complete thermal energy requirement for the establishment of the steady-state profile. They also depend upon the particular initial condition chosen. Since it is now possible to integrate the flame equations for more general models than the single-reaction flame, it appears feasible to develop a more general theory of ignition by extending the techniques of reference (Y1). In particular, it would be interesting to investigate the energy requirements for the generation of the steady-state profile of intermediate species.

D. TRANSITION TO DETONATION

The laminar combustion wave, which is often characterized by the term deflagration, is only one possible mode through which a metastable reaction mixture may be transformed into a set of thermodynamically stable products. The most important features of a deflagration are the dependence of the burning rate on transport phenomena and chemical reaction rates and the subsonic nature of the wave as shown by the unimportance of the momentum equation in most cases. The second stable, steady-state mode of decomposition of a reaction mixture is known as a detonation wave. The velocity of such a wave is a thermodynamically determined quantity. The set of equations which govern the gross motion of detonations are over-all conservation equations for mass, momentum, and energy and as such are algebraic equations as contrasted to the differential equations of deflagration theory. Detonations are essentially supersonic in character. These waves include or are accompanied by powerful shock waves, which are often destructive. The propagation of steady detonation waves is a phenomenon which has been well studied and which is adequately treated in the literature (C6, G4, E2, L10). The processes whereby detonations are initiated or in which deflagrations are converted to detonations constitute a currently active field of investigation. Prevention of detonation is of paramount interest to those concerned with stabilization of slow flames. Recent theoretical and experimental work has uncovered many details of the development of detonation waves in both

gaseous (B5, J4, L1, L2, L13, O2, S1) and condensed phase materials (M2). In this work we shall describe only recent findings in the field of initiation of gaseous detonation.

A detonation wave may be considered to be a shock wave that is maintained by the release of chemical energy rather than by the moving piston of elementary shock theory (C6). The classical picture of a one-dimensional detonation wave [von Neuman, Zeldovitch, Doring theory (E2)] consists of a shock wave traveling ahead of a zone of chemical reaction which is initiated by the elevated temperature behind the shock front. The shock wave is considered to be a mathematical discontinuity. It is well known that transport phenomena prevent the establishment of a mathematical discontinuity in a real substance, so that the shock wave is, in reality, a zone of finite thickness. It has been shown that a sufficiently rapid chemical reaction will merge with a shock wave, so that a detonation wave may consist of a region (very narrow) in which the unreacted mixture changes continuously to a product mixture along with a continuous rise in temperature and pressure (H1). The structure of this zone depends on the general differential equations which govern both deflagration and detonation waves, but the rate at which detonations travel into the undisturbed gases is governed by the previously mentioned algebraic equations. These equations are usually regarded as the boundary conditions on the differential equations of detonation waves.

The preceding remarks all apply to a steadily propagating one-dimensional detonation. It is a relatively simple task to solve the algebraic equation for the over-all steady-state motion. The differential equations for the structure may be solved in the steady state, but the task is tedious and, in addition, detailed knowledge of reaction rates needed in the equation is not available. It is not too difficult to solve the time-dependent over-all equation if a burning velocity for the flame as a function of temperature and pressure is assumed (J4). It is not practicable to solve the time-dependent equations which govern the structure of the wave with any certainty because of the lack of kinetic information, in addition to the mathematical difficulty. The acceleration of the slowly moving flame front as it sends forward pressure waves which coalesce into shock waves that eventually are coupled to a zone of reaction to form a detonation wave has been observed experimentally (L1, L2).

It has been possible to understand the processes that accompany the transition to detonation in gases without being able to integrate the complete set of equations involved because of the hyperbolic character of the dynamical equations (S3). Jones has shown how a discontinuity may develop ahead of an accelerating deflagration (J4). He has considered the energy release required to produce a detonation and shown that some

energy is released at a later stage which thus suggests retonation or detonation in the opposite direction. His work is entirely analytical. Oppenheim has shown how experimental observations of accelerating flames may be analyzed by a graphical use of the method of characteristics to determine the thermodynamic state of the gas as a function of time and distance (O2). The coalescence of the pressure wave ahead of the flame front is depicted in Fig. 7, which is taken from L2.

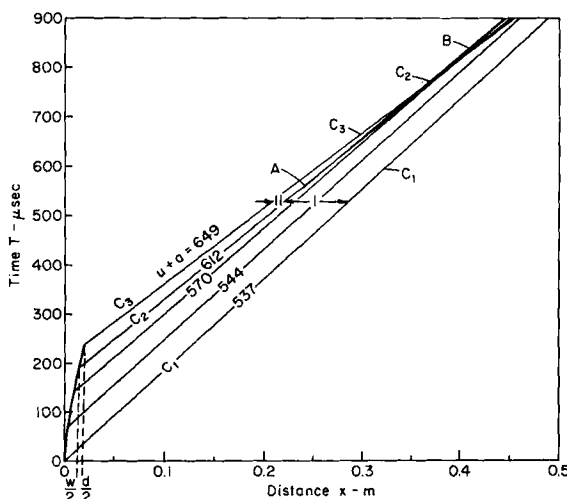


FIG. 7. Collapse of pressure waves ahead of a flame (wave velocities in meters/sec.). Reproduced from Laderman *et al.* (L2).

The general picture of the process that has been developed is that flames (ignited at the end of a closed tube) are accelerated by turbulence generated in the boundary layer. The accelerated flame generates a shock wave which develops into a detonation ahead of the flame itself, so that propagation in both directions is possible. In general the shock wave does not form at the earliest pressure pulse sent out by the flame and does not form at a point but over a region. The reaction is thus effectively initiated as a constant volume explosion. Since it forms in a precompressed region, the detonation wave is initially overdriven and will decay to the constant velocity detonation of classical theory if a sufficient run is available. If the run is short, the overdriven detonation will cause more damage than the steady-state detonation (B5). It is also possible to observe transition to detonation under conditions of short runs in closed containers at an earlier time than for a long run, since reflections of the earliest pressure pulses occur and interact with the later pulses to generate a shock wave.

Recently it has been shown that fully developed turbulence is not at all necessary for the establishment of the shock waves (L1). An increase in flame velocity of several fold which corresponds to a slightly wrinkled flame is responsible for the formation of a shock wave a short distance ahead of the flame. This mild shock travels for some distance before further reinforcement causes the explosive reaction to begin. In general the initiation of detonation waves requires confinement in the region of ignition of the flame. Direct initiation of detonation is possible if the source of ignition is sufficiently strong (L13). The ignition strength is quite critical. An increase in energy from 8.7 to 9.1 joules causes initiation without any precursor shock wave in a bomb 30 cm. in diameter, even though at the lower energy only deflagration occurs.

IV. Burning of Solid Propellants

Solid propellants are substances which may be caused to decompose exothermically into gaseous products. The hot gases are generally used as the working fluid of a rocket engine but occasionally may be used to drive turbine devices which are usually designed as standby sources of power. They have been used also as the source of an oxidizing atmosphere for the study of combustion of metal particles (F10). The primary concern of chemical engineers with respect to solid propellants has been in the areas of formulation and processing of these materials, but these topics will not be considered here. Instead, the relationship between the principles of gaseous combustion and those of solid burning will be discussed. Particular stress will be placed on our knowledge of the structure of the burning zone and the factors which determine the burning rate of solid propellants. In addition to the interaction between fluid flow, transport phenomena, and chemical rate processes, solid propellant combustion involves a necessary change of phase.

Solid propellants may be classified as monopropellants or composite propellants. Monopropellants are substances in which the fuel and oxidizer are both contained within the same molecule or at least in a single phase. These materials may either burn slowly at subsonic rates or may decompose rapidly in detonation. Depending on the use to which this type of material is put, it may be classified either as propellant or high explosive. In general, useful monopropellants are difficult to detonate.⁶ The typical example of a monopropellant is the so-called double-base propellant. This substance consists of nitrocellulose which has been colloided by nitroglycerine along with various minor constituents which have been added to

⁶ See the introduction to reference (M2) for a discussion of this distinction.

control the quality of the burning. The mixture, as far as its burning characteristics are concerned, behaves as a continuous phase. A composite propellant is made up of a mixture of at least two phases. Usually the oxidizer phase is a crystalline inorganic substance. Particles of oxidizer are imbedded in a continuous phase of organic fuel, which is called the binder. Either the oxidizer or the fuel may also be a monopropellant, but the greater part of the heat released is due to the final reaction between the decomposition flame products and the unreacted fuel or oxidizer. Although composite propellants contain as much or more stored chemical energy as conventional high explosives, the mixing process, necessary to release this energy, prevents easy detonation of these materials. Their use is desirable therefore for safety purposes. Common oxidizers are ammonium nitrate and ammonium perchlorate, which are both also monopropellants. A wide variety of organic polymers are used as fuel binders.

A review of the mechanism of solid propellant combustion was presented by Geckler in 1953 (G3). His topic was limited largely to the burning of double-base propellants. Since that time a great deal of experimental work has been done on the burning of the composite type of propellant, while the theory of monopropellant burning has been refined considerably. A limitation on the utility of the theory exists, as with gaseous combustion, due to a lack of fundamental data on the chemical rate processes occurring during the combustion.

Significant features of solid propellant burning which are observed experimentally are the dependence of burning rate on pressure, convection, and various additives. The dependence on pressure is somewhat surprising at first, since the burning velocity of gaseous mixtures is nearly independent of pressure due to the peculiar pressure dependence of transport and reaction rates (H3). However when one realizes that heat transfer to the solid is important in the gasification process and that the temperature gradient is proportional to the pressure for gaseous burning, it is clear that burning rates will increase with pressure. The exact pressure dependence is complicated, however, because of the coupling of solid and gas phase processes. Convection tends to increase burning rates in the usual manner by affecting the heat transfer through temperature gradients. All fundamental theories of propellant burning consider that the gases issue from the surface in a laminar fashion with no component parallel to the surface (linear regression). Convectional effects are determined empirically. Additives, known as ballistic modifiers, are used to control the burning rate. They often have been chosen for supposed catalytic activity, but it is suspected that they usually operate through the mechanism of thermal radiation (L4). Propellants, burning within rockets, at times oscillate strongly. Since this difficulty is largely a ballistic problem not primarily

concerned with the flame processes themselves, the reader is referred to the literature on the subject.⁷

The simplest model usually considered for monopropellant combustion is that of a laminar gaseous flame coupled to the solid surface by the heat transfer necessary to gasify the solid propellants. For a simple sublimation process, the vapor phase flame model needs only to be changed at the cold boundary in a manner precisely the same as the nonadiabatic flame considered by Spalding (S5). If a reaction occurs in or on the condensed phase, the conservation equations must be written for this phase and solved simultaneously with the vapor phase equations by matching conditions at the phase boundary. By a simple manipulation of his approximate technique for gas phase flames, Spalding has obtained solutions for the case of a single-reaction flame supported by a solid which may or may not be reactive (S6). Johnson and Nachbar (J1, J2) have investigated the existence of solutions to the single-reaction monopropellant problem and shown with reasonable assurance that a minimum value of the flame velocity eigenvalue is responsible for the lower pressure limits of burning for ammonium perchlorate (L4). Their work however did include one parameter whose value was assigned somewhat arbitrarily.

The crystalline inorganic monopropellants decompose directly from the solid to the vapor phase and are approximately described by the above mentioned theoretical work, in spite of the fact that the gas phase processes are simplified. However, the double-base propellants and other organic materials liquefy before vaporizing. In their combustion, so-called foam and fizz zones occur before the vapor phase processes. Much work has been done attempting to apply the conservation equations to the series of processes. This work forms the basis for the summary by Geckler (G3). It is the viewpoint of this author that too many parameters are determined empirically in this application of the theory, so that useful extrapolations are not possible. One must admire the manipulative skill of the early workers in this field and also their determination to formulate a complete theory. When and if the rate parameters become available, a useful theory will be developed with the aid of this early work.

A theory for calculation of burning rates for composite propellants is even more difficult to devise because of the intermediate mixing process necessary. Recent experimental work has led to a semitheoretical description of the structure of composite propellant flames (A2, C5, S7, S8). It is possible to vaporize each of the ingredients of a composite propellant by the application of a heat flux. Experimentally it is possible to measure

⁷ References to the earlier literature may be found in the relevant papers of the *Symposium on Combustion, 9th, Cornell Univ., Ithaca, N.Y., 1962*, published by Academic Press, 1963.

the linear pyrolysis rate of the surface of each pure ingredient in a separate experiment as a function of the temperature of a heated plate. It is expected that the surface temperature of the substances will be reasonably approximated by the plate temperature. A two-temperature model for the surface temperature of a burning composite propellant is then based on the assumption that each substance must have its surface regress at the same average linear rate. The surface temperature of each substance is then determined at the measured burning rate from the linear pyrolysis rate, as in Fig. 8. This model is quite plausible if one of the constituents is a

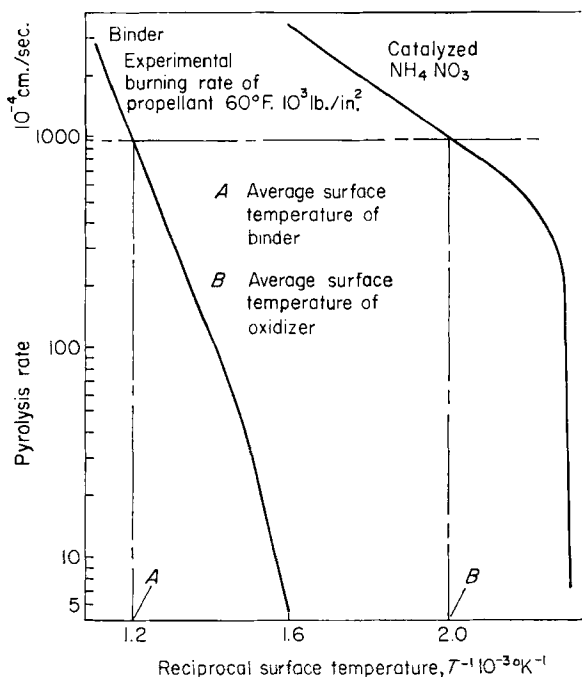


FIG. 8. Estimation of surface temperature from the two-temperature theory of (A2). Reproduced with the permission of Butterworths.

monopropellant whose flame temperature is greater than the surface temperatures. Such is the case for ammonium nitrate propellants. The complete burning process then consists of a monopropellant flame near the surface of the oxidizer particles along with heat transfer to the binder at a lower temperature. A final reaction region where the gaseous intermediates burn in a diffusion flame then completes the process. The model is thought to be applicable to ammonium perchlorate flames in a limited fashion, since surface temperatures about 200°C. higher than the flame

temperature of an ammonium perchlorate flame (about 970°C.) are required for pyrolysis at the observed burning rate. The required temperature increment may be provided by a contribution from the diffusion flame. The importance of the diffusion flame in the combustion of ammonium perchlorate is demonstrated by the dependence of burning rate on particle size. An empirical method for separating the effects of diffusion and premixed flames has been presented by Summerfield (S8). The difficulty in getting accurate information in this field may be seen by realizing that the total flame thickness is only about $100\ \mu$ in some regions of interest. Oxidizer particles smaller than $10\ \mu$ in diameter are difficult to obtain, and one would expect to see diffusional effects with $100\text{-}\mu$ particles. The latest attempts to derive a theory for a diffusion-type flame are those of Nachbar (S8), which fail to yield the desired pressure dependence.

V. Chemical Synthesis in Flames

A. VARIOUS CHEMICAL SYSTEMS CAPABLE OF SUSTAINING A STABLE FLAME

The simplest example of a flame-supporting medium is a pure chemical compound which decomposes exothermically. The widespread interest in such flames is due to their possibilities as monopropellants. Many studies are motivated by purely fundamental considerations, since a decomposition flame can be a kinetically simple flame. The most widely used and studied combustion reactions are those between hydrocarbons or hydrocarbon derivatives and air or oxygen. However, many other chemical substances may be substituted for the common fuels and/or oxidizers. Flames of uncommon fuels and oxidizers are most important because of their possibility of surpassing ordinary hydrocarbon oxidation as a source of energy. Some unusual flames are discussed in reference (P1).

A list of substances which have been used or considered to support decomposition flames is shown in Table I. Almost all of these substances have been studied at one time or another to provide fundamental information for the evaluation of the theory of flame propagation. As previously mentioned, the ozone decomposition has proved most useful as the basis of a flame which is amenable to both theoretical and experimental study. The NO decomposition flame provided a situation where a clear-cut prediction was made possible by flame theory (P2). On the basis of a flame calculation it was predicted that a strong preheat would permit the stabilization of this flame at a measurable flame velocity, since it was known that a flame would not propagate into the gas at room temperature. Subsequent experimental work confirmed the prediction by stabilizing a flame with approximately the predicted value. This places a great deal of

TABLE I
EXAMPLES OF SUBSTANCES THAT SUPPORT STABLE FLAMES

Decomposition flames		Special fuels		Special oxidizers	
Hydrazine	N_2H_2	Ammonia	NH_3	Nitric acid (fuming)	
Ozone	O_3	Hydrogen sulfide	H_2S	Oxides of nitrogen	E.g., NO
Nitric oxide	NO	Cyanogen	C_2N_2	Halogens	Br_2 , Cl_2 , F_2
Hydrogen peroxide	H_2O_2	Silanes	E.g., $(\text{CH}_3)_4\text{Si}$	Perechloryl fluoride	ClO_3F
Acetylene	C_2H_2	Boranes	E.g., B_2H_6		
Ethylene oxide	$\text{C}_2\text{H}_4\text{O}$	Metal particles	Al, Mg, Ti, Zr		
Methyl nitrite	CH_3ONO	Metal alkyls	E.g., $\text{Al}(\text{CH}_3)_3$		
Nitromethane	CH_3NO_2	Volatile metal halides	TiCl_4		
Ethyl nitrate	$\text{C}_2\text{H}_5\text{NO}_3$				

confidence on the magnitude of the chemical rate constants which were used in the calculation.

The most interesting feature of the decomposition flames is their analogy to flames of the solid monopropellants. In fact, many of these substances, which are ordinarily liquids, may support a flame directly from the liquid phase without auxiliary vaporization of the liquid. In this case, the flame supplies the necessary heat of vaporization or decomposition in exact analogy to the solid propellant flame.⁸ The principal usefulness of a decomposition flame is found in the simplicity of design and control of a rocket powered by such a flame, even though more powerful fuels are readily available. A recent example, which has been featured in the news, is the hydrogen peroxide attitude-control rocket used in the artificial earth satellites of the U.S.A.

It should be noted that the products of the decomposition flames contain either fuels or oxidizers. All of these materials are often used to support premixed flames.

Also listed in Table I are special fuels which are defined for the purpose of this article as fuels which are not hydrocarbons or oxygenated hydrocarbon derivatives. Special oxidizers listed there are those other than air or oxygen.

Several of these special fuels are presently in use or have great potentialities for practical usage. They are all most interesting because of the characteristics of their laminar premixed flames. Cyanogen, for example, supports a flame with the highest temperature of any gaseous premixed flame with gaseous products, because of the fact that N_2 and CO do not readily dissociate.⁹ The boranes support fascinating two-stage flames, each stage of which shows up as a visible reaction zone (P3). This feature is due to the separation of the processes which release heat. The solid-producing stage of the reaction apparently does not occur until the fuel has been consumed. The borane flames show great promise because of their high energy content, although the technical problem of production at reasonable costs has not been solved. Their ultimate use depends as well upon the design of engines which can handle the severe problems involved with the production of solids by a flame (O1). Combustion of metals produces flames of high energy content. Premixed flames of metal

⁸ In condensed phase materials, a differentiation between deflagration or detonation is vaporization by endothermic or exothermic processes. If exothermic reaction is initiated within the volume occupied by condensed materials, constant pressure processes are precluded. It has been shown that, by carefully avoiding shock initiation, the most powerful high explosives may be burned in a deflagrating manner (K3).

⁹ A most interesting account of recent work on very high temperatures produced by flames and other chemical means has been presented by Grosse (G5).

dust clouds are known to exist. Heat transfer in such flames is predominately by radiative processes, which therefore must be considered in the conservation equations. The necessary modifications to flame theory have been discussed (E1). Metals combustion however is usually studied because of the potential value of their addition to solid propellants. This function depends upon two phenomena. Extra heat is released by the metal oxidation, while the competition of the metal for oxygen may be used to free hydrogen and thus lower the average molecular weight of the products with a resultant enhancement of specific impulse.

Flames using the special oxidizers also have both practical and theoretical values. Fuming nitric acid and fluorine support flames with a high energy content. Nitric acid and oxides of nitrogen support interesting two-stage flames, in which the second stage is due to the high temperature necessary to decompose the NO produced as an intermediate (M5, P2). Bromine reacts with hydrogen to give a very low temperature flame which has served as the basis of a great deal of fundamental work.

B. THE FLAME AS A REACTOR

There are three principles by which a flame process may be designed. A flame may form a desirable product by reacting to a favorable equilibrium state. The stabilization of an intermediate species may be achieved by quenching. Finally, the condensation of solids from flame products may be controlled to give desirable physical properties to the solids.

In general, the stable thermodynamic products of ordinary flames have little worth, but many of the uncommon flames have products of value. The chlorination of hydrocarbons may be carried out in a flame process which was recently announced (A4). A most fascinating example is the formation of boron nitride from the flame reaction between diborane and hydrazine, two compounds which are ordinarily thought of as fuels (B2, V1). The stabilization of this flame depends upon the proper preparation of the premixed gases, since a solid adduct between the reactants prevents flame stabilization if the preflame residence time is too great.

The quenching of a reaction mixture is made possible by the passage of the hot gases through a DeLaval nozzle. It may be desirable to do this in order to prevent a shift in chemical equilibrium as flame gases are cooled slowly. It is also possible to withdraw nonequilibrium gases from within the reaction zone of a flame through a probe, analogous to the sampling process of reference (F14). It seems quite reasonable to expect that, with careful design, specialized materials could be manufactured in such a fashion.

The production of carbon black is the classical example of a partial flame process in which quenching is important. Soot formation is a non-

equilibrium process since it can form in the cooler parts of a flame by pyrolysis and remain out of equilibrium with the gases by thermal radiation to the surroundings (M7). The fixation of nitrogen in a rocket-type reactor in an impressive, if not necessarily economic, yield has been described (W3). The production of hydrazine by the partial oxidation of ammonia has been suggested (P4). The partial oxidation of hydrocarbons to yield acetylene is a process in which close control of conditions has resulted in economic operation. An interesting diffusion flame process for producing acetylene and ethylene from propane has recently been described (A5).

The condensation of solids from flame gases is suggested as a means of preparing finely divided solids. The difficulty of designing a suitable process is discussed in a review of the problem of nucleation and condensation processes in flow systems (C7). The closely allied production of tiny hollow spheres of alumina from the combustion of aluminum is a fascinating, if not necessarily useful, process (S9, F10).

Modern flame processes for the production of pure silica, titania, and ferric and other oxides are currently the object of strong industrial interest. These processes are made possible by the enhancement of flame temperatures through the addition of an extra fuel. At the time of this writing, announcement will have been made of the construction of new facilities for the production of pigment grade titanium dioxide using processes covered by German and French patents (A3). In these processes, titanium tetrachloride is burned with oxygen and carbon monoxide to regenerate the oxide in the finely divided state.

ACKNOWLEDGMENTS

This work was made possible by the support of the author's research on flames by the National Science Foundation and the Petroleum Research Fund of the American Chemical Society. He is indebted to Doctor R. M. Fristrom for many discussions on flame structure. The bulk of this work was written while the author was associated with the Johns Hopkins University.

Nomenclature

G_i	Fraction of mass flux	x_i	Mole fraction
z	Distance	n	Mole density
m_i	Molecular weight	D_{ij}	Binary diffusion coefficient
K_i	Reaction rate	q_0	Flux of heat at cold boundary
M	Mass flux	ρ	Density
λ	Thermal conductivity	s, r	Integers
T	Absolute temperature	c_p	Specific heat at constant pressure (average)
H_i	Specific enthalpy		

i, j Species*i, j* Species

∞ Burned gas conditions

0 Unburned gas conditions

- A1. Adams, II, E. N., Univ. Wisconsin Naval Res. Lab., C F 957 (1948).
- A2. Anderson, W. H., Bills, K. W., Mishuck, E., Moe, G., and Schultz, R. D., *Combust. Flame* **3**, 301 (1959).
- A3. Anonymous, *Chem. Eng. News* **41**, 25 (1963).
- A4. Anonymous, *Chem. Eng.* **68** (1), 52-54 (1961).
- A5. Arthur, J. R., and Napier, D. H., *Combust. Flame* **4**, 19 (1960).

- B1. Belles, F. M., and Swett, C. C., NACA Rept. 1300 Chapt. III, p. 83 (1959).
- B2. Berl, W. G., and Wilson, W. E., *Nature* **191**, 380 (1961).
- B3. Botha, J. P., and Spalding, D. B., *Proc. Roy. Soc.* **A225**, 71 (1954).
- B4. Boys, S. F., and Corner, J., *Proc. Roy. Soc.* **A197**, 90 (1949); Corner, J., *ibid.* **A198**, 388 (1949).
- B5. Brinkley, Jr., S. R., and Lewis, B., *Symp. Combust. 7th London Oxford* 1958 p. 807 (1959). Butterworths, London.
- B6. Bulewicz, E. M., James, C. G., and Sugden, T.M., *Proc. Roy. Soc.* **A235**, 89 (1956).

- C1. Calcote, H. F., *Combust. Flame* **1**, 385 (1957).
- C2. Calcote, H. F., *Symp. Combust. 9th Cornell Univ., Ithaca, N.Y. 1962* p. 622 (1963). Academic Press, New York.
- C3. Campbell, E. S., *Symp. Combust. 6th Yale Univ. 1956* p. 213 (1957). Reinhold, New York.
- C4. Campbell, E. S., Heinen, F. J., and Shalit, L., *Symp. Combust. 9th Cornell Univ. Ithaca, N.Y. 1962* p. 72 (1963) Academic Press, New York.
- C5. Chaiken, R. F., *Combust. Flame* **3**, 285 (1959).
- C6. Courant, R., and Friedrichs, K. O., "Supersonic Flow and Shock Waves." Wiley (Interscience), New York, 1948.
- C7. Courtney, W. G., *Symp. Combust. 9th Cornell Univ., Ithaca, N.Y., 1962* p. 799 (1963). Academic Press, New York.

- D1. de Sendagorta, J. M., *Combust. Flame* **5**, 305 (1961).
- D2. Dixon-Lewis, G., and Williams, A., *Symp. Combust. 9th Cornell Univ., Ithaca, N.Y., 1962* p. 576 (1963). Academic Press, New York.

- E1. Essenhigh, R. H., and Csaba, J., *Symp. Combust. 9th Cornell Univ., Ithaca, N.Y., 1962* p. 111 (1963). Academic Press, New York.
- E2. Evans, M. W., and Ablow, C. M., *Chem. Rev.* **61**, 129 (1961).

- F1. Ferguson, F. A., and Phillips, R. C., *Advan. Chem. Eng.* **3**, 61 (1962).
- F2. Fenimore, C. P., and Jones, G. W., *J. Phys. Chem.* **61**, 651 (1957); **63**, 1154, 1834 (1959); **65**, 2200 (1961); *Symp. Combust. 9th Cornell Univ., Ithaca, N.Y., 1962* p. 597 (1963). Academic Press, New York.
- F3. Fenimore, C. P., and Jones, G. W., *J. Phys. Chem.* **62**, 178 (1958).
- F4. Fox, M. D., and Weinberg, F. J., *Proc. Roy. Soc.* **A268**, 222 (1962).

- F5. Frank-Kamenetski, D. A., "Diffusion and Heat Exchange in Chemical Kinetics," p. 203. Princeton Univ. Press, Princeton, New Jersey 1955. (Translated by N. Thon.)
- F6. Frazier, G. C., Fristrom, R. M., and Wehner, J. F., *A.I.Ch.E. (Am. Inst. Chem. Engrs.) J.* **9**, 689 (1963).
- F7. Friedman, R., *Symp. Combust. 4th Cambridge, Mass., 1952* p. 259 (1953). Williams & Wilkins, Baltimore, Maryland.
- F8. Friedman, R., and Cyphers, J. A., *J. Chem. Phys.* **23**, 1875 (1955).
- F9. Friedman, R., and Grover, J. H., *Ind. Eng. Chem.* **51**, 1067 (1959); **49**, 1470 (1957); **53**, 1020 (1961).
- F10. Friedman, R., and Maček, A., *Symp. Combust. 9th Cornell Univ., Ithaca, N.Y., 1962* p. 703 (1963). Academic Press, New York.
- F11. Fristrom, R. M., *Symp. Combust. 9th Cornell Univ., Ithaca, N.Y., 1962* p. 560 (1963). Academic Press, New York.
- F12. Fristrom, R. M., *Science* **140**, 297 (1963).
- F13. Fristrom, R. M., and Westenberg, A. A., "Flame Structure—Its Measurement and Interpretation." McGraw-Hill, New York (to be published).
- F14. Fristrom, R. M., Grunfelder, C., and Favin, S., *J. Phys. Chem.* **64**, 1386 (1960); **65**, 587 (1961).
- G1. Gaydon, A. G., "Spectroscopy of Flames." Wiley, New York, 1957.
- G2. Gaydon, A. G., and Wolfhard, H. G., "Flames," 2nd ed., Macmillan, New York, 1960.
- G3. Geckler, R. D., "Selected Combustion Problems," p. 289. Butterworths, London, 1954.
- G4. Gross, R. A., and Oppenheim, A. K., *ARS (Am. Rocket Soc.) J.* **29**, 173 (1959).
- G5. Grosse, A. V., *Science* **141**, 781 (1963).
- H1. Hirschfelder, J. O., and Curtiss, C. F., *Advan. Chem. Physics* **3**, 59 (1961).
- H2. Hirschfelder, J. O., and McCone, Jr., A., *Phys. Fluid* **2**, 551 (1959).
- H3. Hirschfelder, J. O., Curtiss, C. F., and Campbell, D. E., *Symp. Combust. Cambridge, Mass., 1952* p. 190 (1953). Williams & Wilkins, Baltimore, Maryland.
- J1. Johnson, W. E., *Arch. Rat. Mech. Anal.* **13**, 46–54 (1963).
- J2. Johnson, W. E., and Nachbar, W., *Symp. Combust. 8th Pasadena, Calif., 1960* p. 678 (1962). Williams & Wilkins, Baltimore, Maryland.
- J3. Johnson, W. E., and Nachbar, W., *Arch. Rat. Mech. Anal.* **12**, 58–92 (1963).
- J4. Jones, H., *Proc. Roy. Soc. A* **248**, 333 (1958).
- J5. Jost, W., "Explosion and Combustion Processes in Gases." McGraw-Hill, New York, 1946.
- K1. Kaskan, W. E., *Combust. Flame* **3**, 39; 49 (1959).
- K2. Kilpatrick, M., and Baker, Jr., L. L., *Symp. Combust. 5th Pittsburgh, 1954* p. 196 (1955). Reinhold, New York.
- K3. Kistiakowski, G. B., *Symp. Combust. 3rd Madison, Wis., 1948* p. 560 (1949). Williams & Wilkins, Baltimore, Maryland.
- K4. Kläukens, H., and Wolfhard, H. G., *Proc. Roy. Soc. A* **193**, 512 (1948).
- K5. Klein, G., *Phil. Trans. Roy. Soc. London* **A249**, 389 (1957).
- L1. Laderman, A. J., and Oppenheim, A. K., *Proc. Roy. Soc. A* **268**, 153 (1963).

- L2. Laderman, A. J., Urtiew, P. A., and Oppenheim, A. K., *Symp. Combust. 9th Cornell Univ., Ithaca, N.Y. 1962* p. 265 (1963). Academic Press, New York.
- L3. Lask, G., and Wagner, H. G., *Symp. Combust. 8th Pasadena, Calif., 1960* p. 432 (1962). Williams & Wilkins, Baltimore, Maryland.
- L4. Levy, J. B., and Friedman, R., *Symp. Combust. 8th Pasadena, Calif., 1960* p. 663 (1962). Williams & Wilkins, Baltimore, Maryland.
- L5. Lewis, B., and von Elbe, G., *J. Chem. Phys.* **2**, 537 (1934).
- L6. Lewis, B., and von Elbe, G., *Ind. Eng. Chem.* **45**, 1921 (1953).
- L7. Lewis, B., and von Elbe, G., "Combustion, Flames and Explosion of Gases," 2nd ed., p. 220. Academic Press, New York, 1961.
- L8. Lewis, B., and von Elbe, G., "Combustion, Flames and Explosion of Gases," 2nd ed., p. 310. Academic Press, New York.
- L9. Lewis, B., and von Elbe, G., "Combustion, Flames and Explosion of Gases," 2nd ed., p. 323. Academic Press, New York.
- L10. Lewis, B., and von Elbe, G., "Combustion, Flames and Explosion of Gases," 2nd ed., pp. 511-528. Academic Press, New York.
- L11. Lewis, B., and von Elbe, G., "Combustion, Flames and Explosion of Gases," 2nd ed., p. 590. Academic Press, New York.
- L12. Linnett, J. W., and Simpson, J. S. M., *Symp. Combust. 6th Yale Univ., 1956* p. 20 (1957). Reinhold, New York.
- L13. Litchfield, E. L., Hay, M. H., and Forshay, D. R., *Symp. Combust. 9th Cornell Univ., Ithaca, N.Y. 1962* p. 282 (1963). Academic Press, New York.
- M1. McCullough, Jr., F., and Jenkins, Jr., H. P., *Symp. Combust. 5th Pittsburgh, 1954* p. 181 (1955). Reinhold, New York.
- M2. Maček, A., *Chem. Rev.* **62**, 41 (1962).
- M3. Mallard, E., and Le Chatelier, H., *Ann. Mines* [8] **4**, 274 (1883); see (J5).
- M4. Mayer, E., *Combust. Flame* **1**, 438 (1957).
- M5. Mertens, J., and Potter, R. L., *Combust. Flame* **2**, 181 (1958).
- M6. Mikhelson, V. A., *Ann. Phys.* **37**, 1 (1889); quoted in (Z1).
- M7. Millikan, R. C., *J. Phys. Chem.* **66**, 794 (1962).
- M8. Minkoff, G. J., and Tipper, C. F. H., "Chemistry of Combustion Reactions," Chaps. 10 and 11. Butterworths, London, 1962.
- O1. Olsen, W. T., and Setze, P. C., *Symp. Combust. 7th London Oxford, 1958* p. 883 (1959). Butterworths, London.
- O2. Oppenheim, A. K., and Stern, R. A., *Symp. Combust. 7th London Oxford, 1958* p. 837 (1959). Butterworths, London.
- P1. Parker, W. G., *Combust. Flame* **2**, 69 (1958).
- P2. Parker, W. G., and Wolfhard, H. G., *Symp. Combust. 4th Cambridge, Mass., 1952* p. 420 (1953). Williams & Wilkins, Baltimore, Maryland.
- P3. Parker, W. G., and Wolfhard, H. G., *Fuel* **35**, 323 (1956).
- P4. Penner, S. S., "Introduction to the Study of Chemical Reactions in Flow Systems," p. 60. Butterworths, London, 1955.
- P5. Penner, S. S., "Chemistry Problems in Jet Propulsion." Pergamon, New York, 1957.
- P6. Penner, S. S., and Jacobs, T. A., *Ann. Rev. Phys. Chem.* **11**, 391 (1960).
- P7. Penner, S. S., and Mullins, B. P., "Explosions, Detonations, Flammability and Ignition." Pergamon, New York, 1959.

- P8. Penner, S. S., and Williams, F. A., *Astronaut. Acta* **7**, 171 (1961).
- P9. Potter, Jr., A. E., *Progr. Combust. Sci. Technol.* **1**, 145 (1960).
- P10. Powling, J., *Fuel* **28**, 25 (1949).
- P11. Prescott, R., Hudson, R., Foner, S., and Avery, W. H., *J. Chem. Phys.* **22**, 145 (1954).
- R1. Rosen, G., *Symp. Combust. 7th London Oxford, 1958* p. 339 (1959). Butterworths, London.
- S1. Salamandra, G., and Sevastyanova, I. K., *Combust. Flame* **7**, 169 (1963).
- S2. Simon, D. M., "Selected Combustion Problems," p. 59. Butterworths, London, 1954.
- S3. Sneddon, I. N., "Elements of Partial Differential Equations," p. 119. McGraw-Hill, New York, 1957.
- S4. Spalding, D. B., *Combust. Flame* **1**, 287 (1957).
- S5. Spalding, D. B., *Proc. Roy. Soc. A* **240**, 83 (1957).
- S6. Spalding, D. B., *Combust. Flame* **4**, 59 (1960).
- S7. Schultz, R. D., Green, Jr., L., and Penner, S. S., "Combustion and Propulsion: 3rd AGARD Colloquium," p. 367. Pergamon, New York, 1958.
- S8. Summerfield, M. (ed.), *Progr. Astron. Rocketry* **1**, Pt. B (1960).
- S9. Summerfield, M. (ed.), *Progr. Astron. Rocketry* **1**, Pt. C (1960).
- V1. Vanpee, M. W., Clark, A. H., and Wolfhard, H. G., *Symp. Combust. 9th Cornell Univ., Ithaca, N.Y., 1962* p. 127 (1963). Academic Press, New York.
- V2. von Kármán, T., *Symp. Combust. 6th Yale Univ., 1956* p. 1 (1957). Reinhold, New York.
- V3. von Kármán, T., and Penner, S. S., "Selected Combustion Problems," p. 5. Butterworths, London, 1954.
- W1. Wehner, J. F., *Combust. Flame* **7**, 309 (1963).
- W2. Weinberg, F. J., "Optics of Flames." Butterworths, London, 1963.
- W3. Weisenberg, I. J., and Winternitz, P. F., *Symp. Combust. 6th Yale Univ., 1956* p. 813 (1957). Reinhold, New York.
- W4. Westenberg, A. A., and Fristrom, R. M., *J. Phys. Chem.* **64**, 1393 (1960); **65**, 591 (1961).
- W5. Wilde, K. A., *J. Chem. Phys.* **22**, 1788 (1954).
- Y1. Yang, C. H., *Combust. Flame* **6**, 215 (1962).
- Z1. Zeldovich, Y. B., NACA TM 1282 (1951); refers to his publication with D. A. Frank-Kamenetski in *Zh. Fiz. Khim.* **12**, 100 (1938).

BIFUNCTIONAL CATALYSIS

J. H. Sinfelt

Esso Research and Engineering Company,
Linden, New Jersey

I. Introduction	37
II. Nature of Bifunctional Reforming Catalysts	38
A. General Description of Platinum Reforming Catalysts	38
B. Characterization of the Metal Component	39
C. Properties of the Acidic Component	40
III. Nature of Reactions Occurring over Bifunctional Catalysts	42
A. Description of Catalytic Reforming Reactions	42
B. Thermodynamic Considerations	44
C. General Aspects of Reaction Mechanisms	46
D. Independent Action of Metal and Acidic Centers of the Catalyst	48
IV. Kinetics and Mechanism of Individual Hydrocarbon Reactions	49
A. Dehydrogenation of Cyclohexanes	50
B. Isomerization Reactions	55
C. Further Considerations of the Role of Hydrogen in Isomerization Kinetics	61
D. Dehydrocyclization of Paraffins	64
E. Miscellaneous Related Reactions	69
V. Conclusion	71
Nomenclature	71
References	73

I. Introduction

The use of bifunctional catalysts in the catalytic reforming of petroleum naphthas to produce gasolines of high antiknock quality represents one of the most outstanding applications of heterogeneous catalysis over the past decade (C6). The bifunctional catalysts of most interest consist of a hydrogenation-dehydrogenation component, for example, platinum, palladium, or nickel, supported on an acidic component such as alumina or silica-alumina. Such catalysts are termed bifunctional, since they are found to promote simultaneously such reactions as the isomerization and dehydrogenation of saturated hydrocarbons, as was disclosed by Haensel (H1) and by Ciapetta (C1) over a decade ago. While other examples of

bifunctional catalysis are known (K2), the application in catalytic reforming is by far the best known and the one on which most research work has been done.

This review is concerned with a discussion of the reactions of hydrocarbons over bifunctional catalysts, primarily from the viewpoint of mechanism and kinetics. Some discussion will also be given of the structure and properties of typical bifunctional reforming catalysts, since this is somewhat helpful in understanding how the catalyst functions in promoting the various reactions. In addition, at appropriate places in the article, the practical application of the principles of bifunctional catalysis in commercial reforming processes will be considered.

II. Nature of Bifunctional Reforming Catalysts

A. GENERAL DESCRIPTION OF PLATINUM REFORMING CATALYSTS

As already pointed out, the common bifunctional reforming catalysts consist of a metal dispersed on an acidic support. In the case of platinum on alumina catalysts, the amount of platinum present is commonly within the range of 0.1 to 1.0 wt.%. The catalysts frequently contain comparable percentages of halogens, such as chlorine or fluorine. One common method of preparing such a catalyst involves impregnation of alumina with chloroplatinic acid, followed by calcination in air at temperatures in the range 550 to 600°C. (K1, S7). The aluminas commonly used have surface areas, as determined by the method of Brunauer *et al.* (B5), in the range of 150 to 300 m.²/g., corresponding to average pore radii of 60 to 30 Å. The catalytic properties of the alumina depend to a marked extent upon the source or the method of preparation of the alumina (P3). A number of different crystalline phases of alumina have been identified with the use of X-ray diffraction (N1). The different phases can be prepared by varying the conditions of preparation and dehydration of the alumina.

Platinum on alumina reforming catalysts are commonly used commercially in the form of cylindrical pellets about $\frac{1}{8} \times \frac{1}{8}$ in. in size, since this is about the smallest size acceptable from the standpoint of avoiding excessive pressure drop. For fundamental studies in small-scale reactors, where pressure drop limitations are less severe, it may be preferable to use the catalyst in the form of small granules to minimize diffusional limitations.

Catalysts other than platinum catalysts have been considered for reforming. Included among these are certain metal oxides, e.g., chromia and molybdena. However, these catalysts are much less active than platinum and also less selective toward the reactions of most interest in reforming, at least under the conditions usually employed in commercial

catalytic reforming operations, namely, high hydrogen partial pressures of the order 10–30 atm. (C6). Furthermore, since chromia and molybdena catalysts must be used near atmospheric pressure to obtain good activity and selectivity, the activity declines rapidly. This is because operation at low hydrogen pressure results in the extensive formation on the surface of carbonaceous residues, which strongly inhibit the reactions.

The foregoing paragraphs have described platinum on alumina catalysts in a very general way and have also attempted to give a brief discussion of the reason why platinum is so commonly used as a reforming catalyst. In the following sections, the physical and chemical properties of platinum-alumina catalysts will be discussed in more detail, since this information will be of considerable help in understanding the way in which these catalysts function.

B. CHARACTERIZATION OF THE METAL COMPONENT

On the basis of hydrogen chemisorption measurements, Spenadel and Boudart (S7) have concluded that freshly prepared platinum on alumina catalysts are characterized by extremely high dispersion of platinum over the support. If the platinum is present as crystallites, these authors point out that the crystal size must be less than about 10 Å. The authors also suggest that the platinum may be dispersed in the form of two-dimensional patches, but probably not as isolated atoms. This was based on the observation that the amount of adsorption of hydrogen corresponded to about one atom of hydrogen per atom of platinum, and that more than 90% of the adsorption of hydrogen was instantaneous. If the platinum were dispersed as isolated platinum atoms, the distance between platinum atoms would be of the order of 100 Å. In the act of adsorption, the hydrogen molecule would then dissociate in such a manner that one hydrogen would be adsorbed on a platinum site and the other on an adjacent alumina site. To satisfy the requirement of one hydrogen atom adsorbed per atom of platinum, the latter hydrogen atom would then have to migrate over the alumina to another platinum site. However, as Spenadel and Boudart point out, such a surface diffusion process should be of the slow activated type, in contrast with the observation that the adsorption was almost wholly instantaneous.

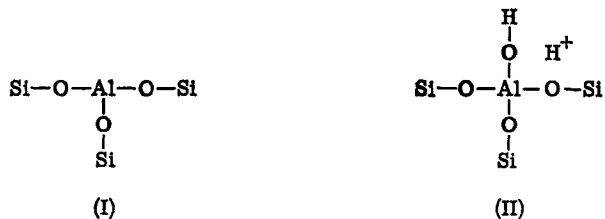
The high degree of dispersion of platinum on alumina has also been confirmed by the hydrogen chemisorption measurements of Keavney and Adler (K1), and by the chemisorption studies of Gruber (G2). In addition, high dispersion of platinum on silica-alumina has been observed by Hughes and associates, using a carbon monoxide chemisorption technique (H10).

McHenry and co-workers (M1) have suggested that platinum on alumina catalysts, which are active for the dehydrocyclization of paraffins,

contain the platinum in the form of a complex, in which the platinum has a valence of four. The platinum complex is characterized by its solubility in aqueous hydrofluoric acid or acetylacetone. However, the work of Kluksdahl and Houston (K4) indicated that solubility of the platinum in hydrofluoric acid may simply be a consequence of exposure of the catalyst to oxygen. These workers found that essentially no soluble platinum was observed for any of a number of reduced platinum catalysts which were not exposed to oxygen. The authors, therefore, suggest that the platinum-alumina complex postulated by McHenry and co-workers does not exist under reforming conditions, i.e., after reduction with hydrogen. Furthermore, they point out that soluble platinum can be observed with platinum on silica catalysts and in the absence of chlorine, so that no evidence exists for a specific soluble platinum-alumina-chlorine complex. They suggest that the species which dissolves in hydrofluoric acid is simply the platinum metal upon which oxygen is chemisorbed.

C. PROPERTIES OF THE ACIDIC COMPONENT

The alumina or silica-alumina supports used in bifunctional catalysts have been shown to be acidic in nature. The acidic properties are readily demonstrated by the affinity of these solids for adsorption of basic compounds such as ammonia, trimethylamine, *n*-butylamine, pyridine, and quinoline (O1, R5). Furthermore, adsorption of certain acid-base indicators such as butter yellow gives a coloration similar to that observed in acid media (B3, B4). With regard to the origin of the acidity, Tamele (T1) has suggested in the case of silica-alumina that aluminum atoms replace silicon atoms in the surface of the silica structure, giving rise to surface sites of the form



in which the first (I) acts as a Lewis acid and the second (II) as a Brønsted acid.

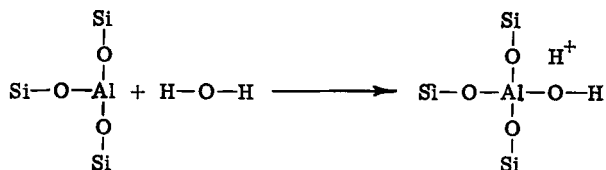
A Lewis acid is defined as a species that can accept a pair of electrons from a base. This is a very general definition of an acid proposed by G. N. Lewis in 1923 (L1). In the case of structure (I), the Al atom is not completely coordinated, i.e., it is bonded to three oxygen atoms instead of four. The aluminum atom thus has a total of six valence electrons instead

of the maximum eight. It therefore has the potential of accepting a pair of electrons from another species to complete a stable octet. Electron-rich species capable of donating a pair of electrons are referred to as Lewis bases. To illustrate the interaction of a Lewis acid and a Lewis base, we can consider the way in which a molecule of ammonia could bond with the aluminum atom in structure (I):



The ammonia molecule donates a pair of electrons to the electron-deficient aluminum atom in the above reaction, thus completing a stable octet of electrons. This example is a pertinent one, since adsorption of ammonia has been used as a way of measuring the acidity of solid catalyst surfaces.

A Brønsted acid is simply defined as a species that can donate a proton to another species (L2). In the case of structure (II) shown for a surface site, it is to be noted that the aluminum atom is completely coordinated by oxygen atoms and has a proton associated with it. The formation of this type of site might simply be visualized as resulting from the interaction of a Lewis acid site of the type just discussed with a molecule of water:



That is, the Brønsted acid site can be thought of as a hydrated Lewis acid site. Since the Brønsted site can donate a proton to another species, we can represent its reaction with ammonia simply as the interaction of a proton with the unshared electron pair on the nitrogen atom of the ammonia molecule:



The interaction leads to the formation of an ammonium ion at the surface.

Thus, we have seen that the surface of a solid such as silica-alumina has acidic properties. Similar considerations also apply to alumina, although alumina alone is appreciably less acidic than the silica-alumina compositions used as cracking catalysts. Treatment of alumina with

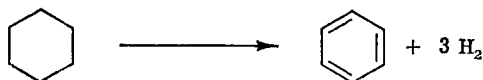
halogens such as Cl or F tends to make the acidic properties of alumina more pronounced, in the sense that it increases the activity of alumina for the catalysis of typical acid-catalyzed reactions, such as the skeletal isomerization of olefins and various cracking reactions of hydrocarbons (M3, R2, S3). It has been suggested that incorporation of halogens in the surface of alumina involves partial replacement of OH groups, known to exist on alumina (P2), by Cl or F. The enhancement of acidic properties is then attributed to the halogens having higher electron affinities than oxygen, thus causing the residual hydrogen atoms on the surface to become more acidic. The experiments of Webb (W1) are of interest with respect to the nature of the effect of halogen acids on the acidity of alumina. Briefly, these experiments showed that treatment of alumina with HF increases the strength of the acid sites for ammonia adsorption but does not alter the number of acid sites appreciably. At any rate, regardless of the detailed mechanism of enhancement of the acidity of alumina, halogens serve as effective promoters for the acid-catalyzed reactions which occur over platinum-alumina reforming catalysts.

III. Nature of Reactions Occurring over Bifunctional Catalysts

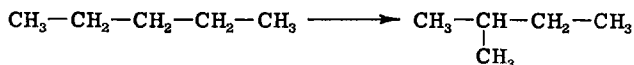
A. DESCRIPTION OF CATALYTIC REFORMING REACTIONS

Some of the typical reforming reactions catalyzed by the bifunctional, metal-acidic oxide catalysts, along with a specific example of each, are listed below:

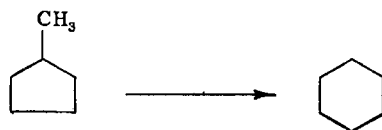
(a) Dehydrogenation of cyclohexanes to aromatics



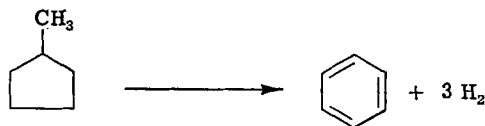
(b) Isomerization of *n*-paraffins to branched paraffins



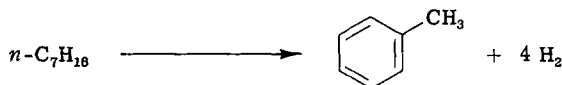
(c) Isomerization of alkylcyclopentanes to cyclohexanes



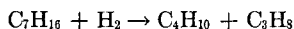
(d) Dehydroisomerization of alkylcyclopentanes to aromatics



(e) Dehydrocyclization of paraffins to aromatics



(f) Hydrocracking to low molecular weight paraffins



Early reported studies on the application of bifunctional catalysts to the foregoing reactions were those of Haensel and Donaldson (H2), Ciapetta and Hunter (C2, C4, C5), Heinemann and co-workers (H3), and Hettinger and co-workers (H7). These reactions form the heart of catalytic reforming and have been exploited commercially in a number of processes, including the following:

(a) Platforming	Universal Oil Products Company
(b) Catforming	Atlantic Refining Company
(c) Houdriforming	Houdry Process Corporation
(d) Sinclair-Baker process	Sinclair Research Laboratories joint with Baker and Company
(e) Ultraforming	American Oil Company
(f) Powerforming	Esso Research and Engineering Company

These processes have been described extensively in a comprehensive article by Ciapetta *et al.* (C6), to which the reader is referred for details. Here we will simply point out that the processes are all fixed bed processes using platinum catalysts and operate at relatively high pressures (15–35 atm.) with recycle of hydrogen-rich gases.

The major part of the antiknock improvement obtained in the catalytic reforming of petroleum naphthas is due to the formation of aromatics. Lesser contributions result from the isomerization of straight-chain paraffins to branched paraffins and hydrocracking of high molecular weight components to lower molecular weight components in the gasoline boiling range.

Of all the reactions taking place in catalytic reforming, the dehydrogenation of cyclohexanes occurs by far the most readily. Isomerization

reactions also occur readily, but not nearly so fast as the dehydrogenation of cyclohexanes. The limiting reactions in most catalytic reforming operations are hydrocracking and dehydrocyclization, which generally occur at much lower rates.

Prior to discussing the mechanistic aspects of reforming reactions, we will next consider the thermodynamics of some of the more important reactions involved in the process. This will be done in the following section.

B. THERMODYNAMIC CONSIDERATIONS

The thermodynamics of the more important reactions in catalytic reforming can be discussed conveniently by referring to the equilibria involved in the various interconversions among certain of the C_6 hydrocarbons. Some thermodynamic equilibrium constants at 500°C., a typical temperature in catalytic reforming, and heats of reaction are given in Table I. The equilibrium constants in Table I apply when the partial pressures of the various components are expressed in atmospheres.

TABLE I
THERMODYNAMIC DATA FOR TYPICAL REFORMING REACTIONS

Reaction	K (R4)	ΔH_R , kcal./mole (R4)
Cyclohexane \rightarrow benzene + 3 H_2	6×10^6	52.8
Methylcyclopentane \rightarrow cyclohexane	0.086	-3.8
<i>n</i> -Hexane \rightarrow benzene + 4 H_2	0.78×10^6	63.6
<i>n</i> -Hexane \rightarrow 2-methylpentane	1.1	-1.4
<i>n</i> -Hexane \rightarrow 3-methylpentane	0.76	-1.1
<i>n</i> -Hexane \rightarrow 1-hexene + H_2	0.037	31.0

The dehydrogenation of cyclohexane and the dehydrocyclization of *n*-hexane to yield benzene are seen to be strongly endothermic, so that increasing temperature has a marked effect on improving the extent of conversion to aromatics. Hydrogen partial pressure obviously has a marked effect on the extent of formation of benzene, and from the viewpoint of equilibria alone, it is advantageous to operate at as high a temperature and as low a hydrogen partial pressure as possible to maximize the yield of the aromatic. However, other considerations, such as catalyst deactivation due to formation of carbonaceous residues on the surface, place a practical upper limit on temperature and a lower limit on hydrogen partial pressure in catalytic reforming operations. The thermodynamic considerations in the formation of aromatics from higher molecular weight paraffins and cycloparaffins are qualitatively the same as for formation of benzene,

but it should be noted that the equilibrium tends to shift more in favor of the aromatic as the molecular weight increases. Thus, for example, the formation of toluene from methylcyclohexane is thermodynamically more favorable than the formation of benzene from cyclohexane, as shown below:

Reaction	K at 500°C. (R4)
Cyclohexane \rightarrow benzene + 3 H ₂	6×10^5
Methylcyclohexane \rightarrow toluene + 3 H ₂	2×10^6

The dehydrogenation of paraffins to olefins, while it does not take place to a large extent at typical reforming conditions (equilibrium conversion of *n*-hexane to 1-hexene is about 0.3% at 510°C. and 17 atm. hydrogen partial pressure), is nevertheless of considerable importance, since olefins appear to be intermediates in some of the reactions. This matter will be discussed in more detail in a subsequent section. The formation of olefins from paraffins, similar to the formation of aromatics, is favored by the combination of high temperature and low hydrogen partial pressure. The thermodynamics of olefin formation can play an important role in determining the rates of those reactions which proceed via olefin intermediates, since thermodynamics sets an upper limit on the attainable concentration of olefin in the system.

The equilibria in the case of isomerization reactions are much less temperature sensitive than in the case of dehydrogenation reactions, since the heats of reaction are relatively small. Furthermore, it is seen that the equilibrium between methylcyclopentane and cyclohexane favors the former, indicating that the five-membered ring structure is more stable than the six-membered ring. In the case of the equilibria between *n*-hexane and the methylpentanes, it can be seen that the 2-methylpentane is the favored isomer over 3-methylpentane, which is reasonable from the simple statistical consideration that the substituent methyl group can occupy either of two equivalent positions in the former molecule as compared to one in the latter. Thermodynamic calculations would indicate the presence of appreciable quantities of dimethylbutanes at equilibrium (about 30 to 35% of the total hexane isomers at 500°C.), but such quantities of these isomers are not observed in reforming. While equilibrium tends to be established rather readily in the case of *n*-hexane and the methylpentanes, this does not appear to be true for the dimethylbutanes. This suggests that a strong kinetic barrier resists the rearrangement of singly branched to doubly branched isomers (C6), which apparently does not exist in the case of the rearrangement of the normal structure to the singly branched structures.

C. GENERAL ASPECTS OF REACTION MECHANISMS

Indications of the mechanism of isomerization of saturated hydrocarbons were obtained by Ciapetta (C3), who observed that olefins were isomerized over nickel-silica-alumina catalyst at appreciably lower temperatures than were the corresponding saturated hydrocarbons, suggesting that olefins were intermediates in the reaction. Ciapetta also suggested that the rearrangement of the carbon skeleton took place via a carbonium

TABLE II

ROLE OF INDIVIDUAL FUNCTIONS OF BIFUNCTIONAL REFORMING CATALYSTS;
EFFECT OF CATALYST TYPE AND HYDROCARBON STRUCTURE ON PRODUCT (M2)^a

Charge	Product	Vol. % of liquid product		
		Catalyst		
		Isomeriza- tion	Dehydro- genation	Dual function
Cyclohexane	Aromatic	2	92	92
	Olefin	0	1	2
	Naphthene	98	2	1.5
	Paraffin	0	5	4.5
	C ₆ /C ₅ ring ratio ^b	> 50 to 1	> 25 to 1	1 to 4
Methylcyclopentane	Aromatic	3	7	49
	Olefin	0	4	2
	Naphthene	95	80	23
	Paraffin	2	9	26
	C ₆ /C ₅ ring ratio ^b	Traces of cyclohexane	Traces of cyclohexane	1 to 4
Cyclohexene	Aromatic	8	92	83
	Olefin	86	3	2
	Naphthene	5	0	11
	Paraffin	7	5	4
	C ₆ /C ₅ ring ratio ^b	Approx. 1 to 10	> 50 to 1	Approx. 1 to 4
Methylcyclopentene	Aromatic	7	16	48
	Olefin	74	2-3	1
	Naphthene	19	48-70	13
	Paraffin	0	34-11	38
	C ₆ /C ₅ ring ratio ^b	1 to 14	< 1 to 50	< 1 to 25

^a 950°F., 300-lb./sq. in. gauge; liquid hourly space velocity = 3, H₂/hydrocarbon = 4.

^b In naphthene and olefin product.

ion mechanism. Further support for such a mechanism was obtained by Mills and co-workers (M2), who made experiments on three different types of catalysts, the first containing only an acidic function, the second only a dehydrogenation function, and the third containing both functions. Data were obtained on cyclohexane, methylcyclopentane, cyclohexene, and methylcyclopentene, as shown in Table II. It was found that the conversion of cyclohexane to benzene proceeded as well over the dehydrogenation catalyst as it did over the bifunctional catalyst but did not take place over the catalyst which contained only an acidic function. The isomerization-dehydroisomerization of methylcyclopentane to cyclohexane and benzene was found to occur to a significant extent only in the case of the bifunctional catalyst. Isomerization of cyclohexene to methylcyclopentene was found to require only an acidic function. Based on these observations, Mills and co-workers proposed the scheme shown in Fig. 1 to describe the

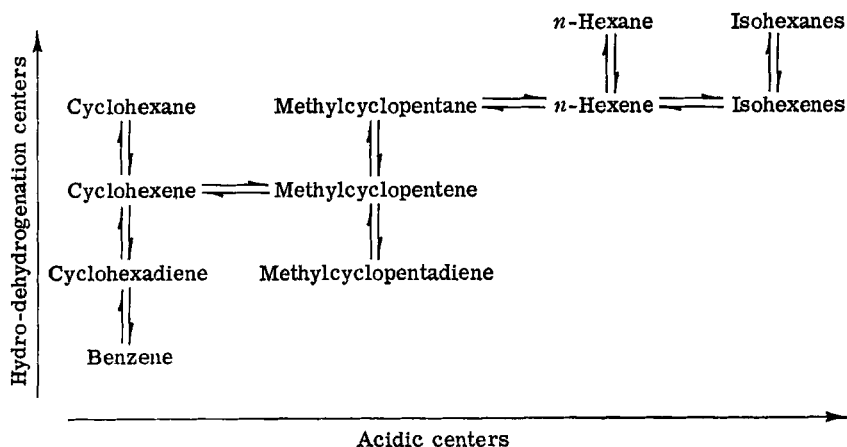


FIG. 1. Reaction paths in reforming C_6 hydrocarbons (M2).

reforming of C_6 hydrocarbons over a bifunctional catalyst. The vertical reaction paths in the figure take place on the hydrogenation-dehydrogenation centers of the catalyst and the horizontal reaction paths on the acidic centers. According to the mechanism, the conversion of methylcyclopentanes on hydrogenation-dehydrogenation centers of the catalyst, followed by isomerization to cyclohexene on acidic centers. The cyclohexene then returns to hydrogenation-dehydrogenation centers where it can either be hydrogenated to cyclohexane or further dehydrogenated to benzene, the relative amounts of these products depending on reaction conditions.

In the reaction scheme in Fig. 1, the dehydrocyclization of n -hexane

is indicated to proceed via formation of *n*-hexene on dehydrogenation centers, followed by cyclization of the *n*-hexene to methylcyclopentane on acidic centers. The methylcyclopentane then is converted to benzene in the manner just described. Alternatively, it has been suggested (B1) that the initial steps in the reaction sequence more likely involve dehydrogenation to the diolefin, hexadiene, followed by cyclization on acidic centers to the cyclic olefin, methylcyclopentene. The mechanism of dehydrocyclization will be considered in more detail in a subsequent section.

Hydrocracking reactions over bifunctional catalysts are quite complex. Thus, over platinum-alumina or platinum-silica-alumina catalysts, both cracking on platinum metal sites and acid-catalyzed cracking can occur (M3). It has been suggested that olefins formed on platinum sites are intermediates in hydrocracking, in a manner similar to isomerization (M3). However, it has been found that appreciable hydrocracking of saturated hydrocarbons can also take place over alumina or halogenated alumina (S2, S3), although no active dehydrogenation component is present.

D. INDEPENDENT ACTION OF METAL AND ACIDIC CENTERS OF THE CATALYST

In the case of the bifunctional platinum-acidic oxide catalysts, it has been demonstrated that the platinum sites and acidic sites can act independently. Thus, Weisz and Swegler (W5) have shown that mechanical mixtures, in which the dehydrogenation and acidic functions were present on separate particles, were active for the isomerization of *n*-paraffins. Provided the catalyst particles were small enough, the extent of isomerization was found to be comparable to that observed when both catalytic functions were present on the same particle (Fig. 2). Similarly, Hindin *et al.* (H8) found that such mechanical mixtures were active for the dehydroisomerization of methylcyclopentane to benzene. The results of these experiments indicate that the above-mentioned reactions can proceed via gas phase intermediates (olefins), which diffuse from one type of catalytic site to the other. Thus, it appears that a reaction like isomerization or dehydroisomerization of a saturated hydrocarbon can proceed satisfactorily by a succession of steps involving dehydrogenation to an olefin on platinum sites, followed by desorption and subsequent diffusion through the gas phase to acidic sites, where the isomerization step takes place. The isomerized olefin can then diffuse through the gas phase to a platinum site, where it can undergo hydrogenation or dehydrogenation to form the final reaction products.

While mechanically mixed catalysts have been shown to be successful for the isomerization or dehydroisomerization of saturated hydrocarbons,

they do not appear to be so satisfactory for the dehydrocyclization reaction (M1, W2). This suggests that dehydrocyclization proceeds to a lesser degree by a mechanism involving gas phase transport of intermediates between separate dehydrogenation and acidic centers. Retaining the idea

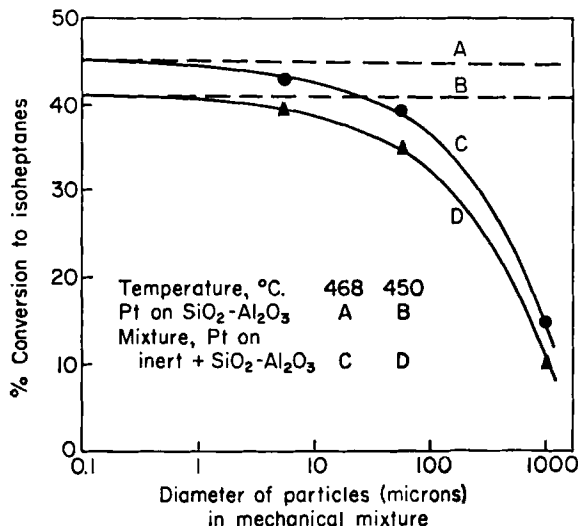


FIG. 2. Isomerization of *n*-heptane over mixtures of particles of silica-alumina and particles of inert-supported platinum (W5). The dashed lines represent conversions over platinum-impregnated silica-alumina. Conditions of runs: 25 atm., $H_2/nC_7 = 4/1$, space velocity = 0.7 g. nC_7 per hour per gram of catalyst.

that the reaction proceeds through a diolefin stage, it might then be postulated that the diolefin does not readily desorb from the platinum site on which it is formed, but rather migrates to an acidic site by surface diffusion, or interacts with an acidic site in very close proximity to the platinum. The active center for dehydrocyclization might then be visualized as a platinum-acid co-site, or alternatively as a complex (M1).

IV. Kinetics and Mechanism of Individual Hydrocarbon Reactions

In the preceding paragraphs we have discussed bifunctional catalysis from the standpoint of the nature of the catalyst surface as well as the kinds of reactions which take place and have summarized the results of certain critical experiments from which a mechanistic picture has evolved. With this background in mind, we will now discuss the results of kinetic studies in the following sections.

A. DEHYDROGENATION OF CYCLOHEXANES

As pointed out earlier, the dehydrogenation of cyclohexanes to aromatics over a supported platinum catalyst requires only platinum sites. The properties of the support do not appear to be critical, provided that the platinum is well dispersed.

The conversion of cyclohexanes to aromatics is a highly endothermic reaction ($\Delta H \simeq 50$ kcal./mole) and occurs very readily over platinum-alumina catalyst at temperatures above about 350°C. At temperatures in the range 450–500°C., common in catalytic reforming, it is extremely difficult to avoid diffusional limitations and to maintain isothermal conditions. The importance of pore diffusion effects in the dehydrogenation of cyclohexane to benzene at temperatures above about 372°C. has been shown by Barnett *et al.* (B2). However, at temperatures below 372°C. these investigators concluded that pore diffusion did not limit the rate when using $\frac{1}{8}$ in. catalyst pellets.

A study of the kinetics of methylcyclohexane dehydrogenation to toluene in the temperature range 315 to 372°C. has been reported by

TABLE III
SUMMARY OF RATE DATA FOR METHYLCYCLOHEXANE
DEHYDROGENATION OVER Pt-Al₂O₃^a (S6)

Temp. (°C.)	p_M^b (atm.)	p_H^c (atm.)	r^d
315	0.36	1.1	0.012
315	0.36	3.0	0.012
315	0.07	1.4	0.0086
315	0.24	1.4	0.011
315	0.72	1.4	0.013
344	0.36	1.1	0.030
344	0.36	3.1	0.032
344	0.08	1.4	0.020
344	0.24	1.4	0.034
344	0.68	1.4	0.034
372	0.36	1.1	0.076
372	0.36	4.1	0.080
372	1.1	4.1	0.124
372	2.2	4.1	0.131

^a 0.3% Pt on alumina catalyst.

^b Methylcyclohexane pressure, atm.

^c Hydrogen pressure, atm.

^d Rate of dehydrogenation, gram-moles of toluene formed per hour per gram of catalyst.

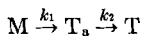
Sinfelt and associates (S6) for a 0.3% platinum on alumina catalyst. At these temperatures diffusional effects are much less important than at the usual reforming temperatures. Over the range of methylcyclohexane and hydrogen partial pressures investigated, 0.07 to 2.2 atm. and 1.1 to 4.1 atm., respectively, the reaction was found to be zero order with respect to hydrogen and nearly zero order with respect to methylcyclohexane (Table III). The kinetic data were found to obey a rate law of the form

$$r = \frac{k'bp_M}{1 + bp_M} \quad (1)$$

where k' and b are parameters which are functions of temperature. Data obtained on 1:1 blends of methylcyclohexane with either benzene or *m*-xylene indicated that the reaction was only slightly inhibited by aromatics.

In the interpretation of the kinetics, it was concluded that a mechanism involving adsorption equilibrium between methylcyclohexane in the gas phase and methylcyclohexane molecules adsorbed on platinum sites was not very likely. If Eq. (1) were interpreted on such a basis, then b would be an adsorption equilibrium constant. From the temperature dependence of b , one would calculate a heat of adsorption of 30 kcal./mole, which seems too high for adsorption of methylcyclohexane molecules as such. Furthermore, the small inhibition by aromatics casts doubt on such a picture, since the extent of adsorption of aromatics would be expected to be considerably greater than that of methylcyclohexane molecules at equilibrium, in view of the unsaturated nature of aromatics.

In view of the above considerations, it was proposed that adsorption equilibria are not established and that the small inhibiting effect of aromatics indicates that the rate of adsorption of aromatics is lower than that of methylcyclohexane. A simple kinetic scheme was proposed to account for the observed kinetics:



Here M and T represent methylcyclohexane and toluene in the gas phase, and T_a represents adsorbed toluene. The first step in the above reaction sequence represents the adsorption of methylcyclohexane with subsequent reaction to form toluene, while the second step is the desorption of toluene from the surface. Very likely the first step represents a series of steps involving partially dehydrogenated hydrocarbon molecules or radicals. However, at steady-state conditions the rates of the intermediate steps would all be equal, and the kinetic analysis is, therefore, not complicated by this factor. To account for the near zero-order behavior of the reaction, it was suggested that the active catalyst sites were heavily covered with

toluene. Assuming that coverage of the active sites by components other than toluene was very small, the following steady-state expression for the net rate of formation of adsorbed toluene was proposed

$$\frac{dT_a}{dt} = k_1 p_M (1 - \theta_T) - k_2 \theta_T = 0 \quad (2)$$

where θ_T represents the fraction of the active sites covered by toluene and p_M represents the methylcyclohexane partial pressure. The rate of desorption of toluene, and hence the rate of reaction, is given by

$$r = k_2 \theta_T \quad (3)$$

Solving Eq. (2) for θ_T and substituting in Eq. (3), the rate expression becomes

$$r = \frac{k_2 (k_1/k_2) p_M}{1 + (k_1/k_2) p_M} \quad (4)$$

which is of the form of Eq. (1) with $k' = k_2$ and $b = k_1/k_2$. From the temperature dependence of k' (or k_2), an activation energy of 33 kcal./mole was determined for the desorption of toluene from the surface. From the temperature dependence of b (or k_1/k_2), a difference of 30 kcal./mole between the activation energies of the first and second steps was found, so that the activation energy for adsorption of methylcyclohexane was 3 kcal./mole. A low activation energy for adsorption of methylcyclohexane does not appear unreasonable, in view of the observation that exchange of cyclohexane with deuterium over platinum takes place readily, even at room temperature (A1, F1).

At 315°C. the rate constant k_1 has a value of 7.0×10^{16} molecules/sec.-cm.²-atm. From the definition of k_1 , this represents the rate of adsorption of methylcyclohexane per cm.² of bare platinum surface at a methylcyclohexane partial pressure of 1 atm. From kinetic theory and statistical mechanics, one can calculate the number of molecules striking a unit area of surface per unit time with activation energy E_a . This is given by

$$r = \frac{1}{4} n \bar{c} \exp(-E_a/RT) \quad (5)$$

where n is the number of molecules per cm.³ and \bar{c} is the average velocity of the molecules in cm./sec., given by $(8RT/\pi M)^{1/2}$, where M is the molecular weight. At 315°C. and 1 atm. methylcyclohexane pressure, this expression gives a value of 18.6×10^{21} for r . This is over 10^6 times as high as the value of k_1 derived from the kinetic data, indicating that only about one out of a million methylcyclohexane molecules striking the surface with the required activation energy is adsorbed. Low "steric" factors such as this have been reported for other cases of activated adsorption (P1).

In their paper, the authors showed that the activation energy of 33

kcal./mole for the desorption step was in fair agreement with a calculation using absolute rate theory. According to absolute rate theory, the rate of desorption is given by

$$r = C_a \frac{kT}{h} \exp(-E/RT) \quad (6)$$

where C_a is the number of molecules adsorbed per unit surface, kT/h is a frequency factor, and E is the activation energy. Substituting an experimentally determined value of the rate for r , and assuming C_a is given simply by the number of platinum atoms per unit area of platinum surface (fully covered surface with one molecule adsorbed per platinum atom), a value of 37 kcal./mole is calculated for the activation energy E . This is in fair agreement with the value of 33 kcal./mole derived from the temperature dependence of k_2 .

Thus it appears that an interpretation not involving adsorption equilibria is reasonable in accounting for the observed kinetics of dehydrogenation of methylcyclohexane to toluene. However, some additional information, such as data on the heat of adsorption of toluene on supported platinum, would be desirable in establishing the correctness of this interpretation.

For purposes of comparison, it is of interest to consider the results of kinetic studies of the dehydrogenation of cyclohexane to benzene over certain other catalysts. Herington and Rideal (H6) studied the kinetics at 400–450°C. using a chromia-alumina catalyst containing 12% Cr_2O_3 . These authors concluded that cyclohexene was an intermediate in the reaction, so that desorption and readsorption of cyclohexene were essential

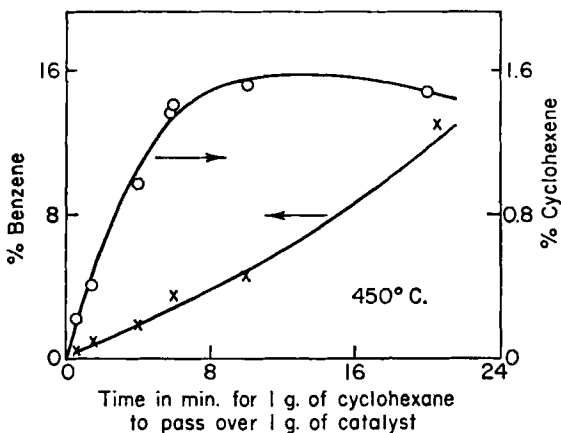


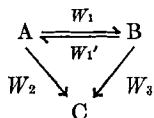
FIG. 3. Dehydrogenation of cyclohexane to cyclohexene and benzene over chromia-alumina (H6).

steps in the conversion to benzene. In the range of 5–10% conversion to benzene, a stationary concentration of cyclohexene was attained (Fig. 3). In the simplified consecutive reaction scheme,



where CH, CH[−], and Bz represent cyclohexane, cyclohexene, and benzene, respectively, the ratio of first-order rate constants (k_2/k_1) was found to be 55 at 450°C. The measured activation energy of 36 kcal./mole was attributed to the loss of the first two hydrogen atoms on the surface, i.e., to the formation of cyclohexene in the adsorbed state.

In a more recent study of the dehydrogenation of cyclohexane to benzene over a chromium oxide catalyst at 450°C., Balandin and co-workers (D1) concluded that benzene was formed by two routes. One of these, the so-called consecutive route, involves cyclohexene as a gas phase intermediate, while the other proceeds by a direct route in which intermediate products are not formed in the gas phase. It was concluded that the latter route played a larger role in the reaction than did the former. These conclusions were derived from experiments on mixtures of cyclohexane and C¹⁴-labeled cyclohexene, which made it possible to evaluate the individual rates W_1 , W_1' , W_2 , and W_3 in the reaction scheme



where A, B, and C refer to cyclohexane, cyclohexene, and benzene, respectively. In the case of a supported rhenium catalyst at 336°C., the formation of benzene was reported to take place almost completely via a direct route not involving gas phase cyclohexene as an intermediate. In line with this, our earlier discussion pointed out that gas phase intermediates do not appear to be involved in the dehydrogenation of methylcyclohexane to toluene over a platinum catalyst. According to Balandin and co-workers (D1), cyclohexene is rarely found in the products of dehydrogenation of cyclohexane over metal catalysts.

For the cases where gas phase cyclohexenes do not appear to be intermediates, the question arises as to the nature of the surface reaction. Thus, does cyclohexane simultaneously lose six hydrogen atoms via the sextet mechanism (T3) originally proposed by Balandin in 1929, or does the reaction take place in a stepwise fashion without desorption of intermediate products? According to the sextet theory, the active catalyst unit is an aggregate of metal atoms which must be spaced within certain definite limits consistent with the geometry of the cyclohexane ring. While there

is much experimental evidence attesting to the importance of geometrical factors in the catalytic dehydrogenation of six-membered rings (T3), certain difficulties are encountered with a sextet mechanism. For example, in the exchange of deuterium with cyclohexane over platinum films (A1), the primary product of exchange is $C_6H_{11}D$ rather than $C_6H_6D_6$. The latter should have been the main primary product if the sextet mechanism predominated in the chemisorption of cyclohexane. In addition, for the very active supported metal catalysts such as platinum on alumina, where the amount of metal is low (0.5% or less) and the degree of dispersion of the metal is extremely high, it is questionable whether the metal crystallites could accommodate the cyclohexane ring in the manner envisioned in the sextet mechanism (S6). Therefore, it seems probable that the dehydrogenation of cyclohexanes on such surfaces takes place in a stepwise manner involving intermediate surface species of varying degrees of dehydrogenation, despite the fact that these species may not appear in the gas phase.

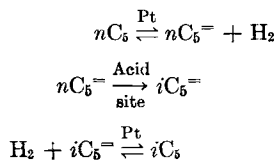
B. ISOMERIZATION REACTIONS

A study of the kinetics of isomerization of *n*-pentane at 372°C. over a platinum on alumina catalyst (0.3% platinum) has been reported by Sinfelt *et al.* (S4). The rate measurements were made in a flow system at low conversion levels (4–18%). The *n*-pentane was passed over the catalyst in the presence of hydrogen at total pressures ranging from 7.7 to 27.7 atm. and at hydrogen to *n*-pentane ratios varying from 1.4 to 18. Over this range of conditions the rate was found to be independent of total pressure and to increase with increasing *n*-pentane to hydrogen ratio (Fig. 4). The rate data were correlated by an expression of the form

$$r = k \left(\frac{p_{nC_5}}{p_{H_2}} \right)^n \quad (7)$$

where *r* represents the rate in gram moles isomerized per hour per gram of catalyst and the parameters *k* and *n* have the values 0.040 and 0.5, respectively, for the particular catalyst used in the study.

The kinetic data were interpreted in terms of a mechanism involving *n*-pentene intermediates:



According to this mechanism the *n*-pentane dehydrogenates to *n*-pentenes on platinum sites. The *n*-pentenes are then adsorbed on acid sites, where

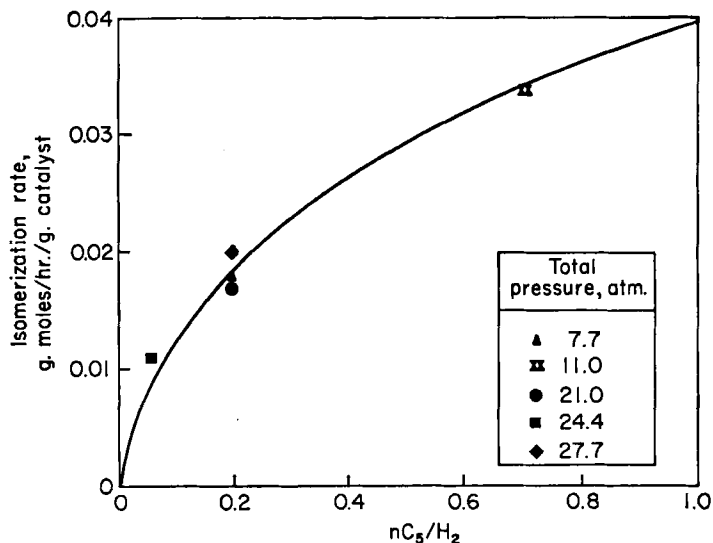
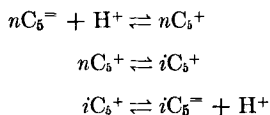


FIG. 4. Effect of nC_5/H_2 ratio on nC_5 isomerization at 372°C. over platinum-alumina catalyst (S4).

they are isomerized to isopentenes. The latter are then hydrogenated to isopentane on platinum sites, thus completing the reaction. The isomerization step on the acid sites presumably takes place via a carbonium ion mechanism (K3):



The initial formation of the ion is pictured as taking place by protonation of the n -pentenes. The n -pentyl ion then rearranges to an isopentyl ion, which in turn can eliminate a proton to form isopentenes.

At the conditions of the study, it was postulated that the isomerization of the n -pentenes on the acid sites was the rate-limiting step, so that the rate is given by

$$r = k'[nC_5^-] \quad (8)$$

where k' is a rate constant and $[nC_5^-]$ represents the concentration of n -pentenes on the acid sites. Assuming that an equilibrium is effectively established between n -pentenes, n -pentane, and hydrogen in the initial dehydrogenation step, the partial pressure of n -pentenes is given by

$$p_{nC_5^-} = K \frac{p_{nC_5}}{p_{H_2}} \quad (9)$$

where K is an equilibrium constant. If we further assume that an adsorption equilibrium is established between n -pentenes in the gas phase and on the acid sites and that the equilibrium can be expressed simply by

$$[nC_5^-] = bp_{nC_5}^n \quad (10)$$

the rate expression becomes, after substituting (9) and (10) in (8),

$$r = k' b K^n \left(\frac{p_{nC_5}}{p_{H_2}} \right)^n = k \left(\frac{p_{nC_5}}{p_{H_2}} \right)^n \quad (11)$$

which is identical with Eq. (7), derived from the data.

Data obtained on the rate of skeletal isomerization of 1-pentene over a sample of catalyst containing only the acid function (no platinum) provided additional strong support for the proposed mechanism. This can be seen quite simply by referring to Fig. 5, in which the circles and the

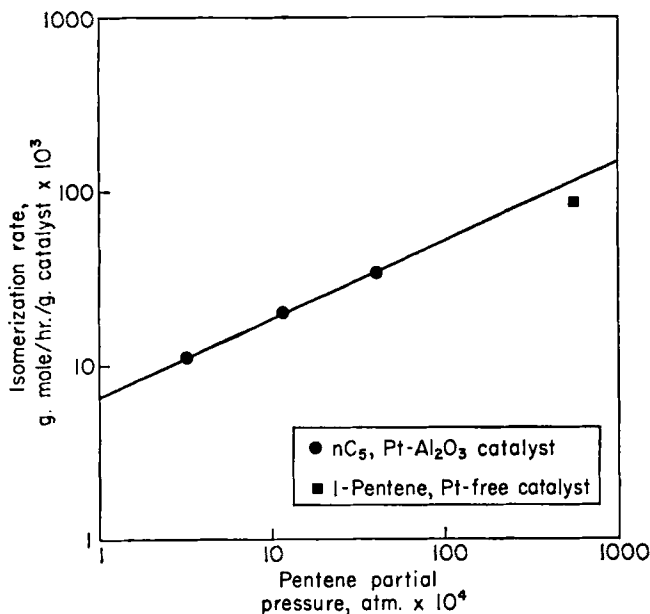


FIG. 5. Isomerization rate versus pentene partial pressure (S4). Comparison of n -pentane isomerization rate over platinum-alumina catalyst with the rate of skeletal isomerization of 1-pentene over the platinum-free catalyst; 372°C.

line represent the rate of isomerization of n -pentane over the bifunctional platinum catalyst as a function of the calculated equilibrium partial pressure of n -pentenes. If the mechanism proposed in the preceding paragraphs applies, then the rate of isomerization of n -pentenes over a sample of catalyst containing only the acid function, when plotted as a function of the partial pressure of the reactant n -pentenes, should fall along the same

line. The result of a run on 1-pentene over the acidic part of the catalyst alone is shown by the square point on the plot. The observed rate of skeletal isomerization of the 1-pentene is seen to fall within about 20 to 25% of the value indicated by the line through the *n*-pentane rate data. Whether one starts with 1-pentene or 2-pentene in this type of experiment would be expected to make little difference, since the rate of double-bond migration is fast compared to the rate of skeletal isomerization of olefins (C8).

Thus, at 372°C. and over the range of pressures and hydrogen to *n*-pentane ratios covered in the investigation, it appears that the proposed mechanism can account in large part for the observed kinetic data. However, Starnes and Zabor (S8) have proposed an alternative mechanism, based on their studies of *n*-pentane isomerization over platinum-alumina-halogen catalysts. They postulate that the paraffin is adsorbed on platinum sites with dissociation of a hydrogen atom, followed by polarization of the adsorbed species.



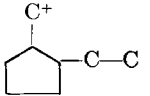
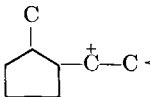
The authors suggest that the support confers Lewis acid properties on the platinum, which in turn accounts for the polarization of the adsorbed alkyl group to a carbonium ion type of structure. The latter then undergoes the usual carbonium ion reactions. The mechanism involves a single type of catalytic site instead of two different types of sites, as envisioned in the previously discussed mechanism. While this type of mechanism may play a role in paraffin isomerization, there seems to be little reason to discount the mechanism involving separate dehydrogenation and acidic centers, as can be seen from the considerable evidence summarized in this review. The objections raised by Starnes and Zabor to the two-site mechanism are based on several experimental observations: (a) When *n*-pentane was isomerized over a mixture of pellets of Pt-alumina and HF-promoted alumina, the rate increased with time on stream, coinciding with transfer of the fluoride to the Pt-containing pellets. (b) Although the olefin content of the products remained constant at the equilibrium level, the rate suddenly increased about 7- or 8-fold when the platinum content of the catalyst was increased from 0.3 to 0.4%. (c) The rate was proportional to the olefin partial pressure to a power somewhat lower than unity. These objections have been answered by Keulemans and Schuit (K2), who suggest that (a) and (b) do not refute a two-site mechanism, but simply reflect diffusion limitations in the experiments of Starnes and Zabor. Furthermore, other data on the effect of platinum content on the rate of paraffin isomerization (S4, S5) do not agree at all with those of Starnes

and Zabor, but rather indicate the rate to be essentially independent of platinum content above 0.1% Pt. Regarding objection (c), it is not at all clear why the rate should have to be proportional to the first power of the olefin (*n*-pentene) partial pressure for the two-site mechanism to be valid. In the study of Sinfelt *et al.* (S4) discussed at the beginning of this section, a two-site mechanism for *n*-pentane isomerization appears to be quite consistent with a square root dependence of the isomerization rate on olefin partial pressure.

Up to this point, we have not said much about the nature of the rearrangement of olefin intermediates on acidic sites, except to indicate that a carbonium ion mechanism is likely involved. Formation of the ion presumably takes place via reaction of the olefin with a proton from the catalyst surface. Keulemans and Voge (K3), in their study of the dehydroisomerization of alkylcyclopentanes to aromatics at 350°C., assumed that ion formation was fast relative to the subsequent skeletal rearrangement of the ions. Relative rates of formation of various aromatics were found to agree quite well with predicted values obtained by simply multiplying relative carbonium ion stabilities by a statistical factor which accounts for the number of ways in which a certain ion can rearrange to give a particular product. The relative stabilities, and hence abundances of primary, secondary, and tertiary carbonium ions, were taken to be 1:16:32. In predicting actual conversions of alkylcyclopentanes to the various aromatics, an empirical rate factor of 0.684 was chosen to fit the average total aromatics formed from the various trimethylcyclopentanes. The same empirical rate factor was then used for all the cyclopentanes; i.e., the specific rate of isomerization was assumed to be constant, so that differences

TABLE IV

CALCULATION OF CONVERSION OF 1-METHYL-2-ETHYLCYCLOPENTANE TO C₈ AROMATIC ISOMERS OVER PLATINUM-ALUMINA-HALOGEN CATALYST (K3)^a

Ion	Product	Relative amount of ion	Statistical factor	Empirical factor	Yield (wt. %)
	Ethylbenzene	1	2	0.684	1.4
	<i>o</i> -Xylene	16	1	0.684	10.9
	<i>m</i> -Xylene	16	1	0.684	10.9

^a For same conditions as shown in Table V.

TABLE V
CONVERSION OF CYCLOPENTANES OVER PLATINUM-ALUMINA-HALOGEN CATALYST (K3)^a

Reactant	Product (wt. %) ^b									
	Benzene		Toluene		Ethylbenzene		<i>m</i> - + <i>p</i> -Xylene		<i>o</i> -Xylene	
	Obs.	Calc.	Obs.	Calc.	Obs.	Calc.	Obs.	Calc.	Obs.	Calc.
Methylcyclopentane	2.6	1.4								
C ₇ Cyclopentanes										
Ethyl			25.0	21.9						
1,1-Dimethyl			2.0	2.7						
1- <i>cis</i> -2-Dimethyl			2.9	2.7						
1- <i>trans</i> -2-Dimethyl			3.9	2.7						
1- <i>cis</i> -3-Dimethyl			1.4	2.7						
1- <i>trans</i> -3-Dimethyl			1.5	2.7						
C ₈ Cyclopentanes										
<i>n</i> -Propyl					26.4	21.9	0	0	0	0
Isopropyl					0	0	0	0	28.0	43.8
1-Methyl-1-ethyl					1.1	1.4	3.4	0	15.6	21.9
1-Methyl- <i>cis</i> -2-ethyl					2.5	1.4	8.5	10.9	7.6	10.9
1-Methyl- <i>trans</i> -2-ethyl					1.7	1.4	9.1	10.9	7.5	10.9
1-Methyl- <i>cis</i> -3-ethyl					0.2	1.4	16.4	21.9	0	0
1-Methyl- <i>trans</i> -3-ethyl					0.3	1.4	29.4	21.9	0	0
1,1,2-Trimethyl					0	0	3.4	1.4	0.9	2.7
1,1,3-Trimethyl					0	0	2.4	2.7	0.6	1.4
1- <i>cis</i> -2- <i>cis</i> -3-Trimethyl					0	0	2.8	1.4	1.9	2.7
1- <i>cis</i> -2- <i>trans</i> -3-Trimethyl					0	0	2.9	1.4	2.0	2.7
1- <i>trans</i> -2- <i>cis</i> -3-Trimethyl					0	0	2.1	1.4	1.2	2.7
1- <i>cis</i> -2- <i>trans</i> -4-Trimethyl					0	0	3.5	2.7	0.6	1.4
1- <i>trans</i> -2- <i>cis</i> -4-Trimethyl					0	0	3.6	2.7	1.0	1.4

^a Hydrocarbons fed to reactor as 3-mg. shots (pulse-type operation) in a stream of hydrogen carrier gas.

^b Conditions: 350°C., total pressure = 1 atm., catalyst charge = 1 g., carrier gas rate = 3 liters/hr.

in reactivities of various cyclopentanes were interpreted strictly in terms of carbonium ion stabilities and statistical factors. The method of calculation is illustrated in Table IV for 1-methyl-2-ethylcyclopentane, in which case two different ions can produce aromatics. In Table V predicted conversions are compared with actual conversions for various alkylcyclopentanes at 350°C. Conversions were assumed to be proportional to rates, which, according to the authors, is a good assumption for conversions below 30%. Agreement between observed and predicted conversions to the various aromatics is quite good considering the simplifying assumptions made by the authors in their predictions of relative rates.

C. FURTHER CONSIDERATIONS OF THE ROLE OF HYDROGEN IN ISOMERIZATION KINETICS

In Section IV, B it was pointed out that the rate of isomerization of *n*-pentane decreased with increasing hydrogen pressure over a reasonably wide range of conditions. However, when the range of conditions is extended still further, the nature of the effect of hydrogen changes. This has been observed for both the isomerization of *n*-heptane to methyl hexanes (R3) and the isomerization-dehydroisomerization of methylcyclopentane to form cyclohexane and benzene (S1) over similar platinum on alumina catalysts. In both of these cases it has been found that reaction does not take place in the complete absence of hydrogen, as indicated in Fig. 6 for *n*-heptane and in Table VI for methylcyclopentane. The data at zero

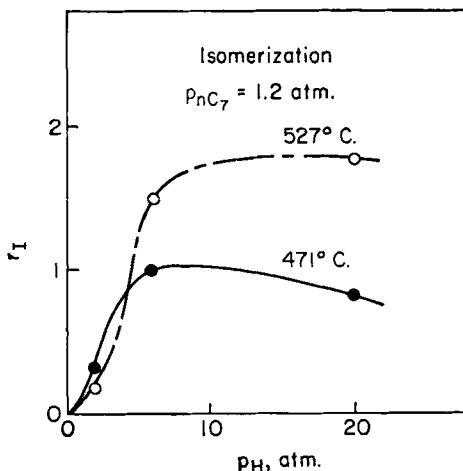


FIG. 6. Effect of hydrogen pressure on rate of isomerization of *n*-heptane over platinum-alumina catalyst (R3). The rate r_I is relative to the rate of isomerization at 471°C., $p_H = 5.8 \text{ atm.}$

TABLE VI
SUMMARY OF RATE DATA ON METHYLCYCLOPENTANE
CONVERSION OVER Pt-Al₂O₃ (S1)

Temp. (°C.)	p_M^a	p_H^b	r_t^c
427	1.0	0 ^d	0
427	0.1	2.0	0.0066
427	0.33	2.0	0.0051
427	1.0	2.0	0.0048
427	1.0	6.0	0.0051
427	1.0	20.0	0.0022
471	1.0	0 ^d	0
471	0.1	2.0	0.0077
471	0.33	2.0	0.0061
471	1.0	2.0	0.0028
471	1.0	6.0	0.019
471	1.0	20.0	0.011
471	10.0	20.0	0.036

^a Methylcyclopentane partial pressure, atm.

^b Hydrogen partial pressure, atm.

^c Rate, gram-mole per hour per gram of catalyst.

^d N₂ substituted for H₂.

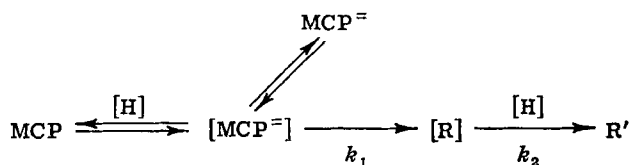
hydrogen pressure were obtained by simply substituting nitrogen for hydrogen. In the presence of hydrogen the reactions take place readily, and the rates are found to increase with increasing hydrogen pressure up to a maximum value, beyond which the rates decrease with further increase in hydrogen pressure.

The change in the nature of the hydrogen effect on the rates has been interpreted as follows. In the absence of hydrogen, or at low hydrogen pressures, the platinum sites become heavily covered with hydrogen-deficient hydrocarbon residues. As a result, the reaction rates are limited by the dehydrogenation activity of the catalyst, i.e., the rate of formation of intermediate olefins. The role of hydrogen is then one of keeping the platinum sites free of surface residues. The extent of coverage of the surface by such residues decreases with hydrogen pressure, thus accounting for the beneficial effect of hydrogen pressure on the over-all rate of isomerization. At sufficiently high hydrogen pressures, however, coverage of platinum sites by surface residues ceases to be a limiting factor, and the rate does not continue to increase with increasing hydrogen pressure. This means that the formation of intermediate olefins is no longer the rate-controlling step, and the over-all reaction becomes limited by the

isomerization of olefins on the acidic centers of the catalyst. The decrease in the rate of isomerization with further increase in hydrogen pressure is attributed to the effect of hydrogen pressure in limiting the concentration of olefin intermediates attainable at equilibrium, as discussed previously for *n*-pentane isomerization.

The suggestion that the dehydrogenation activity of the catalyst limits the isomerization reaction at low hydrogen pressures is supported by data on methylcyclohexane dehydrogenation to toluene at 471°C. (S1), which showed that in the complete absence of hydrogen the conversion was several hundred-fold lower than at 10 atm. hydrogen pressure. Since dehydrogenation of methylcyclohexane requires only the platinum centers of the catalyst, the suggestion that the effect of hydrogen on isomerization at low pressures is associated with the platinum appears quite plausible. That the effect is not associated with acid centers is supported by the finding that variation of hydrogen pressure has little effect on the rate of skeletal isomerization of 2-pentene over an acidic alumina (R2). Furthermore, studies on the dissociative chemisorption of hydrocarbons, such as cyclohexane and cyclopentane, over a variety of metals have given direct evidence for the formation of hydrogen-deficient surface residues, and for their removal by reaction with hydrogen (G1). Studies on the adsorption of benzene on supported platinum catalyst also furnish evidence for the ability of hydrogen to clean up platinum surfaces (P5).

It is of interest to consider the kinetics of isomerization at low hydrogen pressures in more detail. In the case of isomerization-dehydroisomerization of methylcyclopentane at low hydrogen pressures, it has been proposed (S1) that the rate-limiting step is the formation of intermediate methylcyclopentenenes via the reaction scheme:



in which the brackets refer to species on the surface, MCP refers to methylcyclopentane, MCP= to methylcyclopentenenes, and [R] represents the surface residue. According to this scheme, methylcyclopentane dehydrogenates on platinum sites to form methylcyclopentenenes, which in turn can either desorb or undergo further dehydrogenation and polymerization reactions to form the residue [R]. The surface residue is continuously being removed by reaction with adsorbed hydrogen to form gaseous hydrocarbons R'. Making the simplifying assumption that a steady-state concentration of surface residue is approached, one can write

$$\frac{d\theta_R}{dt} = k_1\theta_{M'} - k_2\theta_R\theta_H = 0 \quad (12)$$

where $\theta_{M'}$, θ_R , and θ_H represent coverage of platinum sites by methylcyclopentenes, residue, and hydrogen, respectively. The term $k_1\theta_{M'}$ represents the rate of formation of residue from adsorbed methylcyclopentenes, whereas the term $k_2\theta_R\theta_H$ represents the rate of removal by reaction with hydrogen. The rate of removal has been taken as proportional to the first power of θ_H , in the absence of more detailed knowledge of the nature of the removal reaction. At sufficiently low hydrogen pressures θ_H becomes very small, and the platinum surface is almost completely covered by surface residues, i.e., θ_R approaches unity. Under these conditions $\theta_{M'}$ can be approximated by

$$\theta_{M'} = (k_2/k_1)\theta_H \quad (13)$$

The over-all rate of isomerization-dehydroisomerization is determined by the rate of formation of methylcyclopentene intermediates in the gas phase, as given by

$$r = k'\theta_{M'} \quad (14)$$

where k' is a rate constant for desorption. Since θ_H increases with hydrogen pressure, $\theta_{M'}$ will also increase, thus accounting for the beneficial effect of hydrogen pressure on the rate. Also, since methylcyclopentane and hydrogen may compete for active sites, θ_H would be expected to decrease when methylcyclopentane pressure is increased at a constant hydrogen pressure. This would mean, according to Eq. (13), that $\theta_{M'}$, and hence the rate of reaction, would decrease. A decrease in reaction rate with increasing methylcyclopentane pressure was actually observed in data obtained at 2 atm. hydrogen pressure.

D. DEHYDROCYCLIZATION OF PARAFFINS

The formation of aromatics by the catalytic dehydrocyclization of paraffins with chains of six or more carbon atoms has been known for some time. Certain oxides of the 5th and 6th subgroups of the periodic table, such as chromia and molybdena, were shown early to be particularly effective catalysts for the reaction. Consequently, most of the reported studies of the kinetics and mechanism of the reaction have been carried out using these catalysts (P6, H4, H5). Since the available data on the kinetics of dehydrocyclization over oxide catalysts have been reviewed by Steiner (S9) in 1956, only a brief summary of the work will be made here, primarily for the purpose of orientation. The relatively few kinetic data which have been reported for dehydrocyclization over the bifunctional platinum on acidic oxide catalysts will be discussed subsequent to this.

One of the first reported investigations of the kinetics of dehydrocyclization is that of Pitkethly and Steiner (P6), who studied the conversion of *n*-heptane to toluene over a chromia-alumina catalyst at temperatures in the vicinity of 475°C. The data obtained by these investigators suggested that *n*-heptene was an intermediate in the reaction. Thus, it was observed that at low contact times the concentration of olefins increased much more rapidly with contact time than did the corresponding concentration of aromatics (Fig. 7). After a certain contact

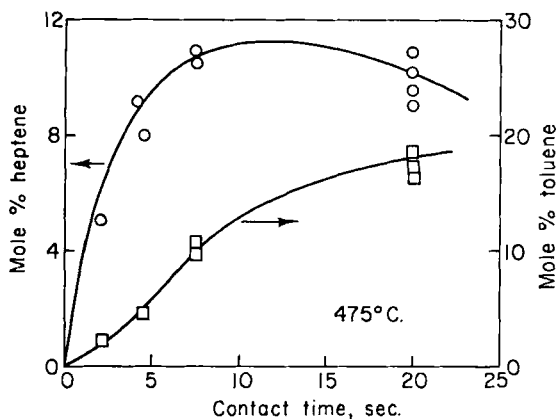
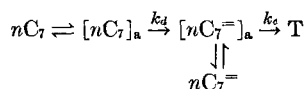


FIG. 7. Conversion of *n*-heptane to heptene and toluene over chromia-alumina (P6).

time, the concentration of olefins passed through a maximum, beyond which the concentration fell slowly while the concentration of aromatics continued to rise. The data were interpreted in terms of the reaction scheme



where nC_7 , $nC_7^=$, and T represent *n*-heptane, *n*-heptene, and toluene, respectively, and the brackets represent adsorbed species. The parameters k_d and k_c are rate constants for the successive dehydrogenation and cyclization steps. A kinetic analysis of the data has been made (S9, T2) assuming that heptane and heptene in the gas phase are in equilibrium, respectively, with heptane and heptene on the surface. The additional assumption was made that heptene was strongly adsorbed relative to heptane. At stationary state conditions, the rate of formation of *n*-heptene from *n*-heptane is equal to the rate of conversion of *n*-heptene to toluene:

$$\frac{k_d A p}{1 + A_0 p_0} = \frac{k_c A_0 p_0}{1 + A_0 p_0} \quad (15)$$

where A and A_0 are adsorption equilibrium constants and p and p_0 are partial pressures of n -heptane and n -heptene, respectively. Solving Eq. (15) for A_0 , the rate r of formation of toluene can be written

$$r = \frac{k_c A_0 p_0}{1 + A_0 p_0} = \frac{k_d A p}{1 + (k_d/k_c) A p} \quad (16)$$

This rate equation satisfactorily accounts for the observed kinetic data, including the 0.6 order of reaction with respect to n -heptane.

At the experimental conditions studied, the value of k_c was found to be about fourfold greater than k_d , indicating that the cyclization of olefins should proceed more readily than that of the corresponding paraffins. Experiments on hexene-1, heptene-1, and heptene-2 bear this out (H9). However, the position of the double bond can have an appreciable effect on the rate of cyclization. Thus hexene-2 cyclizes only about half as fast as hexene-1, and heptene-3 cyclizes at a much lower rate than heptene-1 or heptene-2 (P8). As a result of these findings, Twigg proposed a mechanism for cyclization involving two-point adsorption with opening of the double bond (T4), as illustrated in Fig. 8. It was assumed that ring closure

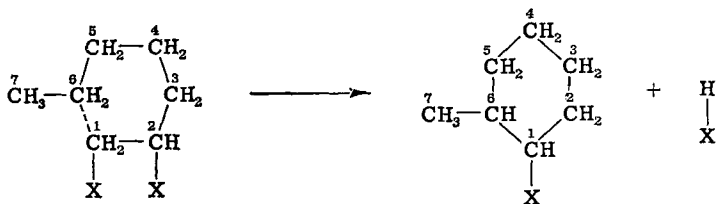


FIG. 8. Twigg's mechanism of cyclization (T4). X = catalyst site.

took place at a carbon atom bonded to the catalyst. In the case of n -heptane, cyclization of the intermediate olefin then requires that adsorption take place at the 1-2 or 2-3 positions. Heptene-3 would thus have to undergo a double bond shift to heptene-1 or heptene-2 prior to cyclization. Such a shift might proceed through a half-hydrogenated state, as suggested by Twigg (T5) for conversion of butene-1 to butene-2 over nickel catalysts.

The work of Herington and Rideal (H4) showed that a good prediction of the relative rates of cyclization of various paraffins could be made based on considerations of the number of ways in which ring closure could be effected, assuming that cyclization involves two-point adsorption in the manner illustrated in Fig. 8. For example, in the dehydrocyclization of n -hexane, five two-point contacts with the surface are possible, but only two can lead to formation of a six-membered ring. By assuming the cyclization rate constant to be given by

$$k_c = \text{constant} \times P \quad (17)$$

where P is the probability of cyclization, e.g., $2/5$ in the case of n -hexane, and taking the constant to be equal to 0.28 at 465°C ., Herington and Rideal calculated conversions to aromatics for a series of hydrocarbons and compared them with the data of Hoog *et al.* (H9). The agreement between predicted and observed values, as shown in Table VII, is quite

TABLE VII
VARIATION OF AROMATIC YIELDS FROM DIFFERENT PARAFFINS
OVER CHROMIA-ALUMINA^a (H4, S9)

Paraffin	P	% Conversion to aromatics	
		Obs.	Calc.
n -Pentane	0	3	0
n -Hexane	0.40	20	23
2-Methylpentane	0	5	0
n -Heptane	0.66	36	35
2-Methylhexane	0.66	31	35
n -Octane	0.84	46	42
3-Methylheptane	0.84	35	42
2,5-Dimethylhexane	1.14	52	52
2,2,4-Trimethylpentane	0	3	0
n -Nonane	1.00	58	48

^a 465°C ., contact time 18–24 sec.

good. It was also demonstrated that the relative amounts of aromatic isomers formed from a given paraffin were generally well predicted, although in certain cases the situation appeared to be complicated by an isomerization step occurring simultaneously with ring closure.

As a result of the studies discussed above, a reasonably consistent picture of the kinetics and mechanism of the dehydrocyclization reaction over oxide catalysts has evolved. However, as pointed out earlier in this section, relatively few kinetic data have been reported for dehydrocyclization over platinum-alumina reforming-type catalysts. The data which have been reported include those of Hettinger and co-workers (H7), who studied the dehydrocyclization of n -heptane over platinum catalysts. These investigators found that the rate of dehydrocyclization decreased with increasing total pressure at a constant hydrogen-to-hydrocarbon ratio (Fig. 9). They also reported that the extent of dehydrocyclization was substantially greater for n -nonane than for n -heptane, which is consistent with the results obtained on oxide catalysts. In a later study of the kinetics

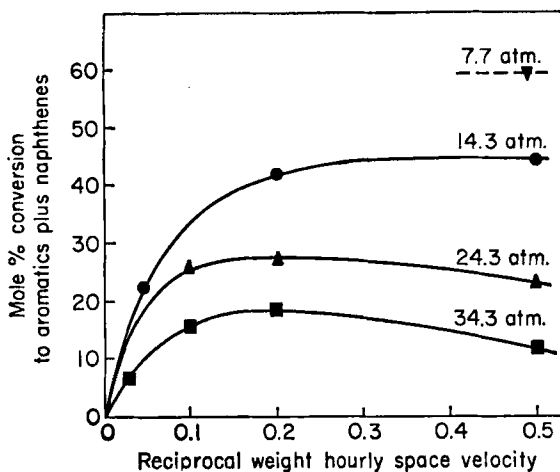


FIG. 9. Effect of total pressure on dehydrocyclization of *n*-heptane over platinum-alumina catalyst (H7). Conditions: 496°C., $H_2/HC = 5/1$.

of *n*-heptane dehydrocyclization over a platinum on alumina catalyst, Rohrer *et al.* (R3) reported initial rate data over a wide range of hydrogen pressures, while maintaining the *n*-heptane partial pressure constant. In the complete absence of hydrogen, no dehydrocyclization was detected. In the presence of hydrogen the rate was found to increase with increasing

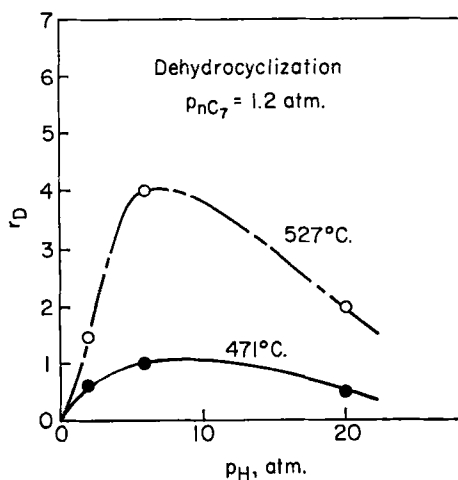
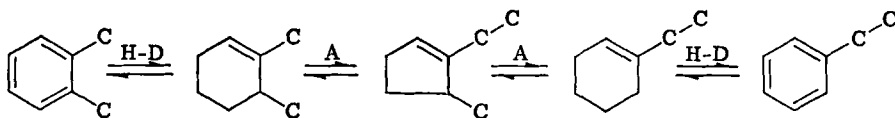


FIG. 10. Effect of hydrogen pressure on rate of dehydrocyclization of *n*-heptane over platinum-alumina catalyst (R3). The rate r_D is relative to the rate of dehydrocyclization at 471°C., $p_H = 5.8$ atm.

hydrogen pressure up to a maximum value, beyond which the rate decreased with further increase in hydrogen pressure (Fig. 10). This behavior is similar to that observed for isomerization and is interpreted in much the same way: The dehydrocyclization reaction involves a preliminary dehydrogenation step prior to ring closure. At sufficiently high hydrogen pressures, where coverage of platinum by carbonaceous residues is not a limiting factor, increasing hydrogen pressure serves to suppress the dehydrogenation step and hence to decrease the rate of dehydrocyclization. However, at low hydrogen pressures (below about 6 atm. at 471 to 527°C.) background reactions involving extensive dehydrogenation and polymerization become important. These reactions lead to extensive coverage of the platinum by carbonaceous residues. The limiting factor in the reaction then becomes the removal of the residues by reaction with hydrogen, thus accounting for the beneficial effect of hydrogen pressure on the rate.

E. MISCELLANEOUS RELATED REACTIONS

The reactions of the various xylenes and ethylbenzene have been studied by Pitts and associates (P7). It was found that isomerization reactions among the three xylenes were catalyzed by acidic catalysts, but that interconversions between the xylenes and ethylbenzene required the presence of a hydrogenation-dehydrogenation component. Furthermore, it was found that the conversion of xylenes to ethylbenzene increased with decreasing temperature. Since lower temperatures are more favorable for hydrogenation, it has been suggested that the reaction proceeds by a sequence of steps such as the following (P7, W3):



In the above diagram, H-D refers to hydrogenation-dehydrogenation centers and A to acidic centers on the catalyst. The reaction sequence involves successive ring contraction and expansion steps, similar to the mechanism proposed by Pines and Shaw (P4) to account for transfer of tagged carbon from the side chain to the ring when ethylcyclohexane was contacted with a nickel-silica-alumina catalyst.

Another reaction which has been studied over a bifunctional catalyst is the hydrogenolysis of benzene and toluene over platinum-alumina, which has been reported by Rohrer and Sinfelt (R1). The reaction was studied over a temperature range of 471 to 527°C. and hydrogen pressure range of 9 to 26 atm. It was found that the rate of formation of the hydrogenolysis products (C_6 and lighter paraffins) was essentially independent

of temperature but was greatly increased by increasing the hydrogen pressure. To account for these observations, it was suggested that the hydrogenolysis involved a hydrogenation step prior to rupture of the ring. It was then suggested that the concentration of hydrogenated intermediates approached an equilibrium value which would be expected to decrease with increasing temperature, thus offsetting any increase in the rate constant for the rupture of the ring and accounting for the independence of the over-all rate on temperature. Since hydrogen pressure would have a strong effect on the equilibrium concentration of hydrogenated intermediates, the large effect of hydrogen pressure on the over-all rate is also readily understood. The bifunctional nature of the catalyst enters into the reaction, in that the initial hydrogenation step would be expected to take place on platinum centers, while the subsequent ring splitting could also involve acidic centers of the catalyst.

Studies using bifunctional catalysts for exchange reactions have also been reported. Myers *et al.* (M4) have investigated the exchange of deuterium between deuterobutane and butane over platinum-acidic oxide catalysts. They concluded that the rate of exchange, while primarily a function of the hydrogenation-dehydrogenation activity of the catalyst, was also dependent to some extent on the acidic activity. Weisz (W3) suggests that direct exchange between olefin intermediates reacting on acidic centers may contribute to the over-all exchange.

Bifunctional catalysis has been shown to play an interesting role in the catalytic conversion of cumene. Thus, Weisz and Prater (W4) found that the incorporation of platinum into a silica-alumina catalyst had a striking effect on the composition of the reaction products. In the absence of platinum, cumene decomposed over silica-alumina to form benzene and propylene. In the presence of platinum, however, an appreciable part of the over-all decomposition resulted in the formation of methylstyrene and hydrogen, although the rate of total disappearance of cumene was essentially unchanged. Thus, the authors indicated that the results could not be explained on the basis of simple additivity of products from the separate catalyst functions. Additional experiments comparing results obtained on mechanical mixtures of 5- μ particles of silica-alumina and platinum-alumina with results on the individual catalysts also indicated that a simple additivity effect was not obtained (W3). The authors therefore proposed that cumene cracking over silica-alumina is accompanied by the formation of a very small amount of unidentified intermediate "B" in equilibrium with cumene on the catalyst. According to the authors, platinum centers catalyze the dehydrogenation of this species to methylstyrene, and since the equilibrium between the intermediate B and adsorbed cumene is readily maintained, this additional reaction path is an effective

drain on the cumene. Weisz (W3) concludes from this example that the mixed catalyst technique offers a powerful tool for detecting the possible participation in a reaction of species which are present in too low a concentration to be detected by available analytical methods.

V. Conclusion

Studies of the mechanisms and kinetics of reactions over the common bifunctional reforming-type catalysts have led to a simple mechanistic picture in which dehydrogenation and acidic components act as separate entities. This picture gives a good explanation of most of the phenomena observed with such catalysts. As a result of its application in catalytic reforming, bifunctional catalysis has become an important branch of the over-all field of catalysis. It is probable that bifunctional catalysis is more widespread than has commonly been realized, since certain supposedly monofunctional catalysts actually appear to be bifunctional in nature (C7). For example, unsupported transition metal oxides such as Cr_2O_3 or MoO_3 , which have generally been considered to be hydrogenation-dehydrogenation catalysts, also appear to have definite acidic properties. Thus, the surfaces of these oxides, and also WS_2 , have sites of both the acid and the hydrogenation-dehydrogenation type. While these substances are inferior bifunctional catalysts in comparison with the two-component metal plus acidic oxide catalyst systems, it is striking that a single compound possesses the two distinctly different types of sites at its surface. Thus, one-component catalysts may exhibit bifunctional behavior.

The possibilities of additional applications, other than catalytic reforming, of the ideas of bifunctional catalysis would seem to be good. In all likelihood, bifunctional-type catalysts will find many new uses in the future.

Nomenclature

A, A_0	Adsorption equilibrium constants for <i>n</i> -heptane and <i>n</i> -heptene, respectively	\AA	Angstrom unit, 10^{-8} cm.
A	Acidic center on catalyst	b	Temperature-dependent parameter in observed rate law for methylcyclohexane dehydrogenation over $\text{Pt}/\text{Al}_2\text{O}_3$ catalyst
A, B, C	Reactants or intermediates in a reaction sequence	b	Proportionality constant in Freundlich adsorption expression
A, B, C, D	Symbols representing different catalyst-temperature combinations in Fig. 2	Bz	Benzene
		\bar{c}	Average molecular velocity, cm./sec.

C_a	Concentration of adsorbed species, molecules/cm. ²	n	Exponent in reaction rate expression
CH, CH ⁻	Cyclohexane, cyclohexene	nC_5, nC_5^-	<i>n</i> -Pentane, <i>n</i> -pentenes
E, E_a	Activation energy, kcal./mole	nC_7, nC_7^-	<i>n</i> -Heptane, <i>n</i> -heptenes
h	Planck's constant, 6.62×10^{-27} erg-sec.	nC_5^+	<i>n</i> -Pentyl carbonium ion
H	Hydrogen atom	p	Partial pressure
H ⁺	Proton	P	Probability of cyclization
H-D	Hydrogenation-dehydrogenation centers	r	Reaction rate, g.-mole/hr./g. of catalyst
ΔH_R	Heat of reaction, kcal./mole	R	Gas constant, 8.31×10^7 erg/°K.
iC_5, iC_5^-	Isopentane, isopentenes	[R]	Concentration of hydrocarbon residues on surface
iC_5^+	isopentyl carbonium ion	R'	Products of removal of hydrocarbon residues from surface
k	Boltzmann constant, 1.38×10^{-16} erg/°K	t	Time
k, k'	Reaction rate constants, g.-mole/hr./g. catalyst	T	Absolute temperature, °K.
k_1, k_2	Rate constants of consecutive reaction steps	T, T _a	Toluene, adsorbed toluene
K	Equilibrium constant	W_1, W_1', W_2, W_3	Rates of individual reaction steps in the reaction sequence leading from cyclohexane to benzene
M	Molecular weight	X	Catalyst site
M	Methylcyclohexane		
MCP, MCP ⁻	Methylcyclopentane, methylcyclopentenes		
n	Molecular concentration, molecules/cm. ³		

GREEK LETTERS

θ	Fraction of active catalyst surface covered	μ	Micron, 10^{-6} m.
----------	---	-------	----------------------

SUBSCRIPTS

1, 2, 3	Successive steps in reaction sequence	I	Isomerization or isomerization-dehydroisomerization
a	Adsorbed	M	Methylcyclohexane or methylcyclopentane
a	Activation (when used as subscript for E)	M'	Methylcyclopentenes
c	Cyclization	nC_5, nC_7	<i>n</i> -Pentane, <i>n</i> -heptane
d	Dehydrogenation	nC_5^-	<i>n</i> -Pentenes
D	Dehydrocyclization	0	<i>n</i> -Heptenes
H	Hydrogen	R	Reaction (when used in ΔH_R)
H ₂	Hydrogen	R	Hydrocarbon residue
		T	Toluene

OTHER SYMBOLS

[] Adsorbed species

REFERENCES

- A1. Anderson, J. R., and Kemball, C., *Proc. Roy. Soc.* **A226**, 472 (1954).
B1. Baeder, D. L., and Boudart, M., private communication, 1958.
B2. Barnett, L. G., Weaver, R. E. C., and Gilkeson, M. M., *A.I.Ch.E. (J. Am. Inst. Chem. Engrs.)* **7**, 211 (1961).
B3. Benesi, H., *J. Am. Chem. Soc.* **78**, 5490 (1956).
B4. Benesi, H., *J. Phys. Chem.* **67**, 970 (1957).
B5. Brunauer, S., Emmett, P. H., and Teller, E., *J. Am. Chem. Soc.* **60**, 309 (1938).
C1. Ciapetta, F. G., U.S. Patent 2,550,531 (1951).
C2. Ciapetta, F. G., *Ind. Eng. Chem.* **45**, 159 (1953).
C3. Ciapetta, F. G., *Ind. Eng. Chem.* **45**, 162 (1953).
C4. Ciapetta, F. G., and Hunter, J. B., *Ind. Eng. Chem.* **45**, 147 (1953).
C5. Ciapetta, F. G., and Hunter, J. B., *Ind. Eng. Chem.* **45**, 155 (1953).
C6. Ciapetta, F. G., Dobres, R. M., and Baker, R. W., *Catalysis* **6**, 495 (1958).
C7. Clark, A., *Ind. Eng. Chem.* **45**, 1476 (1953).
C8. Condon, F. E., *Catalysis* **6**, p. 98 (1958).
D1. Derbentsev, Y. I., Balandin, A. A., and Isagulyants, G. V., *Kinetika i Kataliz* **2**, 741 (1961).
F1. Farkas, A., and Farkas, L., *Trans. Faraday Soc.* **35**, 917 (1939).
G1. Galwey, A. K., and Kemball, C., *Trans. Faraday Soc.* **55**, 1959 (1959).
G2. Gruber, H. L., *J. Phys. Chem.* **66**, 48 (1962).
H1. Haensel, V., U. S. Patents 2,479,109 and 2,479,110 (1949).
H2. Haensel, V., and Donaldson, G. R., *Ind. Eng. Chem.* **43**, 2102 (1951).
H3. Heinemann, H., Mills, G. A., Hattman, J. B., and Kirsch, F. W., *Ind. Eng. Chem.* **45**, 130 (1953).
H4. Herington, E. F. G., and Rideal, E. K., *Proc. Roy. Soc.* **A184**, 434 (1945).
H5. Herington, E. F. G., and Rideal, E. K., *Proc. Roy. Soc.* **A184**, 447 (1945).
H6. Herington, E. F. G., and Rideal, E. K., *Proc. Roy. Soc.* **A190**, 289 (1947).
H7. Hettinger, W. P., Jr., Keith, C. D., Gring, J. L., and Teter, J. W., *Ind. Eng. Chem.* **47**, 719 (1955).
H8. Hindin, S. G., Weller, S. W., and Mills, G. A., *J. Phys. Chem.* **62**, 244 (1958).
H9. Hoog, H., Verheus, J., and Zuiderweg, F. J., *Trans. Faraday Soc.* **35**, 993 (1939).
H10. Hughes, T. R., Houston, R. J., and Sieg, R. P., *Ind. Eng. Chem., Process Design Develop.* **1**, 96 (1962).
K1. Keavney, J. J., and Adler, S. F., *J. Phys. Chem.* **64**, 208 (1960).
K2. Keulemans, A. I. M., and Schuit, G. C. A., "The Mechanism of Heterogeneous Catalysis," p. 159. Elsevier, Amsterdam, 1960.
K3. Keulemans, A. I. M., and Voge, H. H., *J. Phys. Chem.* **63**, 476 (1959).
K4. Kluksdahl, H. E., and Houston, R. J., *J. Phys. Chem.* **65**, 1469 (1961).
L1. Lewis, G. N., "Valence and the Structure of Atoms and Molecules," p. 141. Chemical Catalog, New York, 1923.
L2. Luder, W. F., and Zuffanti, S., "The Electronic Theory of Acids and Bases," pp. 1-106. Wiley, New York, 1946.
M1. McHenry, K. W., Bertolacini, R. J., Brennan, H. M., Wilson, J. L., and Seelig,

- H. S., *Actes Congr. Intern. Catalyse, 2^e, Paris, 1960* Sect. II, Paper No. 117 (1961). Editions Technip, Paris.
- M2. Mills, G. A., Heinemann, H., Milliken, T. H., and Oblad, A. G., *Ind. Eng. Chem.* **45**, 134 (1953).
- M3. Myers, C. G., and Munns, G. W., Jr., *Ind. Eng. Chem.* **50**, 1727 (1958).
- M4. Myers, C. G., Sibbett, D. J., and Ciapetta, F. G., *J. Phys. Chem.* **63**, 1032 (1959).
- N1. Newsome, J. W., Heiser, H. W., Russell, A. S., and Stumpf, H. C., "Alumina Properties." Aluminum Co. of America, Pittsburgh, Pennsylvania, 1960.
- O1. Oblad, A. G., Milliken, T. H., and Mills, G. A., *Advan. Catalysis* **3**, 199 (1951).
- P1. Parravano, G., and Boudart, M., *Advan. Catalysis* **7**, 51 (1955).
- P2. Peri, J. B., and Hannan, R. B., *J. Phys. Chem.* **64**, 1526 (1960).
- P3. Pines, H., and Haag, W. O., *J. Am. Chem. Soc.* **82**, 2471 (1960).
- P4. Pines, H., and Shaw, A. W., *J. Am. Chem. Soc.* **79**, 1474 (1957).
- P5. Pitkethly, R. C., and Goble, A. G., *Actes Congr. Intern. Catalyse, 2^e, Paris, 1960* Sect. II, Paper No. 91 (1961). Editions Technip, Paris.
- P6. Pitkethly, R. C., and Steiner, H., *Trans. Faraday Soc.* **35**, 979 (1939).
- P7. Pitts, P. M., Jr., Connor, J. E., and Leum, L. N., *Ind. Eng. Chem.* **47**, 770 (1955).
- P8. Plate, A. F., and Tarasova, G. A., *J. Gen. Chem. USSR (English Transl.)* **20**, 1193 (1950).
- R1. Rohrer, J. C., and Sinfelt, J. H., *J. Phys. Chem.* **66**, 1190 (1962).
- R2. Rohrer, J. C., and Sinfelt, J. H., *J. Phys. Chem.* **66**, 2070 (1962).
- R3. Rohrer, J. C., Hurwitz, H., and Sinfelt, J. H., *J. Phys. Chem.* **65**, 1458 (1961).
- R4. Rossini, F. D., Pitzer, K. S., Arnett, R. L., Braun, R. M., and Pimentel, G. C., "Selected Values of Physical and Thermodynamic Properties of Hydrocarbons and Related Compounds," API Research Project 44. Carnegie Press, Pittsburgh, Pennsylvania, 1953.
- R5. Ryland, L. B., Tamele, M. W., and Wilson, J. N., *Catalysis* **7**, 1 (1960).
- S1. Sinfelt, J. H., and Rohrer, J. C., *J. Phys. Chem.* **65**, 978 (1961).
- S2. Sinfelt, J. H., and Rohrer, J. C., *J. Phys. Chem.* **65**, 2272 (1961).
- S3. Sinfelt, J. H., and Rohrer, J. C., *J. Phys. Chem.* **66**, 1559 (1962).
- S4. Sinfelt, J. H., Hurwitz, H., and Rohrer, J. C., *J. Phys. Chem.* **64**, 892 (1960).
- S5. Sinfelt, J. H., Hurwitz, H., and Rohrer, J. C., *J. Catalysis*, **1**, 481 (1962).
- S6. Sinfelt, J. H., Hurwitz, H., and Shulman, R. A., *J. Phys. Chem.* **64**, 1559 (1960).
- S7. Spenadel, L., and Boudart, M., *J. Phys. Chem.* **64**, 204 (1960).
- S8. Starnes, W. C., and Zabor, R. C., Symp. Div. of Petrol. Chem. of the Am. Chem. Soc., Boston, Massachusetts, April 5-10, 1959.
- S9. Steiner, H., *Catalysis* **4**, 529 (1956).
- T1. Tamele, M. W., *Discussions Faraday Soc.* **8**, 270 (1950).
- T2. Taylor, H. S., and Fehrer, H., *J. Am. Chem. Soc.* **63**, 1387 (1941).
- T3. Trapnell, B. M. W., *Advan. Catalysis* **3**, 4 (1951).
- T4. Twigg, G. H., *Trans. Faraday Soc.* **35**, 1006 (1939).
- T5. Twigg, G. H., *Proc. Roy. Soc. A* **178**, 106 (1941).
- W1. Webb, A. N., *Ind. Eng. Chem.* **49**, 261 (1957).
- W2. Weisz, P. B., U.S. Patent 2,854,400 (1958).
- W3. Weisz, P. B., *Advan. Catalysis* **8**, 137 (1962).
- W4. Weisz, P. B., and Prater, C. D., *Advan. Catalysis* **9**, 583 (1957).
- W5. Weisz, P. B., and Swegler, E. W., *Science* **126**, 31 (1957).

HEAT CONDUCTION OR DIFFUSION WITH CHANGE OF PHASE

S. G. Bankoff

Department of Chemical Engineering
Northwestern University, Evanston, Illinois

I. Introduction	75
II. Exact Solutions	78
A. No Relative Motion of the Phases	78
B. Relative Motion Between the Phases	84
C. Ablating Slabs	94
D. Growth of a Vapor Film on a Rapidly Heated Plane Surface	102
III. Analytic Approximation Methods	105
A. Quasi-Stationary and Quasi-Steady-State Approximations	105
B. Integral Equation Methods	112
C. Variational Methods	127
D. Boundary Layer Methods	128
E. Expansions for Small Times	131
F. Linear Methods	132
IV. Analog and Digital Computer Solutions	132
A. Passive and Active Analog Solutions	132
B. Numerical Schemes	135
V. Concluding Remarks	142
Acknowledgments	143
Nomenclature	143
References	146

I. Introduction

A large number of technically important problems involve solution of the equation for diffusion of heat, mass, or some other scalar quantity, subject to the existence of a free boundary. This means that the location of the free boundary is in itself dependent, usually as the result of a phase change, upon the amount of diffusant which has been brought up to it in the past. Common examples are the freezing of the surface of a large

lake¹; evaporation from a flat water surface or a single water droplet into surrounding still air; the evaporation of a cloud of fuel droplets; the tarnishing of metal surfaces; the growth of a gas or vapor bubble in a large volume of supersaturated or superheated liquid; the formation of a spherical iron carbide particle by diffusion from a surrounding austenite matrix; and the penetration of a reactant into a spherical ion exchange particle, of a regenerant into a cylindrical viscose fiber or of a fixative into photographic film. In addition, the differential equations and boundary conditions describing quite different phenomena, such as the displacement of a fluid by another immiscible fluid in a porous medium, the growth of a filter cake, and the penetration of a magnetic field into a superconducting medium (C9), are of a similar form. The scope of the subject is truly large, and we shall limit ourselves, therefore, to those cases where the fluid motion is entirely induced by the diffusion process. This eliminates, for example, portions of the active and important field of aerodynamic ablation, but the activity in this field is now so intense as to justify a separate review article.

A number of specialized monographs have been written dealing, wholly or in part, with particular aspects of the subject, but there does not seem to be a comprehensive, unified treatment available in the English language at the present time. It is not the intent of this review to fill this gap, which could be accomplished only by a book-length treatise. It is rather hoped to supplement the existing monographs, to treat in detail areas or methods not fully covered elsewhere, and, above all, to classify in a systematic way the principal contributions which have been made in recent years. The classification system is based upon the mathematical techniques and approximations, rather than the specific nature of the diffusant or the geometry. Whenever possible, comparison of the theory with experimental results is indicated. In a succeeding volume of this series a separate treatment will be given of bubble dynamics, since the equation of motion is coupled to the diffusion equation in this case.

Except for some special cases, the presence of a free boundary introduces a nonlinearity, so that only a few exact solutions are known. These are in all cases self-similar solutions, which means that the differential equation and associated initial and boundary conditions can all be expressed in terms of a single independent variable. The problem is thereby reduced

¹ This particular problem was first studied by Stefan (S10), and the general class of solutions of the diffusion equation subject to a free boundary condition, therefore, are sometimes called Stefan problems. An analogous problem in the freezing of moist soils was previously studied, however, by Lamé and Clapeyron (L1), and in the Russian literature these problems are sometimes given the rather lengthy soubriquet of Lamé-Clapeyron-Stefan problems.

to the solution of an ordinary differential equation with appropriate boundary conditions. This technique is well known in other branches of applied analysis, such as boundary layer theory, and is closely related to the theory of characteristics. Fortunately, the initial and boundary conditions for these exact solutions encompass a number of important physical problems. In some cases the necessary conditions correspond only approximately to the real situation, and the validity of these approximations will then be examined. One may distinguish between analytic (or mathematical) approximations and solutions by numerical or analog methods. In the former category an important general method is the formulation of the problem as a nonlinear integral implicit (or functional) equation for the unknown boundary position, which must then be solved by iterative methods, or from which simpler solutions can be derived for limiting cases. Other integral equation methods (equivalent to macroscopic balances) have been employed to obtain upper and lower bounds for the boundary displacement. An extremely important approximation, which has been extensively applied to the growth and dissolution of precipitates, droplets, and gas bubbles, neglects the convective term in the diffusion equation, as well as the boundary motion, in computing the diffusive flux, and hence may be termed the quasi-stationary assumption. In addition, the time derivative may also be neglected, after a sufficiently long time has elapsed. This simplified approach, known as the quasi-steady-state approximation, has long been used in hygrometry and mass transfer design calculations. In addition, the equations for filter cake deposition are of the same form. On the other end of the scale are perturbation solutions based upon the assumption that the thickness of the diffusion boundary layer increases slowly compared to the displacement of the free boundary. This "thin boundary layer" assumption has been extensively used in bubble dynamics. Finally, various analog and numerical solution schemes, many of which employ transformations which effectively immobilize the free boundary, are treated.

Such purely mathematical problems as the existence and uniqueness of solutions of parabolic partial differential equations subject to free boundary conditions will not be discussed. These questions have been fully answered in recent years by the contributions of Evans (E2), Friedman (F5, F6, F7), Kyner (K8, K9), Miranker (M8), Miranker and Keller (M9), Rubinstein (R7, R8, R9), Sestini (S5), and others, principally by application of fixed-point theorems and Green's function techniques. Readers concerned with these aspects should consult these authors for further references.

The variety of problems which can be posed is so large that it is difficult, as well as unnecessarily confusing, to express the governing equations,

together with the initial and boundary conditions, in the most general form possible. Instead, a semichronological approach is employed in which some of the simpler problems are first taken up, followed by the introduction of various complicating conditions. Early historical material, as well as material adequately treated in the standard reference works, is either omitted or briefly treated. Even so, some judicious choice of material for detailed presentation was necessary. The selection process was, to some extent, necessarily subjective; but it was hoped to present sufficient prototype detail to make clear the major methods which have been employed in free-boundary diffusion theory, together with their limitations.

II. Exact Solutions

A. NO RELATIVE MOTION OF THE PHASES

1. *Diffusion in One Phase Only*

a. Constant Diffusivity. In some cases, as in the melting of ice or the penetration of ions into a polymer particle, it is permissible to ignore the change in density resulting from the motion of the boundary. A number of exact one-dimensional solutions of the melting-freezing problem are reviewed by Carslaw and Jaeger (C1), Crank (C14), Ruddle (R10), and Veinik (V1) and will be considered only indirectly here. The earliest solutions seem to be those of Stefan and Neumann, who considered the melting of a semi-infinite solid at a uniform initial temperature, $T_0 < T_m$, where T_m is the fusion temperature, when the surface temperature is suddenly raised above the melting point. Neumann (N1) assumed a trial form for the solution and established that it satisfied the differential equations and all boundary conditions.² Much later, Boltzmann (B10)³ introduced the new variable $\eta = s/(\alpha t)^{1/2}$ where s is a radial position coordinate in one, two, or three dimensions, α is the thermal diffusivity, and t is the elapsed time. A few solutions of the heat equation exist which are functions of η only, as discussed by Carslaw and Jaeger, so that exact solutions of the moving-boundary problem are possible when the position of the phase interface remains fixed in η -space.

Rieck is quoted by Huber (R6) as generalizing, in an unpublished dissertation, the similarity problem to two and three dimensions. One of the

² Recently Ruoff (R11) has rederived the Stefan and Neumann solutions using the Boltzmann transformation.

³ Actually Boltzmann considered only one-dimensional problems, in which case $s = x$, the distance from the initial slab surface position. Further, his concern was not so much with melting-freezing processes as with temperature-dependent physical properties.

first published similarity solutions under spherically symmetric conditions in n -dimensional space ($n = 1, 2, 3$, corresponding to linear, cylindrical, and spherical geometries) appears to have been presented by Zener (Z2) in a discussion of the growth of spherical precipitates from solid solution.⁴ The immediate applications were to the growth in an austenite matrix of a spherical iron carbide particle, where the carbon atoms are diffusing towards the interface, or of a ferrite particle, where they are diffusing away from the interface. The concentration C' of the diffusant in the newly formed phase is assumed to be a constant, as is its initial concentration in the original phase C_∞ . The concentration just outside the interface, C_i , is assumed to be a constant, dictated by equilibrium considerations. It is of interest that there seems to be no comparable melting-freezing problem, since it is not possible to maintain a finite temperature discontinuity across the phase interface.

With the restriction of uniform mass densities the diffusion equation in n -dimensional space becomes

$$\frac{\partial C}{\partial t} = Ds^{-n+1} \frac{\partial}{\partial s} \left(s^{n-1} \frac{\partial C}{\partial s} \right) \quad (1)$$

where D is a mass diffusivity. A uniform initial concentration, which remains unchanged at infinity, is expressed by

$$C(s, 0) = C_\infty = C_0 \quad (2)$$

It is now assumed that equilibrium conditions prevail at the phase interface. This will be the case if the interface reaction is relatively rapid, so that the growth is diffusion-limited. The mathematical solution requires that η remain constant at the interface, which implies that the radius of

⁴ The author is indebted to Dr. G. Horvay of the General Electric Research Laboratory for bringing to his attention a prior paper by Ivantsov (I1), dealing with a general method for obtaining similarity solutions in the growth of a crystal from a supercooled melt. The differential equation relating the heat conduction at the phase interface to the boundary motion is converted to a nonlinear first-order partial differential equation, having the temperature as the only dependent variable. The complete integral, containing five arbitrary constants and an arbitrary function of the temperature, is obtained by the theory of characteristics. The arbitrary function is determined with the help of the heat conduction equation, and the constants with the aid of the boundary conditions at infinity and at the phase interface. In this way similarity solutions are generated for spherical and cylindrical crystals growing as the square root of time, and needle-shaped (confocal paraboloids) and knife-shaped (confocal parabolic cylinders) growing at constant vertex velocity. Horvay and Cahn (H12) give a different solution for the parabolic cylinder growth, and also extend Ivantsov's solutions to include the growth of elliptical paraboloids and ellipsoids, from which a variety of shapes can be obtained by suitable specialization. These authors also consider modifications of the isothermal phase interface condition due to surface energy effects and to interface kinetics.

the critical nucleus is zero at zero time. Actually, of course, it has a small positive value, determined by surface tension; and surface tension effects remain appreciable for some short time after the critical nucleus begins to grow.⁵ The final results are, therefore, valid after the precipitate particles have attained a size large compared to the critical size of a stable nucleus. The boundary condition at the interface thus becomes

$$C(S(t), t) = C_i \quad (3)$$

where the capital letter is used to denote the time-dependent position coordinate of the free boundary. A material balance at the interface requires that⁶

$$(C' - C_i)\dot{S} = D \frac{\partial C(S(t), t)}{\partial s} \quad (4)$$

where the dot denotes a time derivative.

Since both the governing differential equations and all boundary conditions are homogeneous in the concentrations, \dot{S} can depend upon C' , C_∞ , and C_i only in some dimensionless combination. The only other variables are D and t , so that dimensional considerations require that

$$S = \beta_n (Dt)^{1/2} \quad (5)$$

where β_n is a dimensionless growth constant and n refers to the number of dimensions.

The solution of Eq. (1), which satisfies Eqs. (2)–(5) is

$$c \equiv \frac{C - C_\infty}{C_i - C_\infty} = \psi_n(s/\sqrt{Dt})/\psi_n(\beta_n) \quad (6)$$

where

$$\psi_n(x) = \int_x^\infty \exp(-\tfrac{1}{4}z^2) z^{1-n} dz \quad (7)$$

Upon applying the interface condition, Eq. (4), an expression for the growth coefficient is obtained:

$$(\beta_n)^n = \frac{2c_1 \exp(-\beta_n^2/4)}{\psi_n(\beta_n)}; \quad c_1 = \frac{C_\infty - C_i}{C' - C_i} \quad (8)$$

Zener gives numerical solutions for the growth coefficients for one- and three-dimensional growth, and also asymptotic expansions for large and small values of the growth coefficients:

⁵ Somorjai (S8) discusses the surface energy effect in the early growth of a condensed phase, and Skinner and Bankoff (S6) discuss the error in assuming a zero initial radius in bubble growth.

⁶ When concentrations (or temperatures) in two phases must be considered, the original and newly formed phases will, in general, be designated by the absence or presence of the prime superscript, respectively.

$$\begin{aligned}\beta_1 &= 2\pi^{-1/2}c_1 & \beta_1 &\ll 1 \\ &= 2^{1/2}(1 - c_1)^{-1/2} & \beta_1 &\gg 1\end{aligned}\quad (9)$$

$$\begin{aligned}\beta_3 &= 2^{1/2}c_1^{1/2} & \beta_3 &\ll 1 \\ &= 6^{1/2}(1 - c_1)^{-1/2} & \beta_3 &\gg 1\end{aligned}\quad (10)$$

so that the growth coefficient assumes all positive values as c_1 varies from 0 to 1. From an approximate solution it is shown that a more natural choice of parameters is

$$\beta_1 = K_1 \frac{(C_\infty - C_i)}{(C' - C_\infty)^{1/2}(C' - C_i)^{1/2}}; \quad 1.13 < K_1 < 1.41 \quad (11)$$

for the one-dimensional case and

$$\beta_3 = K_3 \frac{(C_\infty - C_i)^{1/2}}{(C' - C_\infty)^{1/2}}; \quad 1.4 < K_3 < 2.4 \quad (12)$$

for the three-dimensional case, since the dimensionless coefficients K_1 and K_3 show a relatively small range of variation over the entire range of growth coefficient values.

Shortly afterwards Frank (F3) derived the same results and extended the discussion to include the case where both heat and mass diffusion control the phase growth. In this case the melting point depression is related by thermodynamic considerations to the interface concentration, which can be determined either iteratively or by means of a convenient graphical aid. Frank also considers several related problems, such as the growth of a compound, where two dissolved substances which diffuse independently unite to form the new phase.

Problems of this sort have been extensively discussed (not always correctly) and studied experimentally. As an example, Hermans (H7) considers particles diffusing into a medium which contains C_0 "holes" per unit volume, in each of which one particle can be bound and removed from the diffusion process.

Assuming for the present that the holes are immobile, the concentration of unbound particles, C' , and of unfilled "holes," C , is given by

$$\frac{\partial C'}{\partial t} - D \frac{\partial^2 C'}{\partial x^2} = -KCC' = \frac{\partial C}{\partial t} \quad (13)$$

where K is the rate constant for the assumed second-order reaction between molecules and holes.

For K very large, the right-hand side of Eq. (13) will be negligibly small, except in a very thin transition region where the newly diffused molecules are reacting with holes previously not in contact with molecules. In this case a sharp boundary will prevail between the region where the

concentration of free particles is nonzero and that where it is zero. The condition at the free boundary is then

$$-D \frac{\partial C'(X(t), t)}{\partial x} = C_0 \dot{X} \quad (14)$$

The problem thus reduces to the same form as the Stefan problem for the melting of a block of ice initially at the fusion temperature. On the other hand, if the "holes" themselves are mobile, diffusion occurs on both sides of the moving boundary. An example given by Hermans is the penetration of S^{--} ions into a gel containing Pb^{++} ions, precipitating PbS . The problem is now strictly analogous to that solved by Neumann of the melting of ice initially below the fusion point. Adair (A1) has rederived this solution in connection with the mass diffusion problem. Hermans further considers radial penetration into a cylinder⁷ and mentions that Bungenberg de Jong (B15) found experimentally that a quasi-parabolic law was followed:

$$R = k_h[\sqrt{t} + \sqrt{t_{1/2}} - \sqrt{t_{1/2} - t}] \quad (15)$$

where $R(t)$ is the radius of the free boundary and $R(t_{1/2}) = \frac{1}{2}R(0)$. It will be noted that this curve is symmetrical about the point $R(t_{1/2})$. Hermans studied the linear diffusion of thiosulfate ions into both ends of a capillary filled with gel, containing iodine (and starch, to immobilize the iodine) and verified that $Xt^{-1/2} = \text{constant}$. In the penetration of Na_2S into agar gel containing lead acetate, the free boundaries advancing from each end of the capillary were quite sharp initially, but became indistinct as they approached each other, due to depletion of the Pb^{++} ions from the central region by diffusion. Cylindrical diffusion was also studied of $S_2O_3^{--}$ into gelatin gels with I_2 , and Cu^{++} into cellulose xanthate containing bound CS_2 groups. There was a considerable discrepancy in the diffusion coefficients measured in cylindrical and linear diffusion, to be expected in view of the incorrect cylindrical diffusion analysis. Griffin (G8) has reconsidered this problem, using an integral method, and has succeeded in bringing the results into reasonably close agreement.

b. *Concentration-Dependent Diffusivity*. Pattle (P1) has found an interesting class of exact solutions of the diffusion equation when the diffusivity varies as some positive power of the concentration,

$$D = D_0(C/C_0)^b \quad (16)$$

where D_0 is the diffusivity at the reference concentration C_0 . This situation obtains, for example, in the penetration of liquid into a porous body under the influence of capillary forces. In this case the diffusivity increases rapidly as the amount of the liquid in the pores increases, so that the

⁷ Hermans' own solution has an incorrect symmetry condition.

resistance to viscous flow decreases. The equation for outward diffusion from an instantaneous point source in n dimensions into a medium of zero mean motion may be written

$$\frac{\partial C}{\partial t} = s^{1-n} \frac{\partial}{\partial s} \left(s^{n-1} D \frac{\partial C}{\partial s} \right) \quad (17)$$

with the solution

$$C = C_0 \left(\frac{t}{t_0} \right)^{-n/(nb+2)} \left\{ 1 - \frac{s^2}{s_1^2} \right\}; \quad t > 0, \quad s^2 \leq s_1^2 \quad (18a)$$

$$C = 0; \quad s^2 \geq s_1^2 \quad (18b)$$

These equations represent a region of diffusing substance with a definite edge, whose radius s_1 is given by

$$s_1 = s_0 \left(\frac{t}{t_0} \right)^{1/(nb+2)} \quad (19)$$

Assuming that a quantity Q is liberated at time $t = 0$ at a point in an infinite line, plane, or volume, depending upon the number of dimensions, the parameters s_0 and t_0 in Eq. (19) can be determined from

$$s_0^n = \frac{Q}{C_0 \pi^{n/2}} \left\{ \frac{\Gamma(b^{-1} + 1 + \frac{1}{2}n)}{\Gamma(b^{-1} + 1)} \right\} \quad (20)$$

$$t_0 = \frac{s_0^2 b}{2D_0(nb + 2)} \quad (21)$$

As $b \rightarrow 0$, Eqs. (18a) and (18b) tend to the instantaneous point source solution with constant diffusivity:

$$C = \frac{Q \exp(-s^2/4D_0t)}{(4\pi D_0t)^{n/2}} \quad (22)$$

When $b > 1$, the concentration gradient at the boundary of the region is infinite; when $b = 1$, it is finite; and when $b < 1$, it is zero. Note from Eq. (22) that the concentration at any point in space is instantaneously affected by the liberation of a finite quantity of diffusant at the origin, providing that the diffusivity of the medium is a constant. This is a well-known property of parabolic partial differential equations, which implies that the velocity of propagation of a concentration (or temperature) signal is infinite. The introduction of a nonlinearity results in a finite propagation velocity. The appearance of a concentration discontinuity at the outward-moving boundary as b exceeds unity is reminiscent of the appearance of a shock wave in a gas flow when the local Mach number exceeds unity. In the latter case, however, this corresponds to a change in the nature of the characteristics of the linear partial differential equation, and hence is only vaguely analogous to the nonlinear solution discovered by

Pattle. Boyer (B12) has derived these results in a different way and applied them to the release of energy in an ionized gas, as well as to a transmission line problem.

B. RELATIVE MOTION BETWEEN THE PHASES

1. Diffusion in One Phase Only

a. Constant Diffusivity. When the densities of the two phases are constant but unequal a convective motion will be induced by the diffusion process. Chambré (C2) considered the n -dimensional similarity problem for this case but neglected the radial pressure gradients in the equation of motion, with the result that continuity relationships were violated. The first correct solution seems to have been given by Kirkaldy (K2), who was particularly concerned with the applicability of quasi-stationary diffusion theory to the condensation from air of water vapor on ice crystals or water drops. Assuming constant mass density of the exterior phase the mass flux can be expressed as the sum of a convective and a diffusive term

$$\mathbf{J} = C\mathbf{u} - D\nabla C \quad (23)$$

In a symmetrical n -dimensional system the convective term must decrease as s^{n-1} . The time dependence, such that the solution has the form $C = C(\eta)$, turns out to be

$$Cu = \frac{CA_n t^{(n-2)/2}}{2s^{n-1}} \quad (24)$$

where A_n is a constant. On substituting these expressions into the continuity equation

$$\nabla \cdot \mathbf{J} + \frac{\partial C}{\partial t} = 0, \quad (25)$$

one obtains the differential equation

$$\frac{A_n}{2} \frac{t^{(n-2)/2}}{s^{n-1}} \frac{\partial C}{\partial s} - \frac{D}{s^{n-1}} \frac{\partial}{\partial s} \left[s^{n-1} \frac{\partial C}{\partial s} \right] + \frac{\partial C}{\partial t} = 0 \quad (26)$$

The transformation to η -space converts this to the ordinary differential equation

$$\left[\frac{A_n}{2D^{n/2}\eta^{n-1}} - \frac{n-1}{\eta} - \frac{\eta}{2} \right] \frac{dC}{d\eta} = \frac{d^2C}{d\eta^2} \quad (27)$$

The boundary conditions are the same as in Eqs. (2) and (3) with the solution

$$c(\eta) = \phi_n(\eta)/\phi_n(\beta_n) \quad (28)$$

where

$$\phi_n(\eta) = \int_{\eta}^{\infty} z^{1-n} \exp \left(\frac{A_n}{2D^{n/2}} \int z^{1-n} dz - \frac{z^2}{4} \right) dz \quad (29)$$

The constant A_n is determined by reference to the mass balance at the interface. Using Eq. (5), this takes the form

$$C_i(\dot{S} - \mathbf{u}(S, t)) = C'\dot{S} \quad (30)$$

or

$$\mathbf{u}(S, t) = \epsilon \dot{S} = \frac{\epsilon}{2} \beta_n \sqrt{D/t} \quad (31)$$

where $\epsilon = 1 - (C'/C_i)$. This leads to

$$A_n = \epsilon(\beta_n D^{1/2})^n \quad (32)$$

In particular the growth function for spherical symmetry in three dimensions is

$$\phi_3(\eta) = \int_{\eta}^{\infty} z^{-2} \exp\left(\frac{-\beta_3^3 \epsilon}{2z} - \frac{z^2}{4}\right) dz \quad (33)$$

This result was rederived shortly afterwards by Birkhoff, *et al.* (B7), and by Scriven (S4), in considering the growth of gas or vapor bubbles. Finally, from Eqs. (24), (31), and (32), it follows that

$$\mathbf{u}(s, t) = \frac{A_n t^{(n-2)/2}}{2s^{n-1}} = \frac{\epsilon \beta_n^n D^{n/2} t^{(n-2)/2}}{2s^{n-1}} \quad (34)$$

$$= \mathbf{u}(S, t) \left(\frac{S}{s}\right)^{n-1} \quad (35)$$

This is an expression of the continuity equation for the flow of a fluid of constant mass density with n -dimensional spherical symmetry.

In principle, therefore, this solution can be applied to the growth, limited by the diffusion of heat or mass, of slabs, cylinders, or spheres of initially negligible size from a large body of surrounding quiescent fluid of initially uniform concentration and temperature, where the densities of the two phases are constant but not necessarily equal. One further problem remains, consisting of the determination of the growth constant β_n . This follows from an energy or mass balance at the moving interface. These matters will be treated in more detail in the discussion of bubble dynamics.

Griffin (G8) gives a general procedure, based upon the method of intermediate integrals, for finding similarity transformations to the moving-boundary diffusion problem. This method is based upon the Riemann-Volterra theory of characteristics (W2). As a particular example of this method, Kirkaldy's solution for the n -dimensionally symmetric phase growth problem with accompanying convective motion is once again derived.

Horvay (H11) also derives the phase growth and temperature field solutions, and in addition computes the pressure field from the equation of motion. From this it is shown that, for every pressure and temperature

at infinity and for $\epsilon < 0$ ($\rho' > \rho$), there exists a critical spherical nucleus radius which will grow smoothly by influx of liquid to the solid surface; below this size the negative pressure at the surface of the nucleus is sufficiently great to induce cavitation. On the other hand, for a cylindrical shape, cavitation can be expected below some radius for any ϵ , while for a planar form, cavitation is predicted only for $\epsilon > 0$. An example is given of the growth of a nickel nucleus in spherical or cylindrical shape, using a formula deduced by Fisher (F1) for the fracture strength of a liquid, based upon the expected waiting time for the first bubble.

2. Diffusion in Two Regions; Plane Free Boundary

a. Constant Diffusivity. In the preceding sections the concentration of diffusant was uniform in the newly formed phase, so that only the diffusion equation for the exterior phase needed to be considered. More generally, however, there may be concentration or temperature gradients in both phases; there may or may not be induced motion of the phases relative to each other; and the position of the moving interface may or may not be proportional to the total amount of diffusant which has crossed the boundary. As noted previously, nearly all exact solutions of the free-boundary heat diffusion equation in one dimension depend upon the existence of fundamental solutions in terms of the Boltzmann similarity variable, $x/(\alpha t)^{1/2}$. Danckwerts (D1) extended the exact solutions of plane problems to more general types of boundary conditions. The essence of his method is to note that, assuming constant mass densities and diffusivities, each phase is at rest with respect to Lagrangian coordinates, so that solutions of the heat equation written in coordinates appropriate to each phase are readily obtained. Provided suitable restrictions are satisfied, matching conditions can then be found at the interface to relate the motion of one coordinate system to the other. To see how this goes (Fig. 1),

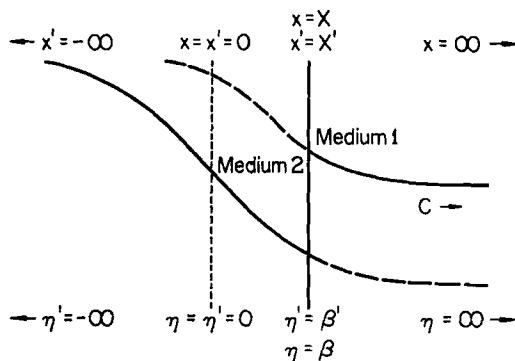


FIG. 1. Coordinate systems (D1). Redrawn by permission of Faraday Society.

consider that the unprimed phase, in which the diffusant concentration is C , occupies the right-hand half-space, and the primed phase the complementary left-hand region. Consider two coordinate systems which are fixed to their respective media, whose origins coincide with the common boundary at $t = 0$. Subject to the simplifications noted above the equations for a single diffusant are

$$\frac{\partial C}{\partial t} = D \frac{\partial^2 C}{\partial x^2}; \quad C = C(x, t), \quad X(t) \leq x < \infty, \quad t > 0 \quad (36)$$

$$\frac{\partial C'}{\partial t} = D \frac{\partial^2 C'}{\partial x'^2}; \quad C' = C'(x', t), \quad -\infty < x' \leq X'(t), \quad t > 0 \quad (37)$$

where $X(t)$ and $X'(t)$ are the positions of the free boundary with respect to the two coordinate systems. The concentrations at the interface are related by an equilibrium expression which may be linearized to the form

$$C_i' = K_1 C_i + K_2 \quad (38)$$

where $C_i = C(X, t)$, $C' = C'(X', t)$, and K_1 and K_2 are physical constants.

Assuming that there is no accumulation of diffusant at the moving interface, a conservation requirement is that

$$D \frac{\partial C(X, t)}{\partial x} - D' \frac{\partial C'(X', t)}{\partial x'} + C_i \dot{X} - C_i' \dot{X}' = 0 \quad (39)$$

Further, the constant proportionality between the rates of movement of the two media relative to the interface implies

$$\dot{X}' = K_3 \dot{X} \quad (40)$$

where K_3 is a constant determined by the physical conditions. Finally, in many cases (such as the growth of a crystal or of a film of tarnish) the position of the interface is proportional to the total flux of diffusant which has crossed it up to that time. That is, some constant K_4 exists such that

$$\dot{X} = K_4 \left[D \frac{\partial C(X, t)}{\partial x} + C_i \dot{X} \right] \quad (41)$$

where the terms on the right represent the contributions of the diffusive and convective fluxes. Upon combining Eqs. (39), (40), and (41), one can obtain a corresponding condition for the second phase

$$\dot{X}' = K_3 K_4 \left[D' \frac{\partial C'(X', t)}{\partial x'} + C_i' \dot{X}' \right] \quad (42)$$

Equations (36) and (37) require two initial conditions and four boundary conditions, as well as two other conditions specifying the parameters X and X' , in order for the solution to be determinate.

The specification, therefore, of two initial conditions and two bounded-

ness conditions at infinity, together with the four equations (38)–(41), serve to define this type of problem (Class A). When Eq. (41) is not applicable it is necessary to have an additional parameter specified, such as one of the interfacial concentrations, besides the initial conditions (Class B). Danckwerts' method of solution is to extend the domain of Eqs. (36) and (37) back to their respective origins, where fictitious constant boundary conditions are imposed. The solutions thus obtained will be valid in the respective physical regions, provided X [and therefore, from Eq. (40), also X'] varies as the square root of time, and the interfacial concentrations remain constant. To provide continuity with previous sections and also to emphasize the self-similar nature of the solution a somewhat different development than that of Danckwerts is given below.

Define the similarity variables and dimensionless concentrations

$$\begin{aligned}\eta &= \frac{x}{\sqrt{Dt}}; & c &= \frac{C - C_0}{C_i - C_0} \\ \eta' &= -\frac{x'}{\sqrt{D't}}; & c' &= \frac{C' - C'_0}{C'_i - C'_0}\end{aligned}\quad (43)$$

where C_0 represents the initial (uniform) concentration in the unprimed phase, which remains unchanged at infinity. At the interface $\eta = \beta$; $\eta' = \beta'$, constant by virtue of the assumption concerning the interface motion. Equation (36) can now be written as an ordinary differential equation

$$\frac{d^2c}{d\eta^2} = -\eta \frac{dc}{d\eta}; \quad c = c(\eta), \quad \beta \leq \eta < \infty \quad (44)$$

subject to the two-point boundary condition

$$c(\infty) = 0; \quad c(\beta) = 1 \quad (45)$$

The solution is readily found to be

$$c(\eta) = \operatorname{erfc} \frac{\eta}{2} / \operatorname{erfc} \frac{\beta}{2}, \quad (46)$$

with the corresponding solution for the primed phase in terms of the appropriate primed variables

$$c'(\eta') = \operatorname{erfc} \frac{\eta'}{2} / \operatorname{erfc} \frac{\beta'}{2}; \quad \eta' - \beta' \geq 0 \quad (47)$$

Define now the dimensionless parameters

$$\begin{aligned}T &= K_4 C_i; & \omega &= \frac{C_0}{C_i} \\ T' &= K_4 C'_i; & \omega' &= \frac{C'_0}{C'_i}\end{aligned} \quad \nu = \sqrt{\frac{D'}{D}} \quad (48)$$

Equations (38), (39), and (40) now become

$$T' = K_1 T + K_2 K_1 \quad (49)$$

$$\frac{dc(\beta)}{d\eta} + \nu\gamma \frac{dc'(\beta')}{d\eta'} + \frac{1}{2(1-\omega)} \left[\beta + \frac{\beta'\nu T'}{T} \right] = 0 \quad (50)$$

$$\beta'\nu = -K_3\beta \quad (51)$$

where

$$\gamma = \frac{C_i' - C_0'}{C_i - C_0} = \frac{T'(1-\omega')}{T(1-\omega)} \quad (52)$$

Similarly Eqs. (41) and (42) may be written

$$\beta(1-T) = 2T(1-\omega) \frac{dc(\beta)}{d\eta} \quad (53)$$

$$\beta'(1-K_3T') = 2K_3T'(1-\omega') \frac{dc'(\beta')}{d\eta'} \quad (54)$$

Upon making use of Eqs. (46) and (47) one has

$$\frac{dc(\beta)}{d\eta} = \frac{2 \exp(-\beta^2/4)}{\pi^{1/2} \operatorname{erfc}(\beta/2)}, \quad \frac{dc'(\beta')}{d\eta'} = \frac{2 \exp(-\beta'^2/4)}{\pi^{1/2} \operatorname{erfc}(\beta'/2)} \quad (55)$$

Besides the two growth constants there are four other parameters defined by Eq. (48) which are not specified as combinations of physical properties of the system. For class A systems there are the four algebraic expressions in Eqs. (49) to (53), so that two other quantities, such as the concentrations at infinity, must be specified. For class B problems, where Eq. (53) is not applicable, three parameters must be specified.

Danckwerts has obtained a variety of interesting results of which we quote a few:

(1) *Absorption by a liquid of a single component from a mixture of gases.*

Let the unprimed phase be a mixture of a soluble gas A and an insoluble gas, the initial mole fraction of A being Y_0 . Similarly the concentration in the primed phase in volumes of dissolved gas per unit volume of liquid is initially equal to C_0' . At the interface a Henry's law expression is satisfied, so that, by Eq. (38), $C'(X, t) = K_1 Y(X, t)$, where K_1 is the solubility of A in the liquid, expressed as volumes of gaseous A per unit volume of liquid per unit mole fraction of A in the gas. The growth constant is then obtained by means of the result

$$\frac{\frac{\beta\pi^{1/2}}{2\nu} - K_1 Y + C_0'}{\frac{\beta\pi^{1/2}}{2\nu} - K_1 + C_0'} = \pi^{1/2} \frac{\beta}{2} \exp \frac{\beta^2}{4} \operatorname{erfc} \frac{\beta}{2} = f\left(\frac{\beta}{2}\right) \quad (56)$$

where the volume of A absorbed per unit area of the liquid surface is

$$V = \beta(Dt)^{1/2} \quad (57)$$

The solution of Eq. (56) proceeds by trial, with the aid of Figs. 2(a) and 2(b). This result was previously given in a less complete form by Arnold (A5).

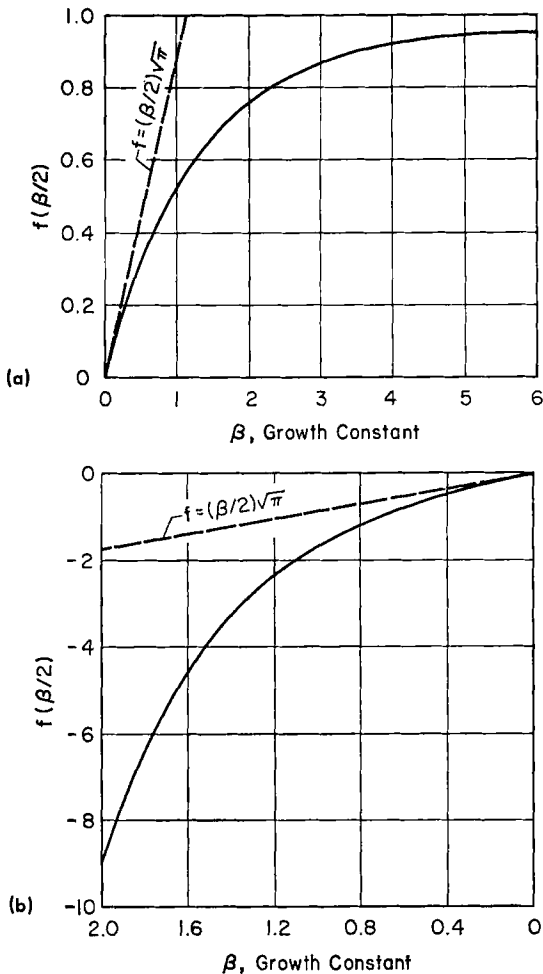


FIG. 2. (a) $f(\beta/2)$, defined by Eq. (56), for positive values of β (D1). Reproduced by permission of Faraday Society. (b) $f(\beta/2)$, defined by Eq. (56), for negative values of β (D1). Reproduced by permission of Faraday Society.

(2) *Tarnishing reactions.* A film of tarnish is formed on the surface of a metal by diffusion of dissolved gas A through the film from an exterior gaseous phase. The reaction rate of gas with metal is assumed to be large,

so that the dissolved gas concentration C_i at the metal-tarnish interface can be taken to be zero. If $C(0)$ is the saturated concentration of gas at the outer surface of the film the growth constant can be determined from

$$\frac{C(0)}{C_A} = \pi^{1/2} \frac{\beta}{2} \exp\left(\frac{\beta^2}{4}\right) \operatorname{erf}\left(\frac{\beta}{2}\right) = g\left(\frac{\beta}{2}\right) \quad (58)$$

where C_A is the concentration of A in the compound formed with the

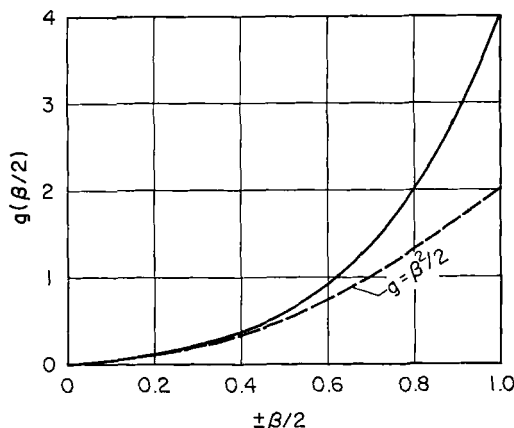


FIG. 3. $g(\beta/2)$, defined by Eq. (58), versus $\beta/2$ (D1). Reproduced by permission of Faraday Society.

metal. A plot of $g(\beta/2)$ is given in Fig. 3. The thickness of the film is found from

$$X = \beta(Dt)^{1/2} \quad (59)$$

This problem was previously considered by Booth (B11). Except at high pressures the left-hand side of Eq. (58) is frequently small, so that a Taylor expansion may be employed. This gives

$$X \cong \left(\frac{2DC(0)t}{C_A}\right)^{1/2} \quad (60)$$

which is the result obtained assuming a linear concentration profile through the film (quasi-steady approximation).

(3) *Condensation of a vapor at the surface of a cold liquid of infinite depth.* Here, heat is the diffusant, and the liquid is initially at a uniform temperature $T_0 < T_s$, the temperature of the saturated vapor in contact with the liquid. The mass condensed per unit of area is then given by

$$M = -X\rho = -\beta\rho(\alpha t)^{1/2} \quad (61)$$

where the growth constant is obtained from

$$\frac{c_p(T_0 - T_s)}{L} = f\left(\frac{\beta}{2}\right) \quad (62)$$

where c_p denotes the specific heat of the liquid and L the latent heat of vaporization. The temperature distribution in the liquid is obtained from Eq. (46)⁸:

$$\theta \equiv \frac{T - T_0}{T_s - T_0} = \frac{\operatorname{erfc}(\eta/2)}{\operatorname{erfc}(\beta/2)} \quad (63)$$

The same equations may be used for evaporation, in which connection this solution was rederived by Knuth (K3). For f small, corresponding to low subcoolings, $f \approx \beta\pi^{1/2}/2$, whence

$$M \cong \frac{2}{L} (T_s - T_0) c_{p\rho} \left(\frac{\alpha t}{\pi}\right)^{1/2} \quad (64)$$

(4) *Progressive freezing of a liquid.* Consider the freezing of a liquid of uniform temperature $T_\infty > T_s$ in contact with a solid wall whose surface is maintained at some constant temperature $T_w < T_s$. There will be an induced motion of the liquid resulting from the density change upon solidification. This is a class B problem, since the thickness of the primed phase (solidified material) is, in general, not proportional to the total amount of heat crossing the interface, in view of the temperature gradients in the solid. The growth constant is found from the expression

$$\frac{c_p(T_\infty - T_s)}{f(\beta/2\alpha^{1/2})} + \frac{c_p'(T_w - T_s)}{g(\rho\beta/2\rho'\alpha'^{1/2})} + L = 0 \quad (65)$$

where f and g are functions given by Eqs. (56) and (58) and L is now the latent heat of fusion. The thickness of the solid at time t is

$$X' = \frac{X\rho}{\rho'} = \rho\beta(t/\rho')^{1/2} \quad (66)$$

while the dimensionless temperature θ' at any point in the solid is

$$\theta' = \frac{T' - T_w}{T_s - T_w} = \frac{\operatorname{erf}[x'/2(\alpha't)^{1/2}]}{\operatorname{erf}[\rho\beta/2\rho'(\alpha')^{1/2}]} \quad (67)$$

Correspondingly the dimensionless temperature of the liquid is

$$\theta = \frac{T - T_\infty}{T_s - T_\infty} = \frac{\operatorname{erfc}[x/2(\alpha t)^{1/2}]}{\operatorname{erfc}[\beta/2(\alpha)^{1/2}]} \quad (68)$$

This solution was rederived by Adams and Seizew (A2), and also by Riazantsev (R5).

b. Concentration-Dependent Diffusivity. Consider the plane melting-freezing problem with specific heats and thermal conductivities of both

⁸ There is a misprint at this point in Eq. (7.14) of the reference.

phases temperature-dependent (H5). It can be seen from the self-similar form of the heat equation (44), with boundary conditions given by Eq. (45), that the only requirements for the existence of a self-similar solution are that the densities of the phases be constant, that the thickness of the new phase increase as the square root of the time, and that the initial and interfacial concentrations (or temperatures) of both phases be constants. This means that the class of self-similar solutions can be extended to cases where the diffusivity is an arbitrary function of concentration in both phases (or the specific heat and thermal conductivity are arbitrary functions of temperature in both phases). The problem then becomes non-linear, and resort to numerical integration is necessary to obtain the exact solutions. It is convenient to define a slightly different similarity variable, $\lambda = x/X$, previously given by Zener (Z2), where $X(t)$ represents the thickness of the solidified layer. The progressive freezing problem posed in the previous section, with the exception that the thermal properties are now temperature-dependent, is considered. The heat equation becomes for the liquid

$$\frac{d}{d\lambda} \left(k \frac{dT}{d\lambda} \right) + 2c_p \rho \beta^{*2} (\lambda - \epsilon) \frac{dT}{d\lambda} = 0; \quad \epsilon = 1 - \frac{\rho'}{\rho}, \quad \lambda \geq 1 \quad (69)$$

and for the solid

$$\frac{d}{d\lambda} \left(k' \frac{dT'}{d\lambda} \right) + 2\rho' c_p' \beta^{*2} \lambda \frac{dT'}{d\lambda} = 0; \quad 0 \leq \lambda \leq 1 \quad (70)$$

where

$$X^2 = 4\beta^{*2}t \quad (71)$$

There are two sets of two-point boundary conditions

$$T(1) = T'(1) = T_s \quad (72)$$

$$T(\infty) = T_\infty; \quad T'(0) = T_w \quad (73)$$

together with the matching condition at the interface resulting from an energy balance,

$$k \frac{dT}{d\lambda} - k' \frac{dT'}{d\lambda} = -2L\rho'\beta^{*2} \quad \text{at } \lambda = 1 \quad (74)$$

The solution of this system by numerical integration in both directions from $\lambda = 1$ is straightforward. Each choice of a growth constant and of the temperature gradient at the interface in one of the phases leads through Eq. (74) to the interfacial gradient in the other phase. An iterative method is employed to determine appropriate starting values for assigned values of T_∞ and T_w . In a numerical example it is found that the freezing rate of a semi-infinite copper melt, initially at the fusion temperature, whose surface is brought to ambient temperature is overestimated by about 10%

when the thermal properties of the solidified copper are evaluated at the average solid temperature.

These results were to some extent anticipated by Tirska (T3), who gave the Boltzmann transformation for self-similar heat conduction solutions in a semi-infinite slab with temperature-dependent thermal properties (although Boltzmann's work is not referenced). For the case considered above, a pair of equations analogous to Eqs. (69) and (70) is obtained, with the exception that motion induced by the phase change is not permitted. The equations are integrated twice to obtain two simultaneous nonlinear integral equations, coupled by a transcendental integral equation for the growth constant β . An iterative process for the solution is suggested, which appears inferior from the point of view of computational effort, to the direct integration procedure employed above (although this point is somewhat difficult to judge, since no numerical examples are given). Tirska also considers similarly Stefan's problem of uniform melting-front velocity, which corresponds to the steady-state ablation of a semi-infinite slab with temperature-dependent physical properties.

3. *Three-Region Problems*

Lightfoot (L5, L6) considered the solidification of a semi-infinite steel mass in contact with a semi-infinite steel mold, where the thermal properties of the phases were taken to be identical. In a later paper, (L7) different thermal constants for the liquid and solid metal and for the mold were assumed. With uniform initial phase temperatures, it is seen that all boundaries of the system are immobilized in η -space. Yang (Y2) rederived this result and further extended the application of the similarity transformation to three-region problems with induced motion. An example is the condensation of vapor, as a result of sudden pressurization, in a tank with relatively thick walls.

C. ABLATING SLABS

1. *Landau's Transformation*

Because of the uncertainty in the position of the free boundary relative to the fixed boundary in finite slabs, it is natural to attempt a transformation which fixes the positions of both boundaries. For example, if a new variable is introduced which expresses the position of a particle as the ratio of its distance from the free boundary to the instantaneous thickness of the original phase, the free boundary is immobilized, while the fixed boundary remains stationary with respect to the new coordinates. This transformation appears to have been given first by Landau (L4) in a

consideration of ablating slabs in which the melt is continuously and immediately removed. The problem is described by

$$\rho c_p \frac{\partial T}{\partial t} = \frac{\partial}{\partial x} \left(k \frac{\partial T}{\partial x} \right); \quad X(t) < x < a, \quad t > 0 \quad (75)$$

$$T(x, 0) = T_0(x) \leq T_m; \quad 0 \leq x \leq a \quad (76)$$

$$\frac{\partial T(a, t)}{\partial x} = 0; \quad t > 0 \quad (77)$$

$$H(t) = -k \frac{\partial T(X(t), t)}{\partial x} + \rho L \dot{X}; \quad t > 0 \quad (78)$$

where $H(t)$ is the heat input, equal to the rate of heat flow into the solid plus the rate of heat absorption by melting. The face at $x = a$ has been assumed to be insulated. There will be a premelting and a postmelting period, defined by

$$\begin{aligned} \dot{X} &= 0 & \text{when } T(X(t), t) < T_m \\ \dot{X} &\geq 0 & \text{when } T(X(t), t) = T_m \end{aligned} \quad (79)$$

The moving boundary is eliminated by the transformation

$$\xi = \frac{a - x}{a - X(t)} \quad (80)$$

so that the boundaries are now fixed at $\xi = 0$ and $\xi = 1$. The governing equation and boundary conditions become

$$\rho c_p \left[\frac{\partial T}{\partial t} + \frac{\xi \dot{X}(t)}{a - X(t)} \frac{\partial T}{\partial \xi} \right] = \frac{1}{[a - X(t)]^2} \frac{\partial}{\partial \xi} \left(k \frac{\partial T}{\partial \xi} \right) \quad (81)$$

$$T(x, 0) = T_0(\xi) < T_m; \quad 0 \leq \xi \leq 1, \quad t = 0 \quad (82)$$

$$\frac{\partial T}{\partial \xi} = 0; \quad \xi = 0, \quad t > 0 \quad (83)$$

$$H(t) = \frac{k}{a - X(t)} \frac{\partial T}{\partial \xi} + \rho L \dot{X}; \quad \xi = 1, \quad t > 0 \quad (84)$$

$$\dot{X} = 0 \quad \text{when } T(1, t) < T_m, \quad \xi = 1 \quad (85)$$

$$\dot{X} \geq 0 \quad \text{when } T(1, t) = T_m, \quad \xi = 1 \quad (86)$$

Equation (82) states that the slab is initially below the melting temperature. Gauss's theorem applied to the heat conduction equation over a region Σ with boundary B in the (x, t') plane bounded by the lines $t' = 0$, $t' = t$, $x = a$, and the curve $x = X(t')$ gives

$$0 = \iint_{\Sigma} \left[\frac{\partial}{\partial x} \left(k \frac{\partial T}{\partial x} \right) - c_p \rho \frac{\partial T}{\partial t'} \right] dx dt' = \int_B \left[k \frac{\partial T}{\partial x} dt' + c_p \rho T dx \right] \quad (87)$$

where

$$\int_B k \frac{\partial T}{\partial x} dt' = \int_0^t [H(t') - \rho L \dot{X}(t')] dt' = \int_0^t H(t') dt' - \rho L X(t) \quad (88)$$

$$\int_B c_p \rho T dx = \int_0^a c_p \rho T_0(x) dx - \int_{X(t)}^a c_p \rho T(x, t) dx - \int_0^t c_p \rho T_m \dot{X}(t') dt' \quad (89)$$

so that

$$\begin{aligned} \int_0^t H(t') dt' &= \int_{X(t)}^a \rho c_p [T(x, t) - T_0(x)] dx \\ &\quad + \rho [(L + c_p T_m) X(t) - \int_0^{X(t)} c_p T_0(x) dx] \quad (90) \end{aligned}$$

The same result can be obtained, in a less elegant manner, by a macroscopic heat balance. For the special case of a semi-infinite slab with constant heat input rate H , the temperature distribution in the premelting period has been given previously by Hartree (H6):

$$\begin{aligned} T(x, t) &= T_0 + 2H \left(\frac{t}{k c_p \rho} \right)^{1/2} \left[\pi^{1/2} \exp \left\{ -\frac{x^2}{4\alpha t} \right\} - \frac{x}{2(\alpha t)^{1/2}} \operatorname{erfc} \left(\frac{x}{2(\alpha t)^{1/2}} \right) \right] \\ &= T_0 + 2H \left(\frac{t}{k c_p \rho} \right)^{1/2} \left[i \operatorname{erfc} \left(\frac{x}{2(\alpha t)^{1/2}} \right) \right] \quad (91) \end{aligned}$$

where, in Hartree's notation,

$$i \operatorname{erfc} x = \int_x^\infty \operatorname{erfc} z dz$$

The time when melting starts is therefore

$$t_m = \frac{\pi}{4} \frac{k c_p \rho}{H^2} (T_m - T_0) = \alpha \left(\frac{L \rho m_1}{H} \right)^2 \quad (92)$$

where

$$m_1 = \frac{\pi^{1/2}}{2} \frac{c_p (T_m - T_0)}{L} \quad (93)$$

is proportional to the ratio of the specific enthalpy of the initial solid and liquid, and the datum condition is taken to be solid at the fusion temperature. For the semi-infinite case an appropriate distance variable for immobilizing the moving boundary is $\xi_1 = x - X(t)$. Since

$$x - X(t) = \lim_{a \rightarrow \infty} a \{ 1 - (a - x) / [a - X(t)] \},$$

this is a special case of the transformation defined by Eq. (80). It is convenient also to introduce the dimensionless variables

$$\theta^* = \theta^*(z^*, y) = \frac{T - T_0}{\pi^{1/2} (T_m - T_0)} \quad (94)$$

$$z^* = \frac{x - X(t)}{(\alpha t_m)^{1/2}} \quad (95)$$

$$y = \frac{t}{t_m} - 1 \quad (96)$$

$$U^* = \frac{\rho L}{H} \frac{X}{t_m} \quad (97)$$

$$U_y^* = \frac{dU^*}{dy} = \frac{\rho L}{H} \frac{dX}{dt} \quad (98)$$

The equations for the melting process now become

$$\frac{\partial \theta^*}{\partial y} = \frac{\partial^2 \theta^*}{\partial z^{*2}} + m_1 U_y^* \frac{\partial \theta^*}{\partial z^*}; \quad z^* > 0, \quad y > 0 \quad (99)$$

$$\theta^* = i \operatorname{erfc} \left(\frac{z^*}{2} \right); \quad z^* \geq 0, \quad y = 0 \quad (100)$$

$$\theta^* \rightarrow 0; \quad z^* \rightarrow \infty, \quad y \geq 0 \quad (101)$$

$$1 = -2 \frac{\partial \theta^*}{\partial z^*} + U_y^*; \quad z^* = 0, \quad y > 0 \quad (102)$$

$$\theta^* = \pi^{-1/2}; \quad z^* = 0, \quad y \geq 0 \quad (103)$$

These equations contain only one parameter m_1 , which is absent from the initial and boundary conditions, so that numerical integration is facilitated.

A steady-state solution, previously given by Soodak (S9), is obtained by setting the left-hand side of Eq. (99) equal to zero in which case U_y^* is a constant from Eq. (102). The steady-state solutions are

$$\theta^* \rightarrow \theta^*(z^*) = \pi^{-1/2} \exp(-m_1 \tilde{U}_y^* z^*) \quad (104)$$

with

$$\tilde{U}_y^* = (1 + 2m_1 \pi^{-1/2})^{-1} \quad (105)$$

or in terms of the original variables

$$\tilde{X} \rightarrow m_2 = \frac{H}{\rho[L + c_p(T_m - T_0)]} \quad (106)$$

To obtain the steady-state thickness melted it is necessary to refer to the integral heat balance, Eq. (90), in dimensionless form

$$U^*(y) = \tilde{U}_y^*(y + 1) - 2 \int_0^\infty \theta^*(z^*, y) dz^* \quad (107)$$

From Eq. (104) this becomes

$$\tilde{U}^*(y) = \tilde{U}_y^*(y + 1) - 2/\pi^{1/2} m_1 \quad (108)$$

or

$$X(t) \rightarrow m_2 t - \frac{k(T_m - T_0)}{H} \quad (109)$$

for large times.

Landau also gives solutions of Eqs. (99) to (103) for the limiting cases

$m_1 = 0$ and $m_1 = \infty$. For $m_1 = 0$ the equations are linear and the solution is

$$\begin{aligned} \theta_0^*(z^*, y) = & \pi^{-1/2} \operatorname{erfc}(z^*/2y) \\ & + (4\pi y)^{-1/2} \int_0^\infty i \operatorname{erfc}\left(\frac{z^*}{2}\right) \\ & \left\{ \exp\left[\frac{-(z^* - z)^2}{4y}\right] - \exp\left[\frac{-(z^* + z)^2}{4y}\right] \right\} dz \quad (110) \end{aligned}$$

This solution, which corresponds to negligible sensible heat effects, can be used to start the numerical integration for any finite m_1 , since, in Eq. (99), $U_y^*(0) = 0$. The case $m_1 = \infty$ is well approximated, for example, by the melting of steel originally at room temperature. Here $m_1 = 27$, so that latent heat effects play a very small role. Some modification of the transformed variables is necessary to get the equations into convenient form for numerical integration.

For $m_1 > 0$ the time derivative was approximated by a forward difference ratio and the space derivatives by central difference ratios. It is known (E4, F2) that the solution to the difference approximation to the heat conduction equation will not be stable unless the ratio $(\Delta y/\Delta z^*) \leq \frac{1}{2}$. Stability implies that small perturbations introduced by rounding off or truncation are damped out instead of being magnified. Taking this ratio to be $\frac{1}{2}$, the difference approximation to Eq. (99)

$$\begin{aligned} \theta^*(i, j+1) - \theta^*(i, j) = & \frac{\Delta y}{\Delta z^*} \left\{ \theta^*(i+1, j) - 2\theta^*(i, j) - \theta^*(i-1, j) \right. \\ & \left. + m_1 U_{ij}^* \frac{\Delta z^*}{2} [\theta^*(i+1, j) - \theta^*(i-1, j)] \right\} \quad (111) \end{aligned}$$

simplifies to

$$\begin{aligned} \theta^*(i, j+1) = & \frac{1}{2}(1 + m_1 U_{ij}^* \Delta z^*/2) \theta^*(i+1, j) \\ & + \frac{1}{2}(1 - m_1 U_{ij}^* \Delta z^*/2) \theta^*(i-1, j) \quad (112) \end{aligned}$$

To compute U_y^* a third-order formula for $(\partial\theta^*/\partial z^*)$ at $z^* = 0$ was used, giving, with Eqs. (102) and (103),

$$U_{ij}^* = 1 + (\Delta z^*)^{-1} [(-11/3\pi^{1/2}) + 6\theta^*(1, j) - 3\theta^*(2, j) + \frac{2}{3}\theta^*(3, j)] \quad (113)$$

This is an initial-value problem, with results for fixed j and all i being computed before going on to $j+1$. The values of the melting rate for a semi-infinite solid are plotted against time in Fig. 4 for various values of the subcooling parameter m_1 . At small times after the start of melting the dimensionless melting rate is nearly the same for all m_1 , but the steady-state condition is approached more rapidly for m_1 large.

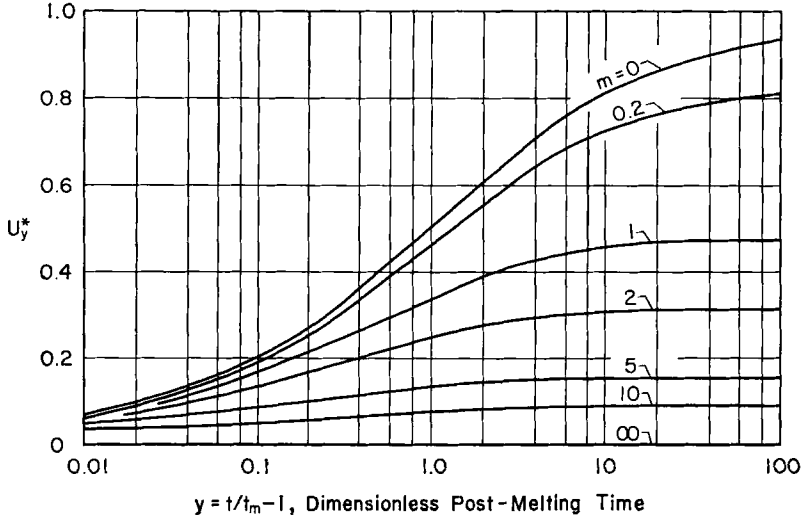


FIG. 4. Rate of melting of semi-infinite solid for various values of m_1 (L4). Reproduced by permission of Quarterly of Applied Mathematics.

2. Temperature-Dependent Thermal Properties

Citron (C4) generalizes Landau's derivation of the steady-state melting rate of a semi-infinite solid with instantaneous removal of the melt to temperature-dependent thermal conductivity and specific heat, expressible in the form

$$\begin{aligned} k(T) &= \sum_{n=0}^{N_1} k_n (T/T_m)^n \\ c_p(T) &= \sum_{n=0}^{N_2} c_{pn} (T/T_m)^n \end{aligned} \quad (114)$$

Under the transformation $\xi_1 = x - X(t)$, the heat equation becomes

$$\frac{\partial}{\partial \xi_1} \left[k(T) \frac{\partial T}{\partial \xi_1} \right] + \rho c_p(T) \dot{X} \frac{\partial T}{\partial \xi_1} = \rho c_p(T) \frac{\partial T}{\partial t}; \quad T = T(\xi_1, t) \quad (115)$$

with boundary conditions

$$T(0, t) = T_m \quad (116a)$$

$$T(\infty, t) = T_\infty \quad (116b)$$

$$T(\xi_1, t_m) = T_0(\xi_1) \quad (116c)$$

$$H_1(t) = -k(T_m) \frac{\partial T(0, t)}{\partial \xi_1} + \rho L \dot{X} \quad (116d)$$

Upon setting the right-hand side of Eq. (115) equal to zero, corresponding to steady-state melting, and making use of Eq. (114), one obtains after an integration

$$\sum_{n=0}^{N_1} k_n \left(\frac{T}{T_m} \right)^n \frac{dT}{d\xi_1} + \rho \tilde{X} T_m \sum_{n=0}^{N_2} \frac{c_{pn}}{n+1} \left(\frac{T}{T_m} \right)^{n+1} = \rho \tilde{X} T_m \sum_{n=0}^{N_2} \frac{c_{pn}}{n+1} \left(\frac{T_\infty}{T_m} \right)^{n+1} \quad (117)$$

With the aid of Eq. (116d), the steady-state melting rate \tilde{X} is found to be

$$\frac{\rho L \tilde{X}}{H_1} = \frac{1}{\{1 + (T_m/L) \sum_{n=0}^{N_2} [c_{pn}/(n+1)][1 - (T_\infty/T_m)^{n+1}]\}} \quad (118)$$

which, for constant specific heat, reduces to

$$\frac{\rho L \tilde{X}}{H_1} = \frac{1}{\{1 + [c_p(T_m - T_\infty)/L]\}} \quad (119)$$

It is shown that the melting rates for copper, evaluated upon the assumptions of temperature-dependent and temperature-independent properties, differ by approximately 10%. This is in agreement with the computation of Hamill and Bankoff (H4) in the solidification of a semi-infinite copper melt. The temperature distribution is found by integration of Eq. (117), and bounds are established for the amount of material melted in a manner similar to that employed by Landau. As expected, the largest melting rate possible is the steady-state one.

The method is later extended to time-varying heat inputs on one face with arbitrary boundary conditions on the back face (C7). Citron also has given a simple method of successive approximations for the finite ablating slab (C6) which is shown to converge rapidly for constant heat input.

3. Transient Heat Conduction in a Finite Slab

Sanders (S1) gives the first exact solution for transient heat conduction in a melting finite slab. The problem is that described by Landau, Eqs. (81)–(86), whose transformation to immobilize the moving boundary, $\xi = (a - x)/[a - X(t)]$, is also employed. Introducing the dimensionless variables $\theta^*(\xi, t) = [T(\xi, t) - T_m]/T_m$; $X^* = X/a$ the problem can be stated as

$$t_c(1 - X^{*2}) \frac{\partial \theta^*}{\partial t} = \frac{\partial^2 \theta^*}{\partial \xi^2} - \xi[(1 - X^*)\dot{X}^* t_c] \frac{\partial \theta^*}{\partial \xi}; \quad \begin{matrix} 0 < \xi < 1 \\ t > 0 \end{matrix} \quad (120)$$

$$\theta^*(\xi, 0) = \theta_0^*(\xi) \quad (121)$$

$$\frac{\partial \theta^*}{\partial \xi}(0, t) = 0 \quad (122)$$

$$\theta^*(1, t) = 0 \quad (123)$$

$$H_2(t) = \frac{T_m k}{a(1 - X^*)} \frac{\partial \theta^*(1, t)}{\partial \xi} + \rho L a \dot{X}^* \quad (124)$$

where the characteristic time t_c is given by

$$t_c = \rho c_p a^2 / k \quad (125)$$

For arbitrary surface heat fluxes the problem must be solved numerically. However, if the desired quantity is the surface heat flux necessary to produce a specified free-boundary motion, Eqs. (120)–(124) become linear. By a judicious choice of X^* a closed-form solution can be obtained. This procedure was previously followed by Baer and Ambrosio (B1) for the semi-infinite slab. With the choice

$$(1 - X^*)^2 = 1 - 4A^2 t / t_c, \quad (126)$$

the bracketed term in Eq. (120) is a constant, namely $2A^2$. After changing independent variables by setting $\xi^+ = A\xi$, Eq. (120) becomes

$$\frac{t_c(1 - X^*)^2}{A^2} \frac{\partial \theta^*}{\partial t} = \frac{\partial^2 \theta^*}{\partial \xi^{+2}} - 2\xi^+ \frac{\partial \theta^*}{\partial \xi^+}; \quad 0 < \xi^+ < A, \quad t > 0 \quad (127)$$

Note that Eq. (126) implies a nonzero initial velocity of the free boundary, in common with previous exact solutions, which were, however, self-similar. The present problem, while linear, is still in the form of a partial differential equation. However, it is readily solved by separation of variables, leading to an ordinary differential equation of the confluent hypergeometric form. The solution appears in terms of the confluent hypergeometric function of the first kind, defined by

$${}_1F_1(\gamma_1; \gamma_2; x) \equiv 1 + \frac{\gamma_1}{\gamma_2} \frac{x}{1!} + \frac{\gamma_1(\gamma_1 + 1)}{\gamma_2(\gamma_2 + 1)} \frac{x^2}{2!} + \dots \quad (128)$$

The eigenvalue equation based on the boundary condition in Eq. (123) is of the form

$${}_1F_1(-\Lambda_1; \tfrac{1}{2}; A^2) = 0 \quad (129)$$

with an infinite number of real roots for the separation constant Λ_1 . A complete set of orthogonal eigenfunctions with real eigenvalues results. The computational labor is considerably lessened if the initial temperature distribution in Eq. (121) is chosen to be given by the eigenfunction corresponding to the lowest eigenvalue, since the orthogonality property then leads to a one-term solution. By examining two heat inputs numer-

ically it is found that \dot{X}^* is considerably more sensitive to small perturbations in the heat flux than $X^*(t)$, as might be expected.

D. GROWTH OF A VAPOR FILM ON A RARIDLY HEATED PLANE SURFACE

An interesting class of exact self-similar solutions (H2) can be deduced for the case where the newly formed phase density is a function of temperature only. The method involves a transformation to Lagrangian coordinates, based upon the principle of conservation of mass within the new phase. A similarity variable akin to that employed by Zener (Z2) is then introduced which immobilizes the moving boundary in the transformed space. A particular case which has been studied in detail is that of a column of liquid, initially at the saturation temperature T_s , in contact with a flat, horizontal plate whose temperature is suddenly increased to a large value, $T_w \gg T_s$. Suppose that the density of nucleation sites is so great that individual bubbles coalesce immediately upon formation into a continuous vapor film of uniform thickness, which increases with time. Eventually the liquid-vapor interface becomes severely distorted, in part due to Taylor instability; but the vapor film growth, before such effects become important, can be treated as a one-dimensional problem. This problem is closely related to reactor safety problems associated with fast power transients. The assumptions made are:

- (1) The vapor obeys the ideal gas law.
- (2) The pressure of the vapor remains constant.
- (3) Radiative heat transfer may be neglected.
- (4) Viscous dissipation due to vapor dilation is negligible.
- (5) The thermal conductivity and specific heat of both vapor and liquid remain constant.

Assumptions (1) and (5) are more restrictive than absolutely necessary and are made principally for simplicity of the development. Actually, all that is necessary is that the physical properties, including density, thermal conductivity, and specific heat, of both phases be specified functions of temperature only.

The principal physical error is probably geometrical. Compared to this, the above assumptions are not unduly restrictive, although extremely fast high-power excursions at low pressures are ruled out by assumptions (2) and (3). Assumption (2) is more nearly fulfilled at high pressures with low liquid heads. Assumption (3) is acceptable in the vapor-film problem even when the radiative flux from the solid surface is appreciable, provided that the liquid (and, of course, vapor) is nearly transparent.

Considering first the case where the liquid is initially at the saturation

temperature, the governing equations for energy transport and continuity in the vapor are

$$\rho c_p \left[\frac{\partial T}{\partial t} + u_x \frac{\partial T}{\partial x} \right] = k \frac{\partial^2 T}{\partial x^2} \quad (130)$$

where u_x is the velocity of the vapor away from the plate and

$$\frac{\partial \rho}{\partial t} + \frac{\partial(\rho u_x)}{\partial x} = 0 \quad (131)$$

The boundary conditions are

$$T(0, t) = T_w; \quad T(X(t), t) = T_s \quad (132)$$

$$-k \frac{\partial T(X(t), t)}{\partial x} = L \frac{d}{dt} \int_0^x \rho dx \quad (133)$$

Upon introducing the Lagrangian coordinate m_* defined by

$$m_*(x) = \int_0^x \rho dx \quad (134)$$

and the ideal gas assumption

$$\rho = p/R_g T \quad (135)$$

one gets

$$\frac{\partial T}{\partial t} = \alpha_* \frac{\partial}{\partial m_*} \left(\frac{1}{T} \frac{\partial T}{\partial m_*} \right) \quad (136)$$

where $\alpha_* = kp/c_p R_g$.

A new similarity variable is now introduced, defined by

$$\psi = \frac{m_*}{M_*}; \quad M_* = m_*(X) \quad (137)$$

so that Eq. (136) becomes

$$\frac{\partial T}{\partial t} - \frac{\psi}{M_*} \frac{\partial T}{\partial \psi} \frac{dM_*}{dt} = \frac{\alpha_*}{M_*^2} \frac{\partial}{\partial \psi} \left(\frac{1}{T} \frac{\partial T}{\partial \psi} \right) \quad (138)$$

It is convenient to introduce the variables

$$\tau_* = \frac{\alpha_* t}{T_s} = \rho_s^2 \alpha_s t; \quad \theta_1 = \frac{T}{T_s}; \quad \Lambda = \frac{L}{c_p T_s}; \quad q = M_*^2 \quad (139)$$

where α_s is the thermal diffusivity of the vapor evaluated at the saturation density ρ_s .

Equation (138) then becomes

$$q \frac{\partial \theta_1}{\partial \tau_*} = \frac{\partial}{\partial \psi} \left(\frac{1}{\theta_1} \frac{\partial \theta_1}{\partial \psi} \right) + \frac{\psi}{2} \frac{\partial \theta_1}{\partial \psi} \frac{dq}{d\tau_*} \quad (140)$$

subject to the conditions

$$\frac{\partial \theta_1(1, \tau_*)}{\partial \psi} = -\frac{L}{2} \frac{dq}{d\tau_*} \quad (141)$$

$$\theta_1(1, \tau_*) = 1, \quad \theta_1(0, \tau_*) = \theta_w(\tau_*) \quad (142)$$

In searching for self-similar solutions, it follows that the left-hand side of Eq. (140) must vanish, and from Eqs. (141) and (142) that $(dq/d\tau_*)$ and θ_w must be constant. Equation (140) then reduces to an ordinary differential equation

$$\frac{d}{d\psi} \left(\frac{1}{\theta_1} \frac{d\theta_1}{d\psi} \right) + \frac{\psi}{2} \frac{d\theta_1}{d\psi} \frac{dq}{d\tau_*} = 0 \quad (143)$$

Defining the growth constant β_* by $dq/d\tau_* = 4\beta_*^2$,

$$M_* = 2\beta_* \tau_*^{1/2} \quad (144)$$

Hence for constant wall temperature the mass of vapor, although not the position of the free boundary, increases as the square root of time. This is thus a generalization of the Stefan constant-density similarity solution. Equation (143), subject to the two initial conditions at $\psi = 1$, is readily solved by numerical integration. A plot of dimensionless flux into the interface versus the dimensionless wall temperature is given in Fig. 5. Analytic approximations by casting the equations into the form of a nonlinear Volterra integral equation can also be established (H3), in good agreement

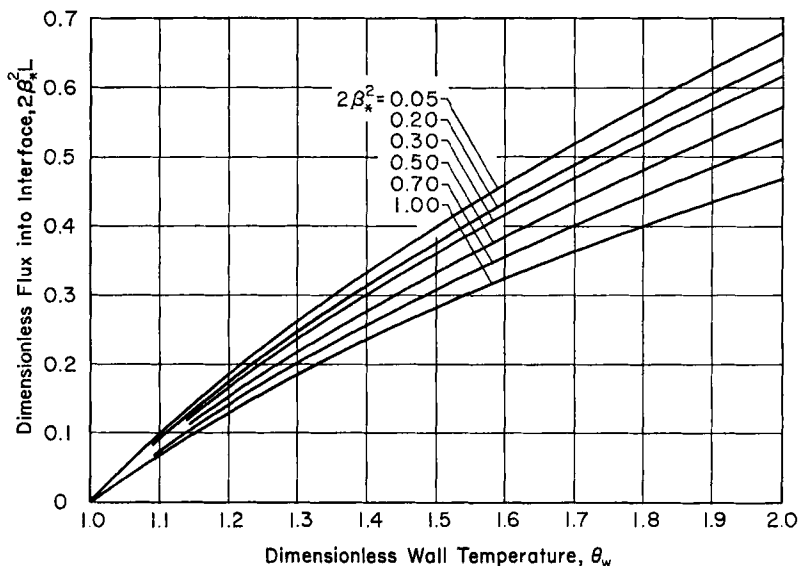


FIG. 5. Dimensionless heat flux versus plate temperature in the growth of a vapor film at the surface of a suddenly heated plate in contact with liquid (H2). Reproduced by permission of Pergamon Press.

with the exact numerical solution. Finally, the restriction that the liquid be initially at the saturation temperature can be relaxed. For any constant liquid subcooling, a fictitious latent heat of vaporization can be defined, which is shown to cast the problem into the same form as for the saturated liquid.

III. Analytic Approximation Methods

A. QUASI-STATIONARY AND QUASI-STEADY-STATE APPROXIMATIONS

1. *Introduction*

On one or both sides of the moving boundary there will be a concentration (or temperature) boundary layer at any instant whose thickness increases with time. Within this layer the concentration has been substantially affected by diffusion to or from the interface. Outside this region the concentration has not been greatly affected by the imposition of the interface boundary condition. It is possible to find approximate solutions when the rate of growth of the boundary layer thickness is either large or small compared to the interface velocity. The former case, where a thin thermal boundary layer is assumed, will be examined in detail in the next volume for the growth of a vapor bubble in a superheated liquid. The latter simplification, which we shall call the quasi-stationary approximation, implies that the boundary motion can be neglected in computing the diffusant distribution. If, in addition, the concentrations on the boundaries of the region are time independent, and the thermal boundary layer thickness is at least comparable to a characteristic dimension of the system, a quasi-steady condition will prevail, governed approximately by the Laplace equation. This method has been applied, for example, to the growth of ice crystals or to the tarnishing of metals. In a sense these are all perturbation methods, in which the solution is expanded in a series of powers of a small parameter, which is a familiar technique in the approximate solution of nonlinear differential equations.

2. *Growth of Small Particles of a Condensed Phase*

The quasi-steady-state theory has been applied particularly where a condensed phase exists whose volume changes slowly with time. This is true, for example, in the sublimation of ice or the condensation of water vapor from air on liquid droplets (M3, M4). In the condensation of water vapor onto a spherical drop of radius $R(t)$, the concentration of water vapor in the surrounding atmosphere may be approximated by the well-known spherically symmetric solution of the Laplace equation:

$$c \equiv \frac{C(r) - C_\infty}{C_i - C_\infty} = \frac{R}{r}, \quad r > R(t) \quad (145)$$

This can be used to compute the diffusive flux at the surface of the sphere, which determines its rate of mass increase:

$$4\pi R^2 C' \dot{R} = 4\pi R^2 D \frac{\partial C(R, t)}{\partial r} = 4\pi R D (C_\infty - C_i) \quad (146)$$

Upon integrating, the radius of the condensed phase is

$$R = \left(\frac{2D(C_\infty - C_i)t}{C'} \right)^{1/2} \quad (147)$$

assuming $R(0) = 0$, and that Eq. (145) holds for all $t > 0$. A heat balance similarly gives

$$LC'R\dot{R} = k(T_i - T_\infty) \quad (148)$$

Finally, an interface equilibrium relation of the form

$$C_i = C_i(T_i) \quad (149)$$

serves, together with Eqs. (147) and (148), to determine uniquely the growth velocity in terms of the atmospheric conditions at infinity, C_∞ and T_∞ .

Kirkaldy (K2) points out that the operation of discarding the time dependence to obtain Eq. (145) and reintroducing it in Eq. (146) is mathematically untenable. This was his motivation in establishing exact similarity solutions (Section II, B, 1, a). Thus, by employing the exact solution [Eqs. (28) and (33)] to evaluate the interfacial concentration gradient in Eq. (146), a means is afforded for testing the quasi-stationary assumption. If it is assumed initially that $\beta_3 \ll 1$, so that the first term in the exponent of Eq. (33) can be neglected, one obtains, upon substituting into the mass balance in Eq. (146),

$$\beta_3 \cong \left[\frac{2(C_\infty - C_i)}{C'} \right]^{1/2} \sim 10^{-4} \quad (150)$$

for the growth of an ice crystal under typical atmospheric conditions, which validates the assumption. The growth velocity is then

$$\dot{R} = \left[\frac{D(C_\infty - C_i)}{2tC'} \right]^{1/2} \quad (151)$$

which is identical with the value obtained from the quasi-stationary theory. Equation (150) is equivalent to the statement that the interface velocity is small compared to the rate of growth of the diffusion boundary layer thickness. Note, however, that an additional approximation is made when the concentration gradient at the interface is computed from the steady-state solution. Kirkaldy is of the opinion that the quasi-steady-

state theory should not be used in infinite regions, since steady-state conditions are not achieved in a finite time. In finite regions, however, after a sufficient time has elapsed for the diffusion boundary layer thickness to equal some characteristic dimension of the system, the steady-state approximation is thought to be more justified. The exact theory is, however, restricted to relatively simple boundary and initial conditions, so that an approximate solution is frequently invoked. What is clear from Kirkaldy's analysis is that the neglect of the convective term in the diffusion equation is justified when the boundary velocity is small compared to that of the edge of the diffusion boundary layer. In this case the problem is reduced to a heat conduction or diffusion problem in a stationary medium, with well-known methods of solution. The literature is quite extensive, several books having been partially devoted to the subject (M5, T5). We shall here content ourselves with indicating briefly the major ideas of some of the more pertinent recent work.

Reiss and La Mer (R4), in a consideration of the nucleation and growth of a cloud of colloidal particles, consider various approximations. Each particle is assumed to lie at the center of a spherical volume, whose radius is determined by the particle concentration. A preliminary approach neglects the boundary motion, so that an exact solution to this approximate problem is readily obtained. A quasi-steady state for the diffusion is now assumed, equivalent to neglecting the time derivative in the diffusion equation, and limiting conditions for the two solutions closely to agree examined. Finally, the approximate method is applied to the moving boundary problem by the methods noted above. Application is made to two problems which arise in practice. One problem deals with the possibility of spontaneous nucleation, in accordance with the Becker-Döring theory (B4), upon suddenly cooling an aerosol system (typically naphthalene) with some predetermined number density of artificial nuclei. No supersaturation can be supported at the surface of these growing particles. Spontaneous nucleation is presumed to occur if the supersaturation at the surface of the surrounding spherical volume reaches the critical value, calculated from fluctuation theory. In the particular case of a naphthalene aerosol, it is found that spontaneous nucleation will not occur if the number density of nuclei exceeds 100/cc. A second problem deals with the rate of growth of sulfur hydrosols, measured by Zaiser and La Mer (Z1). Reiss (R3) shows separately that a nonuniform colloidal dispersion will tend to increase in uniformity as diffusion-controlled growth proceeds, since the rate of increase of the square of the particle radius is approximately the same for all particles at any instant.

Similar methods are applied by Kuczynski and Landauer (K7) to the diffusion of carbon in metallic carbides, in which a metal-carbon

reaction takes place at the free boundary; and by Nielsen (N2) in discussing the kinetics of crystal growth in KClO_4 precipitation. Nielsen also gives an approximate treatment of the increase in diffusional flux resulting from convection of the fluid past the particles. Ham (H1) gives a consolidated statement of the theory of diffusion-limited precipitation of a condensed phase. Only major features are discussed here; the original reference should be consulted for details. In all cases the convective term is neglected in the diffusion equation (quasi-stationary approximation). A simple cubic periodic lattice of spherical precipitate particles is first considered. By replacing the cubic cell surrounding one particle of radius R with a sphere of equivalent radius r_s and initially neglecting the motion of the particle boundary, the diffusion equation for an initially uniform supersaturation can be solved exactly. The eigenfunctions for the spatial variation are trigonometric, while the time-dependence for each term is exponential. After an initial transient, given by $t \gg \tau_1$, where $\tau_1 \cong r_s^2/(4.5)^2 D$, the average supersaturation decreases as $\exp(-t/\tau_0)$, where $\tau_0 \cong r_s^3/3RD$, for $R/r_s \ll 1$. Note that τ_1 represents a time for the diffusion boundary layer radius to become appreciable compared to the cell radius, so that higher-order terms might frequently be expected to be significant. Ham, however, computes that a fractional error of only $(108/175)(R/r_s)^2$ is made in calculating the precipitation during the transient, neglecting all but the leading term. Even when R/r_s is not small, the flux can be calculated for small times as though each particle were isolated in an infinite medium, and for large times by the first term in the eigenfunction expansion. The approximate result thus obtained is nowhere in error by more than 1%. The boundary motion is then taken into account, using only the zero-order eigenfunction and eigenvalue, determined from the instantaneous value of R . This leads to $R\dot{R} = D\bar{C}_e/C_e'$, a result identical with that obtained by Wert and Zener (W3) from a simpler analysis. For large times the unprecipitated fraction of the initial supersaturation decreases exponentially with time and is a weak function of the initial ratio of the mass of precipitate to the excess in solution. A variational method can be employed for small R/r_s and for $t \gg \tau_1$, since the Laplace equation approximately describes the concentration field, and only the lowest eigenvalue need be estimated by the Rayleigh principle. This allows extension to spheroidal and to cylindrical particles, as well as to reaction-controlled precipitation. The effect of a distribution of dissimilar particles or a nonperiodic array is also considered and is shown to be very small for $R/r_s < 0.1$.

Ham further shows that the free-boundary problem, starting with a precipitate particle of negligible dimensions, is not unique, since an arbitrary spheroid will grow at constant eccentricity, its dimensions being

proportional to $t^{1/2}$. The time-dependence of the unprecipitated fraction of the solute is found to be of the form $\exp(-bt^n)$ for small t . For spheroids $n = \frac{3}{2}$, and for cylindrical particles $n = 1$; but regardless of particle shape, the unprecipitated fraction decreases exponentially with time ($n = 1$) when the fraction is less than $\frac{1}{2}$.

Buikov and Dukhin (B14) treat the complete problem of the evaporation or growth of stationary drops by neglecting the convective terms and the boundary motion in solving the diffusion equations. Three coupled diffusion equations are considered: two for the transport of heat and mass in the vapor, and the third for heat conduction within the drop. By a limiting process it is shown that, for sufficiently slow growth rates, the quasi-steady-state approximation applies wherein the drop temperature is spatially uniform, and the vapor density and temperature fields in the vicinity of the drop follow the changes in the drop temperature instantaneously. Dennis (D2) studied the growth of hygroscopic drops in an air stream of controlled humidity and temperature. The 0.5–1 mm. drops were suspended on a pair of crossed filaments, and the motion observed with a microscope. H_2SO_4 , NH_4NO_3 , NaCl , and CaCl_2 solutions were used. The results were found to be in agreement with the quasi-steady-state treatment originally derived by Maxwell (M6), and quoted, among others, by Fuchs (F9) and Mason (M5), employing the simplified humidification equation:

$$R\dot{R} = \frac{k_v(T_0 - T_\infty)}{L\rho} \quad (152)$$

A "ventilation factor" was introduced originally by Frossling (see D2) to account for the increased rate of growth or evaporation in a moving air stream. For evaporating water droplets, Frossling finds this factor to be $(1 + 0.229\text{Re}^{1/2})$ over the Reynolds number range $2.3 < \text{Re} < 1380$. This form was slightly modified by Kinzer and Gunn (K1). Charlesworth and Marshall (C3) considered the evaporation of drops containing dissolved solids.

In some cases, particularly in the growth of aerosol particles, the assumption of equilibrium at the interface must be modified. Frisch and Collins (F8) consider the diffusion equation, neglecting the convective term, and the form of the boundary condition when the diffusional jump length (mean free path) becomes comparable to the radius of the particle. One limiting case is the boundary condition proposed by Smoluchowski (S7), $C(R, t) = 0$, which presumes that all molecules colliding with the interface are absorbed there (equivalent to zero vapor pressure). A more realistic boundary condition for the case when the diffusion jump length, $\langle z \rangle \ll R$, has been shown by Collins and Kimball (C11) and Collins (C10) to be

$$\frac{\partial C(R, t)}{\partial r} = \frac{\gamma}{Z} C(R, t) \quad (153)$$

where $\gamma < 1$ is the probability that an incident vapor molecule will be absorbed at the particle surface and

$$Z = \frac{\int_0^\infty z^2 \phi_1(z) dz}{\int_0^\infty z \phi_1(z) dz} = \frac{\langle z^2 \rangle}{\langle z \rangle} \quad (154)$$

Here $\phi_1(z)$ is the free path length distribution function. It is shown, by reference to the governing integrodifferential equation, that a boundary condition of this form is applicable even for long mean free paths, providing that $t \gg \nu_f^{-1} = \langle z^2 \rangle / 6D$, where ν_f is the mean jumping frequency. For the usual aerosol systems, $t \sim 10^{-6}$ – 10^{-7} sec., and hence is a fraction less than 10^{-3} of the time required to grow a stable droplet. The competition between droplets for the diffusant (equivalent to considering each droplet to be enclosed in a finite vapor volume), and the effect of a time-dependent source function are also considered. In a later paper Frisch and Collins (F8) extend their previous stationary boundary analysis to include the effects of the moving boundary, still neglecting the convective term in the diffusion equation. A growth equation is derived for a plurality of competing sinks, which is shown to be in satisfactory agreement with experimental data for the growth of BaSO_4 crystals. Several interesting extensions are made. One is to the growth of a single particle with a variable absorption probability and a time-dependent source function. If $R_0 \ll \langle z \rangle$, where R_0 is the initial particle volume, γ will not, in general, be constant, because of both surface tension and temperature variation. The appropriate boundary condition is then

$$\frac{\partial C(R, t)}{\partial r} = \frac{\epsilon_1 \gamma(t)}{\rho} C(R, t) \quad (155)$$

where ϵ_1 is a correction factor, of the order of unity, arising from the fact that $\langle z \rangle$ may be large compared to R . This poses difficulties, but it can be cast into more tractable form by defining $C_*(R, t)$, the excess concentration of vapor molecules, as a result of partial reflection, over that which exists when all molecules impinging on the droplet are absorbed:

$$\frac{\partial C}{\partial r} = \frac{\epsilon_1}{Z} (C - C_*) \quad \text{at } r = R \quad (156)$$

This boundary condition is the diffusion analog of Newton's law of cooling in heat conduction theory. A noteworthy conclusion is that a polydisperse self-nucleating sol tends to become monodisperse, i.e., the initial size distribution becomes more peaked as growth progresses. Waite (W1)

gives a more general treatment of the kinetics of diffusion-limited reactions, based upon the change due to diffusion of the joint probability density that reactants A and B shall be some specified distance apart. For the reaction $A + B \rightarrow B$, this can be specialized to the case of the competitive growth of colloidal particles.

The growth of small particles has been followed experimentally by X-ray analysis, resistivity methods, direct observation, and light-scattering techniques. The work of La Mer and co-workers (B2, J1, L2, L3) on sulfur hydrosols, Turnbull (T4) and Collins and Leinweber (C12) on BaSO_4 precipitates, Morin and Reiss (M11) on the precipitation of lithium in germanium, Thomas (T2) on indium in zinc oxide, and Tweet (T6) on copper in germanium, may be especially mentioned. Using Ham's analysis, Morin and Reiss conclude that interstitial lithium precipitates in germanium around isolated lattice vacancies, in view of a measured $n = \frac{3}{2}$. On the other hand, Thomas and Tweet find that $n = 1$ fits their data and conclude that the nucleating centers were dislocation lines. Estimates are given of the nucleation center density.

3. *Accumulation of a Filter Cake*

Surprisingly enough, it is possible for the steady-state assumption in a moving-boundary system to be essentially exact. This occurs in the deposition of a filter cake under the influence of a constant pressure difference. An interesting example is given by Brenner (B13), in a study of the unconfined growth of a filter cake on a circular cloth-covered aperture in a plane wall. It is assumed that the velocity vector of the filtrate within the cake is everywhere and at all times proportional to the pressure gradient (Darcy's law).

$$\mathbf{u} = \frac{k_p g_c}{\mu} \nabla p \quad (157)$$

The fact that the permeability k_p is taken to be a constant scalar indicates that the filter cake is homogeneous, isotropic, and stationary in properties with time. Since the filtrate is incompressible, Eq. (157) leads immediately to Laplace's equation:

$$\nabla^2 p = 0 \quad (158)$$

The governing equation is therefore identical with that for the irrotational flow of an ideal fluid through a circular aperture in a plane wall. The stream lines and equipotential surfaces in this rotationally symmetric flow turn out to be given by oblate spheroidal coordinates. Since, from Eq. (157), the rate of deposition of filter cake depends upon the pressure gradient at the surface, the governing equation and boundary conditions are of precisely the same form as in the quasi-steady-state approximation

to the moving-boundary diffusion problem. Since solutions of Laplace's equation have been studied in detail, it seems probable that the same technique could be used to predict the growth of filter cakes in a variety of geometries with time-independent pressure conditions. The same technique would appear to be useful in predicting the shape of the moving interface in the displacement of a fluid in a porous medium by a second immiscible fluid.

B. INTEGRAL EQUATION METHODS

1. *Introduction*

As noted above, exact solutions for the free-boundary diffusion problem exist only for a restricted class of initial and boundary conditions. Approximation methods, or failing this, a direct numerical attack, are indicated for more general problems. In either case, it is frequently helpful to reformulate the differential equation and associated boundary and initial conditions into integral equation form. One powerful procedure leads to a functional equation for the moving boundary, which may be in suitable form for iterative attack. In other cases the formulation of integral equations leads to maximum and minimum bounds for melting-freezing rate with the aid of mean-value theorems, while still another method employs a polynomial approximation for the temperature, in the manner of the well-known Pohlhausen integral method for momentum boundary layers.

The classical method for solving linear boundary value problems in integral equation form is by means of Green's functions. The Green's function for heat conduction in a solid body with specified boundary conditions is the temperature distribution resulting from an instantaneous point source of heat of unit strength at any particular point in the body, when the initial temperature of the body is zero and homogeneous boundary conditions are imposed at the surface. The solution for the inhomogeneous heat equation with inhomogeneous initial and boundary conditions is obtained by superposing the effects of distributed volume and surface sources and sinks. Because of the nonlinearity of the moving-boundary diffusion problem these methods cannot be directly used to obtain a solution. However, by considering the boundary motion to be an arbitrary, but specified, function of time, the nonlinearity can be concentrated into an integrodifferential equation for the position of the phase interface.

2. *Green's Functions: Lightfoot's Method (L6)*

A natural application of the Green's function approach is to the case where the density, specific heat, and thermal conductivity remain essen-

tially unchanged as a result of the phase transformation, and there is no movement of either phase. In this case, the problem is equivalent to one of heat conduction in a uniform solid with the same initial and boundary conditions, subjected to a moving source surface whose strength is proportional to the local velocity of advance. Before proceeding with a general formulation of the problem, it may be advisable to review the properties of Green's functions for the heat diffusion equation (M2, M12). Consider the inhomogeneous equation

$$\mathfrak{L}\{T\} = \frac{Q(\mathbf{r}, t)}{k}; \quad \mathfrak{L} = \nabla^2 - \frac{1}{\alpha} \frac{\partial}{\partial t}, \quad T = T(\mathbf{r}, t) \quad (159)$$

where Q is the instantaneous volume rate of heat release at the point $P(\mathbf{r})$ in the closed volume V with surface Σ , subject to the initial condition

$$T(\mathbf{r}, 0) = T_0(\mathbf{r}). \quad (160)$$

Denote the value of the gradient of the temperature along the outward pointing normal to the surface by

$$\frac{\partial T(\mathbf{r}_s, t)}{\partial n} = g(\mathbf{r}_s, t) \quad (161)$$

and the value of the temperature on the surface by

$$T_s = T(\mathbf{r}_s, t), \quad t > 0, \quad (162)$$

where $P(\mathbf{r}_s)$ is a point on the surface Σ . The solution for the problem of the temperature distribution is given by

$$\begin{aligned} T(\mathbf{r}, t) &= \frac{1}{k} \int_0^{t^*} \int_V Q(\mathbf{r}_1, t_1) G(\mathbf{r}, t | \mathbf{r}_1, t_1) dV_1 dt_1 + \frac{1}{\alpha} \int_V T_0(\mathbf{r}_1) G(\mathbf{r}, t | \mathbf{r}_1, 0) dV_1 \\ &+ \int_0^{t^*} dt_1 \int_{\Sigma} \left[G(\mathbf{r}, t | \mathbf{r}_{s1}, t_1) \frac{\partial T(\mathbf{r}_{s1}, t_1)}{\partial n_1} - T(\mathbf{r}_{s1}, t_1) \frac{\partial G(\mathbf{r}, t | \mathbf{r}_{s1}, t_1)}{\partial n_1} \right] d\Sigma_1, \end{aligned} \quad (163)$$

where the Green's function G satisfies

$$\nabla^2 G(\mathbf{r}, t | \mathbf{r}_1, t_1) - \frac{1}{\alpha} \frac{\partial G}{\partial t}(\mathbf{r}, t | \mathbf{r}_1, t_1) = -\delta(\mathbf{r} - \mathbf{r}_1) \delta(t - t_1) \quad (164)$$

The delta function product in this case represents an instantaneous source of unit strength at the point in space-time (\mathbf{r}_1, t_1) .

Appropriate boundary conditions are homogeneous Dirichlet, Neumann, or mixed, corresponding to the temperature, heat flux, or some linear combination of the two, vanishing on the surface;

$$G = 0 \quad (165)$$

$$\frac{\partial G}{\partial n} = 0 \quad (166)$$

$$\frac{\partial G}{\partial n} + h_1 G = 0 \quad (167)$$

where $h_1 = h/k$ may be a function of both position on the surface and time. It is seen that the first two equations are special cases of the third, for which the associated inhomogeneous boundary condition for Eq. (159) is

$$\frac{\partial T}{\partial n} + h_1(\mathbf{r}_s, t)T = f(\mathbf{r}_s, t) \quad (168)$$

where the inhomogeneous right-hand side implies that the temperature of the surroundings is a function of both position and time. If the Green's function is required to obey the corresponding homogeneous mixed boundary condition in the source coordinates

$$\frac{\partial G_3(\mathbf{r}, t|\mathbf{r}_{s1}, t_1)}{\partial n_1} + h_1(\mathbf{r}_s, t)G_3(\mathbf{r}, t|\mathbf{r}_{s1}, t_1) = 0 \quad (169)$$

the integral over the surface Σ in Eq. (163) becomes

$$I = \int_0^{t^*} dt_1 \int_{\Sigma} d\Sigma \left[\frac{G_3(\mathbf{r}, t|\mathbf{r}_{s1}, t_1)}{\partial n_1} \frac{f(\mathbf{r}_{s1}, t_1)}{h_1(\mathbf{r}_{s1}, t_1)} \right] \quad (170)$$

where either formulation is acceptable. If h_1 is equal, or nearly equal, to zero, the former representation is appropriate; if h_1 is large, or infinite (f/h_1 remaining finite), the latter representation is employed. In order to switch from observer coordinates to source coordinates, use is made of the reciprocity principle for the diffusion equation

$$G(\mathbf{r}, t|\mathbf{r}_1, t_1) = G(\mathbf{r}_1, -t_1|\mathbf{r}, -t) \quad (171)$$

This leads to the adjoint equation satisfied by G in the source coordinates

$$\nabla_1^2 G + \frac{1}{\alpha} \frac{\partial G}{\partial t_1} = -\delta(\mathbf{r} - \mathbf{r}_1) \delta(t - t_1) \quad (172)$$

where the change in sign of the time derivative is a consequence of the time reversal in the reciprocity principle. Note that the first integral in Eq. (163) represents the effect of distributed volume sources, while the second integral implies that the initial temperature distribution can be obtained by an instantaneous release of volume sources of the required density distribution at $t = 0$. The surface integral indicates that the effect of the boundary conditions can be simulated by placing a layer of sources along the surface in order to achieve the required normal heat flux, or of doublets of strength dictated by the required surface temperature, or of

combinations of sources and doublets to obtain a heat transfer boundary condition.

This leads to a powerful method when the densities, specific heat, and thermal conductivity can be assumed to have constant average values throughout the entire solid-liquid region. In this case, the moving boundary can be considered to be a source surface. As an example, consider the freezing of a semi-infinite region occupied by liquid with arbitrary initial and surface temperature and conditions. In this case Eq. (159) becomes

$$\frac{\partial^2 T}{\partial x^2} - \frac{1}{\alpha} \frac{\partial T}{\partial t} = \frac{L\rho\dot{X}}{k} \delta(x - X) \quad (173)$$

where the strength of the point source at $x = X(t)$ depends upon the latent heat of fusion, the density and the rate of advance of the freezing front, \dot{X} . The initial and boundary conditions can be expressed by

$$T(x, 0) = T_0(x) > T_m \quad (174)$$

$$T(\infty, t) = 0 \quad (175)$$

$$T(0, t) = f(t) < T_m \quad (176)$$

where the requirements that the initial temperature be everywhere above the melting temperature, and the surface temperature everywhere below this temperature, are made in order to insure the presence of a single freezing front at all times. Equation (175) implies that the zero of the temperature scale has been taken to be the temperature at infinity. The appropriate Green's function for this geometry and the boundary condition in Eq. (176) is

$$\begin{aligned} G(x, t|x_1, t_1) &= \left[\frac{1}{4\pi\alpha(t-t_1)} \right]^{1/2} \left[\exp \left\{ -\frac{(x-x_1)^2}{4\alpha(t-t_1)} \right\} - \exp \left\{ -\frac{(x+x_1)^2}{4\alpha(t-t_1)} \right\} \right], \quad t > t_1 \\ &= 0, \quad t \leq t_1 \end{aligned} \quad (177)$$

obtained by the method of images. From Eqs. (163) and (170) the requirement that the freezing front always remain at the melting temperature leads to an integrodifferential equation for the freezing front position, $X(t)$:

$$\begin{aligned} T_m &= \frac{L\rho}{k} \int_0^{t^+} G[X(t), t|X(t_1), t_1] \dot{X}(t_1) dt_1 \\ &\quad + \frac{1}{\alpha} \int_0^\infty G[X(t), t|x_1, 0] T_0(x_1) dx_1 \\ &\quad + \int_0^{t^+} f(t_1) \frac{\partial G}{\partial x_1} [X(t), t|0, t_1] dt_1 \end{aligned} \quad (178)$$

If a step change in surface temperature has been initially applied, $X \sim t^{1/2}$ for small t , as seen from the exact solutions in Section II. Hence the initial conditions for the position and velocity of the interface are specified, and the problem is well suited to iterative attack, progressing forward from $t = 0$. Lightfoot obtained the solution for constant initial and boundary conditions and showed that Eq. (178) gives results in agreement with the exact solution. Carslaw and Jaeger give a compilation of known Green's functions for the heat equation for a variety of geometries and boundary conditions, so that functional equations for the position of the moving boundary can be generated for a large number of problems. Very few of these solutions have as yet appeared in the literature.

3. Kolodner's Method: Source and Doublet Distributions

In most cases, however, it is not satisfactory to assume equal diffusivities in both phases. Moreover, there is often an induced velocity, due to unequal phase densities. In other cases there is actual removal or introduction of mass, as in aerodynamic ablation, so that the boundaries of the domain do not remain stationary with time. Kolodner (K5) has shown how to overcome these limitations by extending the solution over all space, with suitable jump boundary conditions at the moving interface obtained by appropriate single or double layers of sources. The procedure follows that of Holmgren (H9) in the solution of free-boundary potential problems.⁹ Kolodner develops the theory for a single one-dimensional region with a fixed and a moving boundary and later extends the theory by means of examples to other geometries, including multiple regions. A slight specialization is given below. If one considers the one-dimensional heat equation in the region bounded by the fixed and the moving surface, Eq. (159) becomes, with a minor change in coordinates,

$$\mathcal{L}\{T\} = \frac{\partial^2 T}{\partial x^2} - \frac{1}{\alpha} \frac{\partial T}{\partial t} = 0; \quad X(t) < x < 0 \quad (179)$$

A homogeneous boundary condition of the third kind (heat transfer coefficient) at the fixed surface is assumed (although the extension to inhomogeneous conditions is later made)

$$\Gamma\{T(0, t)\} = \frac{\partial T(0, t)}{\partial x} + h_1 T(0, t) = 0; \quad 0 \leq h_1 \leq \infty \quad (180)$$

As before, boundary conditions of the first and second kind are obtained by allowing h_1 to become very large or very small. Two conditions at the

⁹ Such problems arise in steady-state diffusion, such as the equilibrium radius of a vapor bubble attached to a heated surface in contact with liquid. This was considered by Bick (B5), who used spherical Bessel function expansions rather than integral methods.

free boundary usually exist on the interfacial temperature and heat flux:

$$T(X, t) = f(t) \quad (181)$$

$$\frac{\partial T(X, t)}{\partial x} = g(t) \quad (182)$$

where f and g are functions of time determined by the conditions of the problem and the boundary motion. Occasionally they are written $f[X]$ and $g[X]$ to emphasize that they are functionals, which is to say that they are functions of the unknown function $X(t)$. Define now the single- and double-layer heat source functions

$$\mathcal{S}(h|x, t) = \int_0^t G(x, t|X(t_1), t_1) h(t_1) dt_1 \quad (183)$$

$$\mathcal{D}(h|x, t) = \int_0^t \frac{\partial G(x, t|X(t_1), t_1)}{\partial x_1} h(t_1) dt_1 \quad (184)$$

where

$$\begin{aligned} G(x, t|x_1, t_1) &= \left(\frac{1}{4\pi\alpha(t-t_1)} \right)^{1/2} \exp \left\{ -\frac{(x-x_1)^2}{4\alpha(t-t_1)} \right\}, & t > t_1 \\ &= 0, & t \leq t_1 \end{aligned} \quad (185)$$

is the Green's function for a plane source in an infinite one-dimensional domain. It is readily established from Eqs. (183) and (184) that

$$\mathcal{D}(h|x, t) = -\frac{\partial \mathcal{S}(h|x, t)}{\partial x} \quad (186)$$

and less obviously that

$$\begin{aligned} \frac{\partial \mathcal{D}(h|x, t)}{\partial x} &= -\frac{h(0)}{2(\pi\alpha t)^{1/2}} \exp \left\{ -\frac{[x-X(0)]^2}{4\alpha t} \right\} \\ &\quad - \mathcal{D}(h\dot{X}|x, t) - \mathcal{S}(\dot{h}|x, t) \end{aligned} \quad (187)$$

The solution of Eqs. (179)–(182) is found by extending the domain through all space and requiring the temperature to vanish identically for $x < X$. This implies a jump boundary condition at the moving surface both in the temperature and in its gradient, obtained by the use of single and double layers of sources at the free boundary. The resulting temperature distribution is termed the fundamental part of the solution, T_F . To this is added the complementary part of the solution, which is the continuous function satisfying the heat equation in the extended region such that the homogeneous boundary condition, Eq. (180), is satisfied at the fixed surface. Explicitly, an auxiliary functional T_A is defined over the region obtained by extension past the moving boundary. The governing equations and boundary conditions may be written

$$\mathfrak{L}\{T_A(x, t|X)\} = 0, \quad x < 0 \quad (188)$$

$$\Gamma\{T_A(0, t|X)\} = 0 \quad (189)$$

$$T_A(x, 0|X) = 0 \quad (190)$$

$$[T_A] = f[X] \quad (191)$$

$$\left[\frac{\partial T_A}{\partial x}\right] = g[X] \quad (192)$$

where the square brackets imply the jump boundary condition

$$[T_A] = \lim_{\epsilon \rightarrow 0} [T_A(X + \epsilon, t|X) - T_A(X - \epsilon, t|X)] \quad (193)$$

To obtain the fundamental part of the solution the boundary condition at $x = 0$ is replaced by a condition at infinity:

$$\mathfrak{L}\{T_F\} = 0; \quad T_F = T_F(x, t|X); \quad -\infty < x < \infty \quad (194)$$

$$T_F(x, 0|X) = 0 \quad (195)$$

$$T_F(\infty, t|X) = 0 \quad (196)$$

$$[T_F] = f[X] \quad (197)$$

$$\left[\frac{\partial T_F}{\partial x}\right] = g[X] \quad (198)$$

Kolodner shows that the solution for T_F , subject to suitable constraints on the behavior of X , is

$$T_F = \mathfrak{D}(f|x, t) - \mathfrak{S}(g + f\dot{X}|x, t) \quad (199a)$$

$$= \left(\frac{1}{4\pi\alpha}\right)^{1/2} \int_0^t \left[\frac{f(t_1)z(x, t_1)}{(t - t_1)} - \frac{g(t_1) + f(t_1)\dot{X}(t_1)}{(t - t_1)^{1/2}} \right] \exp[-z^2(x, t_1)] dt_1 \quad (199b)$$

where $z(x, t_1) = [x - X(t_1)]/[4\alpha(t - t_1)]^{1/2}$. The auxiliary functional, which coincides with the desired function in the original domain, is given by

$$T_A = T_F + T_a \quad (200)$$

where

$$\mathfrak{L}\{T_a\} = 0, \quad x < 0 \quad (201)$$

$$\Gamma\{T_a + T_F\} = 0, \quad x = 0, \quad t > 0 \quad (202)$$

$$T_a(x, 0|X) = 0, \quad x < 0 \quad (203)$$

$$T_a \text{ and } |t^{1/2}T_a(x, t|X)| < A \quad \text{as } x \rightarrow -\infty \quad (204)$$

Here A is some positive constant. The free boundary problem is now reduced to solving a functional equation for the boundary, expressing the fact that in the domain formed by extension past the free boundary the temperature and its gradient vanish:

$$\lim_{\epsilon \rightarrow 0} [T_A(X - \epsilon, t|X)] = 0, \quad \epsilon > 0, \quad X(0) = 0 \quad (205a)$$

$$\lim_{\epsilon \rightarrow 0} \left[\frac{\partial T_A(X - \epsilon, t|X)}{\partial x} \right] = 0, \quad \epsilon > 0, \quad X(0) = 0 \quad (205b)$$

Other equations resulting from linear combinations of these two are also satisfied. These equations are shown to be equivalent to

$$\mathfrak{D}(X(t), t|f) - \mathfrak{S}(X(t), t|g + f\dot{X}) - \frac{f[X]}{2} + T_a(X(t), t|X) = 0 \quad (206a)$$

$$- \frac{f[X(0)]}{2(\pi\alpha t)^{1/2}} \exp \left\{ -\frac{[X(t) - X(0)]^2}{4\alpha t} \right\} + \mathfrak{D}(X(t), t|g) \\ - \mathfrak{S}(X(t), t|f) - \frac{g[X]}{2} + \frac{\partial T_a(X(t), t|X)}{\partial x} = 0 \quad (206b)$$

As an example, consider the isothermal evaporation of a liquid interface into an unbounded space, previously considered by Danckwerts (D1). The governing equation is now

$$D \frac{\partial^2 c}{\partial x^2} = \frac{\partial c}{\partial t}; \quad c = \frac{C(x, t) - C_\infty}{C_i - C_\infty} \quad (207) \\ \infty > x > X(t); \quad t > 0; \quad X(0) = 0$$

where $C(x, t)$ is the vapor density, whose values at the interface, C_i , and at infinity, C_∞ , are constants. Since there is no fixed finite boundary the solution coincides with the solution for the fundamental part. The boundary conditions are

$$c(x, 0) = 0 \quad (208)$$

$$c(X, t) = 1 \quad (209)$$

$$a_1 D \frac{\partial c(X, t)}{\partial x} = \dot{X}; \quad a_1 = \frac{C_i - C_\infty}{\rho - C_i} \quad (210)$$

$$c(\infty, t) = 0 \quad (211)$$

where ρ is the liquid density, and Eq. (210) has been obtained by a mass balance at the free boundary. On applying Eq. (206b), an integral equation of the second kind is obtained

$$- \frac{1}{(\pi D t)^{1/2}} \exp \left\{ -\frac{[X(t)]^2}{4Dt} \right\} + \frac{1}{2a_1 \pi^{1/2}} \int_0^t \left\{ \frac{\dot{X}(t_1)}{[D(t - t_1)]^{3/2}} [X(t) - X(t_1)] \right. \\ \left. \exp \left[-\frac{\{X(t) - X(t_1)\}^2}{4D(t - t_1)} \right] \right\} dt_1 - \frac{\dot{X}(t)}{a_1 D} = 0 \quad (212)$$

suitable for iterative attack. On the other hand, Eq. (206a) leads to an integral equation of the first kind (fixed limits on the integrals), which must be solved by polynomial approximations of the unknown function

$X(t)$. In the first case the accuracy can be improved, assuming convergence and stability of the iteration, by decreasing the mesh size for the iteration; in the second case, however, an improvement requires a higher order polynomial, which means that the entire solution must be repeated. For details of the extension of this theory to the motion of a plane liquid-vapor interface in a confined medium, the decay by evaporation (or growth by condensation) of a liquid drop in either an infinite region or a finite region (corresponding to the behavior of a cloud of droplets), the dissolution of a gas bubble in a liquid, recrystallization or other changes of phase without appreciable change in density, and two-region problems, such as the freezing of a lake and the solidification of the terrestrial crust, the reader is referred for details to Kolodner's original paper. The constraints necessary for uniqueness and existence of these solutions are also discussed in some detail. It is worthy of note that an existence theorem could not be proven for Eq. (206b) when $\dot{X} > 0$, although it seems reasonable that the sign of the derivative should be immaterial.

This method, powerful as it is, leads to a nonlinear implicit functional equation for the boundary motion, which must be solved by numerical means. In many cases a direct numerical attack on the governing equation and boundary conditions has been preferred; but Kolodner's method has the advantage of being an exact integral formulation which does not require solution of the heat equation throughout all space at each step of the boundary motion.

4. Boley's Method: Fictitious Boundary Temperatures

A closely related method is that of Boley (B8), who was concerned with aerodynamic ablation of a one-dimensional solid slab. The domain is extended to some fixed boundary, such as $X(0)$, to which an unknown temperature is applied such that the conditions at the moving boundary are satisfied. This leads to two functional equations for the unknown boundary position and the fictitious boundary temperature, and would, therefore, appear to be more complicated for iterative solution than the Kolodner method. Boley considers two problems, the first of which is the ablation of a slab of finite thickness subjected on both faces to mixed boundary conditions (Newton's law of cooling). The one-dimensional heat equation is once again

$$\alpha \frac{\partial^2 T}{\partial x^2} = \frac{\partial T}{\partial t}; \quad X(t) \leq x < a, \quad t > 0 \quad (213)$$

where

$$T(0, t_m) = T_m; \quad X(0) = 0 \quad (214)$$

During the premelting period the faces are both subjected to boundary conditions of the form

$$-k \frac{\partial T}{\partial x} + hT = \Psi(t); \quad x = 0, \quad 0 < t \leq t_m \quad (215)$$

$$-k \frac{\partial T}{\partial x} + h_a T = 0; \quad x = a, \quad t > 0 \quad (216)$$

where it has been assumed that the backface ambient temperature is zero. In the post-melting period, the conditions at the free boundary imply that

$$T[X(t), t] = T_m; \quad X(t_m) = 0, \quad t > t_m \quad (217)$$

$$-k \frac{\partial T}{\partial x} + hT_m = \rho L \frac{dX}{dt} + \Psi(t); \quad x = X(t) \quad (218)$$

where the heat transfer coefficient is assumed to be unchanged by the ablation. This restriction is readily removed. The problem is solved by considering the extended domain ($0 \leq x \leq a$), for which Eq. (218) is replaced by

$$-k \frac{\partial T}{\partial x} + hT = \Psi(t) + \Omega(t), \quad x = 0 \quad (219)$$

where $\Omega(t)$ is an unknown function. This problem can be solved by Green's functions, or equivalently in terms of the fundamental solution, T_1 , satisfying Eq. (213) in the extended domain, and the initial and boundary conditions

$$T_1(x, 0) = 0; \quad 0 \leq x \leq a \quad (220)$$

$$-k \frac{\partial T_1}{\partial x} + hT_1 = 1; \quad x = 0 \quad (221)$$

$$-k \frac{\partial T_1}{\partial x} + h_a T_1 = 0; \quad x = a \quad (222)$$

The use of Duhamel's theorem now leads directly to

$$\begin{aligned} T(x, t) = & \int_0^{t_m} \Psi(t') \frac{\partial T_1(x, t - t')}{\partial t} dt' \\ & + \int_{t_m}^t [\Psi(t') + \Omega(t')] \frac{\partial T_1(x, t - t')}{\partial t} dt' \end{aligned} \quad (223)$$

or, more conveniently,

$$\begin{aligned} T(x, t) = & \int_0^t \Psi(t - t') \frac{\partial T_1(x, t')}{\partial t} dt' \\ & + \int_0^{t-t_m} \Omega(t - t') \frac{\partial T_1(x, t')}{\partial t} dt' \end{aligned} \quad (224)$$

Equations (217) and (218) now take the form

$$\int_0^t \Psi(t-t') \frac{\partial T_1[X(t'), t']}{\partial t} dt' + \int_0^{t-t_m} \Omega(t-t') \frac{\partial T_1[X(t'), t']}{\partial t} dt' = T_m \quad (225)$$

$$k \int_0^t \Psi(t-t') \frac{\partial^2 T_1[X(t'), t']}{\partial x \partial t} dt' + k \int_0^{t-t_m} \Omega(t-t') \frac{\partial^2 T_1[X(t'), t']}{\partial x \partial t} dt' = -\rho L \dot{X} - \Psi(t) + hT_m; \quad t \geq t_m \quad (226)$$

which together with

$$X(t_m) = 0 \quad (227)$$

define a set of two functional equations for the unknowns $X(t)$ and $\Omega(t)$. Once the melting rate is known from the solution of these two equations, Eq. (224) gives the temperature directly. As noted previously, for the special case of a semi-infinite solid with prescribed constant heat input, the fundamental solution becomes

$$h = 0; \quad T_1 = -\frac{2(\alpha t)^{1/2}}{k} i \operatorname{erfc} \left\{ \frac{x}{2(\alpha t)^{1/2}} \right\} \quad (228)$$

Boley proceeds to find solutions for short times after melting in powers of the square root of the dimensionless post-melting time and indicates a numerical scheme for continuing the solution. The results are in good agreement with those of Landau for equivalent conditions.

The second example is the solidification of liquid enclosed between parallel boundaries. Here it is necessary to deal with two fictitious bodies of constant dimensions, one representing the liquid and the other the solid. For the solid phase one deals not with an initially finite body whose dimensions are shrinking, but with a body whose dimensions increase from zero. For this reason an imaginary initial temperature turns out to be more appropriate than an imaginary heat input.

More recently, Boley (B9) shows that the method can be extended to find minimum and maximum bounds for ablation rates. The proof is based on a uniqueness theorem deriving from a theorem due to Picone (P3) and leads to the physically obvious result that the higher the heat input rate, the higher the melting rate. The procedure consists of forming a lower bound for the known arbitrary heat input function in terms of a sequence of constant heat flux periods, for which, as noted above, the solution can be written in terms of integrals of the error function. Upper bounds are constructed in a similar manner.

5. Maximum and Minimum Bounds on One-Dimensional Melt Thickness

a. Time-Dependent Boundary Conditions. A transformation which immobilizes the free boundary, analogous to those employed by Zener and Landau, may be used in conjunction with an integral equation formulation to obtain simple, but fairly close, maximum and minimum bounds on freezing-melting rates with time-dependent boundary conditions (H4). For definiteness consider the melting of a semi-infinite solid slab, initially at the fusion temperature, through the application of an arbitrary, but nondecreasing, wall temperature $T_w(t)$ at the surface. It is convenient to introduce the dimensionless variables

$$\lambda = \frac{x}{X}; \quad t^* = \frac{\alpha t}{a^2}; \quad X^* = \frac{X}{a}; \quad \Lambda = \frac{L}{c_p T_m}; \quad \theta_1 = \frac{T}{T_m} \quad (229)$$

where a is any convenient reference length. In terms of these variables the equations for the dimensionless temperature $\theta_1 = \theta_1(\lambda, t^*)$ become

$$X^{*2} \frac{\partial \theta_1}{\partial t^*} = \frac{\partial^2 \theta_1}{\partial \lambda^2} + \lambda X^* \dot{X}^* \frac{\partial \theta_1}{\partial \lambda}; \quad 0 \leq \lambda \leq 1, \quad t^* > 0, \quad (230)$$

$$\theta_1(1, t^*) = 1 \quad (231)$$

$$\frac{\partial \theta_1(1, t^*)}{\partial \lambda} = -\Lambda X^* \dot{X}^* \quad (232)$$

$$\theta_1(0, t^*) = \theta_{1w}(t^*) \quad (233)$$

where $\dot{X}^* = dX^*/dt^*$. This system can be expressed in integral equation form by integrating Eq. (230) twice, from $\lambda = 1$ to λ , and making use of Eqs. (231) and (232), with the result

$$\begin{aligned} X^{*2} \frac{\partial}{\partial t^*} \int_1^\lambda (\lambda - \lambda_1) \theta_1(\lambda_1, t^*) d\lambda_1 &= \theta_1(\lambda, t^*) - 1 + X^* \dot{X}^* (\Lambda - 1)(\lambda - 1) \\ &+ X^* \dot{X}^* \int_1^\lambda (2\lambda_1 - \lambda) \theta_1(\lambda_1, t^*) d\lambda_1 \end{aligned} \quad (234)$$

Upon making use of the boundary condition at $\lambda = 0$ and integrating with respect to t^* one obtains

$$X^{*2} = \frac{\int_0^{t^*} [\theta_{1w}(t_1^*) - 1] dt_1^*}{\int_0^1 \theta_1(\lambda_1, t^*) d\lambda_1 + (\Lambda - 1)/2} \quad (235)$$

For freezing, Λ would be replaced by $-\Lambda$. Equivalently, Λ can be redefined as a dimensionless heat absorbed per unit mass during the phase change. Equation (235) is an exact expression for the melt thickness directly in terms of an integral of the melt temperature profile and the boundary conditions at the plate. It has the usual advantage of integral formula-

tions of being relatively insensitive to small variations in the kernel function from the exact solution. Since $\theta_1(\lambda, t^*) \geq 1$ and θ_{1w} increases monotonically, it follows that

$$\frac{1}{2} < \int_0^1 \lambda_1 \theta_1(\lambda_1, t^*) d\lambda_1 < \frac{\theta_{1w}}{2} \int_0^1 \lambda_1 d\lambda_1 = \frac{\theta_{1w}}{2} \quad (236)$$

whence, from Eq. (235),

$$\frac{2}{\theta_{1w} + \Lambda - 1} \leq \frac{X^{*2}}{\int_0^{t^*} \theta_{1w}(t_1^*) dt_1^* - t^*} \leq \frac{2}{\Lambda} \quad (237)$$

Taking an average of the denominators in the upper and lower bounds one has

$$\frac{X^{*2}}{\int_0^{t^*} \theta_{1w}(t_1^*) dt_1^* - t^*} \sim \frac{2}{\Lambda + (\theta_{1w} - 1)/2} \quad (238)$$

For the constant wall temperature case this reduces to

$$X^{*2} \sim 4\beta_{av}^2 t^* \quad (239)$$

where

$$\beta_{av}^2 = \alpha \left[\frac{2L}{c_p |T_w - T_m|} + 1 \right]^{-1} \quad (240)$$

As noted previously, the growth constant in the exact solution is given by

$$\beta \exp(\beta^2) \operatorname{erf} \beta = \frac{c_p |T_w - T_m|}{\pi^{1/2} L} \quad (241)$$

It is not surprising that the approximate bounds give the correct time dependence for the free boundary motion, since λ is identical, except for constant factors, with the Boltzmann similarity variable. For a block of ice whose surface temperature is subjected to a step increase of 5°C. the upper and lower bounds are within 3% of each other, and the approximate growth constant calculated from Eq. (238) is about 0.5% from the exact value.

For arbitrary, but nondecreasing, wall heat input $H(t)$, Eq. (231) is replaced by

$$-\frac{\partial \theta_1(0, t^*)}{\partial \lambda} = \zeta_0(t^*); \quad \zeta_0 = \frac{H(t)a}{kT_m} \quad (242)$$

Upon repeating the integrations of Eq. (230), using now Eq. (242), as well as Eqs. (231) and (232), the integral formulation for the dimensionless melt thickness turns out to be

$$X^*(t^*) = \frac{\int_0^{t^*} \zeta_0(t_1^*) dt_1^*}{\int_0^1 \theta_1(\lambda_1, t^*) d\lambda_1 + \Lambda - 1} \quad (243)$$

An examination of Eq. (230), which is similar in form to Eq. (81), shows that, for melting, $\partial^2\theta_1/\partial\lambda^2 \geq 0$. From the mean value theorem it follows immediately that an upper bound for the temperature in melting is given by

$$\theta_1 \leq \zeta_0 X^*(1 - \lambda) + 1 \quad (244)$$

upon applying Eq. (242). Upon integration one obtains

$$0 \leq \int_0^1 \theta_1(\lambda_1, t^*) d\lambda_1 - 1 \leq \frac{1}{2} X^* \zeta_0 \quad (245)$$

When inserted into Eq. (243) this leads to

$$\begin{aligned} \int_0^{t^*} \Theta(t_1^*) dt_1^* &\geq X^* \\ &\geq \frac{1}{\Theta(t^*)} \left[-1 + \left\{ 1 + 2\Theta(t^*) \int_0^{t^*} \Theta(t_1^*) dt_1^* \right\}^{1/2} \right] \end{aligned} \quad (246)$$

where $\Theta = \zeta_0(t^*)/\Lambda$. It is seen from an application of the binomial theorem to the root quantity on the right-hand side of Eq. (246) that the upper and lower bounds agree up to third-order terms. The requirement that this series converge rapidly is equivalent to the condition that the superheat energy content of the melt be small compared to its latent heat content.

For constant heat influx H the inequality (246) may be expressed in the form

$$\eta_1 \geq X_1^* \geq \frac{1}{\eta_1} [-1 + (1 + 2\eta_1^2)^{1/2}] = g(\eta_1) \quad (247)$$

where $X_1^* = X^*/\sqrt{t^*}$ is a dimensionless melt thickness, and $\eta_1 = \Theta\sqrt{t^*}$ is a dimensionless thermal boundary layer thickness. For small η_1 one has

$$g(\eta_1) = \eta_1 - \frac{1}{2}\eta_1^3 + \frac{1}{2}\eta_1^5 - \dots \quad (248)$$

so that

$$X_1^* = \eta_1 + O(\eta_1^3) \quad (249)$$

This is an expression of the fact that at constant heat flux the melt thickness initially grows linearly with time. For small times an exact solution of this problem has been given by Evans *et al.* (E3), who expanded $X_1^*(\eta_1)$ in a Maclaurin series and found the first five coefficients by direct substitution:

$$X_1^* = \eta_1 - \frac{1}{2}\eta_1^3 + \frac{5}{8}\eta_1^5 - \dots \quad (250)$$

It is seen that the lower bound $g(\eta_1)$ is correct to $O(\eta_1^5)$.

This representation is useless for $\eta_1 \geq 1$. For large η_1 , $g(\eta_1) \sim \sqrt{2}$, so that the bounds diverge rapidly. However, for $\eta_1 = 1$ and 2, $g(\eta_1)/\eta_1$, which is the ratio of the upper to lower bounds, is 0.76 and 0.62, respectively. Hence, the range of useful solutions has been extended to $\eta_1 \sim 2$.

Some numerical examples are given. For a semi-infinite copper melt initially at the fusion temperature, losing heat with an over-all heat transfer coefficient of 0.5 B.t.u./(hr.)(ft.²)(°F.) to the surroundings at ambient temperature, after 4 hr. $\eta_1 = 0.98$, and the estimated thickness of solidified copper is 44 in. with a $\pm 12\%$ error. A second example is a steel sheet subjected to a slowly flowing stream of very hot gas, such that a uniform heat flux of 10^5 B.t.u./(hr.)(ft.²)(°F.) is imposed at the surface with negligible motion of the melt. After 200 sec., $\eta_1 = 0.68$, and the melt thickness is estimated to be 1.26 in., with a possible error of $\pm 8.6\%$.

Maximum and minimum bounds for the growth of the vapor film at the surface of a rapidly heated plate in contact with a semi-infinite body of liquid initially at the saturation temperature have been deduced in a similar manner for arbitrary monotonic surface temperature or heat flux, following the method of Section II, D (H3).

b. Gutowski Method. An alternative approach is given by Gutowski (G10), who considers the particular case of a radiation boundary condition for the solidification of a semi-infinite liquid mass. The ambient temperature is considered to be constant, and the liquid is initially at the fusion temperature. The heat equation in the solid phase is formulated in the integral form

$$\alpha \int_0^t \left[\frac{\partial T(x, t_1)}{\partial x} - \frac{\partial T(0, t_1)}{\partial x} \right] dt_1 = \int_0^X [T(x_1, t) - T(x_1, 0)] dx_1 \quad (251)$$

with the boundary conditions

$$\frac{\partial T(0, t)}{\partial x} + h_1[T_a - T(0, t)] = 0 \quad (252)$$

$$T[X(t), t] = T_m \quad (253)$$

$$\frac{\partial T[X(t), t]}{\partial x} = \frac{\rho L \dot{X}}{k} \quad (254)$$

In this form this set of equations does not have a unique solution. Additional physical requirements imposed are that $(\partial T/\partial x) > 0$ and $(\partial^2 T/\partial x^2) < 0$, with T and X square integrable, so that

$$X(0) = 0; \quad \dot{X} > 0, \quad \ddot{X} < 0, \quad t \geq 0 \quad (255)$$

which corresponds to the monotonically increasing temperature distribution most favorable for approximate evaluation by integral methods. A one-parameter family of trial functions satisfying Eqs. (252)–(255) is now assumed. For $n > 1$ such a family is

$$\begin{aligned}
T &= T[x, X(t), \dot{X}(t), n] \\
&= - \frac{h_1(T_m - T_a)X - (\rho L/k)X\dot{X}(h_1X + 1)}{(h_1X + n)} \left(1 - \frac{x}{X}\right)^n \\
&\quad - \frac{\rho L}{k} X\dot{X} \left(1 - \frac{x}{X}\right) + T_m
\end{aligned} \tag{256}$$

This is a functional equation for the boundary position X and the unknown constant parameter n . Upon substituting Eq. (256) into Eq. (251) an ordinary differential equation is obtained for $X(t, n)$, and a family of curves in the phase plane (\dot{X}, X) can be obtained. For n sufficiently close to unity two functions in the phase plane can be determined which serve as upper and lower bounds for the trajectories. The choice is guided by reference to the exact solution for the limiting case of constant surface temperature. It is shown that the upper and lower bounds are quite close to the one-parameter phase plane solution, although no comparison is made with a direct numerical solution. The one-parameter solution also agrees well with experiments on the solidification of aluminum under conditions of low surface heat transfer coefficient ($h_1 = 0.02 \text{ cm.}^{-1}$).

C. VARIATIONAL METHODS

Biot and Daughaday (B6) have improved an earlier application by Citron (C5) of the variational formulation given originally by Biot for the heat conduction problem which is exactly analogous to the classical dynamical scheme. In particular, a thermal potential V , a dissipation function D , and generalized thermal force Q_i are defined which satisfy the Lagrangian heat flow equation

$$\frac{\partial V}{\partial q_i} + \frac{\partial D}{\partial \dot{q}_i} = Q_i, \quad i = 1, 2, \dots \tag{257}$$

where q_i is a generalized coordinate which describes the temperature distribution. The problem which is considered is the melting of a unit area of a semi-infinite slab initially at zero temperature, immediately ablating under a constant surface heat flux. For this case

$$V = \frac{1}{2} \int_X^\infty c_p T^2 dx \cong \frac{1}{2} \int_X^{X+q_1} c_p T^2 dx \tag{258}$$

$$D = \frac{1}{2} \int_X^\infty \mathfrak{H}^2 dx \cong \frac{1}{2} \int_X^{X+q_1} \frac{1}{k} \mathfrak{H}_x^2 dx \tag{259}$$

$$Q_i = \int_\Sigma T_m \frac{\partial \mathfrak{H}_n}{\partial q_i} d\Sigma = T_m \frac{\partial \mathfrak{H}_x(X)}{\partial q_i} \tag{260}$$

where \mathfrak{H} is the integrated heat flux vector and q_1 is the depth of penetra-

tion of the thermal boundary layer. A one-parameter cubic temperature profile in the unmelted solid is assumed:

$$T = T_m[1 - (x - X)/q_1]^3 \quad (261)$$

As an admissibility condition, the heat flow per unit area must be consistent with local conservation of energy, which gives

$$\mathcal{H}_x = \int_x^{X+q_1} \rho c_p T \, dx = \frac{q_1}{4} T_m \rho c_p \left[1 - \frac{x - X}{q_1} \right]^4 \quad (262)$$

With these trial functions, Eq. (257) becomes

$$q_1[(4/112)q_1 + (11/112)\dot{X}] = (5/14)\alpha \quad (263)$$

Finally, an over-all energy balance requires that for constant surface heat flux H :

$$\begin{aligned} H \equiv H(t) &= [L + \rho c_p T_m]\dot{X} + \frac{d}{dt} \int_X^{X+q_1} \rho c_p T \, dx \\ &= [L + \rho c_p T_m]\dot{X} + \frac{1}{4}\rho c_p T_m q_1 \end{aligned} \quad (264)$$

from which the nondimensional melting rate can be determined, in connection with Eq. (263). Comparison is made with Landau's exact solution for the problem. As might be expected, the one-parameter trial function is inadequate for small dimensionless times (t/t_m), $t_m = (\pi k \rho c_p T_m^2)/4H^2$, where the curvature of the temperature profile due to the latent heat effect is relatively large, underestimating the melting rate by more than 30%. Excellent agreement, however, is obtained for $t/t_m > 1$, and this agreement is not particularly affected by replacing the cubic temperature profile by a parabolic one. In common with all variational methods, this is a powerful technique when a single quantity, such as the position of the melt boundary, is desired. For a satisfactory description of the temperature field, it is probable that a more sophisticated trial function would be required, with a corresponding increase in algebraic complexity.

D. BOUNDARY LAYER METHODS

1. Goodman's Application of Pohlhausen Method

Instead of attempting to satisfy the heat equation at every point in the domain, it can be reduced to an ordinary differential equation involving only time as the independent variable by integrating over the space domain. The resulting integral quantity, which is proportional to the total sensible heat of the domain, was termed the heat-balance integral by Goodman (G5, G6), who worked out the method in some detail. The procedure is exactly equivalent to the well-known Karman-Pohlhausen momentum integral method in boundary layer theory. The temperature

function in the kernel is approximated by a second- or third-order polynomial in the distance variable, with undetermined coefficients which are functions of time. On substituting into the differential equations satisfied by the integral, a set of ordinary differential equations for the coefficients is generated, whose solution is determined by reference to the boundary conditions. As a simple example, the melting of a semi-infinite slab, initially at the fusion temperature, upon imposition of a step-function increase in surface temperature (Stefan problem) is treated. The equation satisfied by the heat balance integral is

$$\frac{d\theta_I}{dt} = -\alpha \left[\frac{\rho L \dot{X}}{k} + \frac{\partial T(0, t)}{\partial x} \right] \quad (265)$$

where all properties refer here to the liquid, and θ_I , the total energy of the melt, is given by

$$\theta_I = \int_0^{X(t)} T(x, t) dx \quad (266)$$

If a second-order polynomial for the temperature distribution is assumed of the form

$$T = b_1(x - X) + b_2(x - X)^2 \quad (267)$$

the coefficients are determined by reference to the temperature boundary conditions at $x = 0$ and $x = X$. Substitution into Eqs. (265) and (266) then leads to a differential equation for X , which, with the initial condition $X(0) = 0$, results in

$$X = \beta_1 \sqrt{\alpha t} \quad (268)$$

where the growth constant is given by

$$\frac{\beta_1}{2} = \sqrt{3} \left[\frac{1 - (1 + \mu)^{1/2} + \mu}{5 + (1 + \mu)^{1/2} + \mu} \right]^{1/2}; \quad \mu = \frac{2c_p(T_w - T_m)}{L} \quad (269)$$

It will be noted that the heat balance condition at the free boundary, Eq. (254), has not been employed. If this is used instead of Eqs. (265) and (266), a different growth constant is obtained. In order to satisfy, in addition to Eq. (265), two boundary conditions at the melt line and one at the wall, it is necessary to take a third-order polynomial, resulting in a considerably more complicated solution, which is, however, within 2% of the exact solution. Higher order boundary conditions can be generated in a manner similar to the Pohlhausen technique, although this does not seem to be necessary. For example, the curvature of the temperature profile at $x = 0$ must vanish, on account of the constant wall temperature. In a similar manner solutions are given for arbitrary nondecreasing heat input; heat transfer to a surrounding medium (also called a radiation, or mixed boundary condition, or boundary condition of the third kind);

ablating solids (for which excellent agreement is obtained with exact steady-state solution presented by Landau); and vaporization of a melting solid. Later applications are made to the melting of finite slabs (G7). A similar approach appears to have been employed by Mirzadzhanzade and Dzhalilov (M10), Hrycak (H13), and Gadazhieva (G1). Yang (Y1) notes that solutions obtained by the integral method are not unique; and that, furthermore, the accuracy is not necessarily improved by going to higher order polynomials, as has been demonstrated with the Pohlhausen method in boundary layer theory. Koh (K4) suggests that exponential trial functions are more suitable than algebraic polynomials in some cases. Intuitively, it would appear that the integral methods are most reliable when the temperature and its derivatives are monotonic functions over the entire domain for all time. Physically, this implies that the temperature profile is quite smooth. If there are extremal points, or even points of inflection, such as might result from a succession of temperature or heat fluxes at the surface, or even a staircase surface temperature or heat flux function, the method must be approached with caution.

2. Poots' Application of the Tani Method

The Karman-Pohlhausen method appears to fail for cylindrical and spherical geometries, and Poots (P5) shows how a modification of this method, due to Tani (T1), can be applied to melting-freezing problems. The results for the solidification of a cylindrical melt agree within a few percent with the numerical solution of Allen and Severn (A4), obtained by relaxation methods. Poots also applies the exact boundary layer methods of Goldstein and Rosenhead (G4) to the solidification process, in which $X(t)$ is expanded in a Maclaurin series in the dimensionless time variable. Upon substituting into the differential equation for one-dimensional heat conduction in slabs, cylinders, or spheres, and equating coefficients of like powers, a set of ordinary differential equations is generated, which can be solved exactly. The conditions at the fixed and at the free boundary are used to give the Maclaurin series coefficients. Only the first three coefficients are given, and the radius of convergence is difficult to ascertain. Nevertheless, Poots makes clear the direct analogy between the Stefan problem with diffusion on one side of the moving boundary only (original phase at the fusion temperature) and incompressible boundary layer theory, for which a wealth of approaches has been developed (C17, M7). In a later paper the integral boundary layer techniques are extended to two-dimensional solidification problems. The Tani method again agrees within 13% with the relaxation solution of Allen and Severn for the freezing of melt in a uniform prism of square cross section, while the

Karman-Pohlhausen method predicts a time for complete solidification which is too small by more than 40%.

Pleshanov (P4) extends the integral heat balance method to bodies symmetric in one, two, or three dimensions, using a quadratic polynomial for the approximate temperature function. Solutions are obtained in terms of modified Bessel functions which agree well with numerical finite-difference calculations.

E. EXPANSIONS FOR SMALL TIMES

Stefan gave an exact solution for the constant-velocity melting of a semi-infinite slab initially at the fusion temperature. This was extended by Pekeris and Slichter (P2) to freezing on a cylinder of arbitrary surface temperature and Kreith and Romie (K6) to constant-velocity melting of cylinders and spheres by a perturbation method, in which the temperature is assumed to be expressible in terms of a convergent series of unknown functions. To make the method clear, consider the freezing of an infinite cylinder of liquid, of radius r_0 , at constant surface heat flux. For this geometry the heat equation is

$$\frac{1}{r} \frac{\partial}{\partial r} \left(r \frac{\partial T}{\partial r} \right) = \frac{1}{\alpha} \frac{\partial T}{\partial t}; \quad R(t) \leq r \leq r_0 \quad (270)$$

where $R(t)$ is the radius of the freezing front, and it has been assumed that the densities of the two phases are equal. Since the liquid is initially and at all time at the fusion temperature, a heat balance at the free boundary gives

$$\frac{kG_1}{\rho L} = \dot{R}; \quad R(0) = r_0 \quad (271)$$

where $G_1 = (\partial T / \partial r)r = R$ is a constant. In dimensionless form the problem becomes

$$\frac{1}{r^+} \frac{\partial}{\partial r^+} \left(r^+ \frac{\partial T^+}{\partial r^+} \right) = G_1^+ \frac{\partial T^+}{\partial t^+} \quad (272)$$

$$T^+ = T^+(r^+, t^+), \quad R^+ \leq r^+ \leq 1, \quad t^+ > 0$$

$$T^+(R^+, t^+) = 0; \quad \frac{\partial T^+(R^+, t)}{\partial r^+} = \frac{dR^+}{dt^+} = 1; \quad R^+(0) = 1 \quad (273)$$

where

$$\begin{aligned} T^+ &= \frac{T - T_m}{r_0 G_1}; & r^+ &= \frac{r}{r_0}; & R^+ &= \frac{R}{r_0} \\ t^+ &= \frac{tkG_1}{\rho L r_0}; & G_1^+ &= \frac{G_1 c_p r_0}{\rho L} \end{aligned} \quad (274)$$

If now the right-hand side of Eq. (272) is considered to be a small perturbing term, the temperature modulus can be expressed by the series

$$T^+ = T_1 + T_2 + T_3 + \cdots + T_n + \cdots \quad (275)$$

where each term of the series is related to the preceding term by the equation

$$\frac{1}{r^+} \frac{\partial}{\partial r^+} \left(r^+ \frac{\partial T_n}{\partial r^+} \right) = G_1^+ \frac{\partial T_{n-1}}{\partial t_1^+}; \quad t_1^+ = 1 + t^+ \quad (276)$$

subject to homogeneous boundary and initial conditions for $n \geq 2$. Note the implication that T_n is of the order $(G_1^+)^n$. Solutions are obtained for the first five terms, and it is estimated that for $|G_1^+| < 1.5$ the evaluation of T^+ is accurate to within 1–2%. However, the radius of convergence is not given, and there is a logarithmic singularity at the origin, as evidenced by the first term of the solution

$$T_1^+ = t_1^+ \ln \frac{r^+}{t_1^+} \quad (277)$$

which renders the method useless as complete solidification is approached.

A similar solution is obtained for the solidifying sphere.

F. LINEAR METHODS

Redozubov (R1) extends a procedure said to be suggested by Grinberg (G9) [which is also discussed by Gibson (G2, G3)] for obtaining operational solutions to the problem of the ablating semi-infinite slab, for the special case $Xt^{1/2} = \text{constant}$, and $T(x, 0) = Ax + B$. In another paper (R2) these methods are extended to the case of linear motion of the melt line $Xt^{-1} = \text{constant}$, the solid being initially at the fusion temperature. Problems of this type were treated originally by Stefan, as discussed in Carslaw and Jaeger (C1).

Friazinov (F4) deals with a generalized Stefan problem involving finite depth of the two-phase layer, densities and thermal conductivities which are functions of position, and arbitrary initial and boundary conditions, by an approximate expansion in terms of appropriate Sturm-Liouville eigenfunctions.

IV. Analog and Digital Computer Solutions

A. PASSIVE AND ACTIVE ANALOG SOLUTIONS

London and Seban (L8) introduced the method of lumped parameters in melting-freezing problems, whereby the partial differential equation is converted into a difference-differential equation by differencing with respect to the space variable. The resulting system of ordinary differential

equations is suitable for solution on the analog computer. London and Seban simplify the problem by assuming that the heat capacity of the newly formed phase is negligible. Cochran (C8) extends the zero-heat capacity solutions of London and Seban for the slab with specified surface temperature by assuming that the thermal capacity of the newly formed layer is lumped at the midpoint.

Kreith and Romie (K6) consider freezing problems symmetric in one, two, and three dimensions, where the liquid is initially at the fusion temperature. The heat capacity of the solidified phase is taken into account. Thermal properties are considered to be temperature-independent. A passive analog device, in which the thermal system is simulated by an electrical network of resistors and capacitors, is used. It is shown that neglect of the heat capacity of the solidified phase is justified if $L/(T_m - T_\infty)c_p > 25$. The progress of the fusion front is determined by an integrating circuit. When the heat balance around the lump containing the solidification front indicates that liquid is no longer present, a relay system switches the front to the next lump and adjusts the thermal properties accordingly.

Horvay (H10) deals with the more difficult problem, important in casting processes, of the freezing of a growing liquid column, by means of a passive analog circuit. A liquid metal column, initially at one temperature, is supplied at the top with additional metal at a different temperature at a uniform rate, while at the bottom of the column heat is abstracted through a solid plate of finite thickness. The bottom surface of the plate is maintained at ambient temperature. An exact solution, obtained by finite transforms, is given for the case when the ambient temperature is above fusion and the heat capacity of the bottom plate can be neglected. For the more general case, a differencing scheme is employed such that the liquid column is always divided into equal intervals. This is equivalent to the transformation employed by Zener (Z2), Landau (L4), and others, for immobilizing the boundaries of the diffusion region; and, in fact, by a limit process from the difference equation, the Landau equation is again obtained. A passive network is used with voltage sources in parallel with resistors to simulate the heat flow due to mass convection. Several representations are studied, and complete numerical solutions obtained.

Other passive network solutions are given by Hlinka and Paschkis (H8). Otis (O1) employs the Landau transformation for the problem of an ablating slab with uniform initial temperature and specified heat fluxes at the front and back faces,

$$T = T_0; \quad t = 0, \quad X(t) = 0 \quad (278)$$

$$-k \frac{\partial T}{\partial x} + \rho L \dot{X} = H(t); \quad x = X(t) \quad (279)$$

$$-k \frac{\partial T}{\partial x} = H_a(t); \quad x = a \quad (280)$$

With the introduction of the space variable $\xi_2 = (x - X)/(a - X)$, the heat equation becomes [cf. Eqs. (80) and (81)]

$$\frac{\partial T}{\partial t} = \frac{\alpha}{(a - X)^2} \frac{\partial^2 T}{\partial \xi_2^2} + \frac{1 - \xi_2}{a - X} \dot{X} \frac{\partial T}{\partial x} \quad (281)$$

The variable coefficient is eliminated from the first term on the right-hand side of this equation by defining a new dimensionless time variable,

$$\bar{t} = \frac{a^2}{t_{\max}} \int_0^t \frac{dt_1}{[a - X(t_1)]^2} \quad (282)$$

With a dimensionless temperature variable

$$\theta = \frac{T - T_0}{T_m - T_0} \quad (283)$$

Eq. (281) becomes

$$\frac{\partial \theta}{\partial \bar{t}} = \frac{\alpha t_{\max}}{a^2} \frac{\partial^2 \theta}{\partial \xi_2^2} + \frac{1 - \xi_2}{a - X} \dot{X} \frac{\partial \theta}{\partial \xi_2} \quad (284)$$

with boundary conditions

$$\theta = 0; \quad X(t) = 0; \quad \bar{t} = 0 \quad (285)$$

$$-k \frac{T_m - T_0}{a - X} \frac{\partial \theta}{\partial \xi_2} + \rho L \frac{a^2 \dot{X}}{t_{\max}(a - X)^2} = H(t); \quad \xi_2 = 0 \quad (286)$$

$$-k \frac{T_m - T_0}{a - X} \frac{\partial \theta}{\partial \xi_2} = H_a(t); \quad \xi_2 = 1 \quad (287)$$

The moving boundary has now been eliminated and the problem reduced to that of solving the heat conduction equation for a nonmelting solid with internal heat absorption, corresponding to the last term of Eq. (284). This system is then differenced with respect to the space variable and solved on a passive analog system.

Baxter (B3) uses an "enthalpy-flow temperature" method, due originally to Dusinberre (D5, D6) and Eyres *et al.* (E4), whereby the moving-boundary effect is reduced to a property variation. To begin with, the melting of a slab of finite thickness initially at the fusion temperature is considered. At the surface of the melt, which is of the same density as the solid, a heat transfer boundary condition is applied. The technique takes into account latent heat effects by allowing the specific heat to become infinite at the fusion temperature in such a way that

$$\lim_{\epsilon \rightarrow 0} \int_{-\epsilon}^{\epsilon} c_p dT = \int_{0^-}^{0^+} c_p dT = L, \quad (288)$$

where zero temperature is taken to be the fusion point. New variables, consisting of an "enthalpy" and a "flow temperature" defined by

$$H_T(T) = \int_{0^+}^T c_p dT, \quad \text{i.e.,} \quad \frac{dH_T(T)}{dT} = c_p \quad (289)$$

$$\chi_T(T) = \int_0^T k dT, \quad \text{i.e.,} \quad \frac{d\chi_T(T)}{dT} = k \quad (290)$$

are now introduced, when the one-dimensional heat conduction equation becomes

$$\rho \frac{\partial H_T}{\partial t} = \frac{\partial^2 \chi_T}{\partial x^2}; \quad 0 \leq x < a, \quad t > 0 \quad (291)$$

with $\chi_T = \chi_T(H_T)$ and $H_T = H_T(x, t)$. This equation is applicable throughout the entire region, the nonlinearity having been concentrated in the variation of $\chi_T(H_T)$. The equations are then made dimensionless and converted into a set of difference-differential equations which are solved on an active analog computer. Nonlinear function generators are used to simulate $\chi_T(H_T)$ and $T(H_T)$. Solutions are also given for the fusion times of slabs and cylinders. The problem is slightly more complicated when the solid is not initially at the fusion temperature. Illustrative solutions are given for the freezing of a layer of water with various initial temperatures.

In a differential analyzer study of ablating slabs Manci (M1) employs an exponential transformation to reduce the semi-infinite distance interval to a unit interval and to remove the moving boundary. Several approximations are examined at the heated surface; it is shown that second-order differences yield significant improvements in accuracy compared to first-order differences, with negligible increases in computer requirements. Ruddle (R10) gives a detailed experimental and theoretical treatment of solidification rates in molds. Special attention is paid to Schmidt's graphical method (S3) and the method of Sarjant and Slack (S2), and Dusingberre's numerical method, discussed above. Longwell (L9) also applies the Schmidt procedure to freezing problems.

B. NUMERICAL SCHEMES

1. *Relaxation Methods*

Allen and Severn (A3, A4) demonstrate how relaxation methods, originally developed for elliptic partial differential equations, can be extended to the heat conduction equation. With elliptic equations, the value of the dependent variable at any mesh point is determined by all

its nearest neighbors. The relaxation method provides an orderly procedure for minimizing the residual error in a method of successive approximations over the entire domain. With the parabolic differential equations

$$\frac{\partial T}{\partial t} = \alpha \frac{\partial^2 T}{\partial x^2} + \frac{Q}{\rho c_p} \quad (292)$$

where the integration proceeds forward with time, this method is not directly applicable. A preliminary transformation is therefore employed:

$$T = \frac{\partial W}{\partial t} + \alpha \frac{\partial^2 W}{\partial x^2} \quad (293)$$

resulting in

$$\frac{\partial^2 W}{\partial t^2} - \alpha^2 \frac{\partial^4 W}{\partial x^4} - \frac{Q}{\rho c_p} = 0 \quad (294)$$

which is suitable for use with the relaxation method. The method does not appear to have been used extensively for melting-freezing problems, presumably because of the extra computational effort.

2. Finite-Difference Methods

a. Melting and Ablation. Douglass and Gallie (D4) introduce an implicit difference scheme for the numerical integration of a parabolic partial differential equation subject to a moving-boundary condition. In particular, they considered the Stefan problem of the melting of a semi-infinite slab initially at the fusion temperature upon the application of a step function increase in surface temperature. Uniform convergence to the correct solution and stability with respect to small errors was demonstrated. The proof is based upon a maximum principle for parabolic partial differential equations, which essentially states that for bounded initial and boundary temperatures the temperature remains bounded throughout the domain for all time. This is not true for explicit difference equations with an unstable ratio of $\Delta t/(\Delta x)^2$. The procedure employs a fixed space interval with a varying time step, so that the moving boundary is always kept at the right-most mesh point at the time level undergoing computation. An iteration process is therefore required to determine each time step. A second method is also given in which the time is fixed and the boundary is searched for, and which can also be shown to be uniformly convergent and stable but is believed to be inferior from a practical standpoint to the former method.

Ehrlich (E1) uses the Crank-Nicholson (C16) finite-difference procedure for the integration of the diffusion equation, with a three-point approximation of the space derivatives on either side of the moving

boundary. Arbitrary heat input into a finite slab is considered, the liquid phase remaining in contact with the solid.

Murray and Landis (M13) also deal with the fusion of a finite slab with arbitrary initial and boundary conditions. In the first method, the solid is divided into a finite number of equal intervals, which are required to shrink uniformly as the fusion front progresses into the slab. The liquid region is handled in a similar manner. It will be noted that this is equivalent to immobilizing the free boundary with the transformations given by Zener and Landau. In the second method, a fixed space network is employed, but the fusion front is traced as it travels through a particular interval, and the temperature of the lump node is continuously adjusted as the fusion front moves. A three-point slope approximation on both sides of the fusion front is used to determine the free boundary motion. It is necessary to start with some small finite melt thickness. Two sample solutions are shown, carried out both by digital and analog computation. In the conventional method the whole lump containing the free boundary is assumed to remain at the melting point until the free boundary is calculated to pass into the next lump. It is shown from numerical comparisons with the Stefan problem that the fusion front travel is relatively insensitive to the calculation scheme employed, but the temperature histories in the neighborhood of the fusion front are more accurately described by the second method than by either the first method or the conventional method.

Lotkin (L10) gives a scheme for numerical integration of the heat conduction equation in a finite ablating slab, using unequal subdivisions in both space and time variables. Near the melting surface it is advantageous to choose rather small integration steps. Stability characteristics of the method are established.

Sunderland and Grosh (S11) use an explicit numerical scheme for solving the Landau problem. An Eulerian coordinate system is used with the origin at the melt interface. As noted by Landau, the numerical integration is simplified by appropriate choice of the ratio of the space and time intervals. Extension to time-dependent heat flux by either a numerical or a graphical technique is indicated.

Dewey *et al.* (D3) present a numerical scheme for the ablation of an annulus with specified heat fluxes at the outer (ablating) surface and at the inner surface. An implicit finite difference technique is used which permits arbitrary variation of the surface conditions with time, and which allows iterative matching of either heat flux or temperature with external chemical kinetics. The initial temperature may also be an arbitrary function of radial distance. The moving boundary is eliminated by a transformation similar to Eq. (80). In addition a new dependent variable is introduced to

obtain a smooth behavior of the finite difference equations near the boundary:

$$\chi = \int_{T_R}^T k(T_1) dT_1 \quad (295)$$

where T_R is a suitable reference temperature. Time-centered differences are used to replace all derivatives, resulting in

$$\frac{\partial \chi}{\partial t} \approx \frac{(\chi_{i,j+1} - \chi_{i,j})}{\Delta t} \quad (296)$$

$$\frac{\partial \chi}{\partial \xi_2} \approx \frac{(\chi_{i+1,j+1} - \chi_{i-1,j+1} + \chi_{i+1,j} - \chi_{i-1,j})}{4\Delta \xi_2} \quad (297)$$

$$\frac{\partial^2 \chi}{\partial \xi_2^2} \approx \frac{(\chi_{i+1,j+1} - 2\chi_{i,j+1} + \chi_{i-1,j+1} + \chi_{i+1,j} - 2\chi_{i,j} + \chi_{i-1,j})}{2\Delta \xi_2^2} \quad (298)$$

where i represents the space index and j the time index. This leads to a three-point recursion formula for the temperature at an interior mesh point in terms of adjacent temperatures at the same time. The resulting set of simultaneous linear relations is solved by a method which is the equivalent of Gaussian elimination. The constants are successively eliminated in a "forward" direction and determined by substitution in a "rearward" direction, substantially reducing the required time and memory capacity. The stability analysis indicates that, for the thermal conductivity and boundary position varying slowly with time, the difference equation is unconditionally stable. This is to be contrasted with explicit difference procedures in which the temperature at a particular point in space and time is described explicitly in terms of temperatures at a preceding time, with consequent limits on the size of the time interval for stability. The implicit procedure allows the integration interval to be selected to control truncation errors in each step. Some numerical examples are given in terms of typical re-entry conditions.

b. Penetration of a Finite Slab. Crank (C13, C15) poses a problem of particular interest to chemical engineers, consisting of the penetration of a solute from a finite volume of well-mixed solution into a sheet initially free of solute. The solute molecules are adsorbed on fixed sites within the sheet and are thereby removed from the diffusion process. Two methods for the numerical solution of this moving-boundary problem are then described.

To formulate the problem, an infinite sheet of uniform material of thickness $2a$ is placed symmetrically in a solution of extent $2l$, whose initial concentration, expressed in molecules of solute per unit volume, is C_0 . The sheet contains N sites per unit volume, on each of which one diffusing molecule can be rapidly and irreversibly withdrawn from the

diffusion process. Denoting by C the concentration of freely diffusing molecules at any point in the sheet, the concentration of molecules immobilized on the sites changes from 0 to N whenever C assumes a positive value.

From symmetry only one-half the sheet thickness need be considered. In terms of the dimensionless variables

$$x^* = \frac{x}{a}; \quad t^* = \frac{Dt}{a^2}; \quad c^* = \frac{C}{C_0}; \quad N^* = \frac{N}{C_0} \quad (299)$$

the diffusion equation becomes

$$\frac{\partial c^*}{\partial t^*} = \frac{\partial^2 c^*}{\partial x^{*2}}; \quad 0 < x^* < X^* \quad (300)$$

where the diffusion coefficient has been assumed constant. The initial condition is

$$c^* = 0; \quad t^* = 0, \quad 0 < x^* < 1 \quad (301)$$

and the boundary conditions

$$c^* = 0; \quad x^* \geq X^*, \quad t^* > 0, \quad (302)$$

$$\frac{dX^*}{dt^*} = -\frac{1}{N^*} \left(\frac{\partial c^*}{\partial x^*} \right)_{x^*=X^*}, \quad (303)$$

$$c^* = 1 - \frac{a}{l} \int_0^{X^*} (c^* + N^*) dx^*; \quad x^* = 0, \quad t^* \geq 0 \quad (304)$$

where X represents the depth of penetration of solute. Crank proceeds by introducing the Boltzmann similarity variable and a new time variable

$$\eta = \frac{x^*}{\sqrt{t^*}} = \frac{x}{\sqrt{Dt}}; \quad \tau = \sqrt{t^*}; \quad \beta = \frac{X}{\sqrt{Dt}} \quad (305)$$

whereupon Eqs. (300)–(303) become

$$2 \frac{\partial^2 c^*}{\partial \eta^2} = \tau \frac{\partial c^*}{\partial \tau} - \eta \frac{\partial c^*}{\partial \eta} \quad (306)$$

$$c^* = 0; \quad \eta = \infty, \quad \tau = 0 \quad (307)$$

$$c^* = 0; \quad \eta \geq \beta, \quad \tau \geq 0 \quad (308)$$

$$-\frac{1}{2} \frac{d\beta}{d\tau} = \frac{1}{N^* \tau} \frac{\partial c^*(\beta)}{\partial \eta} + \frac{\beta}{2\tau} \quad (309)$$

while the material balance expression, Eq. (304), becomes

$$c^* = 1 - \frac{a}{l} \int_0^\beta (c^* + N^*) \tau d\eta; \quad \eta = 0, \quad \tau \geq 0 \quad (310)$$

For small times Eqs. (306), (309), and (310) become

$$2 \frac{d^2 c^*}{d\eta^2} = -\eta \frac{dc^*}{d\eta} \quad (311)$$

$$\frac{dc^*(\beta)}{d\eta} = -\frac{N^*\beta}{2} \quad (312)$$

$$c^* = 1 \quad \text{at} \quad \eta = 0 \quad (313)$$

Note that for small times the left-hand side of Eq. (309) is small, since the penetration thickness increases as the square root of time, implying that β is constant. From Eq. (58) the first estimate of β is therefore given by

$$\pi^{1/2}\beta \operatorname{erfc}\left(\frac{\beta}{2}\right) \exp\left(\frac{\beta^2}{4}\right) = \frac{2}{N^*} \quad (314)$$

A further transformation to the Zener variable is made by writing

$$\lambda = \frac{\eta}{\beta} = \frac{x}{X}; \quad \tau = \tau; \quad 0 < \tau < 1 \quad (315)$$

whence one obtains

$$2 \frac{\partial^2 c^*}{\partial \lambda^2} = \beta^2 \tau \frac{\partial c^*}{\partial \tau} + \frac{2}{N^*} \frac{\partial c^*}{\partial \lambda} \left[\frac{\partial c^*(1)}{\partial \lambda} \right] \quad (316)$$

$$-\frac{1}{2} \frac{d\beta}{d\tau} = \frac{1}{N^*\tau\beta} \frac{\partial c^*(1)}{\partial \lambda} + \frac{\beta}{2\tau} \quad (317)$$

$$c^* = 1 - \frac{a}{l} \int_0^1 (c^* + N^*) \tau \beta d\lambda; \quad \lambda = 0 \quad (318)$$

These equations are now in convenient form for iterative solution by finite-difference methods, since the free boundary has been immobilized. An implicit method is developed, based on central time differences. Denoting the dimensionless concentration gradient at the moving boundary by

$$A(\tau) = \frac{2}{N^*} \frac{\partial c^*(1)}{\partial \lambda}; \quad A_j = A(j \Delta\tau) \quad (319)$$

and $c_{i,j}^* = c^*(i \Delta\lambda, j \Delta\tau)$; $i, j = 0, 1, 2, \dots$, Eqs. (316) and (317) may be placed in finite-difference form, giving, after some rearrangement,

$$\begin{aligned} & \left\{ \frac{2}{(\Delta\lambda)^2} + \frac{(A_j + A_{j+1})\lambda}{4 \Delta\lambda} \right\} \\ &= \frac{1}{2}(2j+1) \{ \beta_j^2 + \beta_{j+1}^2 \} (c_{i,j+1}^* - c_{i,j}^*) \\ & - \frac{2}{(\Delta\lambda)^2} \{ (c_{i+1,j+1}^* + c_{i+1,j}^*) - 2(c_{i,j+1}^* + c_{i,j}^*) + c_{i-1,j}^* \} \\ & + \frac{(A_j + A_{j+1})\lambda}{4 \Delta\lambda} \{ c_{i+1,j+1}^* + c_{i+1,j}^* - c_{i-1,j}^* \} \end{aligned} \quad (320)$$

$$A_{j+1} = \{j\beta_j^2 - \beta_j\beta_{j+1} - (j+1)\beta_{j+1}^2\} - A_j \quad (321)$$

The iteration procedure begins with an estimate of β_{j+1} , with which A_{j+1} is calculated from Eq. (321). Taking $i = M$ when $\lambda = 1$, and using the approximation

$$\frac{N^*}{2} A_{j+1} = \frac{c_{M-2,j+1}^* - 4c_{M-1,j+1}^*}{2\Delta\lambda}, \quad M = \frac{1}{\Delta\lambda} \quad (322)$$

one notes from Eq. (308) that the special case of Eq. (320) for which $i = M - 1$ enables the calculation of c_{M-1}^* and c_{M-2}^* . This now allows the integration to proceed backwards in Eq. (322) and the value of c^* at $\lambda = 0$ is compared with that obtained from Eq. (318), using any convenient formula for the numerical integration. The initial estimate of β_{j+1} is adjusted until the values agree within some predetermined error, at which point the integration proceeds to the next time interval. Crank shows that quite reasonable accuracy can be obtained in a trial problem with only two steps in time and four in distance, showing that the method is well suited to a desk calculator. The corresponding heat conduction problem is the melting of a slab initially at the fusion temperature when immersed in a well-stirred volume of fluid of limited extent, the initial temperature of the fluid being above the slab melting point, and the melt being constrained to remain immobile.

The problem is extended by Crank to the case where the slab is initially at a uniform temperature below the fusion point, for which a mass transfer analog involves site mobility (*H7*). Note that the center line of the slab is no longer a fixed point in the λ coordinate system. A second spatial coordinate is introduced for the unmelted region

$$\xi_1 = \frac{\eta - \beta}{(1/\tau) - \beta}, \quad \beta \leq \eta \leq \frac{1}{\tau} \quad (323)$$

where $\xi_1 = 0$ at the moving boundary and $\xi_1 = 1$ at the center line. Introducing the dimensionless temperature $\theta = (T - T_0)/(T_b - T_0)$ which ranges from zero at the initial solid temperature to unity at the initial bulk fluid temperature, the diffusion equation for the melt (primed phase) becomes

$$2 \frac{\partial^2 \theta'}{\partial \lambda^2} = \beta^2 \tau \frac{\partial \theta'}{\partial \tau} - \lambda \frac{\partial \theta'}{\partial \lambda} \left(\beta^2 + \beta \tau \frac{d\beta}{d\tau} \right), \quad 0 < \lambda < 1 \quad (324)$$

and for the unmelted solid (unprimed phase)

$$2D\tau \frac{\partial^2 \theta}{\partial \xi_1^2} = (1 - \tau\beta)^2 \frac{\partial \theta}{\partial \tau} + (\xi_1 - 1)(1 - \tau\beta) \left(\beta + \tau \frac{d\beta}{d\tau} \right) \frac{\partial \theta}{\partial \xi_1}, \quad 0 < \xi_1 < 1 \quad (325)$$

The heat balance at the moving interface results in

$$-\frac{1}{2} \frac{d\beta}{d\tau} = \frac{1}{\tau N^*} \left\{ \frac{1}{\beta} \frac{\partial \theta'(1)}{\partial \lambda} - \frac{k'\tau}{k(1-\beta\tau)} \frac{\partial \theta(1)}{\partial \xi_1} \right\} + \frac{\beta}{2\tau} \quad (326)$$

The requirement that the temperatures at the free boundary be equal to the fusion temperature may be written

$$\theta = \theta' = \theta_m; \quad \lambda = 1, \quad \xi_1 = 0 \quad (327)$$

The symmetry requirement at the center line gives

$$\frac{\partial \theta}{\partial \xi_1} = 0, \quad \xi_1 = 1 \quad (328)$$

Finally, a macroscopic heat balance requires that

$$\begin{aligned} \frac{\rho_b c_{pb}}{\rho' c_p'} (1 - \theta') &= \frac{a}{l} \int_0^1 (\theta' + N^*) \tau \beta \, d\lambda \\ &+ \frac{a}{l} \int_0^1 \frac{\rho c_p}{\rho' c_p'} (1 - \tau \beta) \theta' \, d\xi_1; \quad \lambda = 0 \end{aligned} \quad (329)$$

These equations are now in convenient form for a finite-difference scheme along lines similar to that used above. An alternative approach developed in some detail employs the Lagrangian interpolation formula to follow the motion of the boundary in the $(x/a, \tau)$ plane. This is a means of developing finite-difference approximations to derivatives based on functional values and not necessarily equally spaced in the argument. Crank points out that the application of Lagrangian interpolation formulas involves a relatively large number of steps in time, whereas the fixed-boundary procedures require iterative solutions at each time interval, which are, however, far fewer in number.

V. Concluding Remarks

It would appear that the study of the diffusion equation subject to a phase change at one boundary is in a relatively satisfactory state, provided simple boundary conditions of the first, second, or third kind are specified. From a mathematical point of view, the interesting features of the problem arise from the nonlinearity, exhibited for all but a few particular boundary motions. A wide variety of approximate and numerical methods have been employed, and it has frequently been difficult for workers in one specialized field of activity to become conversant with similar approaches made by investigators in other areas. It is hoped that the present work will, to some extent, alleviate this problem.

From a practical point of view, much remains to be learned. For

sufficiently small particles macroscopic diffusion theory is no longer adequate without modification; surface kinetics frequently play an important role, and the growth dynamics of clouds of particles are still not completely understood. Ablation in high-speed flows continues to be a highly active field, both experimentally and computationally. In part this is due to the complexities when the diffusion process is coupled to the external chemical kinetics and boundary layer flow.

Finally, the subject of bubble dynamics, in which the pressure equation is coupled to the convective diffusion equation, offers a number of unsolved problems which will be considered in a succeeding volume of this series.

ACKNOWLEDGMENTS

The author wishes to acknowledge, with appreciation, the invaluable assistance of his student, Mr. V. K. Pai, in assembling and editing this manuscript. The work was supported in part by a grant from the National Science Foundation.

Nomenclature

a	Initial slab thickness or reference length		ence concentration, Eq. (16)
a_1	Constant, Eq. (210)	f	Notation for arbitrary, but specified, function
A, A_1	Constants	${}_1F_1(a, b, x)$	Confluent hypergeometric function
$A(\tau)$	Dimensionless concentration gradient, Eq. (319)	$g(t)$	Arbitrary function of time
b	Positive constant	$g(\gamma_1)$	Function defined by Eq. (247)
b_0, b_1, b_2, \dots	Constants, Eq. (267)	g_c	Gravitational constant
c	$= (C - C_\infty)/(C_i - C_\infty)$, dimensionless concentration	$G(\mathbf{r}, t/\mathbf{r}_1, t_1)$	Green's function for diffusion, Eq. (164), (177), or (185)
c_1	$= (C_\infty - C_i)/(C' - C_i)$, dimensionless concentration, Eq. (8)	G_1	$= (\partial T/\partial r)_{r=R}$, constant, Eq. (271)
c^*	C/C_0 , dimensionless concentration, Eq. (299)	G_1^+	$= (G_1 c_p r_0/\rho L)$, dimensionless, Eq. (274)
c_p	Specific heat at constant pressure	h, h_a	Surface heat transfer coefficients at front and rear faces
C	Concentration	$h_1(\mathbf{r}, t)$	$= (h/k)$, ratio of heat transfer coefficient to thermal conductivity, Eq. (167)
C_*	Excess concentration, Eq. (156)	H	Constant surface heat flux
C_o, C_o'	Excess concentration in old and new phases over saturation in the old phase	$H(t), H_a(t)$	Surface heat flux at front and rear faces
D	Mass diffusivity; or thermal dissipation function, Eq. (259)	\mathcal{H}	Integrated heat flux vector, Eqs. (259) and (262)
$\mathcal{D}(h \mid x, t)$	Double layer heat source function, Eq. (184)	H_T	Enthalpy function, Eq. (289)
D_0	Diffusivity at some refer-		

i	Index of space interval	R_g	Universal gas constant
I	Notation for integral	s	Generalized position coordinate
j	Index of time interval	s_0	Fixed distance parameter, Eq. (19)
J	Mass flux, Eq. (23)	s^+	$= y/R$, dimensionless variable
k	Thermal conductivity	s_1	Generalized coordinate denoting the radius of the region containing diffusant, Eq. (18)
k_H	Henry's law constant	S	Generalized position of interface
k_h	Constant in Eq. (15)	$S(h x, t)$	Single layer heat source function, Eq. (183)
k_p	Filter-cake permeability	t	Time
k_v	Ventilation factor, Eq. (152)	t_0	Reference time
K	Rate constant, Eq. (13)	$t_{1/2}$	Time for penetration to half-radius, Eq. (15)
$K_1, K_2 \dots$	Constants	t^*	$= (\alpha t/a^2)$ or (Dt/a^2) , dimensionless time
l	Length, Eq. (304)	t^+	$= (AkG_1/\rho Lr_0)$, dimensionless, Eq. (274)
L	Latent heat of phase change	t_1^+	$= 1 + t^+$, dimensionless, Eq. (276)
\mathcal{L}	Notation for diffusion operator, Eq. (179)	\bar{t}	$= (a^2/t_{\max})$ $\left(\int_0^t [a - X(t_1)]^{-2} dt_1 \right)$, dimensionless, Eq. (282)
m_1	$= \pi^{1/2} c_p (T_m - T_0)/2L$, dimensionless, Eq. (93)	t_c	Characteristic diffusion time for finite slab, Eq. (125)
m_2	$= H/\rho[L + c_p(T_m - T_0)]$, steady-state melting rate, Eq. (106)	t_m	Time when the melting starts
m_*	$= \int_0^x \rho dx$, Lagrangian coordinate, Eq. (134)	T	Temperature
M	Mass condensed per unit area	T^+	$= (T - T_m)/r_0 G_1$, dimensionless temperature, Eq. (274)
M_*	$= m_*(X)$, Eq. (137)	T_a	Ambient temperature
N	Number of sites for diffusion, per unit volume	T_a	Auxiliary functional, Eq. (200)
N_1, N_2	Constants, dimensionless, Eq. (114)	T_A	Auxiliary functional, Eq. (188)
N^*	N/C_0 , dimensionless, Eq. (299)	T_b	Bulk temperature
p	Pressure	T_F	Fundamental temperature solution, Eqs. (194)–(198)
q	$= M_*^2(X)$, Eq. (139)	u	Velocity vector
q_i	Generalized coordinate describing temperature distribution, Eq. (257)	u_x	Component of the velocity vector in x -direction
Q	Volume rate of heat release		
Q_i	Generalized thermal force, Eq. (260)		
r	Radial coordinate		
r_0	Fixed or reference radial coordinate		
r^+	$= r/r_0$, dimensionless radial coordinate, Eq. (274)		
R	Radius of the free boundary		
R^+	$= R/r_0$, dimensionless, Eq. (274)		

U^*	$= \rho L X(t) / H t_m$, dimensionless, Eq. (97)	X_1^*	$= X^* / \sqrt{t^*}$
V	Volume; or thermal potential function, Eq. (258)	y	$= (t/t_m) - 1$, dimensionless time variable, Eq. (96)
W	Transformation variable for temperature, Eq. (293)	Y	Mole fraction
x	Cartesian coordinate	z	Dummy variable, or function defined in Eq. (199b)
x^*	$= x/a$, dimensionless space coordinate, Eq. (299)	$\langle z \rangle$	Mean diffusant jump length, Eq. (154)
$X(t)$	Position of interface in Cartesian coordinate	z^*	$= [x - X(t)] / (\alpha t_m)^{1/2}$, dimensionless variable, Eq. (95)
X^*	$= X/a$, dimensionless position of interface, Eq. (120)	Z	Function defined in Eq. (154)

GREEK LETTERS

α	Thermal diffusivity		or $(T - T_\infty) / (T_s - T_\infty)$, dimensionless temperature
α^*	$= kp / c_p R_0$, Eq. (136)	θ^*	$= (T - T_m) / T_m$ or $(T - T_s) / T_s$, dimensionless temperature
β, β'	Growth coefficients ($\eta = \beta$ and $\eta' = \beta'$ at free boundary)	θ_1	$= 1 + \theta^*$
β_n	Growth coefficient in n -dimensional space	θ_I	Heat balance integral, Eq. (266)
β^*	Growth coefficient defined in Eq. (71)	Θ	$= \xi_0(t^*) / \Lambda$ dimensionless variable, Eq. (246)
β^*	Growth coefficient defined in Eq. (144)	λ	$= x / X(t)$, dimensionless space coordinate
γ	Accommodation coefficient	Λ	$= L / c_p T_s$ or $L / c_p T_m$, dimensionless
Γ	Gamma function; linear operator, Eq. (180)	μ	$=$ Viscosity; or $2c_p(T_w - T_m) / L$, Eq. (269)
$\delta(x), \delta(t)$	Delta functions in space and time	ν	$= (D' / D)^{1/2}$, dimensionless, Eq. (48)
δ	Boundary layer thickness	ν_f	Mean jump frequency of the diffusant
Δ	Standard notation for difference	ξ	$= (a - x) / [a - X(t)]$, Landau's transformation
ϵ	$= [1 - (C' / C_i)]$, or $[1 - (\rho' / \rho)]$, dimensionless term	ξ_1	$= x - X(t)$, space variable, Eq. (115)
ϵ_1	Correction factor, Eq. (155)	ξ_2	$= 1 - \xi$
ζ_0	$= aH(t) / kT_m$, Eq. (242)	ρ	Density of original phase
ζ_1	$= (\eta - \beta) / [(1/\tau) - \beta]$, space variable, Eq. (323)	Σ	Surface of volume V or region in (x, t') plane
η	Boltzmann transformation variable, $(= s / (\alpha t)^{1/2}$ or $x / (\alpha t)^{1/2}$ or $s / (Dt)^{1/2}$ or $x / (Dt)^{1/2}$	τ	$= (t^*)^{1/2}$, dimensionless time variable, Eq. (305)
η_1	$= \Theta \sqrt{t^*}$, dimensionless thermal boundary layer thickness, Eq. (247)	τ^*	$= (\alpha s t / \tau_s)$, time variable, Eq. (139)
θ	$= (T - T_0) / (T_m - T_0)$, or $(T - T_0) / (T_b - T_0)$,	T	$= K_4 C_i$, dimensionless variable, Eq. (48)

ϕ_1	Mean free path length distribution function, Eq. (154)	$\psi_n(z)$	Function defined in Eq. (7)
$\phi_n(\eta)$	Function defined in Eq. (29)	$\Psi(t)$	Arbitrary heat input function, Eq. (215)
$\chi(T)$	Flow temperature function, Eq. (295)	ω	$= C_0/C_i$, dimensionless concentration, Eq. (48)
$\chi^T(T)$	Flow temperature function, Eq. (290)	$\Omega(t)$	Fictitious heat input function, Eq. (219)
ψ	$= m_*/M_*$, dimensionless variable, Eq. (137)		

SUBSCRIPTS (UNLESS OTHERWISE NOTED)

0	Initial condition	i	Interface
1	Source coordinates, or dummy variable	m	Melting
∞	Condition at infinity	max	Maximum
a	Condition at $x = a$, or ambient	n	Coordinate or summation index
b	Bulk fluid	r	Radial
f	Liquid phase	s	Condition of saturated vapor
		w	Condition at the wall

SUPERSCRIPTS (UNLESS OTHERWISE NOTED)

\cdot	Time derivative	\sim	Steady state
$'$	Newly formed phase (where properties of both phases are considered)	$*$	Dimensionless variable
		$+$	Dimensionless variable

REFERENCES

- A1. Adair, G. S., *Bio. Chem. J.* **14**, 762 (1920); **15**, 620 (1921).
A2. Adams, K. A., and Seizew, M. R., *ARS (Am. Rocket Soc.) J.* **31**, 1595 (1961).
A3. Allen, D. N. de G., and Severn, R. T., *Quart. J. Mech. Appl. Math.* **5**, 447 (1952).
A4. Allen, D. N. de G., and Severn, R. T., *Quart. J. Mech. Appl. Math.* **15**, 53 (1962).
A5. Arnold, J. H., *Trans. Am. Inst. Chem. Engrs.* **40**, 361 (1944).
B1. Baer, D., and Ambrosio, A., TR-59-0000-00610, Space Technology Laboratories, Inc., Los Angeles, California, 1959; cf. Sanders, R. W., *ARS (Am. Rocket Soc.) J.* **30**, 1030 (1960).
B2. Barnes, M. D., Kenyon, A. S., Zaiser, E., and La Mer, V. K., *J. Colloid Sci.* **2**, 349 (1947).
B3. Baxter, D. C., *J. Heat Transfer* **84C**, 317 (1962).
B4. Becker, R., and Doring, W., *Ann. Physik* [5] **24**, 719 (1935).
B5. Bick, J. H., *Trans. Am. Nucl. Soc.* **3**, 146 (1960).
B6. Biot, M. A., and Daughaday, H., *J. Aero/Space Sci.* **29**, 227 (1962).
B7. Birkhoff, G., Margulies, R. S., and Horning, W. A., *Phys. Fluids* **1**, 201 (1958).
B8. Boley, B. A., *J. Math. Phys.* **40**, 300 (1961).
B9. Boley, B. A., *Quart. Appl. Math.* **21**, 1 (1963).
B10. Boltzmann, L., *Ann. Physik* [3] **53**, 959 (1894).
B11. Booth, F., *Trans. Faraday Soc.* **44**, 796 (1948).
B12. Boyer, R. H., *J. Math. Phys.* **40**, 41 (1961).
B13. Brenner, H., *A.I.Ch.E. (Am. Inst. Chem. Engrs.) J.* **7**, 666 (1961).

- B14. Buikov, M. V., and Dukhin, S. S., *Intern. Chem. Eng.* **2**, 399 (1962).
- B15. Bungenberg de Jong, H. G., Unpublished research (1926); cf. Hermans, J. J., *J. Colloid Sci.* **2**, 387 (1947).
- C1. Carslaw, H. S., and Jaeger, J. C., "Conduction of Heat in Solids." Oxford Univ. Press, London and New York, 1959.
- C2. Chambré, P. L., *J. Appl. Phys.* **30**, 1683 (1959).
- C3. Charlesworth, D. H., and Marshall, W. R. Jr., *A.I.Ch.E. (Am. Inst. Chem. Engrs.) J.* **6**, 8 (1960).
- C4. Citron, S. J., *J. Aero/Space Sci.* **27**, 470 (1960).
- C5. Citron, S. J., *J. Aero/Space Sci.* **27**, 317 (1960).
- C6. Citron, S. J., *J. Aero/Space Sci.* **27**, 219 (1960).
- C7. Citron, S. J., *Proc. U. S. Natl. Congr. Appl. Mech.*, 4th, Univ. Calif., Berkeley, Calif. 1962 Vol. 2, p. 1221, A.S.M.E., New York, 1962.
- C8. Cochran, D. L., Rate of solidification—application and extension of theory. Dept. Mech. Eng., Stanford Univ., Stanford, California, Tech. Rep. No. 24 (1955).
- C9. Cohen, H., and Miranker, W. L., On boundary layers' behavior in the superconductor transition problem. IBM Res. Rept. RC-284 (1960).
- C10. Collins, F. C., *J. Colloid Sci.* **5**, 499 (1950).
- C11. Collins, F. C., and Kimball, G. E., *Ind. Eng. Chem.* **41**, 2551 (1949).
- C12. Collins, F. C., and Leinweber, J. P., *J. Phys. Chem.* **60**, 389 (1956).
- C13. Crank, J., *Phil. Mag.* [7] **39**, 140 (1948).
- C14. Crank, J., "Mathematics of Diffusion." Oxford Univ. Press, London and New York, 1959.
- C15. Crank, J., *Quart. J. Mech. Appl. Math.* **10**, Pt. 2, 220 (1957).
- C16. Crank, J., and Nicholson, P., *Proc. Cambridge Phil. Soc.* **45**, 50 (1947).
- C17. Curle, N., "The Laminar Boundary Layer Equations." Oxford Univ. Press (Clarendon), London and New York, 1962.
- D1. Danckwerts, P. V., *Trans. Faraday Soc.* **46**, 701 (1950).
- D2. Dennis, W. L., *Discussions Faraday Soc.* **30**, 78 (1960).
- D3. Dewey, C. F., Jr., Schlesinger, S. I., and Sashkin, L., *J. Aero/Space Sci.* **27**, 59 (1960).
- D4. Douglass, J., Jr., and Gallie, T. N., *Duke Math. J.* **22**, 557 (1955).
- D5. Dusenberre, G. M., *Trans. Am. Soc. Mech. Engrs.* **67**, 703 (1945).
- D6. Dusenberre, G. M., *Trans. Am. Soc. Mech. Engrs. Paper No. 58-HT-7* (1958).
- E1. Ehrlich, L. W., *J. Assoc. Comput. Machinery* **5**, 161 (1958).
- E2. Evans, G. W., *Quart. Appl. Math.* **9**, 185 (1951).
- E3. Evans, G. W., Isaacson, E., and MacDonald, J. K. L., *Quart. Appl. Math.* **8**, 312 (1950).
- E4. Eyres, N. R., Hartree, D. R., Ingham, J., Jackson, R., Sarjant, R. J., and Wagstaff, B., *Phil. Trans. Roy. Soc.* **A240**, 1 (1946).
- F1. Fisher, J. C., *J. Appl. Phys.* **19**, 1062 (1948).
- F2. Fowler, C. M., *Quart. Appl. Math.* **3**, 361 (1946).
- F3. Frank, F. C., *Proc. Roy. Soc.* **A201**, 586 (1950).
- F4. Friazinov, I. V., *Zh. Vychislitelnoi Mat. I. Mat. Fiz.* **1**, 972 (1961); cf. *Appl. Mech. Rev.* **16**, 917 (1963).
- F5. Friedman, A., *J. Math. Mech.* **8**, 499 (1959).

- F6. Friedman, A., *J. Math. Mech.* **9**, 19 (1960).
 F7. Friedman, A., *J. Math. Mech.* **9**, 885 (1960).
 F8. Frisch, H. L., and Collins, F. C., *J. Chem. Phys.* **20**, 1797 (1952); **21**, 2158 (1953).
 F9. Fuchs, N. A., "Evaporation and Droplet Growth in Gaseous Media." Pergamon, New York, 1959.
- G1. Gadazhieva, M. G., *Uch. Azerb. In-ta* **4**, 3 (1955); cf. *Appl. Mech. Rev.* **12**, 355 (1959).
 G2. Gibson, R. E., *Quart. Appl. Math.* **16**, 426 (1959).
 G3. Gibson, R. E., *Z. Angew. Math. Phys.* **9**, 198 (1960).
 G4. Goldstein, S., and Rosenhead, L., *Proc. Cambridge Phil. Soc.* **32**, 392 (1936).
 G5. Goodman, T. R., *Trans. Am. Soc. Mech. Engrs.* **80**, 335 (1958).
 G6. Goodman, T. R., *J. Heat Transfer* **83C**, 83 (1961).
 G7. Goodman, T. R., and Shea, J. J., *J. Appl. Mech.* **82E**, 16 (1960).
 G8. Griffin, J. R., Ph.D. thesis, Purdue Univ., Lafayette, Indiana, 1963.
 G9. Grinberg, G. A., *Zh. Tekhn. Fiz.* **21**, No. 3 (1951); cf. Redozubov, D. V., *Soviet Phys.—Tech. Phys. (English Transl.)* **5**, 570 (1960).
 G10. Gutowski, R., *Bull. Acad. Polon. Sci., Ser. Sci. Tech.* **10**, 183 (1962).
- H1. Ham, F. S., *Phys. Chem. Solids* **6**, 335 (1958).
 H2. Hamill, T. D., and Bankoff, S. G., *Chem. Eng. Sci.* **18**, 355 (1963).
 H3. Hamill, T. D., and Bankoff, S. G., *Chem. Eng. Sci.* **19**, 59 (1964).
 H4. Hamill, T. D., and Bankoff, S. G., *A.I.Ch.E. (Am. Inst. Chem. Engrs.) J.* **9**, 741 (1963).
 H5. Hamill, T. D., and Bankoff, S. G., *Ind. Eng. Chem. Fundamentals* **3**, 177 (1964).
 H6. Hartree, D. R., *Mem. Proc. Manchester Lit. Phil. Soc.* **80**, 85 (1935–1936).
 H7. Hermans, J. J., *J. Colloid Sci.* **2**, 387 (1947).
 H8. Hlinka, J. W., and Paschkis, V., *Trans. Am. Soc. Metals* **51**, 353 (1959).
 H9. Holmgren, E., *Arkiv Mat.* **4** (14, 18); cf. Kolodner, I., *Commun. Pure Appl. Math.* **9**, 1 (1956).
 H10. Horvay, G., *J. Heat Transfer* **82C**, 37 (1960).
 H11. Horvay, G., *Proc. U. S. Natl. Congr. Appl. Mech., 4th, Univ. Calif., Berkeley, Calif. 1962* Vol. 2, p. 1315 (1962).
 H12. Horvay, G., and Cahn, J. W., *Acta Met.* **9**, 695 (1961).
 H13. Hrycak, P., *A.I.Ch.E. (Am. Inst. Chem. Engrs.) J.* **9**, 585 (1963).
- I1. Ivantsov, G. P., *Dokl. Akad. Nauk SSSR* **58**, 567 (1947) (Mathematical Physics); translated by G. Horvay, Report No. 60-RL-(2511M), General Electric Research Laboratory, Schenectady, New York, 1960.
- J1. Johnson, I., and La Mer, V. K., *J. Am. Chem. Soc.* **69**, 1184 (1947).
- K1. Kinzer, G. D., and Gunn, R., *J. Meteorol.* **8**, 98 (1951).
 K2. Kirkaldy, J. J., *Can. J. Phys.* **36**, 446 (1958).
 K3. Knuth, E. L., *Phys. Fluids* **2**, 84 (1959).
 K4. Koh, J. C. Y., *J. Aero/Space Sci.* **28**, 989 (1961).
 K5. Kolodner, I., *Commun. Pure Appl. Math.* **9**, 1 (1956).
 K6. Kreith, F., and Romie, F. E., *Proc. Phys. Soc. (London)* **68**, 277 (1955).
 K7. Kuczynski, G. C., and Landauer, R., *J. Appl. Phys.* **22**, 952 (1951).

- K8. Kyner, W. T., *J. Math. Mech.* **8**, 483 (1959).
 K9. Kyner, W. T., *Quart. Appl. Math.* **17**, 305 (1959).
- L1. Lamé, G., and Clapeyron, B. P. E., *Ann. Chim. Phys.* **47** (1831); cf. Gutowski, R., *Bull. Acad. Polon. Sci., Ser. Sci. Tech.* **10**, 183 (1962).
 L2. La Mer, V. K., and Barnes, M. D., *J. Colloid. Sci.* **1**, 71 (1946); **1**, 79 (1946).
 L3. La Mer, V. K., and Kenyon, A. S., *J. Colloid. Sci.* **2**, 257 (1947).
 L4. Landau, H. G., *Quart. Appl. Math.* **8**, 81 (1950).
 L5. Lightfoot, N. H. M., *J. Iron Steel Inst. (London)* **119**, 364 (1929).
 L6. Lightfoot, N. H. M., *Proc. London Math. Soc.* **31**, Pt. 2, 97 (1930).
 L7. Lightfoot, N. H. M., *Iron Steel Inst. (London) Spec. Rept.* **2**, 1962 (1932).
 L8. London, A. L., and Seban, R. A., *Trans. Am. Soc. Mech. Engrs.* **65**, 771 (1943).
 L9. Longwell, P. A., *A.I.Ch.E. (Am. Inst. Chem. Engrs.) J.* **4**, 53 (1958).
 L10. Lotkin, M., *Quart. Appl. Math.* **18**, 79 (1960).
- M1. Mancj, O. J., Ph.D. thesis, Univ. Michigan, Ann Arbor, Michigan (1960); cf. *Dissertation Abstr.* **21**, 2230 (1961).
 M2. Margenau, H., and Murphy, G. M., "The Mathematics of Physics and Chemistry." Van Nostrand, Princeton, New Jersey, 1944.
 M3. Marshall, J. S., and Langleben, M. P., *J. Meteorol.* **11**, 104 (1954).
 M4. Mason, B. J., *Quart. J. Roy. Meteorol. Soc.* **79**, 104 (1953).
 M5. Mason, B. J., "The Physics of Clouds." Oxford Univ. Press, London and New York, 1957.
 M6. Maxwell, J. C., "Collected Scientific Papers," Vol. 11 Cambridge Univ. Press, London and New York, 1890.
 M7. Meksyn, D., "New Methods in Laminar Boundary Layer Theory." Pergamon, New York, 1961.
 M8. Miranker, W. L., *Quart. Appl. Math.* **16**, 121 (1958).
 M9. Miranker, W. L., and Keller, J. B., *J. Math. Mech.* **9**, 67 (1960).
 M10. Mirzadzhanzade, A. K., and Dzhalilov, K. N., *Zh. Tekhn. Fiz.* **25**, 1800 (1955); cf. *Appl. Mech. Rev.* **12**, 355 (1959).
 M11. Morin, F. S., and Reiss, H., *Phys. Chem. Solids* **3**, 196 (1957).
 M12. Morse, P. M., and Feshbach, H., "Methods of Theoretical Physics," Vol. 1. McGraw-Hill, New York, 1953.
 M13. Murray, W. D., and Landis, F., *J. Heat Transfer* **81C**, 106 (1959).
- N1. Neumann, F., Cf. Frank, P., and von Mises, R., "Die Differential und Integral Gleichungen der Mechanik und Physik," Vol. 2. Vieweg, Braunschweig, 1927.
 N2. Nielsen, A. E., *J. Phys. Chem.* **65**, 46 (1961).
- O1. Otis, D. R., *Heat Transfer Fluid Mech. Inst., Stanford Univ. Press, Stanford, Calif.*, p. 29 (1956).
- P1. Pattle, R. E., *Quart. J. Mech. Appl. Math.* **12**, 407 (1959).
 P2. Pekeris, C. L., and Slichter, L. B., *J. Appl. Phys.* **10**, 135 (1939).
 P3. Picone, M., *Math. Ann.* **101**, 701 (1929).
 P4. Pleshanov, A. S., *Soviet Phys.—Tech. Phys. (English Transl.)* **7**, 70 (1962).
 P5. Poots, G., *Intern. J. Heat Mass Transfer* **5**, 339, 525 (1962).

- R1. Redozubov, D. B., *Soviet Phys.—Tech. Phys. (English Transl.)* **2**, 1993 (1957).
R2. Redozubov, D. B., *Soviet Phys.—Tech. Phys. (English Transl.)* **5**, 570 (1960).
R3. Reiss, H., *J. Chem. Phys.* **19**, 482 (1951).
R4. Reiss, H., and La Mer, V. K., *J. Chem. Phys.* **18**, 1 (1950).
R5. Riazantsev, I. S., *J. Appl. Math. Mech.* **25**, 1706 (1961).
R6. Rieck, R., Unpublished dissertation (1924); cf. Huber, A., *Z. Angew. Math. Mech.* **19**, 1 (1939).
R7. Rubinstein, L. I., *Izv. Akad. Nauk SSSR* **11**, 37 (1947).
R8. Rubinstein, L. I., *Dokl. Akad. Nauk SSSR* **62**, 195 (1948).
R9. Rubinstein, L. I., *Dokl. Akad. Nauk SSSR* **79**, 45 (1951).
R10. Ruddle, R. W., "The Solidification of Castings." Inst. Metals, London, England, 1957.
R11. Ruoff, A. L., *Quart. Appl. Math.* **16**, 197 (1958).

S1. Sanders, R. W., *ARS (Am. Rocket Soc.) J.* **30**, 1030 (1960).
S2. Sarjant, R. J., and Slack, M. R., *J. Iron Steel Inst. (London)* **177**, 428 (1954).
S3. Schmidt, E., "Festschrift zum Siebzigsten Geburtstag August Föppl," p. 179. Springer, Berlin, 1924.
S4. Scriven, L. E., *Chem. Eng. Sci.* **10**, 1 (1959).
S5. Sestini, G., *Riv. Mat. Univ. Parma* **3**, 3, 103 (1952).
S6. Skinner, L. A., and Bankoff, S. G., *Phys. Fluids* **7**, 1 (1964).
S7. Smoluchowski, M. V., *Ann. Physik* [4] **48**, 1103 (1915).
S8. Somorjai, G. M., *J. Chem. Phys.* **35**, 655 (1961).
S9. Soodak, H., Ph. D. thesis, Duke Univ., Durham, North Carolina, 1943.
S10. Stefan, J., *Ann. Phys. Chem. (Wiedemann)* [N. F.] **42**, 269 (1891).
S11. Sunderland, J. W., and Grosh, R. J., *J. Heat Transfer* **83C**, 409 (1961).

T1. Tani, I., *J. Aeron. Sci.* **21**, 487 (1954).
T2. Thomas, D. G., *Phys. Chem. Solids* **9**, 31 (1958).
T3. Tirsii, G. A., *Soviet Phys.—Tech. Phys. (English Transl.)* **4**, 288 (1959).
T4. Turnbull, D., *Acta Met.* **1**, 684 (1953).
T5. Turnbull, D., *Solid State Phys.* **3**, 226 (1956).
T6. Tweet, A. G., *Phys. Rev.* **106**, 221 (1957).

V1. Veinik, A. L., "Approximate Calculation of Heat Conduction Processes." Gose-nergoizdat, Moscow, USSR, 1959. (In Russian.)

W1. Waite, T. R., *Phys. Rev.* **107**, 463, 471 (1957).
W2. Webster, A. G., "Partial Differential Equations of Mathematical Physics." Stechert, New York, 1927.
W3. Wert, C., and Zener, C., *J. Appl. Phys.* **21**, 5 (1950).

Y1. Yang, K. T., Discussion following paper by T. R. Goodman, *J. Heat Transfer* **83C**, 83 (1961).
Y2. Yang, W. J., Phase change of one-component system in a container. 6th Natl. Heat Transfer Conf., A.I.Ch.E.-A.S.M.E., Boston, Massachusetts, 1963. A.I.Ch.E. Preprint No. 48.

Z1. Zaiser, E., and La Mer, V. K., *J. Colloid Sci.* **3**, 571 (1948).
Z2. Zener, C., *J. Appl. Phys.* **20**, 950 (1949).

THE FLOW OF LIQUIDS IN THIN FILMS

George D. Fulford *

Department of Chemical Engineering,
University of Birmingham, Birmingham, England

I. Introduction	151
II. Description of Film Flow	153
A. Types of Film Flow	153
B. The Regimes of Film Flow	154
III. Theoretical Treatments of Film Flow	155
A. Introduction	155
B. Laminar Flow	156
C. The Onset of Wavy Flow (Theoretical Stability Considerations)	163
D. Wavy Laminar Film Flow	166
E. Turbulent Film Flow	170
F. Film Flow in the Presence of an Adjoining Stream	172
IV. Experimental Results and Comparison with Theory	176
A. Mean Film Thicknesses	177
B. Onset of Turbulence in Films	185
C. Onset of Rippling in Film Flow	186
D. Surface Waves on Films	189
E. Effect of Wall Roughness on Film Flow	200
F. Film Velocities and Velocity Profiles	201
G. Static Pressure Drop in the Gas Stream of a Wetted-Wall Column	204
H. Wall Shear Stress in the Liquid Film	206
V. Conclusions	207
Nomenclature	209
Appendix. Brief Chronological Résumé of Papers on Film Flow and Related Topics	210
References	228

I. Introduction

The flow of liquids in thin layers is frequently observed in everyday life; a common example is the flow of rain water on window panes, road surfaces, and roofs.

* *Present address:* E. I. du Pont de Nemours & Company, Inc., Photo Products Department, Research Division, Parlin, New Jersey.

Film flow is a special case of two-phase flow. In the present survey the flow of free liquid sheets (i.e., films bounded by two free surfaces) will not be considered; attention will be confined to film flow along a solid surface of some sort, with only one free surface. The second phase in contact with the free surface of the film may be either a gas or a second (immiscible) liquid, which may be at rest or in motion relative to the solid surface on which the film flows. Film flow is distinguished from other forms of two-phase flow by the presence of large interfaces of basically simple geometrical configuration. Two-phase flows are also often further classified as single-component (e.g., steam-water) or multicomponent flows, but this distinction is not of great importance in the study of the flow behavior of films.

The occurrence and applications of film flow in modern technology are numerous and important. Omitting the field of chemical engineering for the moment, the following applications of thin liquid flows have been found in the recent literature:

- (1) Film cooling of rocket motors, turbine blades, reactor tubes, etc. (T17, K18, Y3).
- (2) Refrigeration problems (C5).
- (3) Conveying of liquids by cocurrent gas streams, e.g., in oil pipelines, boiler tubes, etc. (H17, K23).
- (4) Design of channels, camber of roads, drainage works (C8, I3).
- (5) Design of dam spillways (B1).
- (6) Design of drain pipes and overflow lines (E2, V4).
- (7) Study of the transport of radioactive materials by rain water (B12).
- (8) Combating soil erosion (I1).
- (9) Heat transfer from wavy films of molten materials, e.g., on spacecraft (Z5).

The flow of thin liquid films in channels and columns has also served as the basis of fundamental studies of wave motion (M7), the effects of wall roughness in open-channel flow (R4), the effects of surface-active materials (T9-T12), and the like.

A very early application of liquid film flow in the chemical industry is mentioned in a patent of 1836 (G5): hydrogen chloride gas produced in the Leblanc soda process was absorbed by water films flowing over packings. Much later the film coolers and evaporators used in the German beet sugar industry inspired the earliest detailed theoretical and experimental studies of flow and heat transfer in falling films (C10, N6, N7). Chemical engineering interest in film flow has increased rapidly in recent years.

Typical modern applications of gas/film flows in the process industries

are in trickling-type cooling towers, packed and wetted-wall towers for rectification and gas absorption (or desorption), and in various types of coolers and evaporators. Most vapor condensers also make use of film flow, since droplet condensation is comparatively rare. In recent years swept-film equipment has been finding increasing application for solving difficult separation problems (B20, H21).

Extensive treatments of general two-phase flow problems have been given in the monograph by Kutateladze and Styrikovich (K25) and in recent surveys by Dukler and Wicks (D17), and Scott (S4), all of which indicate clearly the important place of film flow in the over-all scheme of two-phase flow phenomena. Film flow is more amenable to detailed study than most other types of two-phase flow, and a detailed knowledge of the phenomena occurring in film flow (with or without an adjacent gas stream) would assist greatly in understanding many of the more complex types of two-phase flow and the mechanisms of heat and mass transfer in such flows. Numerous experimental studies have been made of various two-phase transfer processes, but these have led mainly to empirical correlations of more or less limited applicability.

An attempt is made in the present survey to collect and review the more important results of the studies of liquid film flow scattered throughout the literature. It is hoped that this will avoid future duplication of work and enable investigators to concentrate on the many aspects of film flow which have been insufficiently studied in the past.

Studies of heat and mass transfer to films and film condensation are considered only insofar as the results throw light on the flow behavior; a brief review of such studies has been published elsewhere (F6). In addition, annular gas/liquid flow in horizontal ducts will not be considered here, since this is usually complicated by droplet entrainment.

II. Description of Film Flow

A. TYPES OF FILM FLOW

As in other flows, various types of film flow can be distinguished. The most important of these are steady flow and uniform flow, in which the properties of the flow are constant with respect to time and with respect to distance in the direction of flow.

Thus, the flow of a smooth film outside the acceleration zone is both steady and uniform. The flow in the smooth entry zone of a wetted-wall column where acceleration occurs is steady but nonuniform, while certain wavy film flows are both unsteady and nonuniform.

B. THE REGIMES OF FILM FLOW

A dimensional analysis of the problem of film flow (F7) has shown that in general the properties of a film flow *may* depend on the Reynolds, Weber, and Froude numbers of the flow, a dimensionless shear at the free surface of the film, and, for wavy flows, a Strouhal number formed from the frequency of the surface waves, and various geometrical ratios, e.g., the ratios of the wave amplitude and length to the mean film thickness.

The general dependence on the Reynolds, Froude, and Weber numbers appears to be the most useful. In this survey the following definitions of these groups are used:

$$N_{Re} = \bar{u}\bar{b}\rho/\mu = W/\mu \quad (1)$$

(a Reynolds number four times as large, based on the hydraulic diameter of an infinitely wide film, is frequently used in the literature, but appears to offer no particular advantage):

$$N_{We} = \bar{u}/(\sigma/\rho\bar{b})^{1/2} \quad (2)$$

$$N_{Fr} = \bar{u}/(g\bar{b})^{1/2} \quad (3)$$

This definition of N_{Fr} is of particular physical significance in film flow, since here the Froude number denotes the ratio of the mean film velocity to the celerity of a gravity wave in shallow liquid. (Wave celerity is defined as the velocity of a wave relative to the liquid on which the wave propagates.) The Weber number is defined by analogy.

It is well known in fluid flow studies that below a certain critical value of the Reynolds number the flow will be mainly laminar in nature, while above this value, turbulence plays an increasingly important part. The same is true of film flow, though it must be remembered that in thin films a large part of the total film thickness continues to be occupied by the relatively nonturbulent "laminar sublayer," even at large flow rates ($N_{Re} \gg N_{Re_{crit}}$). Hence, the transition from laminar to turbulent flow cannot be expected to be so sharply marked as in the case of pipe flow (D12). Nevertheless, it is of value to subdivide film flow into laminar and turbulent regimes depending on whether ($N_{Re} \leq N_{Re_{crit}}$).

However, the flow regime of a film cannot be defined uniquely as laminar or turbulent, as in the case of pipe flow, due to the presence of the free surface. Depending on the values of N_{Fr} and N_{We} , the free surface may be smooth, or covered with gravity waves or capillary or mixed capillary-gravity waves of various types. Thus, under suitable conditions, it is possible to have smooth laminar flow, wavy laminar or turbulent flow, where the wavy flows may be subdivided into gravity or capillary

types. It is to be noted particularly that the presence of waves is no indication that the flow as a whole is turbulent.

It can be seen that a large number of film-flow regimes exists. In the past it has been customary to describe the boundaries between the various regimes in terms of the Reynolds number only. This has given rise to a large number of "critical Reynolds numbers" for the first formation of waves, the appearance of capillary waves, the onset of turbulence, etc. (cf. B14). Recently it has been shown that it is possible to describe the various film-flow regimes in terms of N_{Re} , N_{Fr} , and N_{We} , and a rational nomenclature has been proposed (F7). The most important flow regimes discussed in this survey are the smooth laminar, the wavy laminar, and the (wavy) turbulent regimes. For instance, in the case of water films flowing on steep or vertical walls, smooth laminar flow occurs only at very low flow rates, gravity-type surface disturbances predominate at moderate N_{Re} , while capillary effects become important mainly at larger flow rates. (For water films, the Froude number is larger than the Weber number at a given flow rate except at very small slopes of the wall.)

It is clear that the flow regime is a complicated but predictable function of the physical properties of the liquid, the flow rate, and the slope of the channel. It has been shown that, for water films, gravity waves first appear in the region $N_{Fr} = 1-2$, capillary surface effects become important in the neighborhood of $N_{We} = 1$, and the laminar-turbulent transition occurs in the zone $N_{Re} = 250-500$ (F7).

III. Theoretical Treatments of Film Flow

A. INTRODUCTION

From the brief discussion above it is apparent that the flow of viscous liquids in the form of thin films is usually accompanied by various phenomena, such as waves at the free surface. These waves greatly complicate any attempt to give a general theoretical treatment of the film flow problem; Keulegan (K14) considers that certain types of wavy motion are the most complex phenomena that exist in fluid motion. However, by making various simplifying assumptions it is possible to derive a number of relationships which are of great utility, since they describe the limits to which the flow behavior should tend as the assumptions are approached in practice.

In the present section the general equations are set up, and the main results of the various treatments of smooth laminar flow, wavy flow, turbulent flow, and flow of films with an adjoining gas stream will be reviewed briefly.

B. LAMINAR FLOW

1. General Equations

The most general equations for the laminar flow of a viscous incompressible fluid of constant physical properties are the Navier-Stokes equations. In terms of the rectangular coordinates x, y, z , these may be written:

$$u \frac{\partial u}{\partial x} + v \frac{\partial u}{\partial y} + w \frac{\partial u}{\partial z} + \frac{\partial u}{\partial t} = - \frac{\partial \Omega}{\partial x} - \frac{1}{\rho} \frac{\partial p}{\partial x} + \nu \nabla^2 u \quad (4)$$

$$u \frac{\partial v}{\partial x} + v \frac{\partial v}{\partial y} + w \frac{\partial v}{\partial z} + \frac{\partial v}{\partial t} = - \frac{\partial \Omega}{\partial y} - \frac{1}{\rho} \frac{\partial p}{\partial y} + \nu \nabla^2 v \quad (5)$$

$$u \frac{\partial w}{\partial x} + v \frac{\partial w}{\partial y} + w \frac{\partial w}{\partial z} + \frac{\partial w}{\partial t} = - \frac{\partial \Omega}{\partial z} - \frac{1}{\rho} \frac{\partial p}{\partial z} + \nu \nabla^2 w \quad (6)$$

where u, v, w are the velocities in the x, y, z directions, t is the time, ρ and ν are the density and kinematic viscosity, p is the pressure, Ω is the force potential of the field in which flow occurs, and ∇^2 is the Laplacian operator.

In addition, the continuity equation

$$\frac{\partial u}{\partial x} + \frac{\partial v}{\partial y} + \frac{\partial w}{\partial z} = 0 \quad (7)$$

must be satisfied.

Since only gravity fields will be considered here, the negative derivatives of Ω are merely equal to the components of g in the respective directions.

For flow on flat plates, the following coordinate convention will be used, except where otherwise noted: the x -axis is directed along the plate surface in the direction of the greatest slope, the z -axis is directed across the plate, and the y -axis is taken perpendicular to the plate.

The forms assumed by the general equations for various simplified cases together with the boundary conditions and solutions will now be discussed, starting with the simplest possible case.

2. Smooth, Laminar, Two-Dimensional Film Flow

If the flow is steady, uniform, and two-dimensional (i.e., flow of a smooth film on an infinitely wide plate outside the acceleration zone), Eqs. (4) to (6) reduce directly to the very simple case originally obtained by Hopf (H18) and Nusselt (N6):

$$\frac{d^2 u}{dy^2} + \frac{g}{\nu} \sin \theta = 0 \quad (8)$$

$$\frac{dp}{dy} = \rho g \cos \theta \quad (9)$$

$$\frac{dp}{dz} = 0 \quad (10)$$

where θ is the slope of the wall. The continuity equation is satisfied automatically. With the boundary conditions

$$u = 0 \quad \text{at} \quad y = 0 \text{ (no slip at wall)}$$

$$\frac{du}{dy} = 0 \quad \text{at} \quad y = b \text{ (no drag at interface)}$$

the velocity distribution is given by the semiparabolic equation:

$$u = \frac{g}{\nu} (\sin \theta) \left(by - \frac{y^2}{2} \right) \quad (11)$$

The surface velocity (at $y = b$) is therefore

$$u_s = \frac{gb^2}{2\nu} \sin \theta \quad (12)$$

By integrating (11) over the film thickness, the mean velocity is found to be

$$\bar{u} = \frac{gb^2}{3\nu} \sin \theta \quad (13)$$

whence

$$u_s/\bar{u} = 1.5 \quad (14)$$

The volumetric flow rate per wetted perimeter is

$$Q = b\bar{u} = \frac{gb^3}{3\nu} \sin \theta \quad (15)$$

In the absence of drag at the free surface, the wall shear stress must support the total body force on the film, so that

$$\tau_w = b\rho g \sin \theta = (3\rho^2 g^2 \mu Q \sin^2 \theta)^{1/3} \quad (16)$$

Using the film Reynolds number defined as

$$N_{\text{Re}} = b\bar{u}/\nu = Q/\nu \quad (17)$$

the results above can be rewritten to give

$$\bar{u} = \left[\frac{\nu g \sin \theta}{3} \right]^{1/3} N_{\text{Re}}^{2/3} \quad (18)$$

$$b = \left[\frac{3\nu^2}{g \sin \theta} \right]^{1/3} N_{\text{Re}}^{1/3} \quad (19)$$

$$\tau_w = \rho(3\nu^2 g^2 \sin^2 \theta)^{1/3} N_{\text{Re}}^{1/3} \quad (20)$$

If the friction factor for film flow is defined in the usual way, so that $\tau_w = f\rho(\bar{u})^2/2$, then, by substituting for τ_w and \bar{u} from above,

$$f = 6/N_{Re} \quad (21)$$

which can be compared with the analogous value for laminar flow in closed conduits, $f = 8/N_{Re}$.

3. Axisymmetric, Smooth, Laminar Film Flow

When the film flows on a vertical cylindrical surface of radius R , Eq. (8) becomes

$$\frac{d^2u}{dr^2} + \frac{1}{r} \frac{du}{dr} = -\frac{g}{\nu} \quad (22)$$

with r as the radial coordinate, which is to be solved with the boundary conditions

$$\begin{aligned} u &= 0 & \text{at } r &= R \text{ (no slip at tube wall)} \\ du/dr &= 0 & \text{at } r &= R + b \text{ (no drag at interface)} \end{aligned}$$

(The film is assumed to flow on the outer surface of the tube; for flow inside the tube the interface is at $r = R - b$, but the derivation is similar otherwise.)

The velocity profile is found to be

$$u = \frac{g}{4\nu} (R^2 - r^2) + \frac{g}{2\nu} (R + b)^2 \ln\left(\frac{r}{R}\right) \quad (23)$$

and the flow rate per wetted perimeter is

$$Q = \frac{g}{16\nu} \left[\frac{4(R + b)^4}{R} \ln\left(\frac{R + b}{R}\right) - \frac{3(R + b)^4}{R} + 4R(R + b)^2 - R^3 \right] \quad (24)$$

which is the result given by Feind (F2). The equation quoted by Jackson (J1) can be derived from (24) also. However, this equation is inconvenient for frequent use. By expanding the terms above in powers of (b/R) , it is easily shown that

$$Q = \frac{gb^3}{3\nu} \left[1 + \frac{b}{R} + \frac{3}{20} \left(\frac{b}{R}\right)^2 - \frac{1}{40} \left(\frac{b}{R}\right)^3 + \frac{1}{140} \left(\frac{b}{R}\right)^4 \dots \right] \quad (25)$$

which is a more general case of the equation used by Kamei and Oishi (K4).

As the tube radius R tends to infinity, it is seen that (25) tends towards (15) for the infinitely wide wall.

Considering a film 1 mm. thick flowing on a tube of 1 cm. diameter, it is seen that the b/R term in (25) constitutes a correction of 20% to the film thickness calculated by (15), while the next term makes only a very small correction. It can be seen that it is necessary to apply these curvature

corrections in comparing film flow results on tubes with those on flat walls unless the tubes are of large diameter.

Grimley (G11) has shown experimentally that for tubes of very small diameter there is an additional capillary effect on the film thickness.

4. Smooth, Laminar, Three-Dimensional Film Flow

When the film flows in a channel of finite width, with side walls, the flow is no longer two-dimensional in nature, as in Section III, B, 2, but edge effects occur and must be taken into account. Two types of edge effects can occur: viscous edge effects, due to the drag of the side walls, and capillary edge effects, due to the capillary surface elevation at the side walls.

The viscous edge effect will be calculated first. It is assumed that the liquid possesses no surface tension, so that the liquid surface is flat from wall to wall of the channel. In this case, with the other assumptions of Section III, B, 2, Eq. (4) reduces to

$$\frac{\partial^2 u}{\partial y^2} + \frac{\partial^2 u}{\partial z^2} = -\frac{\rho g}{\mu} \sin \theta \quad (26)$$

to be solved with zero velocity on the wall ($y = 0$) and at the side walls ($z = \pm w$) and zero drag at the interface ($y = b$). Several solutions of this equation have been given (C16, F7, H18, O1). These differ somewhat in form, but Owen (O1) has pointed out that, since this is a problem of the Dirichlet type, which is known from potential theory to possess only one regular solution, these must be merely different expressions for the same solution.

For the velocity distribution, Hopf gives (H18)

$$u = \sum_{n=0}^{\infty} (-1)^n \frac{16w^2g \sin \theta}{(2n+1)^3\pi^3\nu} \left[\frac{\cos \left\{ (2n+1) \frac{\pi}{2} \frac{y-b}{w} \right\}}{\cos \left\{ (2n+1) \frac{\pi}{2} \frac{b}{w} \right\}} - 1 \right] \cos \left\{ (2n+1) \frac{\pi}{2} \frac{z}{w} \right\} \quad (27)$$

from which the flow rate is given as

$$2wQ = \frac{4w^4g \sin \theta}{\nu} \left[\sum_{n=0}^{\infty} \left(\left\{ \frac{2}{(2n+1)\pi} \right\}^5 \tan \frac{(2n+1)\pi b}{2w} \right) - \frac{b}{w} \sum_{n=0}^{\infty} \left\{ \frac{2}{(2n+1)\pi} \right\}^4 \right] \quad (28)$$

Provided that the channel width is considerably larger than the film thickness, which is usually the case, Hopf showed that (28) can be greatly simplified to give the mean flow per wetted perimeter as

$$Q = \frac{gb^3 \sin \theta}{3\nu} \left(1 - 0.63 \frac{b}{w} \right) \quad (29)$$

As $w \rightarrow \infty$, (29) tends to the solution for the infinitely wide plate, (15), by comparison with which it is seen that the term $0.63b/w$ is the correction for the viscous edge effect. Since normally $w \gg b$, it is clear that this correction is very small.

The velocity distribution equation (27) indicates that in the absence of surface tension effects the maximum velocity in a film flowing in a flat channel of finite width should occur at the free surface of the film at the center of the channel. The surface velocity should then fall off to zero at the side walls. However, experimental observations have shown (B10, H18, H19, F7) that the surface velocity does not follow this pattern but shows a marked increase as the wall is approached, falling to zero only within a very narrow zone immediately adjacent to the walls. The explanation of this behavior is simple: because of surface tension forces, the liquid forms a meniscus near the side walls. Equation (12) shows that the surface velocity increases with the square of the local liquid depth, so the surface velocity increases sharply in the meniscus region until the side wall is approached so closely that the opposing viscous edge effect becomes dominant.

For this case the velocity equation is the same as (26), since the pressure term $\partial p / \partial x$ in Eq. (4) disappears in uniform flow in which the free surface is in contact with the atmosphere at all points. Equations (5) and (6) reduce to

$$\frac{dp}{dy} = \rho g \cos \theta \quad (30)$$

which shows that there is a hydrostatic pressure distribution across the film thickness and

$$\frac{dp}{dz} = 0 \quad (31)$$

If the film is flat, (31) is automatically satisfied, as in the calculation of the viscous edge effect above, but, with surface tension, the capillary pressure in the curved part of the meniscus must be taken into account, and Eq. (31) provides the condition from which the shape of the free surface can be calculated.

Numerical calculations of the velocity distributions in the meniscus region of a water film flowing in a glass channel have been made (F7) for a few cases. Figure 1 shows the isotaches in the meniscus region for a water

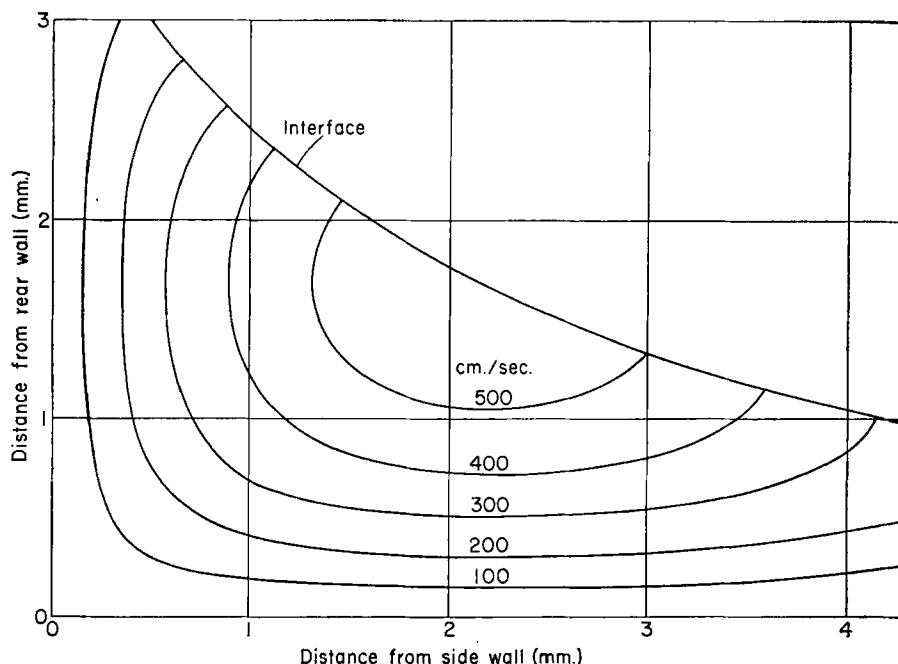


FIG. 1. Calculated lines of constant velocity in a water film flowing near the corner of a rectangular glass channel at 30° to the horizontal; film thickness far from side wall is $\frac{1}{3}$ mm. (F7).

film (at $20^\circ\text{C}.$) of undisturbed thickness $\frac{1}{3}$ mm. (far from the side walls) flowing in a glass channel at 30° to the horizontal. The calculated results for the local flow rates were in fair agreement with experimental data.

The calculations and experimental observations show that the local flow rates near the side walls are considerably larger than the local flow rates prevailing over the central part of the channel. It is clear that this capillary edge effect must be allowed for in film flow experiments in rectangular channels unless the channel is extremely wide (H19, B10). It is clear that the capillary effect noted here could be very important in the flow of films over packings, since menisci may be formed in the angles between packing elements; a relatively large part of the liquid might flow in such regions, due to the greater thickness of the film there, and, because of the greater velocity, the contact-time distribution of elements of the film surface could be greatly disturbed.

5. Inertia Effects in Smooth Laminar Flow

Kasimov and Zigmund (K11) have dealt with film flow on a vertical laterally unbounded surface for the case when the flow is steady but not

necessarily uniform, i.e., taking the inertia terms into account. In this case, Eq. (4) becomes

$$u \frac{\partial u}{\partial x} + v \frac{\partial u}{\partial y} = \nu \frac{\partial^2 u}{\partial y^2} + g \quad (32)$$

and (7) becomes

$$\frac{\partial u}{\partial x} + \frac{\partial v}{\partial y} = 0 \quad (33)$$

Denoting the initial film thickness at $x = 0$ by b_i and assuming a semiparabolic velocity distribution, the following equation was obtained for the local film thickness b_x at $x = x$:

$$\begin{aligned} \frac{5gx}{6Q^2} = & \frac{1}{6b_N^2} \ln \left[\frac{(b_x^2 + b_N b_x + b_N^2)}{(b_x - b_N)^2} \frac{(b_i - b_N)^2}{(b_i^2 + b_N b_i + b_N^2)} \right] \\ & + \frac{1}{b_N^2 \sqrt{3}} \arctan \frac{b_N \sqrt{3}(b_x - b_i)}{b_x(b_i - b_N) + b_N b_i + 2b_N^2} \end{aligned} \quad (34)$$

where b_N is the value of the film thickness given by the Nusselt theory, neglecting inertia [Eq. (15) or (19)].

The flow can be divided into three zones:

- (1) The stabilization zone, where $b_x < b_N$.
- (2) The zone of stabilized flow, where $b_x = b_N$.
- (3) The zone in which inertia forces are important, and $b_x > b_N$.

The usual Nusselt equations, Section III, B, 2, are strictly valid only in the second zone, which is usually only of short extent.

A second approximate solution was obtained without assuming the shape of the velocity profile. In this case the x component of the velocity was found to be

$$u = \frac{g}{\nu} \left(b_x y - \frac{y^2}{2} \right) + \frac{\nu}{6} \left\{ \frac{g}{4\nu^2} \right\}^2 \frac{b_x^2}{x} \left[y^4 - \frac{13}{210} \frac{g}{4\nu^2} \frac{b_x y^7}{x} \right] \quad (35)$$

for the region $x > 2.02$ cm., with a similar relation for v . It will be observed that the Nusselt solution (11) is a special case of this general result. Similar expressions were obtained for the case when a surface drag due to a gas stream was present.

The main prediction of this treatment is that the film thickness should increase gradually in the direction of flow due to the inertia effects. Substitution of values of the physical properties into these equations has shown that these effects are usually small for ordinary mobile liquids, such as water.

C. THE ONSET OF WAVY FLOW (THEORETICAL STABILITY CONSIDERATIONS)

In addition to the general treatments of wavy flow, a number of theories concerning the stability of film flow have been published; in these the flow conditions under which waves can appear are determined. The general method of dealing with the problem is to set up the main equations of flow (usually the Navier-Stokes equations or the simplified Nusselt equations), on which small perturbations are imposed, leading to an equation of the Orr-Sommerfeld type, which is then solved by various approximate means to determine the conditions for stability to exist. The various treatments are lengthy, and only the briefest summary of the results can be given here.

Shibuya (S10) dealt with the case of the onset of instability in film flow on the outer surface of a vertical tube. By assuming a mixed disturbing velocity of the cosine-hyperbolic cosine type, it was found that the numerical value of the Reynolds number for instability was approximately

$$N_{Re_i} = 7 \quad (36)$$

regardless of the physical properties. The wavelength at the onset of rippling was calculated as approximately 2 mm.

In his early paper, Yih (Y1) carried out numerical calculations for stability in the case of flow on a vertical wall, from which it appears that

$$N_{Re_i} = 1.5 \quad (37)$$

Both these treatments omitted surface tension forces.

The Kapitsa treatment of wavy film flow (K7), which is discussed in detail later, indicates that

$$N_{Re_i} = 0.61(K_F \sin \theta)^{-1/11} \quad (38)$$

where K_F is the physical properties group $\mu^4 g / \rho \sigma^3$. The Kapitsa theory is strictly applicable to long waves only ($\lambda/b \geq 13.7$), so this result may not be accurate if the waves at the point of inception are short. This equation gives a numerical result of $N_{Re_i} \cong 5.8$ for water on a vertical wall.

Benjamin (B5) has given a detailed treatment of the onset of two-dimensional instability in film flow, taking capillary effects into account. The expression for neutral stability found in this work can be given as

$$\frac{4n^2}{(3N_{Re})^{5/3}} (K_F \sin \theta)^{-1/3} + \frac{4 \cot \theta}{3N_{Re}} - \frac{8}{5} + 5.5289142n^2 - 0.0000639(nN_{Re})^2 - 14.6352952n^4 = 0 \quad (39)$$

where n is the wave number, defined as

$$n = 2\pi\bar{b}/\lambda \quad (40)$$

It was deduced that surface tension has a stabilizing effect, especially at short wavelengths, but instability cannot be converted to stability merely by increasing the surface tension. It was found that, for a vertical slope,

$$N_{Re} = 0 \quad (41)$$

i.e., vertical film flow is always inherently unstable, though the instability at very low N_{Re} may not be physically manifest. At other slopes there is a small zone of stable flow.

Andreev (A5a) has recently considered the stability of viscous film flow with respect to infinitesimal disturbances. In this treatment, absolute instability was not found for laminar film flow along a vertical wall.

In a simplified treatment for longer waves, Benjamin derived an amplification factor α , defined as the amplification experienced by the wave of maximum instability in traveling a distance of 10 cm. If neutral stability exists, $\alpha = 1$, and if $\alpha > 1$, wavy flow can be expected. For a vertical wall,

$$\alpha = \exp \left(1.7396 [\text{cm.}] \nu^{2/3} g^{2/3} \frac{\rho}{\sigma} N_{Re}^{7/3} \right) \quad (42)$$

Binnie (B10) extended this treatment to cover angles other than the vertical; thus, for water films ($\sim 20^\circ\text{C.}$),

$$\alpha = \exp \left\{ 0.0434 \left(\frac{8}{5} - \frac{4 \cot \theta}{3N_{Re}} \right)^2 (\sin^{2/3} \theta) N_{Re}^{7/3} \right\} \quad (43)$$

Substituting the condition $\alpha = 1$ for neutral stability, it is seen that

$$N_{Re} = \frac{5}{8} \cot \theta \quad (44)$$

This work was later extended to cover the case of three-dimensional instability (B6). The results tended to confirm the earlier results.

Hanratty and Hershman (H2) have given an interesting treatment of the stability problem. For the case of free film flow (i.e., film flow without a bounding gas flow), the condition for neutral stability becomes

$$\frac{\cos \theta}{(N_{Fr})^2} = 3 - n^2 (N_{We})^2 \quad (45)$$

where n is given by (40). It can be shown that Benjamin's result can be expressed in an exactly similar form, apart from replacing the term 3 in Eq. (45) by 3.6.

The treatment of Ishihara *et al.* (I2) leads to results similar to those of the simplified Benjamin theory.

The stability problem in the presence of a bounding gas stream (co-current and countercurrent) has been considered for a number of special cases (F3, G6, M10, Z1). The countercurrent solutions tend to confirm Benjamin's result that the flow is always inherently unstable on a vertical wall.

Recently Yih (Y2) has given a detailed treatment of the stability of film flow on an inclined plane. Three cases are considered in detail: small wave numbers (n), small Reynolds numbers, and large wave numbers. In the first case the results are in agreement with the results of Benjamin noted above, but for large wave numbers and zero surface tension, Benjamin's tentative conclusions are shown to be invalid. The stability curves are considered for film flows on vertical and sloped walls for liquids with and without surface tension.

The stability of flow in open channels has been investigated theoretically from a more macroscopic or hydraulic point of view by several workers (C17, D9, D10, D11, I4, J4, K16, V2). Most of these stability criteria are expressed in the form of a numerical value for the critical Froude number. Unfortunately, most of these treatments refer to flow in channels of very small slope, and, under these circumstances, surface instability usually commences in the turbulent regime. Hence, the results, which are based mainly on the Chézy or Manning coefficient for turbulent flow, are not directly applicable in the case of thin film flow on steep surfaces, where the instability of laminar flow is usually in question. The values of the critical Froude numbers vary from 0.58 to 2.2, depending on the resistance coefficient used. Dressler and Pohle (D11) have used a general resistance coefficient, and Benjamin (B5) showed that the results of such analyses are not basically incompatible with those of the more exact investigations based on the differential rather than the integral ("hydraulic") equations of motion. The hydraulic treatment of the stability of laminar flow by Ishihara *et al.* (I2) has been mentioned already.

It is to be noted that, for laminar open channel flow, the Froude and Reynolds numbers are interrelated. Making use of (1), (3), and (19), it is easily shown that

$$N_{Fr} = (N_{Re}/3)^{1/2} \sin^{1/2}\theta \quad (46)$$

so that for this regime the Reynolds number of instability N_{Re} can be expressed as a critical Froude number, if desired. Similar equations can also be obtained for other flow regimes [see, for instance, (P4), but it is necessary to note that N_{Re} and N_{Fr} are defined differently in this publication].

D. WAVY LAMINAR FILM FLOW

For the case of two-dimensional wavy film flow, Levich (L9) has shown that Eqs. (4) and (5) reduce to the familiar form of the boundary layer equations:

$$\frac{\partial u}{\partial t} + u \frac{\partial u}{\partial x} + v \frac{\partial u}{\partial y} = \frac{-1}{\rho} \frac{\partial p}{\partial x} + \nu \frac{\partial^2 u}{\partial y^2} + g \sin \theta \quad (47)$$

$$\frac{\partial p}{\partial y} = 0 \quad (48)$$

with the following boundary conditions: at the free surface of the film, $y = b$, where $b = f(x, t)$,

$$p = p_\sigma \cong -\sigma \frac{d^2 b}{dx^2} \quad (\text{capillary pressure}) \quad (49)$$

$$\mu \frac{\partial u}{\partial y} = 0 \quad (\text{zero interfacial shear}) \quad (50)$$

at the solid wall ($y = 0$),

$$u = v = 0 \quad (\text{no slip}) \quad (51)$$

The continuity condition can be expressed as

$$\frac{\partial b}{\partial t} = -\frac{\partial}{\partial x} \left(\int u \, dy \right) \quad (52)$$

Kapitsa was the first to attempt the solution of this system of equations (K7). In this original solution the term $v \partial u / \partial y$ in Eq. (47) was omitted, as also in the analysis by Portalski (P3) who resolved Kapitsa's equations to a higher degree of accuracy. By comparing the corrected solution by Bushmanov (B22, L9) with the original result, it appears that the errors caused by the omission of this term are not large.

It is assumed that the velocity distribution in the film can be given by the usual semiparabolic expression [Eqs. (11) and (13)]. Substituting this value of the velocity into (47), making use of (49), and then averaging over the film thickness by integrating with respect to y and dividing by b , it is found that

$$\frac{\partial \bar{u}}{\partial t} + \frac{9}{10} \bar{u} \frac{\partial \bar{u}}{\partial x} = \frac{\sigma}{\rho} \frac{d^3 b}{dx^3} - \frac{3\nu \bar{u}}{b^2} + g \sin \theta \quad (53)$$

while (52) becomes

$$\frac{\partial b}{\partial t} = -\frac{\partial (\bar{u} b)}{\partial x} \quad (54)$$

where \bar{u} is the mean velocity over the film thickness.

It is then further assumed that the waves are long compared to the film thickness, so that the film thickness can be represented as

$$b = \bar{b}(1 + \phi) \quad (55)$$

where \bar{b} is the mean film thickness and ϕ is the local deviation from the mean, and the mean velocity and thickness are then referred to the new variable $(x - ct)$, where c is the phase velocity of the waves. After various rearrangements, the equation for solution becomes, finally, to the first approximation,

$$\frac{\sigma \bar{b}}{\rho} \frac{d^3 \phi}{dx^3} - (c - \bar{u}) \left(\frac{9\bar{u}}{10} - c \right) \frac{d\phi}{dx} - \frac{3\nu}{(\bar{b})^2} (c - 3\bar{u})\phi + g \sin \theta - \frac{3\nu \bar{u}}{(\bar{b})^2} = 0 \quad (56)$$

where \bar{u} is given by $Q = \bar{b}\bar{u}$.

In order for an undamped periodic solution to exist it is necessary that the constant term in this equation and the coefficient of ϕ be equal to zero, so that, to the first approximation,

$$\bar{u} = \frac{(\bar{b})^2 g \sin \theta}{3\nu} \quad (57)$$

$$c = 3\bar{u} \quad (58)$$

Comparison of (57) with (13) shows that, to the first approximation, the film thickness is not affected by the waviness of the flow.

It is of interest to note that the wave-velocity condition obtained by Benjamin (B5) can be written as

$$c = 2(1 - n^2 + \frac{11}{8}n^4 + 0.0077581n^2(N_{Re})^4 - 3.3555556n^6)u_s \quad (59)$$

where u_s is the surface velocity (equal to $1.5\bar{u}$), and n is given by (40). For long waves, (59) reduces to

$$c = 2u_s = 3\bar{u} \quad (60)$$

which is in agreement with the first result of Kapitza above. The same value of c has been obtained by Hanratty and Hershman (H2) and can also be deduced from the general wave theory of Lighthill and Whitham (L11).

Using (57) and (58), Eq. (56) becomes

$$\frac{\sigma \bar{b}}{\rho} \frac{d^3 \phi}{dx^3} + 4.2\bar{u}^2 \frac{d\phi}{dx} = 0 \quad (61)$$

from which the function ϕ defining the surface shape (55) is

$$\phi = \alpha \sin [\bar{u}(4.2\rho/\sigma\bar{b})^{1/2}(x - ct)] \quad (62)$$

where $\alpha\bar{b}$ is the wave amplitude. To this first approximation, it is seen that the surface disturbances are sinusoidal.

In the second approximation, the equation analogous to (56) contains terms to the second order in ϕ . The details of the calculation cannot be included here, but briefly, it is found that in this case the mean film thickness of the wavy flow depends on the wave amplitude α , or

$$(\bar{b})^3 = \frac{3\nu Q}{g} \Phi \quad (63)$$

where Φ is a function of α and c/\bar{u} . In order to estimate the wave amplitude, Kapitza (K7) carried out an interesting analysis of the stability of the wavy flow and determined the conditions under which the energy supplied to the film by the gravity force is balanced by the dissipation of energy by viscous forces. From this it was deduced in general terms that the film will assume a configuration in which its mean thickness is a minimum for the given flow rate; that is, the function Φ in (63), which is unity for smooth flow, but which is always less than unity for wavy flow, must be a minimum. For the particular second-order conditions of this treatment, the equations for Φ as a function of α^2 and of c/\bar{u} are solved graphically, making use of the fact that Φ must be a minimum. In this way, Levich (L9) shows that

$$\alpha = 0.46 \quad (64)$$

$$c = 2.4\bar{u} \quad (65)$$

$$\Phi = 0.8$$

so that, substituting in (63),

$$\bar{b} = 1.34(\nu Q/g)^{1/3} \quad (66)$$

$$\lambda = \frac{2\pi}{\bar{u}} \left\{ \frac{\sigma\bar{b}}{\rho(c/\bar{u} - 1)(c/\bar{u} - 0.9)} \right\}^{1/2} \quad (67)$$

For flow on nonvertical slopes, g is replaced throughout by $g \sin \theta$, where θ is the angle of inclination of the wall, measured from the horizontal.

It is seen from (65) that the wave velocity is considerably smaller than the value given by the first approximation, (58). From (63), the ratio of the mean film thickness in wavy flow to the thickness of a smooth film at the same flow rate is given by $\Phi^{1/3}$ or, from above, 0.93. The corresponding value obtained by Portalski (P3) was 0.94. It is thus seen that for wavy flow of the type assumed here, the mean thickness of the wavy film is 6-7% smaller than the corresponding smooth film. It is pointed out by Kapitza that it does not follow that there may not be some other type of film surface configuration which would lead to a greater reduction in thickness and, therefore, to greater stability of flow.

Based on a treatment like that above, Tailby and Portalski (T2) have

derived an expression for the increase in the surface area of the film due to the waves at the interface:

$$\Delta S = \left(\frac{b\pi\alpha}{\lambda} \right)^2 \left[1 + \left(\frac{g\alpha\rho\lambda^3}{2^4\pi^3\bar{f}\sigma} \right)^2 \right] \quad (68)$$

It is claimed that this relationship is valid up to approximately $N_{Re} = 300$. However, the Kapitza treatment (K7) is shown to be valid only up to the condition that the wavelength is more than 13.7 times as great as the film thickness, which corresponds to $N_{Re} \cong 50$ for a vertical water film.

Semenov (S7) simplified the equations of wavy flow for the case of very thin films, and this approach has also been followed by others (K20, K21). These treatments refer mainly to the case of film flow with an adjoining gas stream and will be considered in Section III, F, 3.

Kapitsa and Kapitza (K10) have shown that the relative change in wavelength for flow on a tube of radius R compared with that on a flat surface at the same flow rate is

$$\Delta\lambda/\lambda = \frac{1}{2}(\lambda/2\pi R)^2 \quad (69)$$

which is quite small except for small values of R .

Recently, Kasimov and Zigmund (K12) have published the first part of a new theoretical treatment of wavy film flow, extending their recent work on smooth laminar film flow (Section III, B, 5) to this case also. It is shown that, with appropriate assumptions, the new theory reduces to the Nusselt solution for smooth films, or to a result similar to the corrected Kapitza solution. The most interesting conclusions to be drawn from the part of the theory so far published are:

(1) The mean film thickness and the wave amplitude should increase in the direction of flow.

(2) The wave amplitude should decrease with increase of the liquid viscosity.

(3) The wavelength is proportional to $(N_{Re})^{1/3}\sigma^{1/3}\nu^{2/9}$.

(4) The wave amplitude on an inclined surface should be smaller than on a vertical surface for the same flow rate and liquid properties, while the wavelength should be greater on the inclined surface.

In addition to the theories reviewed above, there are many treatments in the literature which deal with the hydraulics of wavy flow in open channels. Most of these refer to very small channel slopes (less than 5°) and relatively large water depths. Under these conditions, surface tension plays a relatively minor part and is customarily neglected, so that only gravity waves are considered. For thin film flows, however, capillary forces play an important part (K7, H2). In addition, most of these treatments consider a turbulent main flow, while in thin films the wavy flow is often

laminar. It is of interest to note, however, that Dressler (D9) has shown that gravity waves in steep channels became nonsymmetrical, with steep fronts and gently sloping tails (roll waves). The breakup of an initially uniform wave pattern to form irregular roll waves is also considered by Lighthill (L10) and Mayer (M7). Ishihara *et al.* (I1) have considered gravity roll waves on a laminar main flow and deduced that, for small channel slopes and waves of small amplitude, the wave velocity is

$$c = \frac{g}{5}\bar{u} + [g\bar{b} + \frac{g}{25}(\bar{u})^2]^{1/2} \quad (70)$$

E. TURBULENT FILM FLOW

The problem of turbulent flow in thin films has received comparatively little attention. Because of the great complexity of the flow processes involved, there are no theoretical treatments of the problem of wavy turbulent flow, and the usual procedure is to neglect the surface waves and obtain solutions for the case of smooth turbulent flow.

Keulegan (K13) applied the semiempirical boundary-layer concepts of Prandtl and von Kármán to the case of turbulent flow in open channels, taking into account the effects of channel cross-sectional shape, roughness of the wetted walls, and the free surface. Most of the results are applicable mainly to deep rough channels and bear little relation to the flow of thin films.

Levich (L8, L9) has given an interesting treatment of fully turbulent film flow. In the absence of a flowing gas stream at the interface, Levich deduced that the scale of turbulence and the turbulent velocity normal to the interface must be proportional to the distance from the interface, so that all turbulent pulsations must disappear at the interface itself, leaving there a nonturbulent layer of thickness

$$\delta' \propto b/(N_{Re})^{3/4}$$

A theory of gas absorption by turbulent liquid films has been developed on the basis of this conclusion (L9).

For fully developed turbulent flow with zero interfacial drag, it is shown (L8) that the mean film velocity is

$$\bar{u} = \sqrt{\frac{gb \sin \theta}{K}} \ln \left[\frac{b}{\nu} \sqrt{\frac{gb \sin \theta}{K}} \right] \quad (71)$$

where K is a constant. No numerical value is given for K , but substitution of the value $b = 0.076$ cm. for $N_{Re} = 1000$ obtained experimentally (B14) for a water film ($\nu = 0.01$ cm.²/sec.) on a vertical wall ($\sin \theta = 1$) shows that K should be in the region of $\frac{1}{5}$.

Nearly all of the remaining treatments of turbulent film flow are based on the assumption that the film can be regarded as smooth, and that some

form of the dimensionless velocity profile valid for single-phase flow (pipe flow) can be applied to the flow of films. In principle the treatments differ mainly in the form of the dimensionless velocity profile used, and only one will be discussed in detail.

Dukler and Bergelin (D16) used the universal velocity profile equations of Nikuradse:

$$u^+ = y^+ \quad \text{for } 0 \leq y^+ \leq 5 \text{ (laminar sublayer)} \quad (72)$$

$$u^+ = -3.05 + 5.0 \ln y^+ \quad \text{for } 5 < y^+ \leq 30 \text{ (buffer layer)} \quad (73)$$

$$u^+ = 5.5 + 2.5 \ln y^+ \quad \text{for } 30 < y^+ \leq b^+ \text{ (turbulent zone)} \quad (74)$$

where

$$u^+ = u/u^* \quad (\text{dimensionless velocity}) \quad (75)$$

$$y^+ = yu^*/\nu \quad (\text{dimensionless distance from wall}) \quad (76)$$

$$b^+ = bu^*/\nu \quad (\text{dimensionless film thickness}) \quad (77)$$

$$u^* = (\tau_w/\rho)^{1/2} \quad (\text{friction velocity}) \quad (78)$$

By integrating the dimensionless velocities over the film thickness, it is found for the case of turbulent flow ($b^+ \geq 30$) that

$$N_{Re} = b^+(3.0 + 2.5 \ln b^+) - 64 \quad (79)$$

[For $b^+ < 30$, Portalski (P3, P4) has given a corrected form of the original treatment.] In the case of zero interfacial shear, the wall shear stress is given by (16), so from (77) and (78)

$$b^+ = (g^{1/2} \rho \sin^{1/2} \theta) b^{3/2} / \mu \quad (80)$$

Hence, knowing the values of the physical properties appearing in (80), it is possible to calculate the value of b for any value of N_{Re} using (79) and (80). The values obtained in this way for the film thickness are in good agreement in the laminar zone with the values given by (19).

In the case of flow of the film in a tube of radius R , with a pressure drop per unit length of ψ , a force balance shows that, approximately,

$$\tau_w = (\rho_{gas} g \sin \theta \pm \psi) \frac{R}{2} + b \rho g \sin \theta \quad (81)$$

in place of (80), and in this case a trial-and-error or graphical solution is necessary in order to find b at a given N_{Re} and ψ .

According to this theory, the film becomes turbulent when $b^+ = 30$. Substitution of this value into (79) gives

$$N_{Re_{crit}} = 270 \quad (82)$$

This result has been criticized (B14) on the grounds that recent investigations do not support the view of well-defined zones within the boundary

layer. The critical Reynolds number will be discussed further in Section IV, B.

Kutateladze and Styrikovich (K25) have presented a treatment very similar to that outlined above. Thomas and Portalski (T14) have also used the universal velocity profile concept, but for the case of countercurrent gas flow they have used instead of (81) the more exact form (for a vertical tube):

$$\tau = (b - y)(\rho - \psi) - \frac{(R - b)}{2} (\psi - \rho_{\text{gas}}) \quad (81a)$$

The treatments of Anderson *et al.* (A4, A5), Charvonia (C4), Calvert (C1, C2), and others differ mainly in the manner in which the gas stream pressure drop is taken into account for various cases of gas flow. Labuntsov (L2) has carried out an analysis using two forms of the velocity profile which do not involve the assumption of sharply differentiated zones in the boundary layer; this analysis is mainly concerned with heat transfer in films.

Dukler (D12) has carried out a superior analysis of this type, based on the dimensionless velocity profile of Deissler (D7), but as this is also concerned with the effects of gas flow, it will be considered in the next section.

F. FILM FLOW IN THE PRESENCE OF AN ADJOINING STREAM

In most of the treatments considered above it has been assumed that the phase adjoining the free surface of the film is stationary. In the case of an adjoining stationary gas phase, the buoyancy effect will be small and can be neglected, and, because of the small viscosity of a gas compared with that of the film liquid, it is reasonable to assume that the drag caused by the stationary gas is small. This was confirmed experimentally by Grimley (G11) who showed that similar results were obtained with various degrees of evacuation of the gas space of a wetted-wall column. On the other hand, since there can be no relative slip at the interface, it follows that a thin layer of the "stagnant" gas phase must be entrained by the film surface. This gas-pumping effect of the film surface has been dealt with theoretically and experimentally by Mazyukevich (M8) for the case of film flow inside a tube and has also been noted elsewhere (F2, F7).

1. Flow in the Presence of an Adjoining Liquid Phase

In the case of film flow in the presence of a heavy adjoining phase (density ρ_c), it has been shown (F1) that the results obtained in Section III, B, 2 for laminar flow remain valid provided there is negligible interfacial drag and the quantity $g\rho$ is replaced by the effective value $g(\rho - \rho_c)$

throughout the derivations. In particular, Eqs. (15) and (19) assume the form

$$b = \left[\frac{3Q}{g(\rho - \rho_c) \sin \theta} \right]^{1/3} = (3N_{\text{Re}})^{1/3} \left[\frac{\rho}{\rho - \rho_c} \right]^{1/3} \left[\frac{\nu^2}{g \sin \theta} \right]^{1/3} \quad (83)$$

Even when the adjacent liquid phase is stationary it is clear that the interfacial shear is likely to be considerable because of the large viscosity of the adjoining phase. Film flow with interfacial drag is considered below.

2. Smooth Laminar Film Flow with Interfacial Shear

For smooth laminar film flow with an interfacial shear the equations of motion remain as in Section III, B, 2, but the boundary condition $du/dy = 0$ at $y = b$ must be replaced either by

$$(du/dy)_{y=b} = -\tau_i/\mu$$

with τ_i as the interfacial shear, in which case,

$$u = \frac{g}{\nu} \left(by - \frac{y^2}{2} \right) \sin \theta - \frac{\tau_i y}{\mu} \quad (84)$$

or by

$$u = u_s \quad \text{at} \quad y = b$$

where u_s is no longer equal to $1.5\bar{u}$ as in Section III, B, 2, which leads to

$$u = \frac{\rho g}{2\mu} (by - y^2) \sin \theta + \frac{yu_s}{b} \quad (85)$$

From these, two series of expressions similar to those obtained in Section III, B, 2 can be obtained for use where τ_i or u_s are known.

Semenov (S6) considered the case of smooth film flow with an interfacial shear τ_i (which may be either positive or negative) and a pressure drop in the gas stream of ψ , and it was shown that no fewer than eight regimes of gas-liquid flow may exist for an upward gas stream; however, half of these are unstable and do not normally occur. Semenov's expression for the volumetric flow rate per wetted perimeter was

$$Q = \frac{(\rho g \sin \theta - \psi)}{3\mu} b^3 - \frac{\tau_i b^2}{2\mu} \quad (86)$$

At the commencement of flooding in a wetted-wall column, the net flow is zero ($Q = 0$), and, with this value, various solutions of (86) can be studied. The trivial solution is that $b = 0$. If τ_i is negative (downward cocurrent flow) the equation can only be solved to give a negative value of b , which is not physically meaningful, indicating that flooding cannot occur in this case. With τ_i positive, however (countercurrent flow), flooding commences at a film thickness of

$$b = \frac{3\tau_i}{2(\rho g \sin \theta - \psi)} \quad (87)$$

More recently, Brauer (B18) carried out a detailed analysis of the flow of smooth films and gas streams inside vertical tubes; this work was subsequently extended by Feind (F2). In this treatment, all the possible cases of film/gas flow (countercurrent, upward cocurrent, and downward cocurrent) are dealt with in a unified manner by plotting the calculated results in the form of $|f|$ as a function of $N_{\text{Re}_{\text{gas}}}$. Here $|f|$ is the absolute value of the dimensionless pressure drop in the gas stream:

$$|f| = \frac{2\tau_i}{\rho_{\text{gas}}(\bar{u}_{\text{gas}})^2} = \frac{2(\Delta P)(R - b)}{\rho_{\text{gas}}(\bar{u}_{\text{gas}})^2 L} \quad (88)$$

where $\Delta P/L$ is the pressure drop per unit length of the wetted tube. The gas stream Reynolds number is defined as

$$N_{\text{Re}_{\text{gas}}} = (\bar{u}_{\text{gas}})2(R - b)/\nu_{\text{gas}} \quad (89)$$

Limiting values of the gas stream pressure drops have been obtained for the various flow regimes.

Feind (F2) has shown that the effect of an interfacial shear τ_i due to a countercurrent gas stream is to increase the film thickness in the ratio

$$\frac{b}{b_0} = 1 / \left(1 - \frac{3\tau_i}{2b\rho g} \right)^{1/3} \quad (90)$$

(for a vertical wall), where b_0 denotes the value in the absence of a gas stream. Flooding commences when

$$\frac{\tau_i}{b\rho g} = \frac{2}{3} \quad (91)$$

It is found that the ratio of the wall shear stresses τ_w/τ_{w0} decreases until $\tau_i/b\rho g = \frac{1}{2}$ and then increases sharply. The surface velocity in the presence of the gas stream is shown to be

$$u_s = \frac{g}{\nu} b^2 \left(\frac{1}{2} - \frac{\tau_i}{b\rho g} \right) \quad (92)$$

and it can be deduced that the ratio of the surface velocity to the mean velocity of the film is given by

$$u_s/\bar{u} = 3 \left(1 - \frac{2\tau_i}{b\rho g \sin \theta} \right) / \left(2 - \frac{3\tau_i}{b\rho g \sin \theta} \right) \quad (93)$$

which reduces to the value given by (14) if $\tau_i = 0$.

It is to be noted that these treatments assume that the pressure drop per unit length is constant over the length of the wetted tube and that the film is in smooth laminar flow, which is usually the case only at very low

flow rates. The results above, therefore, represent mainly a limiting case, as recognized by Brauer and Feind.

3. Wavy Flow with an Adjoining Gas Stream

Kapitsa (K8) extended his treatment of wavy free film flow to cover this case also. For the simplest case, in which the gas stream does not seriously affect the wavelength, it was found to a first approximation that the mean film thickness \bar{b} could be given in terms of the flow rate per wetted perimeter Q and the mean gas velocity \bar{u}_{gas} by means of the equation

$$(\bar{b})^3 \pm 0.27 \frac{\rho_{\text{gas}}}{\sigma g \sin \theta} (\bar{u}_{\text{gas}} - c)^2 Q^2 \bar{b} - \frac{2.4\nu Q}{g \sin \theta} = 0 \quad (94)$$

where the \pm sign refers to countercurrent and cocurrent flow, respectively. Hence, in downward cocurrent flow, when increasing \bar{u}_{gas} decreases \bar{b} for a given Q , it follows from the stability considerations mentioned in Section III, D that increased stability will result, while for countercurrent flow an increase of \bar{u}_{gas} leads to an increase of \bar{b} for constant Q ; hence, the film eventually becomes unstable and flooding commences, as observed in practice. Kapitsa derived a condition for the onset of flooding from (94) which was in excellent agreement with published experimental data (F4).

Semenov (S7) simplified the wavy flow equations by omitting the inertia terms, which is permissible in the case of very thin films. Expressions are obtained for the wavelength, wave velocity, surface shape, stability, etc., with an adjoining gas stream; the treatment refers mainly to the case of upward cocurrent flow of the gas and wavy film in a vertical tube.

Konobeev *et al.* (K20, K21) have generalized the Semenov and Kapitsa results for the case of wavy film flow with an adjoining gas stream. In particular, the wavelength expression is obtained as

$$\lambda = \frac{2\pi}{\bar{u}} \left[\frac{\bar{b}\sigma}{\rho(c/\bar{u} - 1)(c/\bar{u} - T)} \right]^{1/2} \quad (95)$$

In the absence of a moving gas stream, the velocity profile is semiparabolic, and $T = 0.9$, so that (95) reduces to (67). For a linear velocity profile, such as might occur in very high-speed cocurrent gas/film flow, $T = \frac{2}{3}$. It has been shown (K21) that the use of $T = 0.8$ gives excellent agreement with wavelengths measured experimentally with very low liquid flow rates and moderate cocurrent gas velocities. It seems that countercurrent flow of the gas and film would require values of T greater than 0.9. Konobeev *et al.* obtained experimental wave velocities on a vertical wall which were in excellent agreement with (95) up to film thicknesses of about 0.28 mm.

It is of interest to note that Zhivaikin and Volgin (Z4) have questioned

the utility of the wavy flow theories of the Kapitsa-Semenov type on the grounds that the regular "sine wave" behavior assumed by these theories is not usually observed in practice. However, these are the only comprehensive wavy flow theories for thin films available at present, and they represent an interesting limiting case of film flow.

4. *Turbulent Film Flow with an Adjoining Gas Stream*

Attention in this section will be confined to the analysis of turbulent film flow by Dukler (D12, D13, D14), which includes the effect of a cocurrent downward gas stream. Film heat transfer under these circumstances is also considered. The Dukler analysis was later extended to cover the case of upward cocurrent gas/film flow by Hewitt (H7).

Briefly, in this treatment a force balance is carried out on an element of the film, taking into account the gas shear on the interface, which is expressed in terms of the pressure drop per unit length in the gas stream (assumed constant). As usual, the interface is assumed to be smooth. In this way an expression is obtained for the shear-stress distribution in the film, and this is converted to a velocity distribution by making use of the dimensionless velocity profiles proposed for channel flow by Deissler (D7) in the zone $0 < y^+ \leq 20$ and by von Kármán (V6) for the zone $y^+ > 20$. The complicated equations obtained in this way were solved on a computer, and the numerical results have been presented graphically and in tabular form (D12, H7).

An important result of this treatment is that the dimensionless velocity u^+ within the film is no longer a unique function of the dimensionless distance from the wall y^+ , as in single-phase pipe flow, but depends significantly on a parameter involving the interfacial shear.

Neither of the treatments above covers the case of countercurrent gas/film flow, but the behavior of a downward film flow in the absence of a gas stream can be obtained from the original Dukler analysis. It is found that in the laminar zone the film thicknesses predicted by the Dukler theory are in agreement with (19). A comparison of the theory with experimental results will be carried out in Section IV, A.

Finally, it may be noted that the error in Dukler's original treatment (D12) pointed out by Hewitt (H7, p. 4) is only apparent, since Hewitt's result can be reduced to a form exactly analogous to the corresponding Dukler equation.

IV. Experimental Results and Comparison with Theory

The results of the more important experimental studies of the flow of thin films will be reviewed briefly in this section, and these results will be

compared with the predictions of the theoretical treatments of film flow which have been outlined in Section III.

A brief chronological review of the more important theoretical and experimental investigations pertinent to the flow of liquids in thin films is given in the Appendix. In general, only those heat and mass transfer investigations which throw light on some aspect of the film flow problem have been included.

For a more detailed survey, it will be most convenient to consider the experimental results under separate headings, e.g., film thicknesses, film velocities, etc., even though it will be apparent that many of the investigations cover several of these topics.

A. MEAN FILM THICKNESSES

1. *Introduction*

A knowledge of the thicknesses of flowing liquid films is of importance in a wide range of practical problems involving film flow. Such problems include the calculation of heat transfer in evaporators and condensers, mass transfer in film-type equipment, the design of overflows and downcomers, etc.

As a result, much experimental work has been carried out to determine the thicknesses of flowing films. The experimental techniques for measuring the film thickness, the most convenient manner of presenting the results, and finally the results with and without a gas stream adjoining the film will be discussed here.

2. *Experimental Techniques and Presentation of Results*

Many techniques have been proposed in the literature for the measurement of film thicknesses, and most have been used by various investigators. These techniques may be classified as:

- (1) Direct determination of the position of the surface by means of a micrometer gauge and pointer, e.g. (C9, H18, J3, J4, K17, R4).
- (2) Improved probe methods, in which contact of the probe with the surface is determined by some nonvisual method (B14, H9, P1, etc.).
- (3) Photography of the film and channel (B4, C6, C11, K10, R3, W4).
- (4) Weighing the channel and film continuously (K4).
- (5) Drainage technique: the feed of liquid to the channel is shut off, and simultaneously the film liquid flowing from the channel is collected and measured. Knowing the wetted area of the channel, the mean film thickness can be determined from the volume of liquid (B21, C10, C15, F1, F5, W1). Improved drainage techniques have been used by (F2, F7, P3, T14).
- (6) Measurement of the electrical resistance between two probes set in the channel wall (A1, B8, C13, G11, H9, K21, M7, V1).
- (7) Measurement of the electrical capacitance between a probe placed above the film surface and the channel wall (B12, D16, H9, P3, S11).
- (8) The light-beam extinction technique, using a dyed film liquid (C4, C14, G7, H11, L13).
- (9) Radioactive tracer method (J1).

Of these methods, the first can give accurate values of the mean film thickness only in the absence of surface waves. The fourth and fifth methods can be used only for the mean film thickness, while methods (2), (3), (6), (7), and (8) may be used for measuring either the local or mean film thicknesses. Black (B12) and Portalski (P4) have discussed the advantages and disadvantages of most of these measurement techniques, and Hewitt and Lovegrove (H11a) have compared the film thickness values measured by three different methods.

Several methods of correlating film thickness data have been published in the literature. Thus, several investigators have plotted the film thickness b as a function of the Reynolds number N_{Re} ; this yields a different curve for each liquid and is not very convenient. Hopf (H18) presented his film thickness results in the form of an apparent liquid viscosity as a function of N_{Re} . This type of plot makes it possible to see very clearly the value of N_{Re} at which turbulence commences, since at this point the apparent viscosity begins to differ from the true viscosity.

Two of the more general correlations may be considered here. The first of these is the film friction-factor correlation. From Eqs. (15), (17), and (21), it can be shown that

$$f = \frac{2b^3g \sin \theta}{Q^2} \quad (96)$$

which indicates that the friction factor defined in this way can be regarded as a form of dimensionless film thickness, as pointed out by Brauer (B14). A plot of f as a function of N_{Re} should therefore correlate all film thickness data, and this method of correlation has been applied by several workers (B14, C15, F1, S13, Z3). However, it is to be noted that (96) gives a true value of the friction factor only for steady uniform laminar film flow in a wide channel. For other flow regimes the value of f calculated from (96) can be regarded only as a dimensionless film thickness, and it is somewhat misleading to take these values of f as friction factors in these cases. It has been shown that the true value of the friction factor as calculated from wall shear stress measurements in the wavy flow regime is not the same as that given by (96) (F7). For this reason, the second method of correlation given below seems to be preferable.

By rearranging Eq. (83), which is a generalized form of Eq. (19), it can be shown that

$$b(g \sin \theta / \nu^2)^{1/3} \left(\frac{\rho - \rho_c}{\rho} \right)^{1/3} = (3N_{Re})^{1/3} \quad (97)$$

The group on the left side of this equation is a form of dimensionless film thickness and has been termed the Nusselt film thickness parameter N_T (D12). Equation (97) indicates that a plot of N_T against N_{Re} on double-logarithmic coordinates should give a straight line of slope $\frac{1}{3}$ for the

regime of smooth laminar flow. It has been found that this type of plot successfully correlates film thickness data obtained in the other flow regimes also (though the lines have a slope different from $\frac{1}{3}$ for the other regimes), and also data obtained with various liquids and on walls of various slopes. When the fluid phase adjoining the free surface of the film is gaseous the density correction term in (97) can be omitted, since then $\rho \gg \rho_c$.

3. Discussion of Film Thickness Data in the Absence of a Gas Stream

A search of the literature up to 1959 revealed some 1013 values of the film thickness which were tabulated or plotted on graphs large enough to be read accurately. These measurements were obtained for a wide variety of liquids, varying from very mobile hydrocarbon oils to glycerol, for film flow on vertical walls and at slopes down to about 1° to the horizontal. These values of the film thickness were recalculated and plotted as the dimensionless thickness parameter N_T against N_{Re} (F7). Figure 2 shows the

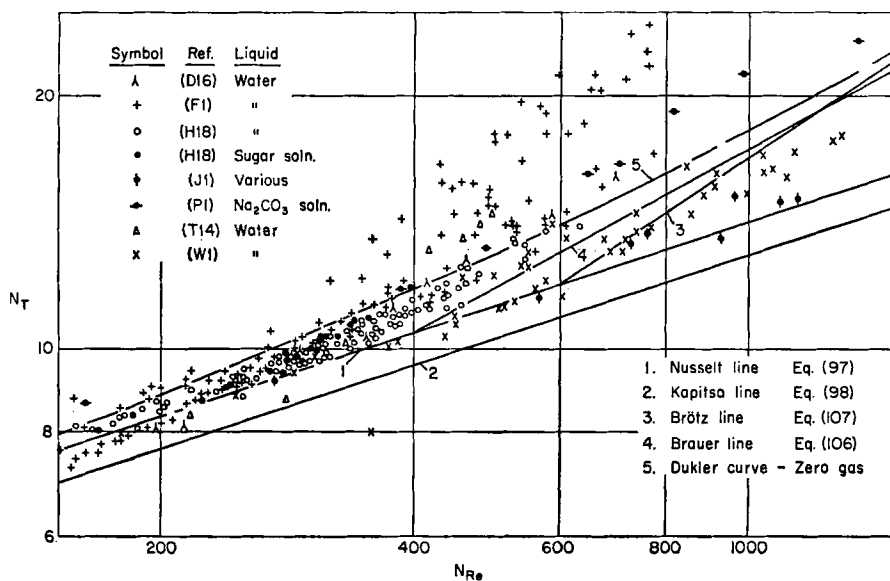


FIG. 2. Sample of earlier film thickness data near the critical Reynolds number plotted in terms of the Nusselt thickness parameter N_T and the Reynolds number N_{Re} , for the case of zero gas flow.

part of this plot in the region of the critical Reynolds number; the total range extended from (N_T, N_{Re}) of $(0.5, 4 \times 10^{-2})$ to $(50, 4 \times 10^3)$. As can be seen from this figure, many of the early film thickness data, which were

obtained mainly by the micrometer or simple drainage techniques, were not of a high degree of accuracy. However, in the laminar region the values fell near the line given by Eq. (97) for the most part. Above N_{Re} values of about 300–400, the experimental values deviated systematically from this line. In the laminar regime, even when waves were present, the N_T values appeared to agree better with Eq. (97) for a smooth film than with the predictions of the Kapitza theory of wavy film flow, $N_{T(wavy)} = 0.93N_{T(smooth)}$ (see Section III, D).

More recent film thickness measurements in the laminar wavy regime obtained by improved techniques (F2, F7, P3) have shown that there are appreciable reductions in the mean film thickness in the wavy regime for both vertical and sloped surfaces, as predicted by the Kapitza theory.

Feind (F2) measured the thickness of various films of kinematic viscosities 1 to 19.7 centistokes flowing in a vertical tube. An improved drainage technique was used. At the lowest values of N_{Re} (smooth laminar flow regime) the values of N_T fell along the line given by Eq. (97). Once wavy flow commenced, the values deviated towards the Kapitza line,

$$N_T = (2.4N_{Re})^{1/3} \quad (98)$$

At larger values of N_{Re} there was a gradual transition back towards the Nusselt line, Eq. (97), which was finally crossed at about $N_{Re_{crit}} = 350$. In the turbulent zone the experimental values of N_T fell above the Nusselt line.

Feind's empirical relationships may be written as

$$N_T = (\nu')^{0.025} 3^{0.333} (N_{Re})^{0.333} (\nu')^{-0.11} \quad (99)$$

for the region $0.72K_F^{-0.1} < N_{Re} \leq 1.35K_F^{-0.1}$;

$$N_T = (\nu')^{-0.005} 3^{0.333} (N_{Re})^{0.333} (\nu')^{-0.03} \quad (100)$$

for the region $1.35K_F^{-0.1} < N_{Re} \leq 6.0K_F^{-0.1}$;

$$N_T = (\nu')^{-0.055} 3^{0.333} (N_{Re})^{0.333} (\nu')^{0.025} \quad (101)$$

for the region $6.0K_F^{-0.1} < N_{Re} \leq 400$,

where K_F is the physical properties group given by

$$K_F = \mu^4 g / \rho \sigma^3 = (N_{We})^6 / (N_{Re})^4 (N_{Fr})^2 \quad (102)$$

and ν' is a "relative viscosity" given by

$$\nu' = \nu \text{ (in m.}^2\text{/sec.)} / 0.6 \times 10^{-6} \quad (103)$$

so that $\nu' = 1.495$ for water at 25°C.

For the turbulent region ($N_{Re} > 400$), it was found approximately that

$$N_T = (0.369) 3^{1/3} N_{re}^{1/2} \quad (104)$$

The results of recent measurements of the thicknesses of water films flowing in a channel of slope $7\frac{1}{2}^\circ$ to 90° (F7) can be represented approximately over the range $30 < N_{\text{Re}} < 300$ by the empirical relationship

$$N_T = 1.28(\sin \theta)^{-0.065} N_{\text{Re}}^{0.337} \quad (105)$$

which indicates that the effect of the waves on the film thickness varies with the slope of the wall on which the film flows. The data of Kamei and Oishi (K4) also indicate that there is a reduction in the mean film thickness in the wavy laminar regime, but these data are not presented in a form suitable for exact comparison.

Portalski's experimental results (P4) for several liquids flowing as films on a vertical plate show that the measured film thicknesses are smaller than those calculated by the Nusselt theory for smooth laminar flow, except in the presence of surface-active materials. In certain cases the measured film thicknesses were also smaller than those predicted by the Kapitza theory. Good agreement was also observed between the measured film thicknesses in the turbulent and laminar regimes (except at the lowest flow rates) and the predictions of the treatment based on the universal velocity profile [see Eq. (80), etc.]. At the lowest flow rates (in the smooth laminar regime), Portalski's experimental film thicknesses fall well below the Nusselt line and show a trend away from this line, and it is deduced that the Nusselt theory (Section III, B, 2) cannot be used for calculating the film thickness, even in this zone. However, these results are not in agreement with other recent measurements (F2, F7), which agree with or tend towards the Nusselt line in the smooth laminar zone.

Hence, the trend predicted by the Kapitza theory is supported by the recent, more accurate, film thickness measurements. This does not indicate, however, that the Kapitza theory will apply in detail over the whole wavy laminar regime of film flow, since Kapitza (K7) pointed out that such a reduction in the mean thickness should result for other types of wavy flow besides the particular case considered in his theory.

Turning to the turbulent regime of film flow, there are several empirical relationships to be found in the literature. The experimental data of Brauer (B14) for the zone $N_{\text{Re}} > 400$ can be represented by the equation

$$N_T = 3^{1/3} N_{\text{Re}}^{8/15} (400)^{-1/5} \quad (106)$$

Feind's results (F2) have been given already by Eq. (104). Partly from dimensional considerations, Brötz (B21) showed that, in the turbulent region,

$$N_T = (3N_{\text{Re}}^2/590)^{1/3} \quad (107)$$

By analogy with pipe flow, Zhivaikin and Volgin (Z4) obtained for the turbulent region

$$N_T = 0.141(4N_{\text{Re}})^{7/12} \quad (108)$$

It can be seen that the empirical equations predict that N_T will vary with some power of the Reynolds number between $\frac{1}{2}$ and $\frac{2}{3}$. These equations are plotted in Fig. 3 on which is also shown the curve given by

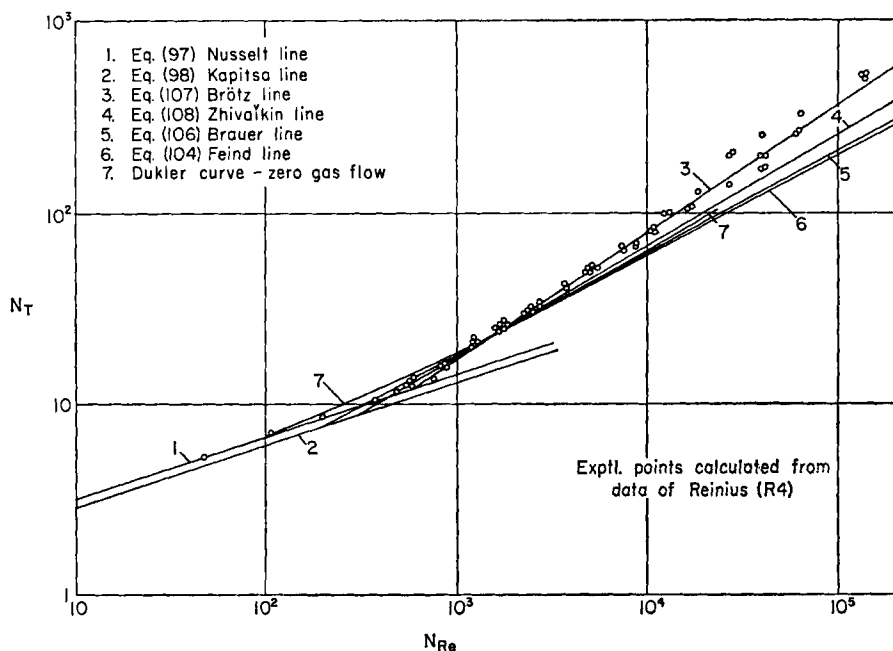


FIG. 3. Comparison of various correlations for the film thickness in the turbulent film flow regime in the absence of a gas flow.

the Dukler theory (Section III, F, 4) for the special case of zero interfacial drag. The experimental film thickness data obtained by Reinius (R4) for the flow of water in a smooth channel of small slope are also plotted on Fig. 3, and it is clear that the Brötz relationship, Eq. (107), is in excellent agreement with the experimental values over this very wide range of Reynolds numbers. However, at the smaller values of N_{Re} normally encountered in falling films, there is little difference between the predictions of these relationships; and the Dukler curve, which avoids a sharp transition between the laminar and turbulent regimes, lies close to many of the data in the transition and lower turbulent zones.

As noted earlier, the equation for turbulent film flow obtained by Levich (18) [Eq. (71)] contains an unspecified constant and therefore cannot be readily compared with the other relationships for turbulent films.

4. *Film Thicknesses in the Presence of a Gas Stream*

There have been numerous studies of the effects of gas streams on the thicknesses of liquid films flowing in contact with them. Cases studied in the literature refer mainly to gas/film flow in vertical tubes or channels or horizontal pipes. The latter case will not be considered here. The gas/film flows may be countercurrent, cocurrent upwards, or cocurrent downwards. Only the most important studies can be discussed here.

Semenov (S6) considered generally the effects of a gas drag at the film interface for all the cases listed above for smooth laminar film flow (see Section III, F, 2), and later experimental work confirmed these results (K20, K10, S7) for the case when the film thickness is very small, with no waves present on the film surface, and at moderate gas flow rates. The early treatment by Nusselt (N6, N7) also gave results in agreement with the experimental data obtained under these restricted conditions. Brauer's treatment of the problem (Section III, F, 2) (B18) also assumed laminar flow of the film and absence of surface waves. The experimental work of Feind (F2), which refers to countercurrent gas/film flow in a vertical tube, showed that, although such a treatment was useful in predicting the qualitative effects of the gas stream on the film thickness and other properties, the Reynolds number range in which it applied strictly was very limited.

In general, the various treatments predict that, as the velocity of the gas stream is increased, the mean film thickness for a given liquid flow rate decreases in the case of downward cocurrent flow of the two phases, due to the acceleration of the surface by the gas stream drag. With countercurrent flow of the gas and film, the opposite effect occurs, until a point is reached at which the film no longer has a net downward flow, and "flooding" is imminent. If the liquid is introduced at the lower end of the channel and if the gas velocity is large enough, it is possible to have upward cocurrent flow of the film and gas, and, as in downward cocurrent flow, the mean thickness of the film at a given liquid flow rate decreases as the gas velocity increases. This general behavior has been confirmed experimentally (cocurrent upward: A5, C14, H9, H10, M5, K21, S6, Z3; cocurrent downward: C4, K5, K21, S6, Z3; countercurrent: F2, F4, F7, G10, H20, K4, N2, S6, S11, T14, Z3, among others).

For wavy flow the experimental results of Konobeev *et al.* (K20, K19) are generally in quite good agreement with the theoretical predictions outlined in Section III, F, 3 for very low liquid flow rates. At larger flow rates there are serious deviations from the predictions.

In the case of turbulent film flow with an adjoining gas stream, there is a wealth of experimental studies reported in the literature. Only the briefest review of these can be given here. In general, the difficulty en-

countered in such studies is to convert the measured pressure drop in the gas phase to a drag at the film/gas interface. It is frequently assumed that, if the gas stream is made to pass through a long calming section to form a fully developed flow profile before being introduced into the wetted section, the entry effect will be negligible, so that the interfacial shear stress can be calculated directly from the pressure drop per unit length. However, even if the gas stream is fully developed with respect to the dry entry tube, it will no longer be fully developed with respect to the wetted section, where the new boundaries of the gas stream are in motion relative to the inlet section walls. In general, it is necessary in such cases to make use of the more complicated relationship quoted by Eckert *et al.* (E1) for calculating the interfacial shear. In using this relationship, it is necessary to know the manner in which the gas stream velocity profile changes in the direction of flow, and this information is not often available.

In most of the work reported in the literature it is assumed that the wetted tube over which the pressure drop is measured is sufficiently long that such entry effects can be neglected. No account is taken of the waves at the film surface, or of the fact that they may move faster than the mean surface velocity of the film, and the energy lost or gained by the gas stream in accelerating or decelerating the liquid surface near the inlet is also neglected.

In spite of these apparently seriously restricting assumptions, Dukler (D15) has shown that his theory for downward cocurrent flow is in agreement with experimental gas/film thickness data reported by Charvonia (C4) and McManus (M3). Hewitt *et al.* (H10) and Collier and Hewitt (C13) have carried out analyses of numerous experimental data on the thicknesses of liquid films in upward cocurrent flow in terms of the Dukler theory and other simpler theories such as those due to Anderson and Mantzouranis (A5) and Calvert and Williams (C2) (Section III, F, 4). The experimental and calculated values are in moderate agreement in the case of the Dukler and the Anderson and Mantzouranis treatments. The discrepancies are probably due to the simplifying assumptions made in the theoretical treatments.

Zhivaikin (Z3) has recently published the results of a detailed investigation of the effects of a gas stream on the film thickness for upward cocurrent, downward cocurrent, and countercurrent flow of the phases over a wide range of flow rates. Thus, downward cocurrent flow is little affected by gas velocities up to about 4 m./sec. For gas velocities between 4 m./sec. and the velocity at which spray formation commences (which has been determined experimentally as a function of the flow rates of gas and liquid and their physical properties), the film thickness is given by

$$N_T = [1 - 0.022(v_g - 4)](3N_{Re})^{1/3} \quad (109)$$

where v_g is the gas velocity, measured in meters per second.

For upward cocurrent flow, in the zone extending up to the formation of spray, it was found experimentally that

$$N_T = 1.18(v_g)^{1/3}(N_{Re})^{1/2}v_g^{-3/4} \quad (110)$$

where v_g is the gas velocity in meters per second as before. The conditions for flooding in countercurrent flow are also reported.

Feind (F2) has shown that, in countercurrent flow of the film and gas stream, there is a zone at low gas velocities in which the film thickness is hardly altered by the gas stream. At larger gas flow rates the film thickness increases; this point of initial increase of the film thickness occurs at lower gas Reynolds numbers as the film Reynolds number is increased, as might be expected. With countercurrent flow of liquid core streams, when the interfacial drag is much larger than with gas cores, Strang *et al.* (S13) and Treybal and Work (T16) have noted much larger increases in the film thicknesses.

From the remarks above, it can be seen that, although there are many experimental data available on the thicknesses of liquid films in the presence of gas streams, further work, both experimental and theoretical, will be required before film thicknesses can be predicted accurately under such conditions.

B. ONSET OF TURBULENCE IN FILMS

There are several reports in the literature of the critical Reynolds number at which turbulent film flow commences. These values of $N_{Re_{crit}}$ are usually determined from the breaks which appear in the curves of film thickness, surface velocity of the film, heat or mass transfer coefficients in the film, etc., when plotted against N_{Re} . Some of the numerical values proposed by various investigators are listed in Table I.

Several of these investigators have quoted an upper and lower critical value, enclosing a transition region, and Schoklitsch (S3) has given three values, the lowest, $N_{Re} = 144$, at which turbulence could be first detected, the second, $N_{Re} = 389$, at which the turbulent part of the flow became important, and an upper value, $N_{Re} = 900$, at which the film became "fully turbulent."

Dukler (D12) and Zhivaikin and Volgin (Z4) have pointed out that the transition to turbulence in a thin film is likely to be a gradual process, so that it is not reasonable to expect a single, sharply defined critical Reynolds number. The scatter in the experimental values of $N_{Re_{crit}}$ tabulated below can be explained in this way. However, the bulk of the evidence

TABLE I
VALUES OF THE CRITICAL REYNOLDS NUMBER

Investigator and Date	Ref.	$N_{\text{Re crit}}$
Hopf, 1910	(H18)	250-300
Schoklitsch, 1920	(S3)	144, 389, 900
Jeffreys, 1925	(J4)	310
Monrad and Badger, 1930	(M12)	350
Schmidt <i>et al.</i> , 1930	(S2)	280-430
Kirkbride, 1934	(K17)	500
Cooper <i>et al.</i> , 1934	(C15)	525
Horton <i>et al.</i> , 1934	(H19)	550-750
Fallah <i>et al.</i> , 1934	(F1)	500
Kutateladze, 1939 (reported by Z4)	(Z4)	375
Grigull, 1942	(G8)	350
Dukler and Bergelin, 1952	(D16)	270
Grigull, 1952	(G9)	310-450
Emmert and Pigford, 1954	(E4)	300
Brötz, 1954	(B21)	590
Stirba and Hurt, 1955	(S12)	below 300
Brauer, 1956	(B14)	400 \pm 10
Thomas and Portalski, 1958	(T14)	290
Belkin <i>et al.</i> , 1959	(B4)	325-500
Feind, 1960	(F2)	400, 800
Kutateladze and Styrikovich, 1960	(K25)	100-400
Reinius, 1961 (smooth channel data)	(R4)	400
Zhivalkin and Volgin, 1961	(Z4)	400, 1000
Saveanu <i>et al.</i> , 1962	(S1)	362
Wilke, 1962	(W3)	400, 800
Fulford, 1962	(F7)	260-330

seems to support a lower value $N_{\text{Re crit}}$ in the region of 250-400, with a less well-marked upper value of about 800.

Brauer (B14) and Kamei and Oishi (K4) have reported experimental values of the critical Reynolds numbers of films containing small quantities of surface-active materials in solution. In this case, the value of $N_{\text{Re crit}}$ appeared to depend on the surface tension of the solution; this effect is probably due to the layer of surface-active material present at the interface.

C. ONSET OF RIPPLING IN FILM FLOW

As reported in Section III, C, there are numerous theoretical treatments of the problem of the onset of rippling in a falling film. By way of comparing these predictions, the theoretical lines giving the Reynolds number at the onset of rippling, $N_{\text{Re,}}$ as a function of the channel slope

are plotted in Fig. 4, using the Benjamin simplified theory (B5), Eq. (44), Kapitza's theory [Eq. (38)], and the theory of Ishihara, *et al.* (I2), which reduces to a form similar to Eq. (44). The physical properties substituted in the equations in making this plot are those of water at room temperature.

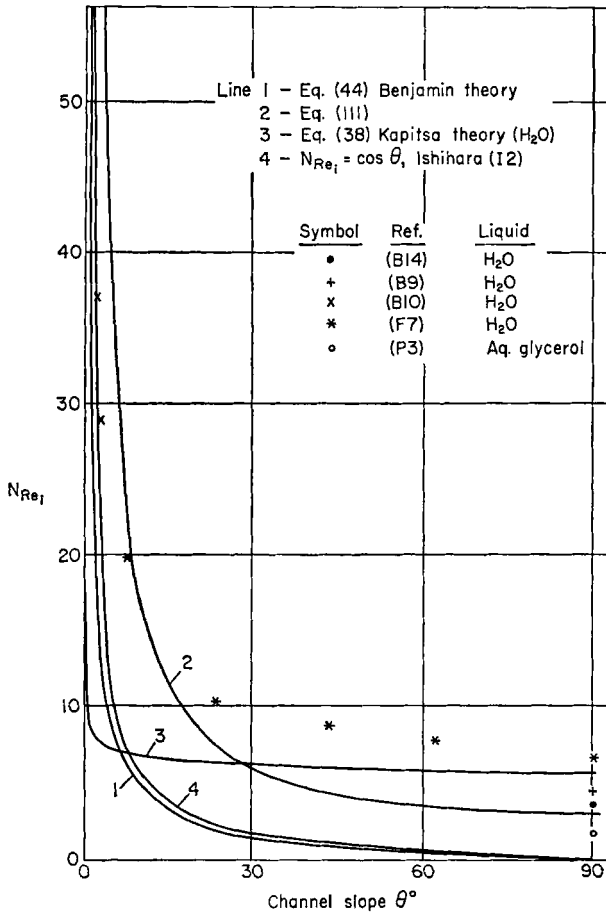


FIG. 4. Variation of the Reynolds number for wave inception, N_{Re_i} , with channel slope.

Making use of the condition that waves can only be stable if the Froude number of the flow is equal to unity (or exceeds unity), and using Eq. (46), it is seen that

$$N_{Re_i} = 3 \operatorname{cosec} \theta \quad (111)$$

The stability criterion of Hanratty and Hershman (H2) cannot be plotted

on Fig. 4, since it contains the relative wavelength as a parameter. However, for long waves this reduces to a form very similar to the conditions of Benjamin and of Ishihara *et al.*

The various hydraulic stability analyses mentioned in Section III, C lead to the criterion $N_{Fr} \geq n$, where $n = 0.58-2.0$, instead of 1.0 as assumed above, and these reduce to conditions similar to Eq. (111) for the onset of rippling, but with numerical constants other than 3.

Also shown in Fig. 4 are the experimental values of the Reynolds number at which waves were first detected on water films flowing in channels of various slopes (B9, B10, B14, F7). These values were determined by careful visual observation of the free surface of the film (B9, F7), from photographs (B10), or by an electronic "feeler" (B14).

It is seen that in general the various theories are in reasonable agreement with each other, especially the Benjamin and the Ishihara theories. The simple condition $N_{Fr} = 1$ shows a similar trend with channel slope, but the values lie slightly higher at all slopes. The Kapitsa theory predicts that the values of N_{Re} will change little with slope except at very small slopes.

The experimental values lie above the theoretical curves but indicate a similar trend with channel slope. Binnie (B10) has shown that the exact value of N_{Re} , obtained depends to some extent on the method used for detecting the waves; waves are detected at smaller values of N_{Re} when more sensitive methods are used. Since many of the experimental points in Fig. 4 were determined visually, which is not a particularly accurate method, it is reasonable to expect that they should fall high, for the Benjamin and Ishihara curves give a lower limit of N_{Re} . It can be seen that the condition $N_{Fr} = 1$ seems to be in moderate agreement with the experimental values of the Reynolds number at which waves are clearly visible for water films in channels of various slopes. It is interesting to note that, by analyzing his own and previously published experimental results on the onset of rippling in vertical columns using a number of liquids of widely different physical properties, Jackson (J1) also deduced that the criterion for wave formation was $N_{Fr} \geq 1$. Belkin *et al.* (B4) arrived at the same conclusion. It seems, therefore, that the condition $N_{Fr} = 1$, or its equivalent, Eq. (111), represents a useful working equation for calculating the onset of rippling.

Unfortunately, the experimental results mentioned above do not throw any light on an interesting aspect of the Benjamin theory of film stability, namely, the prediction that films flowing on vertical walls are unstable at all flow rates (see Section III, C). This is due to the fact that, although the theory predicts that vertical films will always be wavy, the waves may be very small at low flow rates. The fact that the use of more sensitive

methods of wave detection leads to smaller experimental values of N_{Re} , (see above) may be indirect confirmation of the theory.

Brauer (B14) carried out very careful determinations of the values of N_{Re} , for films of water and aqueous diethylene glycol solutions flowing on vertical tubes. The results were correlated by the empirical relationship

$$N_{Re_i} = 0.306(K_F)^{-0.1} \quad (112)$$

where K_F is the dimensionless group given by Eq. (102). Rather earlier, Grimley (G10), using less sensitive methods of detection, obtained a similar correlation,

$$N_{Re_i} = 0.3(K_F)^{-1/8} \quad (113)$$

which gives slightly higher numerical values of N_{Re_i} for the liquids used.

A careful analysis of the experimental results of Brauer in terms of Benjamin's theory (Section III, C) indicated (F7) the interesting fact that, for all the pure liquids (i.e., liquids not containing surface-active materials in solution), the rate of increase of the Benjamin amplification factor with the Reynolds number, $d\alpha/d(N_{Re})$, was the same at the point of onset of rippling.

Benjamin (B7) has also indicated that, if constant amplification of the most unstable wave per wavelength is assumed, it can be derived from the theory that

$$N_{Re_i} \propto (K_F)^{-1/11} \quad (114)$$

and it is interesting to note that this relationship is quite similar to the experimental correlation obtained by Brauer, Eq. (112).

D. SURFACE WAVES ON FILMS

1. General Observations of Wavy Flow

Perhaps the most interesting features of film flow are the wave patterns which appear at the free surface of the flowing film at all except the lowest liquid flow rates. Numerous investigators have made observations of these waves under various flow conditions, e.g. (A2, A3, B6, B9, B10, B14, B15, B16, B20, C4, D17, E4, F2, F7, G10, H16, H19, H2, I2, J4, K1, K10, K18, L10, L11, L12, L13, M7, R2, S7, S11, T3, T5, T7, T13, T14, V1, V4, W2, W3), among others. It has been mentioned earlier (Section III, C) that wavy film flow is usually so complex that no satisfactory general theory of wavy film flow has yet been possible. For the same reason the experimental determination of the parameters characterizing the wave patterns is extremely difficult. Many of the earlier descriptions of wavy film flow are purely qualitative, and it is only in recent years that attempts have been made to measure mean wavelengths, amplitudes, etc., for any but the regular ("sine wave") regime of wavy flow.

In general, the wave patterns may be described qualitatively as follows. At very low flow rates ($N_{Re} < N_{Re_i}$), the film surface is completely smooth and mirror-like, troubled only occasionally by small random "dimples," which are rapidly damped out in the

direction of flow of the film. At slightly larger Reynolds numbers, small, symmetrical, regular waves appear. The wave fronts are almost straight and perpendicular to the direction of flow. At still larger flow rates, the regular symmetrical waves tend to become less regular, and the cross section of the wave assumes the nonsymmetrical shape usually described as a "roll wave" (D9), with a steep front and a long, gently sloping tail. Frequently each roll wave is preceded by a number of small waves [termed "push waves" by Brauer (B14)] which move as a group with the main wave (B14, C6, F7, M7). (It appears likely that, although the wavelength of the main roll waves is large enough to make capillary effects negligible over most of the wave, the curvature of the steep front is sufficiently great to lead to the formation of capillary ripples at the toe of the main wave.) In this zone of flow the wave fronts are no longer straight at all times but show a tendency to form bulges or to split or overtake each other. Similar observations have been made recently for the case of upward cocurrent gas/film flow (T7).

As the liquid flow rate is increased a stage is reached when the main waves and their accompanying push waves have become so randomly mixed that the individual wave fronts can scarcely be distinguished, and the surface appears to be covered with a mass of small jagged "turbulent" waves. A number of photographs of this type of wave pattern have been published, e.g., by Bressler (B20), by Dukler and Bergelin (D16), and by Tailby and Portalski (T4). Certain observers (B14, T7) have noted larger wave rings or disturbance waves superimposed on this rough surface.

The presence of a gas stream appears to increase the size and randomness of the waves on the film surface (C4, F2, F7). Countercurrent gas flow leads to a decrease in the wave velocity, with the opposite effect for cocurrent flow.

2. *The Smooth Entry Zone*

In nearly all of the observations of wavy flow, it has been noted that there is initially a smooth region near the liquid inlet before waves appear on the film surface. The length of this smooth entry zone varies with the liquid flow rate, the flow rate of the adjoining gas stream, if present, and to some extent on the manner in which the liquid is introduced (T5). In general, the length of the smooth zone increases as the flow rate increases, but the increase is not in direct proportion to the flow rate (C6, J1, F2, M2, F7, T5, B14). Chien (C7) has noted that, as the flow rate is increased above a certain value, local disturbances occur within this initially smooth zone, leading to an apparent decrease in its length; however, it appears that the length of the zone without sustained wavy flow continues to increase with increasing flow rate. The observation made by Grimley (G11), that his films ceased to be wavy above a certain liquid flow rate, is probably due to the length of the entry region exceeding the total length of his wetted surfaces at the larger flow rates.

The cause of this initial smooth zone and the subsequent fairly sudden transition to wavy flow is not completely clear. Working on a much larger scale, with mostly turbulent flow of the liquid layers on dam spillways, Bauer (B1) has shown that the length of the smooth initial region is the same as the distance required for the turbulent boundary layer, which

begins to form at the point of introduction of the liquid, to reach the thickness of the whole liquid layer, which in this initial zone accelerates and becomes thinner in the direction of flow. MacLeod (M2) arrived at a similar conclusion for flow rates normally encountered in wetted-wall columns, i.e., that the waves appeared at the end of the acceleration zone of the film, when the boundary layer (laminar or turbulent) had reached the same thickness as the film. Unfortunately, it is not a simple matter to calculate the film thickness in the acceleration zone; there is some dispute as to the length of the acceleration zone (S5, L14), and, in any case, the exact manner of introducing the liquid will affect the length of this zone to some extent (see F2, L14, W4). However, recent measurements of the film thicknesses near the liquid inlet have indicated a marked decrease in the film thickness in the direction of flow (C6, C7, F7, M7, T7), and it has been found that in many cases the film acceleration continued at an ever-decreasing rate as far as the point of wave inception (F7).

It seems possible, therefore, that in this initial region the upper part of the film, outside the growing boundary layer, is in potential-like flow, and that once the boundary layer reaches the free surface, its vorticity is sufficient to trigger the wave disturbances, which can then propagate or not, depending on whether the flow is unstable or stable ($N_{Fr} > 1$ or $N_{Fr} < 1$).

On the other hand, since the film is accelerating in this initial zone, it follows that the Froude number of the flow, which may be taken as the criterion for gravity-wave instability, increases from some very small value at the inlet to its equilibrium value for the particular flow rate and channel slope. Depending on the flow conditions, it is possible for the Froude number of the flow to reach the critical value before the end of the acceleration zone is reached. In this case it can be supposed that waves could occur before the end of the acceleration zone if some triggering mechanism were available. This appears to be the case in fact, for Tailby and Portalski (T5) have noted that when an adjacent gas stream (either cocurrent or countercurrent) is present, the length of the smooth entry zone decreases markedly.

Chien (C7) has proposed an energy mechanism for explaining the initial decrease in film thickness and subsequent formation of waves. Mayer (M7) has dealt with the manner in which the waves, which are initially fairly regular near the inception line, later develop into roll waves, etc., downstream, and Lighthill (L10) has also considered the manner in which waveforms may change by amplitude and frequency dispersion.

It is clear that further detailed work is required in order to explain the initial smooth zone adequately.

3. *Effect of Surface-Active Materials on Wavy Films*

It is well known that many types of waves and ripples can be damped by interfacial films of surface-active materials, as shown theoretically by Levich (L6, L7). There have been a number of investigations into the effects of surface-active additives on the flow of wavy films (E4, H2, H20, I2, J1, L15, M7, S11, S12, T3). In addition, surface-active materials have also been used in various studies of mass and heat transfer to films, and some of these results throw light on the flow behavior of the films, e.g. (H13, M11, R1, T9, T10, T11, T12).

Most of the investigators have found that surface-active additives greatly reduce or completely eliminate the surface ripples. The mechanism by which the surface-active materials suppress the waves is discussed by Emmert and Pigford (E4). In the mass-transfer studies, it has been found that the addition of surface-active materials greatly reduces the rate of mass transfer at a given liquid flow rate. It is interesting to note that by adding surface-active material to an initially wavy water film, Ternovskaya and Belopol'skiĭ (T11) found that the rate of absorption of SO_2 at small Reynolds numbers decreased by 25–38%, while Kapitsa (K9) has calculated that, in the regime of regular waves, the increase in the mass-transfer rate due to the waves is of the same order, namely 20–30%. Hence it seems that the change in the mass-transfer rates under these circumstances is due purely to the changes in the hydrodynamics of the flowing surface. It has been shown experimentally that the change in surface tension brought about by the surface-active additives has little effect as such on the mass-transfer rates (T9). Lynn *et al.* (L15, L16, L17) have shown that surface-active materials may lead to the formation of a stagnant “skin” over the lower part of a film surface, and this may become important in measuring rates of mass-transfer in short wetted-wall columns.

Emmert and Pigford (E4), Ternovskaya and Belopol'skiĭ (T9–T12), and Tailby and Portalski (T3) have carried out detailed investigations of the effects of surfactants, using several different surfactants, each at a number of concentrations. In nearly all cases it was found that, as the concentration of surfactant was increased, the waves were rapidly damped out as far as some optimum concentration, beyond which there was either little further damping of the waves, or the waviness increased again. Ternovskaya and Belopol'skiĭ calculated that the optimum concentrations for wave damping corresponded to quantities of surfactant just sufficient to form a saturated monolayer at the interface (T10).

It is of interest to note that Brötz (B21) and Jackson (J1) could find little effect of the addition of surface-active materials on film flow. It is possible that these experiments were carried out in a region where the waves were mainly of the gravity type, i.e., of

fairly long wavelength, and hence less likely to be affected by capillary forces. In this connection, it may be noted that Keulegan (K15) has found that surface-active materials may prevent waves being formed in the first place, but that, once formed, they do little to prevent gravity waves from propagating in the usual way. In dealing with wave problems of the present sort it is clearly important for experimenters to specify whether the Froude and Weber numbers are above the critical values, so that it can be decided whether the waves are likely to be controlled mainly by gravity forces, capillary forces, or a combination of both; surface-active materials will have a much larger effect on the capillary waves with their shorter wavelengths and hence greater surface curvatures.

4. Wavelengths, Wave Velocities, Maximum and Minimum Film Thicknesses

a. Wavelengths. In recent years there have been several investigations of the wavelengths of the surface waves appearing on films or, alternatively, the wave frequencies, from which the wavelengths can be calculated if the wave velocities are known (A3, B10, C4, C6, F7, G7, G11, I1, I2, K10, K20, K21, M7, S7, T4, T7).

It has already been noted that the wavelengths are regular only near the line of wave inception, except at low liquid flow rates, when regular waves extend over the remainder of the film surface also.

Tailby and Portalski (T4) have reported measurements of the wavelengths near the point of wave inception on vertical films of various liquids. Even in this case, it was found that the wavelengths were considerably greater than predicted by the Kapitsa theory, Eq. (67), even in the cases in which the conditions of the theory were satisfied. Similar results have been obtained for water films on walls of various slopes (F7).

For most flow rates the wavelength in the region away from the line of inception varies considerably with time, and it is possible to obtain a mean wavelength only by averaging the distances between the fronts of a large number of waves. It has been found that after a zone at low Reynolds numbers in which the wavelength decreases with increasing N_{Re} , as predicted by the Kapitsa theory, there is a marked increase in the mean wavelength in the roll-wave zone (F7). The maximum wavelength is reached at $N_{Re} = 100-160$ (depending on the channel slope), after which there is again a decrease in the mean wavelength. The locus of the maxima on the wavelength-Reynolds number curves has been found to agree closely with the line $N_{We} = 0.7-1.0$, which indicates that the initial sharp increase in the wavelength is due to the action of gravity-type roll waves, while the subsequent decrease is probably due to the formation of shorter capillary waves near the critical Weber number of unity.

These results also show that, at a given liquid flow rate, the wavelength increases rapidly as the slope of the wetted wall is decreased.

The standard deviation of the individual waves from the mean wavelength was also calculated, giving some measure of the randomness of the

wave patterns. (The wavelengths appeared to follow a Gaussian distribution quite closely.) The standard deviation increased in the roll-wave region, then decreased in the zone immediately above $N_{\text{Wcritical}}$ and finally increased again, slowly, in the turbulent region.

Although there are numerous published investigations in which records of the wavy surface profile have been obtained, e.g. (H9, D16, S11), not many of these have been analyzed for information on wavelengths, most being concerned with wave-size (height) distributions. However, it may be noted that the experimental wavelengths of Kapitsa and Kapitsa (K10) show a trend in the direction of the data reported above, even at very small Reynolds numbers ($N_{\text{Re}} < 25$). It seems, therefore, that the Kapitsa theory is applicable only at very small flow rates, as far as wave characteristics are concerned, in the case of the free flow of wavy films. Allen (A3) has reported a similar conclusion.

On the other hand, Konobeev and his co-workers (K20, K21) have shown that Eq. (95), which is a simplified and generalized form of the Kapitsa equation for the wavelength, is in good agreement with experimental data for the wavelengths appearing in upward cocurrent gas/film flow. However, these investigations were confined to very small liquid flow rates. At larger flow rates, Taylor *et al.* (T6, T7) have shown that the wave patterns in upward cocurrent gas/liquid flow are quite complex, though even at moderate liquid flow rates the wavelengths appear to be more uniform than in free film flow. It was found that the wave frequency was relatively insensitive to the air flow rate but increased with the liquid flow rate.

There appears to be little information available on the effect of a countercurrent gas stream on the wavelength.

b. Wave Velocities. The Kapitsa theory [Eq. (65)] predicts that the wave velocity should be 2.4 times the mean film velocity, while the theories of Benjamin (B5) and Hanratty and Hershman (H2) predict that $c = 3\bar{u}$. Ishihara *et al.* (I2) have shown that the wave velocity in the laminar region can be given as

$$c = \bar{u} \left\{ \frac{6}{5} + \sqrt{\frac{6}{25} + \frac{3}{N_{\text{Re}} \sin \theta}} \right\} \quad (115)$$

The experimental results of Mayer indicate that the wave velocity is proportional to $N_{\text{Re}}^{1/3}$ (M7). Since \bar{u} is proportional to $N_{\text{Re}}^{2/3}$ [Eq. (18)], it follows that the ratio c/\bar{u} must decrease with increasing Reynolds numbers. Similar experimental conclusions have been reported elsewhere also, e.g. (F7).

In order to compare the theoretical predictions with experimental values, the ratio c/\bar{u} is plotted as a function of the Reynolds number in

Fig. 5. The lines $c/\bar{u} = 3$ and $c/\bar{u} = 2.4$ corresponding to the theories of Benjamin and Hanratty and Hershman and of Kapitza are shown, together with the line given by Eq. (115), using $\theta = 7\frac{1}{2}^\circ$. The remaining lines represent smoothed experimental wave velocity data (F7) for water films on wetted walls of slopes $7\frac{1}{2}$, 62 , and 90° .

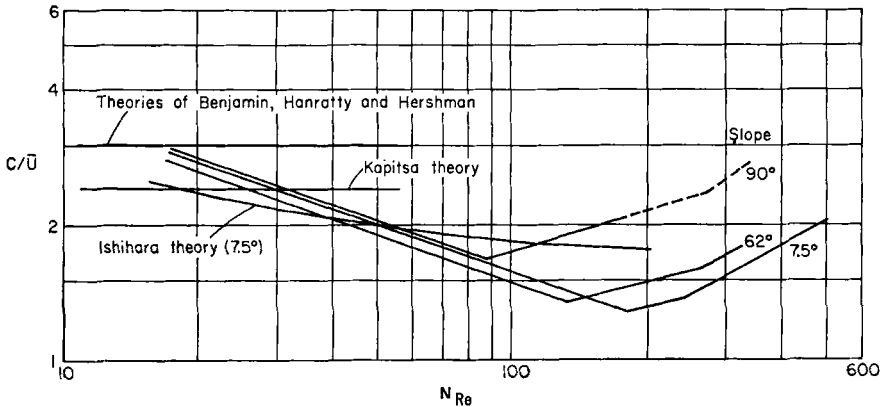


FIG. 5. Ratio of the wave velocity to mean film velocity, c/\bar{u} , in the absence of gas flow as a function of N_{Re} : comparison of various theories with smoothed experimental data (F7) for water films in inclined channel.

It can be seen immediately that the experimental values of c/\bar{u} reach a value of 3 only at very small flow rates, near the flow rate for the onset of rippling, which is the zone for which Benjamin's theory is strictly applicable. The experimental values fall below the Kapitza value of 2.4 at $N_{Re} = 30$. The theoretical relationship by Ishihara *et al.* predicts that c/\bar{u} will decrease as N_{Re} increases, but less rapidly than observed experimentally. However, this theory is strictly applicable only at very small channel slopes and for waves of negligibly small amplitude, so that exact agreement cannot be expected.

The experimental results show that c/\bar{u} decreases up to a certain flow rate at which it was found that $N_{We} = 0.8$, after which a different behavior is exhibited, with an increase in c/\bar{u} as N_{Re} increases. At $N_{Re} = 280$, a further break was observed; this is due to the onset of turbulence in the film, which alters the manner in which \bar{u} varies with N_{Re} . Hence, as in the case of the wavelengths, there appears to be an important change in the wave characteristics near the critical Weber number of unity.

The experimental wave velocities of Kapitza and Kapitza (K10) for vertical water films are in agreement with the results given above, but these investigators only covered the range up to $N_{Re} = 25$. The experimental wave velocities for water films given by Portalski (P3) (90°) and

Mayer (M7) (small slopes) show the same trend as these results, but the numerical values of c at a given N_{Re} are rather larger.

An interesting feature of the experimental results plotted in Fig. 5 is that the ratio c/\bar{u} may be less than 1.5 under certain flow conditions. It will be shown later (Section IV, F) that the surface velocity of the film is equal to $1.5\bar{u}$, so that in this flow zone it appears that the surface waves move less rapidly than the surface of the film. Under these circumstances, the waves might tend to steepen at the upstream end, and the sudden transition from steep-fronted to steep-backed waves might explain the increase in the randomness of the waves in this flow zone, as illustrated by the standard deviation of the wavelengths mentioned in the last section.

Taylor *et al.* (T6, T7) have reported on wave velocities in upward cocurrent gas/film flow. It was found that the wave velocity increased rapidly with increasing gas flow rate but varied little with liquid flow rate. It was found, furthermore, that the individual wave velocities were not uniformly distributed around the mean value under given flow conditions, but that certain "preferred velocities" appeared to exist. The reasons for such behavior are not clear at present. More recently, Nedderman and Shearer (N1a) have carried out similar studies over a wider range of gas and liquid flow rates. Although the results were similar in many respects, it seems that the wave frequencies, of the large disturbance waves in particular, are dependent on the geometry of the apparatus. These results showed that, at constant water flow rate, the wave velocity for upward cocurrent flow varied with the square root of the air velocity relative to the waves.

There is again a lack of detailed measurements for the case of counter-current gas/film flow. Qualitative observations (F7) indicate that the wave velocity first increases slightly as the gas flow rate increases, perhaps due to an increase in the size of the waves, and then decreases due to gas phase drag.

c. Maximum and Minimum Film Thicknesses. Brauer (B14) carried out the first detailed investigation of the distribution of wave sizes on a vertical film and reported on the maximum film thickness (height to the highest wave crest), the minimum film thickness (liquid thickness from the wall to the deepest wave trough), and also the frequencies of waves of various sizes, for the case of zero gas flow.

More recently, similar studies have been carried out for other cases of flow; Shiotsuka *et al.* (S11) have given empirical relationships for the mean wave heights as a function of the gas and liquid flow rates for the case of countercurrent gas/film flow. Lilleleht and Hanratty (L12, L13) and McManus (M3) have considered the amplitude characteristics of the waves at a horizontal liquid surface in the presence of a gas stream. Similar studies have been carried out for cocurrent gas/film flow by Hewitt *et al.*

(H9, H11) and Konobeev *et al.* (K20, K21) for the case of upward flow, and by Charvonia (C4), Chien (C7), and Konobeev *et al.* (K20, K21) for downward flow of the phases.

Brauer (B15, B16, B17) has pointed out that information on the frequency of the waves, regarded as surface disturbances, may be of considerable importance in calculating the rates of heat and mass transfer through the wavy film interface, and, in fact, Konobeev *et al.* (K20, K21) have shown that the rate of absorption of CO_2 by a water film in wavy cocurrent flow can be correlated in terms of the length and amplitude of the surface waves over the range of small liquid flow rates investigated.

In most cases, it is found that there is a considerable spread in the wave amplitudes, but that for given gas and liquid flow rates there is a certain wave height which occurs most frequently, and which can therefore be regarded as a characteristic of the wavy flow. The manner in which this characteristic frequency varies with the flow rates has been given in the literature, e.g. (B14, C4, H9).

In addition to the effects on heat and mass transfer, the wavy film surface also acts as "rough wall" to the adjoining gas phase (L12, C4, G3). This aspect of such flows will be considered more fully in Section IV, G.

In spite of the detailed investigations mentioned above, much work remains to be done on this aspect of film flow before it will be possible to characterize the wave amplitude behavior accurately for all the film flow regimes. Once wavelengths and wave amplitudes can be predicted accurately, it may be expected that a better understanding of transfer processes at wavy film interfaces will result.

5. Increase of Interfacial Area Due to Waves

Wetted-wall columns have been used for many years for determining mass-transfer coefficients on the assumption that the interfacial area across which mass transfer occurs can be obtained accurately from the dimensions of the column and a knowledge of the film thickness. It is therefore of considerable practical interest to determine whether the interfacial waves lead to an appreciable increase in the interfacial area of the film, which would introduce a grave uncertainty into such methods of determining mass-transfer coefficients.

Portalski (T2) has extended Kapitsa's treatment of wavy film flow to obtain an expression for the increase in interfacial area due to the waves [Eq. (68)]. For mobile liquids this relationship predicts that the increase in interfacial area will be very large, reaching 150% for 2-propanol at $N_{\text{Re}} = 175$, for example, though the applicability of the Kapitsa theory at such large Reynolds numbers is in doubt. Experimental values of the

increase in interfacial area were presented (T2) for films of 82% glycerol solution on a vertical wall and found to be in good agreement with the value predicted by Eq. (68) at $N_{Re} \cong 12$ (3% experimental, 3.3% calculated). Dukler and Bergelin (D16) also obtained records of the wavy surface profiles of vertical films and claimed that the increase in interfacial area was appreciable, though numerical values were not given.

Levich (L8) has shown that, for capillary waves, the relative increase in interfacial area is given by

$$\frac{\Delta S}{S} = \left(\frac{\alpha}{\lambda}\right)^2 \quad (116)$$

where α and λ are the wave amplitude and wavelength. Since, usually, $\lambda \gg \alpha$, this formula predicts that $\Delta S/S$ will be small.

The wave profile photographs published by Kapitsa and Kapitsa for vertical films of water and ethanol at small Reynolds numbers indicate that the increase in surface area can only be small. Brauer (B14) obtained numerous profile photographs of wavy films over the range $25 < N_{Re} < 1675$, and measured a maximum increase in the interfacial area of about 3%. From similar photographic studies, Belkin *et al.* (B4) and Vouyoucalos (V7) arrived at increases of not more than 10% and 8%, respectively. Portalski (T2, discussion) has criticized the results of Belkin and Brauer on the grounds that exact orthogonal views of the film profile were not obtained by the photographic technique used, and that the measured increases in interfacial area were too low, due to partial blocking of troughs by other crests in the photographs. Nevertheless, Shiotsuka *et al.* (S11), who obtained film profiles by means of a capacitance probe similar to Portalski's, have obtained increases in surface area of less than 0.2% up to liquid Reynolds numbers of 160, even in the presence of a countercurrent gas stream (water films). These workers have shown that it is difficult to obtain accurate values of the increase in surface area from a recorder chart of the wave profile, which is normally considerably exaggerated in the direction perpendicular to the film surface.

Ternovskaya and Belopol'skii (T12) claim that the decrease in surface area due to damping of waves is small, and Allen (A3) has shown that the increase of surface area by the waves is smaller than predicted by Portalski.

In general, it seems that, although there must be a measurable increase in the interfacial area of a wavy film, this is not likely to be too important in practice.

6. *Mixing Effect of Surface Waves*

It is well known from the literature that the waves appearing at the surfaces of flowing films lead to increases in the rates of heat and mass

transfer to such films. Zotikov and Bronskiĭ (Z5) have shown that surface waves lead to an increased rate of heat transfer, and Labuntsov (L1) has reported a correction to the Nusselt heat transfer equations for condensate films to take into account the effects of interfacial waves. Zhavoronkov *et al.* (Z2) and Kamei and Oishi (K3) have reported increases in mass-transfer rates to wavy films, which are up to several times as large as the values calculated for smooth flow of the same Reynolds number. Similarly Hikita (H12) and Stirba and Hurt (S12) have reported that the rates of mass transfer to wavy laminar films are much larger than those predicted from the theory for smooth laminar flow, but that when surface-active materials were added to damp out the waves, the results were in agreement with the theories of Pigford (S9) or Vyazovov (V8). Recently Heartinger (H5) has proposed a model to account for mass transfer in wavy films also, while Brauer (B14, B16) has reviewed a mass of experimental data and proposed a semi-empirical method of calculating mass and heat transfer in wavy films.

In order to explain these large increases in the transfer rates to wavy films, Jackson (J1) has postulated that the waves in a wetted-wall column behave as sources of localized mixing action moving over the film, which may otherwise be in laminar motion. Stirba and Hurt (S12) have carried out dye tracer experiments in a wetted-wall column, which indicated that even well within the laminar zone the dye streaks are broken up by the waves. When the waves were damped out by the use of surface-active materials the dye streaks remained undisturbed at the same liquid flow rates. Ishihara *et al.* (I1) have reported tracer studies in waves appearing on a laminar water flow at small slopes and concluded that there must be a considerable degree of turbulent mixing along the fronts of such waves. Mayer (M7) has published photographs of laminar roll waves and has shown that these waves are characterized by ridges of high vorticity with quiescent interwave zones. Allen (A3) has also suggested that the increased rates of heat and mass transfer in wavy films are due to mixing in the fluid streams.

On the theoretical side, Dmitriev and Bonchkovskaya (D8) have shown that in principle turbulence should spread from waves. Kapitsa (K9) has calculated a general tensor quantity, termed the coefficient of wavy transfer, which is applicable to any flow with periodic disturbances, such as pulsations or surface waves. This treatment predicts an appreciable increase in the rates of heat and mass transfer in wavy films, though this increase does not appear to be as large as that observed experimentally under certain conditions.

Davies (D4, D5, D5a, D6) has reported that when a potassium permanganate dye streak was injected through a fine capillary tube below

the surface of a water film in vertical wavy laminar flow, the surface waves appeared to have no effect on the width of the streak, indicating that there was no lateral mixing action in the wave fronts. From a consideration of the original Kapitza treatment of wavy film flow, Portalski (P5) has shown theoretically that circulating eddies may arise as a result of the zones of reversed flow predicted in the wave troughs by this theory. Such eddies would explain the increased rates of heat and mass transfer to wavy films in the absence of lateral mixing in the wave fronts. However, recent experiments in which a potassium permanganate dye streak was injected carefully onto the surface of a water film have shown that the dye streak became appreciably wider in the wave fronts and eventually became very diffuse, even at $N_{Re} < 90$, i.e., well within the laminar zone; the disappearance of the sharply defined dye streak was accelerated in the presence of a countercurrent gas stream (F7). It is possible that the persistence of the dye streaks in the earlier experiments is connected with the manner in which the dye trace was injected; in studying the flow of films over roughness elements, Vouyoucalos (V7) showed that dye streaks behaved differently if injected near the free surface (which is likely to be most affected by the waves) or deeper in the film.

Finally, brief mention must be made of a series of recent papers in which it is shown that the mixing action usually ascribed to discontinuities (e.g., mixing between packing elements in a packed column) may be, in fact, a result of the action of ripples present on the film flowing over the packing at the discontinuities (A7, R3, W5). It is clear that the flow patterns in wavy film flow and their effects on transfer processes merit a great deal of further study.

E. EFFECT OF WALL ROUGHNESS ON FILM FLOW

Although nearly all of the theoretical and experimental studies of film flow have dealt with the flow of films along hydrodynamically smooth surfaces, it is of interest to review the limited information available on the effects of wall roughness in view of their possible importance.

Using channels of glass and roughened brass, Hopf (H18) found that the critical Reynolds number appeared to be independent of the wall roughness in film flow. For vertical tubes of different roughnesses, Claassen (C10) found that the thicknesses of flowing films varied little, though the amount of liquid remaining on the wall after draining increased with the roughness of the surface.

There are numerous reports of investigations of the effects of roughness on flow in open channels. For instance, Reinius (R4) has reported on the effects of surfaces covered with various types of roughnesses (spheres, sand, etc.) on the flow of water in open channels, while Hama (H1) has reported

the effects of other types of roughness elements on flow in a flume. Unfortunately, in most of these investigations the channel slopes are extremely small, and the conditions are not the same as in the flow of thin films on steep walls.

Vouyoucalos (V7) carried out experiments with film flow over regular transverse wall roughness elements of very large size compared with the film thickness and showed that interesting back-mixing patterns could occur in the zones between the roughness elements. Bressler (B20) has also shown that the use of a plate with horizontal ridges increases the turbulence in a film flowing over it and improves heat transfer to such a film. Saveanu *et al.* (S1) investigated the effects of introducing small roughness elements of various sizes on an otherwise smooth vertical wall. These elements were placed at intervals equal to the characteristic wavelength appearing at the free surface. It was found that, with elements of height only 0.2 mm., the critical Reynolds number at which turbulence became important was reduced from its value of 362 for a smooth wall to 287. Increase of the roughness to 0.5 mm. led to little additional change.

The most detailed investigation of the effects of roughness on film flow available at present is due to Brauer (B14). In these experiments fine wires of 0.1-, 0.2-, and 0.3-mm. diameter were placed around a wetted tube 20 mm. above a device for measuring the local heat transfer coefficient to the film. The critical Reynolds numbers obtained for the three sizes of disturbance were 380, 360, and 340, respectively, compared with the value of 400 for the smooth wall, and for the 0.2-mm. disturbance, the local heat transfer coefficient at $N_{Re} = 800$ was at least 12% larger than for the smooth wall. When the roughness elements were placed 40 mm. or more above the heat transfer device, no change could be detected compared with the smooth wall, indicating that the effects of the roughness elements die out rapidly downstream.

It seems that it would be of practical interest to investigate the effects of wall roughness in greater detail, since it might be possible by means of suitably arranged small roughness elements to increase the rates of heat and mass transfer in film-type equipment.

F. FILM VELOCITIES AND VELOCITY PROFILES

A knowledge of the velocity profiles within falling films under various flow conditions would be of very great value, making it possible to calculate the rates of convective heat and mass transfer processes in flowing films without the need for the simplified models which must be used at present. For instance, the analyses of Hatta (H3, H4) and Vyazovov (V8, V9) indicate clearly the differences in the theoretical mass-transfer rates due to the assumption of linear or semiparabolic velocity profiles in smooth

laminar films. The importance of the shape of the velocity profile in studies of heat transfer to films has also been stressed by Wilke (W2) and others; up to the present there have been no direct checks as to whether the various velocity profiles assumed for turbulent film flow (Sections III, E and III, F, 4) are in fact observed in the flow of films.

Unfortunately, the thinness of most liquid films makes it difficult to measure the velocity profiles experimentally, since it is practically impossible to introduce any of the usual fluid-velocity probes into a film which may be less than 1 mm. thick without grossly distorting the flow patterns. Nevertheless, film velocity profile measurements have been reported for a few special cases.

Grimley (G10, G11) used an ultramicroscope technique to determine the velocities of colloidal particles suspended in a falling film of tap water. It was assumed that the particles moved with the local liquid velocity, so that, by observing the velocities of particles at different distances from the wall, a complete velocity profile could be obtained. These results indicated that the velocity did not follow the semiparabolic pattern predicted by Eq. (11); instead, the maximum velocity occurred a short distance below the free surface, while nearer the wall the experimental results were lower than those given by Eq. (11). It was found, however, that the velocity profile approached the theoretical shape when surface-active material was added and the waves were damped out, and, in the light of later results, it seems probable that the discrepancies in the presence of wavy flow are due to the inclusion of the fluctuating wavy velocities near the free surface.

Clayton (C11) measured velocity profiles in vertical films of various liquids by a chronophotographic method, and this work was continued by Wilkes and Nedderman (W4), using improved techniques. Almost instantaneous values of the velocity are obtained at different distances from the wall in this method, so that the difficulty noted above is eliminated. It has been shown in this way (W4) that in the smooth laminar flow regime the velocity profiles are in very close agreement with the predictions of Eq. (11). In the presence of waves at the film surface the local velocities scatter about the theoretical curve, which, however, continues to give an excellent approximation to the time-averaged local velocities. This investigation was confined to quite small Reynolds numbers (regime of regular waves), and further results for other wavy regimes would be of great interest.

Wilke (W2, W3) obtained velocity profiles by means of a traversing scoop, which collected the liquid flowing within the part of the film between the free surface and the lip of the scoop. These results were complicated

by the fact that the flow is periodic in the part of the film between the highest wave crests and deepest wave troughs, but, by applying suitable corrections, Wilke showed that useful information on the velocity profiles could be obtained.

However, for the most part it is necessary to concentrate on the determination of the mean film velocity (from the flow rate and the mean film thickness, see Section IV, A) and the true surface velocity of the film. If the ratio u_s/\bar{u} is equal to 1.5 [see Eq. (14)] this will be an indication that the velocity profile is semiparabolic.

It is well known that in turbulent pipe flow the parabolic profile present in laminar flow becomes blunter, so that the ratio u_{\max}/\bar{u} decreases. A similar effect has been found for the relatively deep flows in open channels at small slopes by Jeffreys (J4), who obtained values of u_s/\bar{u} down to 1.06, and by Horton *et al.* (H19), who measured values as low as 1.1. It can be expected that in the flow of thin films the ratio will decrease in turbulent flow from the value of 1.5, but by a very much smaller amount than observed in the deep flows noted above.

Several workers have reported experimental values of the ratio u_s/\bar{u} for film flow, e.g., Friedman and Miller (F5), Grimley (G11), and Chew (C6), who timed the movement of dye drops at the free surface, Brauer (B14) and Jaymond (J3) who used plastic "confetti" as surface tracers, and Asbjørnsen (A6), who used an interesting residence-time technique. Jackson *et al.* (J2) have deduced the effective film surface velocities from pressure drop measurements in an adjoining gas stream, neglecting the effects of the surface roughness due to the waves.

These studies show that up to the Reynolds number of wave inception, $N_{\text{Re}i}$, the ratio u_s/\bar{u} is equal to the theoretical value of 1.5 [Eq. (14)]. Above $N_{\text{Re}i}$, all the investigators above found a sharp increase in u_s/\bar{u} to a value between 1.9 and 2.25, followed by a more gradual decrease to a value of 1.5, again in the region of $N_{\text{Re}ii}$ (except Jackson *et al.*, who did not observe the subsequent decrease to 1.5).

On the other hand, Portalski (P4) found values of u_s/\bar{u} which fell near or below the theoretical value of 1.5 for all the flow rates investigated, including the range in which other workers found values of 2.0 or greater. It seems clear that the earlier workers have measured an "effective" surface velocity in the region of large waves, which lies between the true surface velocity of the film and the wave velocity. It is of interest to note that the maximum values of u_s/\bar{u} have been reported in the zone in which the wavelengths appeared to pass through a maximum, i.e., near $N_{\text{We}} = 1$ (see Section IV, D, 4, a), and the effective surface velocities tend towards the theoretical value of the surface velocity in the zone near $N_{\text{Re}iii}$, where

the wave velocities tend towards the value of the surface velocity (Section IV, D, 4, b) and where Kirkbride (K17) has reported a decrease in the wave heights.

Unfortunately, in the light of the paper of Tinney and Bassett (T15), it is not clear that the method used by Portalski for measuring the surface velocity of the film (measurement of the rate of propagation of a surge front at the given flow rate on a just-wetted surface) will give accurate values of this quantity. More recently (F7), other measurements of the surface velocities of water films have been made, in which the surface velocity has been calculated from the wavelengths of the standing waves on the film surface formed upstream of a stationary pointer just touching the surface. The theory underlying this method has been treated by Lamb (L5) under the title of Lord Rayleigh's "fishline problem." The experimental values, which covered the range $N_{Re} = 180-750$, fell about the line $u_s/\bar{u} = 1.5$ and showed no tendency to increase towards the value of 2.0 at the lower Reynolds numbers. Although there was a fairly large experimental scatter, the average of 226 readings was $(u_s/\bar{u})_{av} = 1.543$, quite close to the theoretical value.

It seems, therefore, that the true surface velocity of the film does not vary much from the theoretical value over the range of flow rates normally encountered in wetted-wall columns.

It was also found that, although u_s decreased in the presence of an air counterflow, the ratio u_s/\bar{u} remained almost unchanged at moderate gas flow rates ($N_{Re, gas}$ up to 24,000), since the film thickness increased, and hence \bar{u} decreased as well as u_s . This is in agreement with Eq. (93), which predicts that u_s/\bar{u} will be only slightly smaller than 1.5, unless the interfacial shear stress is large.

Feind (F2) has indicated that, in determining the effect of a liquid film flow on an adjoining gas stream, the velocity of the gas relative to the film surface is an important parameter. At present there are few measurements of film surface velocities for the various cases of gas/film flow, and the problem remains as to whether the gas velocity should be considered relative to the true surface velocity of the film in the wavy regime, or to the wave velocity, or to some effective surface velocity.

G. STATIC PRESSURE DROP IN THE GAS STREAM OF A WETTED-WALL COLUMN

Numerous pressure-drop measurements have been made in the gas streams of wetted-wall equipment under various geometric and flow conditions. For the case of vertical tubes, pressure drops have been reported for downward cocurrent gas/film flow by Charvonia (C4), Chien (C7), and Zhivalkin and Volgin (Z4a), for upward cocurrent flow by Bennett and

Thornton (B8), Calvert and Williams (C2), Hewitt and co-workers (C13, G3, H8, H9, H10), and Mahrenholtz (M5), and for countercurrent flow by Clayton (C11), Feind (F2), Jackson *et al.* (J2), Kamei and Oishi (K2), and Thomas and Portalski (T14). Pressure-drop measurements have also been reported for other geometries of the wetted channel (F7, H6, M3, among others). In addition, values have been reported for the small static pressure drops occurring in wetted-wall equipment in the absence of a net gas flow due to the entraining action of the liquid film surface (F2, F7, M8).

Attempts have been made to compare the experimentally measured pressure drops with various of the theories discussed in Section III, F and with the more generalized empirical two-phase friction-factor correlations of the type discussed by Dukler and Wicks (D17). Hewitt *et al.* (H10) have compared their experimental data for upward cocurrent flow with one such empirical correlation and with the theories of Anderson and Mantzouranis (A5) and of Dukler (D12) and Hewitt (H7). In most cases there was good qualitative agreement only.

The theoretical treatments assume that the pressure drop per unit length of the wetted-wall column is a constant quantity, that is, that the gas and liquid streams are both in steady-state flow, with no changes in their velocity profiles in the direction of flow of each phase. In many cases the experimental pressure gradients reported in the literature have been obtained by measuring the pressure drop over the whole length of a wetted wall column and dividing this value by the length of the column, which is clearly valid only so long as the pressure gradient is constant over the whole length of the column. Recent careful experimental measurements in countercurrent flow (F2, F7), in upward cocurrent flow (G3), and in downward cocurrent flow (Z4a) have shown that the pressure gradient is not always constant in the direction of flow of the gas, due to changes in the shape of the gas stream velocity profile and to changes in energy on accelerating or decelerating the liquid film near the inlet. Until it is possible to correct accurately for these effects, or until pressure gradient measurements referring specifically to the steady-state flow regions are available, it seems to serve little useful purpose to compare the theories with the experimental values, which may be valid only for the specific column dimensions investigated, and only a general discussion can be given here.

A particularly interesting feature of gas flow in a tube wetted by a wavy film is that the pressure drop for a given gas velocity is considerably larger than in the case of flow in a dry tube (M4), as shown very clearly by the data of Feind (F2). In an attempt to explain this effect, Laird (L3) investigated gas flows along tubes with flexible walls which performed sine wave oscillations. It was concluded that a large part of the increase in the

pressure drop over the value for a smooth tube was due to changes in the gas stream profile. Later measurements by Laird *et al.* (L4) in tubes with wavy stationary walls showed that the pressure drop in this case was not greatly in excess of the value for a smooth tube, from which it was concluded that the boundary shape alone could not be the cause of the large increase in the pressure drop in columns wetted by wavy films. Konobeev and Zhavoronkov (K22) carried out similar studies for both long-wave and short-wave stationary wall roughnesses and pointed out that in wetted-wall columns the pressure drop increase would be greater than in a tube with stationary solid waves on the walls, due to the moving, irregular, and deformable nature of the roughness elements. In the case of countercurrent gas/film flow, Feind (F2) has suggested that the thin layer of gas entrained at the surface of the liquid film (to satisfy the condition of zero slip) must travel in a direction opposite to the main gas flow, so that the effective gas velocity gradient at the interface (and hence the pressure drop) will be increased.

Attempts have been made to characterize the effects of the interfacial waves on the gas stream by calculating an equivalent sand roughness for the wavy interface from velocity profile measurements in the gas stream (G2, H6, L13). Lilleleht and Hanratty (L12) have shown that a sand roughness calculated in this way is in good agreement with the root-mean-square wave heights. However, more recently Gill *et al.* (G3) have shown that the effect of a wavy film surface on a gas stream in contact with it is not the same in some respects as that of a solid rough wall. One grave complication in the approach of regarding the film surface as a rough surface relative to which the gas stream moves is that, in this case, the "roughness elements" are themselves in motion relative to the "wall," since it has been shown in Section IV, D, 4, b that the wave velocity usually differs from the film surface velocity.

From the brief discussion above, it can be seen that our knowledge of the pressure drop and the interfacial shear stress in the gas stream of a wetted-wall column is very unsatisfactory at present. Since the pressure drop is an important quantity in more complicated two-phase flows, of which gas/film flow is the simplest case, this is particularly unfortunate, and a great deal of detailed experimental work is necessary on this topic.

H. WALL SHEAR STRESS IN THE LIQUID FILM

Experimental measurements of the wall shear stress exerted by a falling liquid film have been reported for the cases of film flow outside a vertical tube (B14) and in a channel of variable slope (F7). In both cases the experimental results in the zone of smooth laminar flow were in agreement

with the predictions of Eq. (16) or (20), and the friction factors calculated from the wall shear stresses are therefore given by Eq. (21).

In the wavy laminar regime, however, the experimental values of the film wall shear stress, and hence of the film friction factor, are appreciably greater than predicted by the theoretical equations mentioned above. The deviation between the experimental and theoretical values at a given value of N_{Re} increased with increasing slope of the channel (F7). The increase in the wall shear stress is due at least partly to the decrease in the mean film thickness in the wavy flow regime, which leads to a greater mean velocity and velocity gradient at the wall. In the turbulent zone of film flow, Brauer (B14) has shown that the wall shear stress is given (for vertical film flow) by

$$\tau_w = 0.0465(N_{Re})^{2/5}$$

which corresponds to a friction factor of

$$f = 0.408/(N_{Re})^{3/15}$$

Preliminary results (F7) show that, in the case of countercurrent gas/film flow, the film wall shear stresses decrease with increasing gas velocity, due to the increase in the mean film thickness (and hence decrease in the velocity gradient at the wall) at a given liquid flow rate.

As yet there appear to be no reports of wall shear stress measurements in liquid films with cocurrent gas streams.

V. Conclusions

In the preceding sections an attempt has been made to summarize the information available at present on a number of aspects of film flow.

In his review of research in the field of film condensation, Colburn (C12) summed up the situation in 1951 by saying, “. . . the direction of most promising research is in studying fluid flow characteristics of liquids in layers, with and without a superimposed gas velocity. The types of turbulence in layers needs to be investigated, and also the nature of a laminar layer containing ripples. . . .” It is interesting to note that a significant part of the work on film flow carried out since that time has been concerned in one way or another with the wavy nature of flowing films and with the interactions between films and adjacent gas streams. However, in spite of several important advances, the field of gas/film flow is so vast that the remarks above remain quite valid today.

In recent years there has been a considerable increase in the amount of information available on the more macroscopic aspects of film flow under various conditions, such as the film thicknesses, general wave

patterns, over-all pressure drops in the gas streams of wetted-wall columns, surface velocities of the film, the various critical flow rates at which changes occur in the flow behavior of the film, and the like. However, the situation is rather less satisfactory as regards the finer features of such flows, particularly in the wavy flow regime. For example, much work remains to be done in the investigation of the flow patterns and velocity profiles inside films and, in particular, inside the waves at the film surface; the interfacial shear stress exerted by a gas stream at a wavy film surface and the related local gas stream pressure drop also urgently require closer study, and a number of other features of film flow which seem to merit more detailed investigation have been mentioned in the earlier sections.

As regards the theoretical studies of film flow, it has been shown that it is possible to predict quite accurately the flow behavior in the smooth laminar flow regime of the film; unfortunately, this flow regime is not of great practical importance. The Kapitza theory for wavy film flow appears to apply over only a very limited part of the total wavy flow regime (flow with regular waves). Apart from this theory, there appears to be no general theory available for the wavy flow of thin films on steep surfaces, and the mathematical difficulties in the way of developing such a theory appear to be enormous. It seems probable that it will be necessary to use empirical relationships, based on a suitably wide mass of experimental results, for describing the flow behavior in the wavy flow regime, but it will be some time before sufficient results are available.

It is of interest to note that several new experimental techniques for the study of film flow have been developed in recent years, including improved methods for studying local film thicknesses and wave profiles (e.g., H9, L13, S11), a method for obtaining instantaneous and undisturbed velocity profiles in films (W4) and for obtaining wall shear stresses and local heat transfer coefficients in films (B14, W3), to mention but a few. In this way it has become possible within the last few years to measure many of the features of film flow which were previously beyond the reach of experimentation, while the speed and accuracy of other measurements have been greatly increased. In view of the expanding interest in film flow (see the Appendix), it can be expected that this intense experimental activity will continue, eventually providing sufficient information to enable many of the puzzling features of film flow to be explained, thus laying a firm foundation for the study of more complex two-phase flows.

ACKNOWLEDGMENTS

The present review of the literature on film flow was carried out in its original form at the Department of Chemical Engineering, University of Birmingham, Birmingham, England. The writer would like to express his gratitude to the Department of Chemical

Engineering and to the Esso Petroleum Company for financial assistance, and to Professor F. H. Garner, O.B.E., for his interest in this work.

Nomenclature

α	Amplification of most unstable wave in traveling 10 cm.
b	Film thickness
b_i	Initial film thickness at $x = 0$
b_N	Film thickness given by Nusselt equation [Eq. (15)]
b_x	Value of variable film thickness at $x = x$
b^+	Dimensionless film thickness, Eq. (77)
\bar{b}	Mean film thickness
c	Phase velocity of waves
f	Function of; or friction factor for film flow
g	Acceleration of gravity
K	Constant
L	Length of column
n	Integer (1, 2, 3 . . .) in summations; or wave number, Eq. (40)
p	Pressure
p_c	Capillary pressure, Eq. (49)
Δp	Pressure drop
Q	Volumetric flow rate per unit wetted perimeter
r	Radial coordinate
R	Tube radius
S	Interfacial area
ΔS	Increase in interfacial area due to waves
t	Time
T	Velocity profile shape factor, Eq. (95)
u	Velocity in x -direction
u_s	Surface velocity of film
u^+	Dimensionless velocity in x -direction, Eq. (75)
u^*	Friction velocity, Eq. (78)
\bar{u}	Mean velocity in film
v	Velocity in y -direction
v_g	Gas stream velocity
w	Velocity in z -direction; or half-width of wetted channel (Section III, B, 4)
W	Weight flow rate per wetted perimeter
x	Coordinate in direction of flow
y	Coordinate measured from wall across thickness of film
y^+	Dimensionless distance from wall, Eq. (76)
z	Coordinate across channel

GREEK LETTERS

α	Wave amplitude
δ'	Thickness of nonturbulent surface layer
Δ	Change in quantity
θ	Angle of channel bed, measured from horizontal
λ	Wavelength

μ	Dynamic viscosity
ν	Kinematic viscosity
ν'	Relative viscosity, defined by Eq. (103)
ρ	Density
ρ_c	Density of adjacent phase
σ	Surface tension
τ	Shear stress
τ_i	Interfacial shear stress
τ_w	Wall shear stress
ϕ	Quantity defined in Eq. (55)
Φ	Quantity defined in Eq. (63)
ψ	Pressure drop per unit length
Ω	Force potential of field

NAMED DIMENSIONLESS GROUPS

K_F	$= \mu^4 g / \rho \sigma^3$, physical properties group
N_{Fr}	Froude number, defined by Eq. (3)
N_{Re}	Reynolds number of film, defined by Eq. (1)
$N_{Re_{crit}}$	Critical Reynolds number for onset of turbulence
$N_{Re_{gas}}$	Reynolds number of gas stream
N_{Re_i}	Reynolds number at onset of instability
N_T	Nusselt dimensionless film thickness parameter, defined by Eq. (97)
N_{We}	Weber number, defined by Eq. (2).

SUPERScript

+	Dimensionless quantity
---	------------------------

SUBSCRIPTS

crit	Critical value of quantity
gas	Gas phase quantity
0	Value of quantity in absence of gas stream.

OTHER SYMBOLS

∇^2	Laplacian operator
$ q $	Absolute value of quantity q

APPENDIX. BRIEF CHRONOLOGICAL RÉSUMÉ OF PAPERS ON FILM FLOW AND RELATED TOPICS

Authors and Date	Remarks
Hopf (H18), 1910	Film flow experiments (water, sugar solution) in channel 5.2×40 cm., slope $\frac{1}{2}-3\frac{1}{2}^\circ$; $N_{Re} = 150-600$. Observations of film thickness, surface velocity, wave formation, effects of wall roughness. Theory of film flow in rectangular channel in absence of surface tension forces.

Authors and Date	Remarks
Nusselt (N6), 1916	Theoretical treatment of flow and heat transfer in smooth laminar films, with and without interfacial drag. Inertia forces neglected.
Claassen (C10), 1918	Experimental studies of film flow of water, NaCl solutions, and molasses on vertical tubes. Measurements of film thickness, liquid adhering after draining, effects of roughness.
Schoklitsch (S3), 1920	Flow studies in channel at small slopes (below 2°) with water; $N_{Re} = 22$ –45,000. Thicknesses, critical Reynolds number, onset of turbulence studied.
Nusselt (N7), 1923	Extension of earlier work (N6), and comparison with experiments of Claassen.
Jeffreys (J4), 1925	Water flow in channel 10.2×364 cm. at small slopes, large range of N_{Re} . Measurements of velocities, ratio of mean to maximum velocity, thicknesses; $N_{Re, crit} = 310$. Dye tracer experiments used to deduce thickness of laminar sublayer, eddy viscosity, friction factors. Theoretical work on bores, waves, instability of flow.
Chwang (C9), 1928	Study of thicknesses of water, oil films on plates at slopes up to 13° . $N_{Re} = 0.9$ –110.
Cornish (C16), 1928	Theory of flow with free surface in rectangular channel of finite width, neglecting interfacial drag.
Warden (W1), 1930	Flow of water films inside tubes, $N_{Re} = 69$ –1830. Film thicknesses reported.
Cooper and Willey (C15), 1934	Flow of films of dilute H_2SO_4 inside tube, diameter 1.13 cm. $N_{Re} = 1.53$ –192. Film thicknesses reported.
Hatta (H3), Hatta and Katori (H4), 1934	Theoretical and experimental work on absorption of CO_2 by water film on channel 1.5 cm. \times various lengths, slopes 1° – 90° . Shows inapplicability of "two film" theory to most cases of gas absorption by liquid films.
Horton <i>et al.</i> (H19), 1934	Laminar water flow studied in channel, 14.3×86.4 cm. at slopes up to 2° . Measurements of thickness, surface velocity, ratio u_s/\bar{u} . Capillary edge effect noted. Onset of turbulence discussed.
Kirkbride (K17), 1934	Flow of water and 4 oils outside tubes, $N_{Re} = 0.04$ –2000. Film thicknesses (maximum wave heights) measured by micrometer. Wavy flow is described, and corrections to Nusselt theory derived for heat transfer in laminar wavy film flow.

Authors and Date	Remarks
Cooper <i>et al.</i> (C15), 1934	Earlier film thickness data correlated in form of film friction factor plot.
Fallah <i>et al.</i> (F1), 1934	Flow of water films inside tubes, with second phase of air, white oil, stationary and countercurrent kerosine. Film thicknesses of this and previous work correlated by film friction factor plot.
Holmes (H16), 1936	Observations of traveling waves in steep channels.
Bays and McAdams (B2), 1937	An improved correlation for heat transfer in laminar film flow is presented.
Strang <i>et al.</i> (S13), 1937	Flow of water films ($N_{Re} = 6-150$) inside tubes with stationary second phase of tetralin, kerosine, and 4 oils of various densities and viscosities. Effect of buoyancy forces on film thickness determined.
Keulegan (K13), 1938	Extension of Prandtl-von Kármán turbulent flow theories to turbulent flow in open channels. Effects of wall roughness, channel shape, and free surface on velocity distribution are considered.
Verschoor (V3), 1938	Hold-up in wetted-wall columns.
Sexauer (S8), 1939	Experimental study of heat transfer to and through condensate films.
Keulegan and Patterson (K16), 1940	Determination of criterion for wave formation in turbulent flow in steep channels: $N_{Fr} > \frac{3}{2}$ or $N_{Fr} > 2$, depending on use of Manning or Chézy coefficients for resistance term.
Levich (L6), 1940	Theory of the damping of waves by insoluble surface-active materials.
McAdams <i>et al.</i> (M1), 1940	Correlation of heat transfer coefficients in falling-film heaters, $N_{Re} = 225-15,000$.
Thomas (T13), 1940	Theory of wave propagation in steep channels. Experimental work on wave profiles in channel in which the wetted wall was moved upwards to keep wave profile stationary. Surface tension effects neglected.
Vyazovov (V8, V9), 1940	Observations of flow and absorption of CO_2 by water film (laminar flow) on plate 9.2×110 cm., various slopes. Gas absorption by smooth laminar film dealt with theoretically, assuming linear and semiparabolic velocity profiles.
Friedman and Miller (F5), 1941	Flow of films of water, oil, toluene, and kerosine inside tubes, $N_{Re} = 0.02-115$. Measurements of thickness, surface velocity, onset of wavy flow.

Authors and Date	Remarks
Levich (L7), 1941	Theory of damping of waves by soluble surface-active materials: shows that damping coefficient passes through a maximum as concentration of surfactant increases.
Grigull (G8), 1942	Treatment of heat transfer in condensate film on vertical surface, assuming applicability of Prandtl pipe-flow relationships. Comparison with experimental data.
Treybal and Work (T16), 1942	Thicknesses of aqueous acetic acid films inside tubes with moving second phase of benzene. Wide range of N_{Re} .
Semenov (S6), 1944	Experimental thicknesses of water films inside tube 1.38×23 cm.; $N_{Re} = 2-77$. Theoretical treatment of smooth laminar flow with interfacial drag due to cocurrent or countercurrent gas flow, and onset of flooding.
Grimley (G10), 1945	Film flow in tubes and channels (water, water + surfactant), co- and counter-flow of air. Wave observations, onset of rippling, surface velocity, velocity distribution, film thicknesses, effects of surface tension and surfactants.
Vedernikov (V2), 1946	Theoretical treatment of wavy flow in open channels. Wavy flow and turbulent flow clearly distinguished.
Fradkov (F4), 1947	Theory of laminar film flow with interfacial drag. Experimental work on film flow of liquid air with counter-flow of air; conditions for onset of flooding determined.
Grimley (G11), 1947	Amplification of earlier work (G10), and experimental work on CO_2 absorption by water film. Photos of wavy films.
Kapitsa (K7, K8), 1948	Theoretical treatment of wavy flow of thin films of viscous liquids, including capillary effects. Only regular waves considered. Wavy flow shown to be more stable than smooth film, and about 7% thinner than smooth film at same flow rate. Also calculates wave amplitudes, wavelengths, etc., onset of wavy flow, effects of countercurrent gas stream, heat transfer. Theory applicable only if wavelength exceeds 14 film thicknesses. Error in treatment pointed out by Levich (L9).
Levich (L8), 1948	Considers theoretically mass transfer across liquid/fluid interfaces, with special treatment of gas absorption by turbulent liquid films.

Authors and Date	Remarks
Dressler (D9), 1949	Mathematical treatment of roll waves in inclined open channel, including effects of slope, resistance to flow, but neglecting surface tension effects.
Kapitsa and Kapitsa (K10), 1949	Wavy flow of water and alcohol films on outside of tube of diameter 2 cm., $N_{Re} < 100$, studied photographically and stroboscopically. Experimental data at low flow rates in agreement with Kapitsa theory; waves become random at large flow rates.
Semenov (S7), 1950	Extension of earlier work to wavy film flow. Kapitsa theory simplified by omitting inertia terms, and applied to wavy film flow with co- or counter-flow of gas to give thickness, velocity, wavelength, wave velocity, stability, onset of flooding, etc.
Ternovskaya and Belopol'skiĭ (T9, T10), 1950	Experimental study of absorption of SO_2 in water film with various surfactant additives. Rate of absorption decreased rapidly then increased slowly as concentration of surfactant increased (cf. Levich, L7); this effect is shown to be due to damping of waves.
Tsien (T17), 1950	Describes applications of film cooling.
Carpenter and Colburn (C3, C12), 1951	Review of research on film condensation; shows importance of gas stream effects, waves, transition to turbulence, etc.
Jackson <i>et al.</i> (J2), 1951	Experimental study of film flow inside tube with counter-flow of gas. Film surface velocity deduced from pressure drop readings in gas stream, neglecting wave roughness effects. Surface velocities appear to exceed the theoretical values in the wavy flow regime.
Kapitsa (K9), 1951	Deals theoretically with heat and mass transfer to periodic flows, e.g., to wavy liquid films.
Shibuya (S10), 1951	Mathematical treatment of onset of wavy flow in liquid films on vertical tubes. Waves appear for $N_{Re} > 7$. Wavelength of first waves $\cong 3$ film thicknesses.
Zhavoronkov <i>et al.</i> (Z2), 1951	Mass transfer studies (CO_2 into water film) in two diameters of wetted-wall column and on wetted-plate packing (liquid mixed at intervals). Gas velocity had little effect on transfer rates.
Calvert (C1), 1952	Theory for case of upward cocurrent gas/film flow in tubes. Numerous experimental results on film thicknesses, pressure drops, etc.
Craya (C17), 1952	Treatment of stability problem in open channel flow.

Authors and Date	Remarks
Dressler (D10), 1952	Treatment of stability and roll-wave formation in open channels, using general resistance formula.
Grigull (G9), 1952	Correlation and discussion of heat transfer results for film condensation.
Ishihara <i>et al.</i> (I1), 1952	Theoretical treatment of stability of laminar film flow: waves possible for $N_{Fr} > 0.58$. Experiments in channel 20×500 cm., slopes up to 15° . Measurements of wavelength, wave velocities, and frequencies, onset of rippling and turbulence. Tracer studies of turbulence in wave fronts.
Pennie and Belanger (P1), 1952	Film thickness measurements in film of 5% aqueous sodium carbonate solution flowing inside tube (diameter 1.28 cm.). $N_{Re} = 13$ –3250.
Dukler and Bergelin (D16), 1952	Study of water films on vertical plate, 61.4×204 cm. $N_{Re} = 120$ –750. Film thicknesses (local and mean) by capacitance proximity meter; wave profiles; photos of wave patterns. Theoretical treatment assuming applicability to film flow of pipe-flow universal velocity profiles.
Sherwood and Pigford (S9), 1952	Much information on absorption, distillation, and vaporization in wetted-wall columns. Details of Pigford's theoretical treatment of gas absorption by smooth laminar films.
Ternovskaya and Belopol'skii (T11, T12), 1952	Extension of earlier work (T10) on effects of surfactants on rates of gas absorption by water films, giving explanation of mechanism.
Chew (C6), 1953	Film thicknesses of water films on plates of various slopes measured. Observations of entry region and wave patterns. Surface velocity measurements.
Dressler and Pohle (D11), 1953	Treatment of hydraulic instability of turbulent flow in open channels, using general resistance law.
Brötz (B21), 1954	Study of films of water, pentadecane, and a refrigerating oil inside tubes of various diameters; kinematic viscosities 1.0–8.48 cs.; $N_{Re} = 100$ –4300. Measurements of film thicknesses, rate of absorption of CO_2 . Effective diffusivity in turbulent zone determined from dye tracer studies. Relationship derived for turbulent film thicknesses.
Emmert and Pigford (E4), 1954	Experimental work on mass transfer to water films and comparison with theory. O_2 and CO_2 absorption and desorption studied; $N_{Re} = 2$ –250. Observations of

Authors and Date	Remarks
	waves, onset of rippling, effect of surfactants. Mass transfer agrees with theory only in absence of waves.
Kamei and Oishi (K2), 1954	Experimental determination of pressure drops in air stream flowing countercurrently to liquid films inside columns of 4.5 and 20.3 cm. diameter. Liquids included water, soap solutions, glycerol solutions, $N_{Re} = 0.2-250$; $N_{Re_{gas}} = 4000-200,000$.
Kamei <i>et al.</i> (K5), 1954	Thicknesses of films flowing inside tubes of diameters 1.90–5.09 cm. measured with zero and cocurrent gas flows.
Kamei <i>et al.</i> (K6), 1954	Experimental determination of flooding points in wetted-wall columns of i.d. 1.89–4.91 cm., using various liquids and air counter-flow.
Knuth (K18), 1954	Experimental study of film cooling; conditions for film attachment to wall, entrainment, instability.
Laird (L3), 1954	Experimental study of pressure drop in gas stream in tubes with sine-wave oscillations of tube wall. Shows that large pressure drop is partly due to change in shape of gas velocity profiles.
Owen (O1), 1954	Derives equations for flow in open rectangular channel of finite width; considers transition to turbulence.
Yih (Y1), 1954	Mathematical treatment of stability of laminar flow with free surface (neglecting surface tension). Numerical calculations for film on vertical surface give $N_{Re} \cong 1.5$.
Calvert and Williams (C2), 1955	Presentation and discussion of work by Calvert (C1) on velocity distribution, flow rate, pressure drop, shear stresses, profile drag, etc., for upward cocurrent film/gas flow.
Garwin and Kelly (G1), 1955	Study of heat transfer between water film and heated plate at various inclinations.
Jackson (J1), 1955	Flow of films of ethyl acetate, methanol, water, water + surfactant, 2-propanol, glycerol solutions (with and without surfactant), inside tube of 3.6 cm. diameter. Film thicknesses by radioisotope tracer method; heights of waves measured. Surface tension had little effect.
Kamei and Oishi (K3), 1955	Experimental measurements of absorption of CO_2 by water film inside tubes, 4.76×250 cm., with zero and countercurrent gas flow. Large range of N_{Re} .
Lynn <i>et al.</i> (L15, L16, L17), 1955	Experimental work on absorption of SO_2 in water films, (1) in long wetted-wall column (rod, film outside); (2)

Authors and Date	Remarks
	in very short wetted-wall columns (no rippling); (3) flowing over spheres. Entry and end effects studied, also effects of adding surfactant.
Malyusov <i>et al.</i> (M6), 1955	Study of distillation in wetted-wall columns, taking into account the effects of laminar and turbulent flow of vapor phase.
Stirba and Hurt (S12), 1955	Experimental work on CO ₂ absorption by water films in vertical tubes of length 3 and 6 ft., and dissolution of tubes of solid organic acids by water films. Effective diffusivity exceeds molecular diffusivity, even at $N_{Re} = 300$. Dye streak experiments show that waves cause mixing; surfactants damp waves to give continuous dye streak and mass transfer results in agreement with theory.
Alimov (A2), 1956	Considers stable form of liquid film condensing on hot horizontal cylindrical surface, and shows that stable annular wave patterns are formed for certain flow rates and temperature differences.
Brauer (B14), 1956	Extensive experimental study of film flow outside tube 4.3×130 cm.; films of water, water + surfactant, aqueous diethylene glycol solutions, kinematic viscosity 0.9–12.7 cs.; $N_{Re} = 20$ –1800. Data on film thicknesses, waves, maximum and minimum thicknesses, characteristic Reynolds numbers of flow, onset of rippling and turbulence, wall shear stress, etc.
Greenberg (G7), 1956	Flow of films (5 liquids) down tube 2.5×30 in. Data on film thickness, wave velocity, frequency, amplitude; analysis of roll waves.
Kamei and Oishi (K4), 1956	Flow of films of water, soap solution, millet-jelly solutions inside tubes of diameter 5.09–1.9 cm. \times 100 cm., with zero and countercurrent air flow. Kinematic viscosities 1.1–40 cs.; $N_{Re} = 1$ –4200. Surface tension found to affect holdup.
Kramers and Kreyger (K24), 1956	Experimental and theoretical study of mass transfer between a soluble wall surface and film flowing on it. Experiments carried out at low N_{Re} on inclined plane surface.
Labuntsov (L1), 1956	Heat transfer to falling films (laminar flow): effects of convective heat transfer and inertia forces (neglected in Nusselt theory) considered experimentally and theoretically.

Authors and Date	Remarks
Mazyukevich (M8), 1956	Experimental study of entrainment of gas by the surface of a film (water, ethylene glycol) flowing inside a tube.
Vivian and Peaceman (V5), 1956	Experimental mass transfer work in short wetted-wall columns (1.9–4.3 cm. long); ripples absent at most flow rates. Rate of desorption of CO_2 independent of gas velocity up to $N_{\text{Re}_{\text{gas}}} = 2200$. Width and type of liquid inlet slot had little effect. Acceleration of film important.
Benjamin (B5), 1957	Theoretical study of wave formation in laminar flow down inclined plane, taking surface tension into account. Films on vertical surfaces shown to be always theoretically unstable. Simplified treatment for long waves presented.
Binnie (B9), 1957	Determination of onset of rippling in water film flowing outside vertical tube: $N_{\text{Re}_i} \cong 4.4$.
Brauer (B15), 1957	Application of results on flow of films (B14) to case of heat transfer in film condensation.
Davidson and Cullen (D1), 1957	Consideration of the flow mechanics and diffusion in a liquid film flowing over a sphere.
Davidson and Howkins (D3), 1957	Calculations of shapes of standing waves formed on surface of film flow in the presence of an accelerating gas stream, and experimental results on same.
Feldman (F3), 1957	Mathematical consideration of stability of a liquid film on a wall with a cocurrent gas stream above it.
Konobeev <i>et al.</i> (K19), 1957	Theoretical and experimental studies of pressure drops and film thicknesses in upward cocurrent flow of gas and film in vertical tubes (1.35×122 cm.).
Konobeev <i>et al.</i> (K20), 1957	Study of CO_2 absorption in water films in upward and downward cocurrent flow; $N_{\text{Re}} = 5$ –200, gas velocities 11.6–39 m./sec. It is suggested that only wavelength and amplitude of interfacial waves affect the rate of mass transfer. Values of wavelength and amplitude measured and compared with previous theories.
Labuntsov (L2), 1957	Heat transfer to condensate films on vertical and horizontal surfaces. In laminar region, Nusselt equations are corrected for (a) inertia effects, (b) variation of physical properties with temperature, (c) effects of waves. In turbulent region various "universal" velocity profiles are used. Results compared with experimental data.
Michalik (M9), 1957	Study of hydraulics of laminar film flow of Newtonian fluid in tubes and on vertical plates. Optimum design parameters for wetted-wall columns derived.

Authors and Date	Remarks
Shirotsuka <i>et al.</i> (S11), 1957	Experiments on film flow in vertical channel, 8 cm. wide; $N_{Re} = 100-1500$; zero or countercurrent air flow. Data on local film thicknesses, wave heights, wave frequencies, increase in surface area due to rippling, with and without air flow.
Brauer (B17), 1958	Application of results on film flow (B14) to case of heat flow in filmwise condensation of pure vapors on vertical walls. Nomograms for practical use.
Brauer (B16), 1958	Same as previous citation, but application to mass transfer in liquid films; comparison with previous experimental work.
Bressler (B19), 1958	Review of research on evaporation from thin liquid films.
Clayton (C11), 1958	Experimental studies of flow of films of water, aqueous glycol solutions, inside tube, 1.27 cm. diameter; $N_{Re} = 0.007-2100$; zero or countercurrent air flow. Flooding conditions investigated; velocity profiles obtained within wavy film by chronophotographic method.
Collins (C14), 1958	Film thicknesses and CO_2 absorption by water film in cocurrent flow with gas stream in vertical tube, 2.05×36 in. Thicknesses by light-absorption technique.
Gay (G2), 1958	Experimental study of interfacial drag between liquid surface (nearly horizontal) and air stream flowing over it (co- or counter-flow). Distortion of gas stream profiles by rough liquid surface; determination of effective surface roughness.
Howkins and Davidson (H20), 1958	Investigation of stability of liquid film flowing over spheres in an upward airstream. Effects of surfactants studied.
Kutateladze and Styrikovich (K25), 1958	Sections deal with film flow in presence of zero, counter-current, upward and downward cocurrent gas streams, including turbulent film flow.
Mahrenholtz (M5), 1958	Experimental and theoretical study of upward cocurrent gas/film flow. Data on mean film thicknesses, range of stability, efficiency of conveying liquid up wall in film, effects of physical properties of liquids.
Nikolaev (N2), 1958	Consideration of distillation in film columns. Includes observations of onset of flooding with counterflow of gas.
Pocza (P2), 1958	Theoretical treatment of binary thin-film distillation.
Scriven and Pigford (S5), 1958	Discussion of effect of acceleration of liquid film near inlet on gas absorption into film. See Lyan, 1960.

Authors and Date	Remarks
Thomas and Portalski (T14), 1958	Experimental study of water film flowing inside tube 1.96×98 cm., $N_{Re} = 141-493$, counterflow of air. Data on film thicknesses, pressure drop, wave characteristics.
Belkin <i>et al.</i> (B4), 1959	Experimental studies of water films flowing outside tubes; observations of film thicknesses, onset of rippling. $N_{Re} = 50-7500$ (mostly turbulent zone).
Binnie (B10), 1959	Experimental studies of water films in channel 8.4×480 cm., small slopes, N_{Re} up to 2500. Data on onset of rippling and turbulence, capillary edge effect. Comparison with Benjamin stability theory (B5).
Charvonja (C4), 1959	Experimental studies of downward cocurrent flow of air and water films in vertical tubes, $2\frac{1}{2} \times 30$ in.; $N_{Re} = 4-445$. Data on local film thicknesses, pressure drops; analysis of amplitude and frequency spectra of surface waves.
Davidson <i>et al.</i> (D2), 1959	Study of film flow over spheres, and absorption of CO_2 by water films. Effects of adding surfactants on mixing between spheres noted.
Dukler (D12), 1959	Theoretical analysis of turbulent film flow (with and without downward cocurrent gas stream) with extension to film heat transfer. Interfacial disturbances are neglected; basic equations are solved by computer giving film thicknesses, velocity profiles, local and mean heat transfer coefficients. Interfacial shear is shown to be of great importance.
Ellis and Gay (E3), 1959	Presentation and discussion of results of Gay (G2).
Hikita (H12), 1959	Experimental study of effects of rippling on rate of absorption of CO_2 by water films containing surfactants (0.0005-0.05 wt. %), with film flow inside tubes 1.3 cm. \times $15-101$ cm. Results approach Emmert and Pigford theory (E4) as rippling is damped by surfactants.
Hikita and Nakanishi (H13), 1959	Film flow over spheres (1.42-4.12 cm. diameter) singly and in vertical groups of up to 5, spaced at 5-mm. intervals. CO_2 absorbed in water films with and without surfactant additives, $N_{Re} = 1-200$. With pure water results for multiple spheres agree with assumption of complete mixing between spheres; deviations with surfactants.
Hikita <i>et al.</i> (H14), 1959	Study of rate of dissolution of wall of vertical steel pipe by film of 0.01 <i>N</i> sulfuric acid flowing on inside wall. Comparison with theory.

Authors and Date	Remarks
Hikita <i>et al.</i> (H15), 1959	Experimental studies of absorption of CO ₂ , H ₂ , Cl ₂ , H ₂ S, SO ₂ by falling films of water, sugar solutions, butanol/methanol, and methanol/benzene solutions in tubes of 0.7–4.35 cm. i.d., 20–103 cm. long. $N_{Re} = 7.5$ –500, $N_{Sc} = 73$ –2600. No effect of gas rate noted up to $N_{Re_{gas}} = 7000$. Results correlated empirically.
Levich (L9), 1959	Final chapter deals with film flow theory (smooth, wavy laminar, turbulent) with and without gas flow. Also considers mass transfer to such films. Correction to theory of Kapitza (K7).
van Rossum (V1), 1959	Experimental studies in horizontal channel, 15×310 cm., using water, kerosine, various oils, $N_{Re} = 0.1$ –5000, cocurrent air flow. Data on local film thicknesses, onset of rippling and entrainment, effects of roughness and surfactants.
Anderson and Mantzouranis (A5), 1960	Experimental and theoretical study of hold-up and film thicknesses for upward cocurrent gas/film flow in vertical tubes. Theory based on use of universal velocity profile. Numerous experimental data on friction factors, etc.
Bird <i>et al.</i> (B11), 1960	Brief theoretical treatments of various cases of film flow (on cone, with variable viscosity, non-Newtonian liquids, etc.) and of heat and mass transfer to films.
Brauer (B18), 1960	Treatment of film flow in vertical tubes with gas streams (countercurrent, cocurrent up and down). Pressure drops and gas stream friction factors are calculated for the various cases. Fully developed gas flow and laminar film flow (smooth) are assumed throughout.
Bressler (B20), 1960	Experimental studies of film flow and heat transfer to films, work is extended to deal with swept-film evaporators.
Davies (D4), 1960	Considers, <i>inter alia</i> , dye-tracer experiments in wetted-wall columns.
Dukler (D13), 1960	Discussion and extension of earlier paper (D12).
Feind (F2), 1960	Experimental studies of film flow (water, aqueous glycol solutions) with countercurrent air flow in vertical tubes (2.0–5.0 cm. diameter). Data on mean film thicknesses, local heat transfer coefficients, pressure drop, wave heights, onset of flooding, gas/film interactions.
Fulford (F6), 1960	Brief review of heat and mass transfer to falling liquid films.

Authors and Date	Remarks
Graebel (G6), 1960	Theoretical treatment of stability of countercurrent film/gas flow.
Heartinger (H5), 1960	Study of gas absorption in wavy liquid film; a simplified model is given and solved by computer to give rates of transfer under various conditions.
Lynn (L14), 1960	Theoretical consideration of acceleration of film near inlet slots of various types. Model studies suggested that acceleration should be complete in a very short distance.
Miles (M10), 1960	Considers stability problem of thin liquid film (linear velocity profile) bounded by a solid wall and a cocurrent gas stream.
Norman and Binns (N3), 1960	Experimental determination of minimum flow rates of liquid to ensure wetting in wetted-wall columns, and effects of surface tension on same.
Norman and McIntyre (N4), 1960	Investigation of effect of surface tension changes caused by heat transfer on minimum flow rates required to ensure wetting of wetted-wall columns.
Portalski (P3), 1960	Extensive study of film flow on vertical plates, with and without gas flow. Liquids included water, aqueous glycerol solutions, methanol. Data on effects of surface tension changes and surfactants, wave and surface velocities, increase in interfacial area by waves, etc.
Tailby and Portalski (T2), 1960	Reports on extension of Kapitza theory (K7) to give increase in interfacial area due to waves; experimental measurements of N_{Re} for wave inception, entry length, and increase in interfacial area.
Zaitsev (Z1), 1960	Theoretical treatment of stability of thin film of viscous liquid (with surface tension) on wall in the presence of a cocurrent gas stream.
Adorni <i>et al.</i> (A1), 1961	Experimental studies of upward cocurrent flow of argon and water film in tube 0.987 in. \times 3.3 ft.; gas velocities up to 86 ft./sec. Data on film thicknesses, entrance characteristics, droplets entrained in gas stream.
Anderson <i>et al.</i> (A4), 1961	Theoretical and experimental study of heat transfer to liquid films in vertical long-tube evaporators. Theory based on use of universal velocity profile.
Asbjørnsen (A6), 1961	Residence times in falling water films determined by a pulsed tracer technique. Mean residence time 2-7% greater than calculated from laminar film flow theory.

Authors and Date	Remarks
	Minimum residence time in agreement with Brauer's (B14) effective surface velocity results up to $N_{Re} = 400$. Distribution function agrees with theory in presence of surfactants.
Beda (B3), 1961	Theoretical treatment of film flow of liquid permeating through porous wall, with heat transfer.
Benjamin (B6), 1961	Extension of earlier work (B5) to the case of three-dimensional disturbances on surface of film.
Bennett and Thornton (B8), 1961	Experimental work on annular film/gas flow in vertical tubes. Data on film thicknesses and pressure drops along the wetted tubes.
Black (B12), 1961	Discussion of various methods of measuring local film thicknesses.
Chien (C7), 1961	Investigation of liquid film structure and pressure drops in vertical downward cocurrent gas/film flow. Data on surface waves, entry length, energy dissipation in film, film thicknesses (local and mean), pressure drop.
Collier and Hewitt (C13), 1961	Experimental studies of film thickness, pressure drop, and entrainment in upward, cocurrent gas/film flow, using various liquids. Results compared with earlier theories.
Dukler (D14), 1961	Practical application of the theoretical calculations of film heat transfer coefficients (Dukler, D12, D13).
Dukler (D15), 1961	Comparison of calculated values of the film thickness (Dukler, D12, D13) with published experimental results.
Escoffier (E5), 1961	Analysis of onset of instability in open channel flow and origin of waves of instability. Discussion of earlier instability criteria.
Glaser (G4), 1961	Studies of heat transfer between a vertical tube and a liquid film flowing on it.
Hanratty and Hershman (H2) 1961	Jeffreys' theory (J4) for roll-wave transition on a liquid surface is applied to the cocurrent flow of gas and liquid at small slopes. Experimental data on the initiation and growth of waves on various liquids with and without surfactant additives.
Hewitt (H7), 1961	Extension of Dukler treatment (D12, D13) to case of upward cocurrent flow of gas and liquid film, with heat transfer. Computer solutions presented.

Authors and Date	Remarks
Hewitt <i>et al.</i> (H8), 1961	Experimental study of upward cocurrent flow of air (200–500 lb./hr.) and water film (20–1000 lb./hr.) in 1½-in. vertical tube. Results compared with theory by Hewitt (H7).
Ishihara <i>et al.</i> (I2), 1961	Gives summary of recent Japanese work on wavy flow in open channels, and semitheoretical analysis of problem (wave velocities, frequencies, heights, lengths). Mostly small channel slopes considered.
Jaymond (J3), 1961	Experimental absorption of CO ₂ by laminar film of NaOH solution flowing on plate, 4 × 100 cm., slopes 1–15°, countercurrent gas flow. Film thicknesses and surface velocities also measured. Good agreement with theory in absence of waves.
Kaiser (K1), 1961	Distillation in wetted-wall column. Film theory corrected to allow for oscillations of film surface which were observed.
Konobeev <i>et al.</i> (K21), 1961	Experimental study of CO ₂ absorption by water film, with upward and downward cocurrent gas/film flow, inside tubes 1.05–1.66 cm. i.d., 20–87 cm. long. Gas velocities 6–86 m./sec. $N_{Re} = 5$ –105. Length and amplitude of surface ripples and local film thicknesses measured. Rate of mass transfer stated to be function of wave characteristics only.
Lilleleht and Hanratty (L12, L13), 1961	Local film thicknesses (wave profiles) measured in horizontal channel with cocurrent gas stream and interpreted statistically. Effect of interfacial roughness in increasing the interfacial stress also investigated.
Mayer (M7), 1961	Experimental and theoretical study of wavy flow of water in open channel (slopes up to 5°). Data on growth of turbulent spots, local depths, surface velocity, length of entry zone, wave velocities, heights, frequencies, effect of surface-active materials.
Mirev <i>et al.</i> (M11), 1961	Experimental studies of rates of absorption of C ₂ H ₂ , SO ₂ in water films in wetted-wall columns. Experimental results not in agreement with Vyazovov (V8) and penetration theories. Surfactant reduced rippling but appeared to increase interfacial resistance to mass transfer.
Ratcliff and Reid (R2), 1961	Equations set up for flow of liquid film (water) over sphere in presence of second liquid (benzene). Drag taken into account, surface tension neglected. Experimental data on film thicknesses and mass transfer.

Authors and Date	Remarks
Ratcliff and Holdcroft (R1), 1961	Mass transfer into liquid film flowing on sphere with first-order chemical reaction (theory and experiment).
Reinius (R4), 1961	Studies of water flows in open channels at small slopes, $N_{Re} = 50$ –13,000. Data on film thicknesses, film friction factors, effects of wall roughness.
Tailby and Portalski (T3), 1961	Experimental work on the damping of waves on water films flowing on vertical plate 21×84 in. by surface-active materials. Three surfactants used at various concentrations; optimum concentration for damping was observed in each case.
Taylor and Kennedy (T8), 1961	Discussion of onset of wave formation and wave behavior in open-channel flow.
Vouyoucalos (V7), 1961	Experimental study of absorption and desorption of SO_2 by water film in channel of 10×40 cm., slope 25° . Channel floor covered with regular transverse rugosities of large dimensions. Also dye-tracer studies of flow patterns, wave profiles.
Wilke (W2), 1961	Heat transfer to falling films. More detail in later paper (W3).
Zhivafkin and Volgin (Z4), 1961	Review of film flow literature and experimental work on film thicknesses in tube 2×98 cm., $N_{Re} = 150$ –3500, and surface velocities.
Zucrow and Sellars (Z6), 1961	Experimental study of film cooling of rocket motors. Liquids of various N_P used, with and without chemical reaction.
Allen (A3), 1962	Investigation of characteristics of liquid films on vertical surface, with emphasis on surface features. Kapitza theory shown to be applicable only at low flow rates. Increase in interfacial area reported to be smaller than predicted by Portalski theory.
Boyarchuk and Planovskii (B13), 1962	Study of the kinetics of mass transfer in film-type distillation equipment.
Fulford (F7), 1962	Experimental study of countercurrent flow of water film and air stream in channel ($5\frac{1}{2} \times 30$ in.) at slopes 7 – 90° .
Hewitt <i>et al.</i> (H9), 1962	Description of techniques for measuring properties of liquid films and pressure drops in vertical upward co-current flow of gas and film. Numerous data reported for air/water system in $1\frac{1}{4}$ -in. i.d. tube.
Hewitt and Lovegrove (H11), 1962	Data and techniques for continuous film thickness recording in vertical gas/film flow.

Authors and Date	Remarks
Kasimov and Zigmund (K11), 1962	Theoretical treatment of smooth laminar film flow on vertical surface, with and without gas flow, including inertia effects. Nusselt equations (N6, N7) are shown to be special cases of the present solutions.
Konobeev and Zhavoronkov (K22), 1962	Theoretical and experimental studies of pressure drops in gas streams flowing in tubes with wavy walls (long-wave and short-wave roughnesses). Importance to case of flow of gas adjacent to wavy film pointed out.
Laird <i>et al.</i> (L4), 1962	Deals with laminar flow and transition to turbulence in flow along tubes with wavy walls of various wavelengths. Entry effects also studied.
Ratcliff and Reid (R3), 1962	Deals with smooth and rippling flow of a liquid over a sphere or series of spheres, especially with the problem of mixing in the liquid film at the junctions of spheres.
Saveanu <i>et al.</i> (S1), 1962	Determination of $N_{Re_{rit}}$ for film flow is made from measurements of absorption of CO_2 in water film. Effects of wall roughness on $N_{Re_{rit}}$ were also studied.
Saveanu and Tudose (S1a), 1962	Study of onset of flooding in tubes 8–15.8 mm. diameter, 1200 mm. long with downward water films, counter-current air stream of 0.5–12 m. sec. Gas velocity to cause flooding found to depend on liquid flow rate and tube diameter.
Tailby and Portalski (T4), 1962	Experimental determination of wavelengths near point of onset of rippling on films of various liquids flowing on a vertical wall.
Tailby and Portalski (T5), 1962	Experimental determination of the distance of the line of wave inception on a vertical liquid film from the inlet as a function of liquid flow rate, viscosity, and co- and counter-flows of air.
Taylor and Hewitt (T6), 1962	Considers the motion and frequency of large "disturbance" waves in upward cocurrent flow of air and water films.
Wilke (W3), 1962	Extensive survey of flow and heat transfer in liquid films flowing outside tubes. Measurements of temperature and velocity profiles in films of various liquids are reported, and a heat transfer mechanism is proposed.
Wilkes and Nedderman (W4), 1962	Experimental determination of velocity profiles in films flowing on vertical tube by stereoscopic chronophotographic method. Films included glycerol, aqueous glycerol solutions, liquid paraffin, glycerol + surfactant. In smooth flow, profiles agreed with theoretical semi-

Authors and Date	Remarks
	parabola; with waves, profiles scattered about semi-parabola. Entry effects also studied.
Zhivafkin (Z3), 1962	Experimental work on film flow and upward and downward cocurrent gas/film flow (water and aqueous glycerol solutions). Data on onset of flooding and entrainment, effect of gas velocity.
Adorni <i>et al.</i> (A1a), 1963	An instrument is described for measuring the wall shear stress in a two-phase flow in the presence of a pressure gradient and a changing velocity profile.
Andreev (A5a), 1963	Considers stability of laminar flow of viscous incompressible liquid film on vertical wall with respect to infinitesimal disturbances. Absolute instability is not found.
Atkinson and Taylor (A7), 1963	Study of the effect of discontinuities on mass transfer to a liquid film. It is concluded that the mixing effect at discontinuities is a result of ripple action.
Dukler and Wicks (D17), 1963	General review of gas/liquid flow in conduits, including brief consideration of gas/film flows.
Gill <i>et al.</i> (G3), 1963	Experimental study of upward cocurrent flow of air/water system. Data on pressure drop and film thicknesses (and effects of liquid droplet entrainment) as functions of distance from inlet. Effects of waves on film surface considered.
Hewitt <i>et al.</i> (H10), 1963	Numerous data on pressure drops and liquid holdup in vertical upward cocurrent flow of air and water films, and comparisons with published theories.
Hewitt and Lovegrove (H11a), 1963	Measurements are reported of pressure gradient, holdup, film thicknesses in vertical, upward, cocurrent air/water streams in a tube of 1.25 in. diameter. Film thicknesses by three measurement methods are compared.
Kasimov and Zigmund (K12), 1963	General solution is given to equations of wavy film flow (with corrected continuity equation), using simple parabolic or higher approximation to velocity profile at given plane. It is shown that the film thickness and wave amplitude should increase in direction of flow. Effect of channel slope also considered.
Nedderman and Shearer (N1a), 1963	Deals with the motion and frequency of large disturbance waves in upward cocurrent flow of air and water film, extending work of Taylor and Hewitt (T6).

Authors and Date	Remarks
Niebergall (N1), 1963	Deals with the effects of changes of surface tension during heat and mass transfer in wetted-wall equipment.
Norman and Sammak (N5), 1963	Deals with effects of mixing on rates of mass transfer to a liquid film flowing over packing elements.
Portalski (P4), 1963	Theories of film flow and methods of measuring film thickness are reviewed. Film thicknesses on vertical plate (zero gas flow) reported for glycerol solutions, methanol, isopropanol, water, and aqueous solutions of surfactants. Results compared with values calculated by Nusselt, Kapitza, and corrected Dukler and Bergelin treatments.
Scott (S4), 1963	General survey of cocurrent gas/liquid flows, including gas/film flows.
Tadaki and Maeda (T1), 1963	Experimental study of absorption of CO_2 in downward cocurrent gas/film flow, and comparison with various theories.
Taylor <i>et al.</i> (T7), 1963	Study of large "disturbance" waves in upward cocurrent flow of air and water film in vertical tubes. A "preferred" wave velocity is reported.
Yih (Y2), 1963	A general consideration (theoretical) of the stability of film flow down an inclined plane, including the cases of long and short waves and small N_{Re} . Results for long waves are in agreement with theory of Benjamin (B5). The effects of surface tension and viscosity on stability are discussed.
Portalski (P5), 1964	From Kapitza's theory of wavy film flow, it is shown that regions of reversed flow exist under the wave troughs, leading to the generation of circulating eddies which may explain the increased rates of heat and mass transfer to wavy laminar films.
Zhivalkin and Volgin (Z4a), 1964	Considers pressure drop in downward cocurrent flow of air and films of water, glycerol solutions, water + surfactant, in tubes of diameter 12.9 mm., lengths 150-830 mm. Air velocities 3-45 m./sec. Conditions for droplet entrainment from film also reported.

REFERENCES

- A1. Adorni, N., Casagrande, I., Cravarolo, L., Hassid, A., and Silvestri, M., "Experimental Data on Two-phase Adiabatic Flow: Liquid Film Thickness, Phase and Velocity Distribution, Pressure Drops in Vertical Gas-Liquid Flow". Centro Informazioni Studi Esperienze, Milan, Report R-35, March 1961.

- A1a. Adorni, N., Cravarolo, L., Hassid, A., Pedrocchi, E., and Silvestri, M., *Rev. Sci. Instr.* **34**, 937 (1963).
- A2. Alimov, R. Z., *Dokl. Akad. Nauk SSSR* **109**, 559 (1956).
- A3. Allen, J. M., Some studies of falling liquid films. Ph.D. thesis, Manchester Coll. Sci. and Technology, England, 1962.
- A4. Anderson, G. H., Haselden, G. G., and Mantzouranis, B. G., *Chem. Eng. Sci.* **16**, 222 (1961).
- A5. Anderson, G. H., and Mantzouranis, B. G., *Chem. Eng. Sci.* **12**, 109 (1960).
- A5a. Andreev, A. F., *Zh. Eksperim. i Teor. Fiz.* **45**, 755 (1963).
- A6. Asbjørnsen, O. A., *Chem. Eng. Sci.* **14**, 211 (1961).
- A7. Atkinson, B., and Taylor, B. N., *Trans. Inst. Chem. Engrs. (London)* **41**, 140 (1963).
- B1. Bauer, W. J., *Trans. Am. Soc. Civil Engrs.* **119**, 1212 (1954).
- B2. Bays, G. S., and McAdams, W. H., *Ind. Eng. Chem.* **29**, 1240 (1937).
- B3. Beda, G. A., *Zh. Prikl. Mekhan. i Tekhn. Fiz.* No. 3, 110 (1961).
- B4. Belkin, H. H., MacLeod, A. A., Monrad, C. C., and Rothfus, R. R., *A.I.Ch.E. (Am. Inst. Chem. Engrs.) J.* **5**, 245 (1959).
- B5. Benjamin, T. B., *J. Fluid Mech.* **2**, 554 (1957).
- B6. Benjamin, T. B., *J. Fluid Mech.* **10**, 401 (1961).
- B7. Benjamin, T. B., private communication, 1961.
- B8. Bennett, J. A. R., and Thornton, J. D., *Trans. Inst. Chem. Engrs. (London)* **39**, 101 (1961).
- B9. Binnie, A. M., *J. Fluid Mech.* **2**, 551 (1957).
- B10. Binnie, A. M., *J. Fluid Mech.* **5**, 561 (1959).
- B11. Bird, R. B., Stewart, W. E., and Lightfoot, E. N., "Transport Phenomena." Wiley, New York, 1960.
- B12. Black, R. H., *Trans. Am. Soc. Civil Engrs.* **126** (Pt. I), 88 (1961).
- B13. Boyarchuk, P. G., and Planovskii, A. N., *Khim. Prom.* No. 3, 195 (1962).
- B14. Brauer, H., Strömung und Wärmeübergang bei Rieselfilmen. *VDI (Ver. Deut. Ingr.)-Forschungsheft* **457** (1956).
- B15. Brauer, H., *Kaeltetechnik* **9**, 274 (1957).
- B16. Brauer, H., *Chem.-Ing.-Tech.* **30**, 75 (1958).
- B17. Brauer, H., *Forsch. Gebiete Ingenieurw.* **24**, 105 (1958).
- B18. Brauer, H., *Chem.-Ing.-Tech.* **32**, 719 (1960).
- B19. Bressler, R., *VDI (Ver. Deut. Ingr.) Z.* **100**, 630 (1958).
- B20. Bressler, R., Untersuchung des Wärmeüberganges in einem Dünnschichtverdampfer. *Forschungsber. Landes Nordrhein-Westfalen* **770** (1960).
- B21. Brötz, W., *Chem.-Ing.-Tech.* **26**, 470 (1954).
- B22. Bushmanov, V. K., *Zh. Eksperim. i Teor. Fiz.* **39**, 1251 (1960); English transl.: *Soviet Phys.-JETP*, **12**, 873 (1961).
- C1. Calvert, S., Vertical, upward, annular, two-phase flow in smooth tubes. Ph.D. thesis, Univ. Michigan, Ann Arbor, Michigan, 1952.
- C2. Calvert, S., and Williams, B., *A.I.Ch.E. (Am. Inst. Chem. Engrs.) J.* **1**, 78 (1955).
- C3. Carpenter, E. F., and Colburn, A. P., "Proc. General Discussion on Heat Transfer Problems," p. 20. Inst. Mech. Engrs., London, 1951.
- C4. Charvonia, D. A., A study of the mean thickness of liquid films and surface characteristics in annular two-phase flow in a vertical pipe. Purdue Univ., Lafayette, Indiana, Jet Propulsion Lab., Rept. I-59-1, May 1959.
- C5. Chawla, M. J., *Kaeltetechnik* **12**, 96 (1960).

- C6. Chew, J.-N., Liquids in free fall on a solid surface. Ph.D. thesis, Univ. Texas, Austin, Texas, 1953.
- C7. Chien, S.-F., An experimental investigation of the liquid film structure and pressure drop of vertical, downward, annular, two-phase flow. Ph.D. thesis, Univ. Minnesota, Minneapolis, Minnesota, 1961.
- C8. Chow, V. T., "Open Channel Hydraulics." McGraw-Hill, New York, 1959.
- C9. Chwang, C. T., M.S. thesis, Mass. Inst. Technol., Cambridge, Massachusetts, 1928; data reported by (C15).
- C10. Claassen, H., *Centr. Zuckerind.* **26**, 497 (1918).
- C11. Clayton, C. G. A., The behaviour of liquid films in countercurrent two-phase flow. Ph.D. thesis, Gonville & Caius College, Cambridge, England, 1958.
- C12. Colburn, A. P., "Proc. General Discussion on Heat Transfer Problems," p. 1. Inst. Mech. Engrs, London, 1951.
- C13. Collier, J. G., and Hewitt, G. F., *Trans. Inst. Chem. Engrs. (London)* **39**, 127 (1961).
- C14. Collins, D. E., Co-current gas absorption. Ph.D. thesis, Purdue Univ., Lafayette, Indiana, 1958.
- C15. Cooper, C. M., Drew, T. B., and McAdams, W. H., *Trans. Am. Inst. Chem. Engrs.* **30**, 158 (1934); *Ind. Eng. Chem.* **26**, 428 (1934).
- C16. Cornish, R. J., *Proc. Roy. Soc. A* **120**, 691 (1928).
- C17. Craya, A., *Natl. Bur. Std. (U. S.) Circ.* **521**, 141-151 (1952).
- D1. Davidson, J. F., and Cullen, E. J., *Trans. Inst. Chem. Engrs. (London)* **35**, 51 (1957).
- D2. Davidson, J. F., Cullen, E. J., Hanson, D., and Roberts, D., *Trans. Inst. Chem. Engrs. (London)* **37**, 122 (1959).
- D3. Davidson, J. F., and Howkins, J. E., *Proc. Roy. Soc. A* **240**, 29 (1957).
- D4. Davies, J. T., *Trans. Inst. Chem. Engrs. (London)* **38**, 289 (1960).
- D5. Davies, J. T., *Birmingham Univ. Chem. Engr.* **12**, 5 (1961).
- D5a. Davies, J. T., Fundamental Thought in Chemical Engineering. Inaugural Lecture, Univ. Birmingham, Nov. 3, 1961. Obtainable from the Publications Officer, Univ. of Birmingham, England.
- D6. Davies, J. T., and Rideal, E. K., "Interfacial Phenomena." Academic Press, New York, 1961.
- D7. Deissler, R. G., Analysis of turbulent heat transfer, mass transfer and friction in smooth tubes at high Prandtl and Schmidt numbers. NACA Rep. 1210 (1955).
- D8. Dmitriev, A. A., and Bonchkovskaya, T. V., *Dokl. Akad. Nauk SSSR* **91**, 31 (1953).
- D9. Dressler, R. F., *Commun. Pure Appl. Math.* **2**, 149 (1949).
- D10. Dressler, R. F., *Natl. Bur. Std. (U. S.) Circ.* **521**, 237-241 (1952).
- D11. Dressler, R. F., and Pohle, F. V., *Commun. Pure Appl. Math.* **6**, 93 (1953).
- D12. Dukler, A. E., *Chem. Eng. Progr.* **55** (10), 62 (1959); Appendix as Auxiliary Documentation Institute Microfilm No. 6058, U.S. Library of Congress, Washington, D.C., 1959.
- D13. Dukler, A. E., *Chem. Engr. Progr. Symp. Ser.* **30**, 1-10 (1960).
- D14. Dukler, A. E., *Petrol. Engr. Management* **33** (9), 198 (1961); **33** (11), 222 (1961).
- D15. Dukler, A. E., *ARS (Am. Rocket Soc.) J.* **31**, 86 (1961).
- D16. Dukler, A. E., and Bergelin, O. P., *Chem. Eng. Progr.* **48**, 557 (1952).
- D17. Dukler, A. E., and Wicks, M., in "Modern Chemical Engineering" (A. Acrivos, ed.), Vol. I, pp. 349-435. Reinhold, New York, 1963.

- E1. Eckert, E. R. G., Diaguila, A. J., and Donoughe, P. L., Experiments on turbulent flow through channels having porous rough surfaces with or without air injection. NACA Tech. Note 3339 (1955).
- E2. Ellis, S. R. M., and Betts, R. A., *Birmingham Univ. Chem. Engr.* **13**, 38 (1962).
- E3. Ellis, S. R. M., and Gay, B., *Trans. Inst. Chem. Engrs. (London)* **37**, 206 (1959).
- E4. Emmert, R. E., and Pigford, R. L., *Chem. Eng. Progr.* **50**, 87 (1954).
- E5. Escoffier, F. F., *Trans. Am. Soc. Civil Engrs.* **126** (Pt. I), 535 (1961).
- F1. Fallah, A., Hunter, T. G., and Nash, A. W., *J. Soc. Chem. Ind. (London)* **53**, 369T (1934).
- F2. Feind, K., Strömungsuntersuchungen bei Gegenström von Rieselfilmen und Gas in lotrechten Rohren, *VDI (Ver. Deut. Ingr.)-Forschungsh.* **481** (1960).
- F3. Feldman, S., *J. Fluid Mech.* **2**, 343 (1957).
- F4. Fradkov, A. B., *Kislod 4* (2), 16, (1947).
- F5. Friedman, S. J., and Miller, C. O., *Ind. Eng. Chem.* **33**, 889 (1941).
- F6. Fulford, G. D., *Birmingham Univ. Chem. Engr.* **11**, 23 (1960).
- F7. Fulford, G. D., Gas-liquid flow in an inclined channel. Ph.D. thesis, Univ. Birmingham, England, 1962.
- G1. Garwin, L., and Kelly, E. W., *Ind. Eng. Chem.* **47**, 392 (1955).
- G2. Gay, B., Studies in interfacial shear. Ph.D. thesis, Univ. Birmingham, England, 1958.
- G3. Gill, L. E., Hewitt, G. F., Hitchon, J. W., and Lacey, P. M. C., *Chem. Eng. Sci.* **18**, 525 (1963).
- G4. Glaser, H., *Journées Internat. Transmission Chaleur*, **1**, 1961, 567-578. Institut Français des Combustibles et de l'Énergie Paris (1962).
- G5. Gossage, W., British Patent 7267 (Dec. 24, 1836).
- G6. Graebel, W. P., *J. Fluid Mech.* **8**, 321 (1960).
- G7. Greenberg, A. B., The mechanics of film flow on a vertical surface. Ph.D. thesis, Purdue Univ., Lafayette, Indiana, 1956.
- G8. Grigull, U., *Forsch. Gebiete Ingenieurw.* **13**, 49 (1942).
- G9. Grigull, U., *Forsch. Gebiete Ingenieurw.* **18**, 10 (1952).
- G10. Grimley, S. S., *Trans. Inst. Chem. Engrs. (London)* **23**, 228 (1945).
- G11. Grimley, S. S., Effects of liquid flow conditions on the performance of packed towers. Ph.D. thesis, Univ. London, England, 1947.
- H1. Hama, F. R., *Soc. Naval Architects Marine Engrs. Trans.* **62**, 333 (1954).
- H2. Hanratty, T. J., and Hershman, A., *A.I.Ch.E. (Am. Inst. Chem. Engrs.) J.* **7**, 488 (1961).
- H3. Hatta, S., *J. Soc. Chem. Ind. Japan* **37**, 275B, (1934).
- H4. Hatta, S., and Katori, M., *J. Soc. Chem. Ind. Japan* **37**, 280B (1934).
- H5. Heartinger, D. J., Mass transfer in falling liquid layers. D.Sc. thesis, Washington Univ., St. Louis, Missouri, 1960.
- H6. Hershman, A., The effect of liquid properties on the interaction between a turbulent air stream and a flowing liquid film. Ph.D. thesis, Univ. Illinois, Urbana, Illinois, 1960.
- H7. Hewitt, G. F., Analysis of annular two-phase flow: application of the Dukler analysis to vertical upward flow in a tube. *At. Energy Res. Estab. (Gt. Brit.) Harwell AERE-R 3680* (1961).
- H8. Hewitt, G. F., King, I., and Lovegrove, P. C., Holdup and pressure drop measurements in the two-phase annular flow of air-water mixtures. *At. Energy Res. Estab. (Gt. Brit.) Harwell AERE-R 3764* (1961).

- H9. Hewitt, G. F., King, R. D., and Lovegrove, P. C., Techniques for liquid film and pressure drop studies in annular two-phase flow. *At. Energy Res. Estab. (Gt. Brit.) Harwell AERE-R 3921* (1962).
- H10. Hewitt, G. F., King, I., and Lovegrove, P. C., *Brit. Chem. Eng.* **8**, 311 (1963).
- H11. Hewitt, G. F., and Lovegrove, P. C., The application of the light-absorption technique to continuous film thickness recording in annular two-phase flow. *At. Energy Res. Estab. (Gt. Brit.) Harwell AERE-R 3953* (1962).
- H11a. Hewitt, G. F., and Lovegrove, P. C., Comparative film thickness and holdup measurements in vertical annular flow. *At. Energy Res. Estab. (Gt. Brit.) Harwell, Memo M-1203* (1963).
- H12. Hikita, H., *Chem. Eng. (Tokyo)* **23**, 23 (1959).
- H13. Hikita, H., and Nakanishi, K., *Chem. Eng. (Tokyo)* **23**, 513 (1959).
- H14. Hikita, H., Nakanishi, K., and Asai, S., *Chem. Eng. (Tokyo)* **23**, 28 (1959).
- H15. Hikita, H., Nakanishi, K., and Kataoka, T., *Chem. Eng. (Tokyo)* **23**, 459 (1959).
- H16. Holmes, W. H., *Civil Eng.* **6**, 467 (1936).
- H17. Hoogendoorn, C. J., *Chem. Eng. Sci.* **9**, 205 (1959).
- H18. Hopf, L., *Ann. Physik* [4] **32**, 777 (1910).
- H19. Horton, R. E., Leach, H. R., and van Vliet, R., *Trans. Am. Geophys. Union* **15**, 393 (1934).
- H20. Howkins, J. E., and Davidson, J. F., *Chem. Eng. Sci.* **7**, 235 (1958).
- H21. Rodney Hunt Machine Co., "Mechanically Aided Thermal Processing with the Turba-Film Processor." Orange, Massachusetts, 1958.
- I1. Ishihara, T., Iwagaki, Y., and Ishihara, Y., *Mem. Fac. Eng. Kyoto Univ.* **14**, 83 (1952).
- I2. Ishihara, T., Iwagaki, Y., and Iwasa, Y., *Trans. Am. Soc. Civil Engrs.* **126** (Pt. I), 548 (1961).
- I3. Iwagaki, Y., *Mem. Fac. Eng. Kyoto Univ.* **13**, 139 (1951).
- I4. Iwasa, Y., *Mem. Fac. Eng. Kyoto Univ.* **16**, 264 (1954).
- J1. Jackson, M. L., *A.I.Ch.E. (Am. Inst. Chem. Engrs.) J.* **1**, 231 (1955).
- J2. Jackson, M. L., Johnson, R. T., and Ceaglske, N. H., *Proc. 1st Midwestern Conf. Fluid Dynamics, Urbana, Illinois, 1950*, pp. 226-236. J. W. Edwards, Ann Arbor, Michigan (1951).
- J3. Jaymond, M., *Chem. Eng. Sci.* **14**, 126 (1961).
- J4. Jeffreys, H., *Phil. Mag.* [6] **49**, 793 (1925).
- K1. Kaiser, L., *Intern. J. Heat Mass Transfer* **3**, 175 (1961).
- K2. Kamei, S., and Oishi, J., *Chem. Eng. (Tokyo)* **18**, 421 (1954).
- K3. Kamei, S., and Oishi, J., *Mem. Fac. Eng. Kyoto Univ.* **17**, 277 (1955).
- K4. Kamei, S., and Oishi, J., *Mem. Fac. Eng. Kyoto Univ.* **18**, 1 (1956).
- K5. Kamei, S., Oishi, J., Iijima, H., Kawamura, M., and Itoi, M., *Chem. Eng. (Tokyo)* **18**, 545 (1954).
- K6. Kamei, S., Oishi, J., and Okane, T., *Chem. Eng. (Tokyo)* **18**, 364 (1954).
- K7. Kapitsa, P. L., *Zh. Eksperim. i Teor. Fiz.* **18**, 3 (1948).
- K8. Kapitsa, P. L., *Zh. Eksperim. i Teor. Fiz.* **18**, 19 (1948).
- K9. Kapitsa, P. L., *Zh. Eksperim. i Teor. Fiz.* **21**, 964 (1951).
- K10. Kapitsa, P. L., and Kapitsa, S. P., *Zh. Eksperim. i Teor. Fiz.* **19**, 105 (1949).
- K11. Kasimov, B. S., and Zigmund, F. F., *Inzh. Fiz. Zh. Akad. Nauk Belorussk.* **5** (4), 71 (1962).
- K12. Kasimov, B. S., and Zigmund, F. F., *Inzh. Fiz. Zh. Akad. Nauk Belorussk.* **6** (11), 70 (1963).
- K13. Keulegan, G. H., *J. Res. Natl. Bur. Stds.* **21**, 707 (1938).

- K14. Keulegan, G. H., in "Engineering Hydraulics" (H. Rouse, ed.), pp. 711-768. Wiley, New York, 1950.
- K15. Keulegan, G. H., *J. Res. Natl. Bur. Stds.* **46**, 358 (1951).
- K16. Keulegan, G. H., and Patterson, G. W., *Trans. Am. Geophys. Union* 594 (1940).
- K17. Kirkbride, C. G., *Trans. Am. Inst. Chem. Engrs.* **30**, 170 (1934); *Ind. Eng. Chem.* **26**, 425 (1934).
- K18. Knuth, E. L., *Jet Propulsion* **24**, 359 (1954).
- K19. Konobeev, B. I., Malyusov, V. A., and Zhavoronkov, N. M., *Khim. Prom.* No. 3, 38 (1957).
- K20. Konobeev, B. I., Malyusov, V. A., and Zhavoronkov, N. M., *Dokl. Akad. Nauk SSSR* **117**, 671 (1957).
- K21. Konobeev, B. I., Malyusov, V. A., and Zhavoronkov, N. M., *Khim. Prom.* No. 7, 475 (1961).
- K22. Konobeev, B. I., and Zhavoronkov, N. M., *Intern. Chem. Eng.* **2**, 431 (1962).
- K23. Kosterin, S. I., and Shel'nikov, B. I., *Teploenerg.* No. 6, 71 (1958).
- K24. Kramers, H., and Kreyger, P. J., *Chem. Eng. Sci.* **6**, 42 (1956).
- K25. Kutateladze, S. S., and Styrikovich, M. A., "Hydraulics of Gas-Liquid Systems." Gosénergoizdat, Moscow, 1958; translated by U.S. Dept. Commerce, Office Tech. Serv., Washington, D.C., 1960.
- L1. Labuntsov, D. A., *Teploenerg.* No. 12, 47 (1956).
- L2. Labuntsov, D. A., *Teploenerg.* No. 7, 72 (1957).
- L3. Laird, A. D. K., *Trans. Am. Soc. Mech. Engrs.* **76**, 1005 (1954).
- L4. Laird, A. D. K., Brunner, R. K., and Haughton, K. E., *J. Hydraulics Div. Am. Soc. Civ. Engrs.* **88** (HY1), 1 (1962).
- L5. Lamb, H., "Hydrodynamics," 6th ed. Oxford Univ. Press, London and New York, 1932.
- L6. Levich, V. G., *Zh. Eksperim. i Teor. Fiz.* **10**, 1296 (1940).
- L7. Levich, V. G., *Zh. Eksperim. i Teor. Fiz.* **11**, 340 (1941).
- L8. Levich, V. G., *Zh. Fiz. Khim.* **22**, 721 (1948).
- L9. Levich, V. G., "Fiziko-khimicheskaya Gidrodinamika," 2nd ed. Fizmatgiz, Moscow, 1959; English translation published as "Physico-Chemical Hydrodynamics." Prentice-Hall, Englewood Cliffs, New Jersey, 1962.
- L10. Lighthill, M. J., in "First Symposium on Naval Hydrodynamics," Sept. 24-28, 1956, Washington, D.C., pp. 17-40, Publication No. 515. National Academy of Sciences—National Research Council, Washington, D.C. 1957.
- L11. Lighthill, M. J., and Whitham, G. B., *Proc. Roy. Soc.* **A229**, 281 (1955).
- L12. Lilleleht, L. U., and Hanratty, T. J., *A.I.Ch.E. (Am. Inst. Chem. Engrs.) J.* **7**, 548 (1961).
- L13. Lilleleht, L. U., and Hanratty, T. J., *J. Fluid Mech.* **11**, 65 (1961).
- L14. Lynn, S., *A.I.Ch.E. (Am. Inst. Chem. Engrs.) J.* **6**, 703 (1960).
- L15. Lynn, S., Straatemeier, J. R., and Kramers, H., *Chem. Eng. Sci.* **4**, 49 (1955).
- L16. Lynn, S., Straatemeier, J. R., and Kramers, H., *Chem. Eng. Sci.* **4**, 59 (1955).
- L17. Lynn, S., Straatemeier, J. R., and Kramers, H., *Chem. Eng. Sci.* **4**, 64 (1955).
- M1. McAdams, W. H., Drew, T. B., and Bays, G. S., *Trans. Am. Soc. Mech. Engrs.* **62**, 627 (1940).
- M2. MacLeod, A. A., Liquid turbulence in a gas-liquid system. Ph.D. thesis, Carnegie Inst. Technol., Pittsburgh, Pennsylvania, 1951.
- M3. McManus, H. N., *Proc. Sixth Midwestern Conf. Fluid Mech. Austin, Texas, 1959* pp. 292-302. Univ. Texas Press, Austin, Texas.
- M4. McManus, H. N., *ARS (Am. Rocket Soc.) J.* **29**, 144 (1959).

- M5. Mahrenholtz, O., *Kaeltechnik* **10**, 150 (1958).
- M6. Malyusov, V. A., Umnik, N. N., and Zhavoronkov, N. M., *Dokl. Akad. Nauk SSSR* **105**, 779 (1955); **106**, 1057 (1955).
- M7. Mayer, P. G., *J. Hydraulics Div. Am. Soc. Civil Engrs.* **85** (HY7), 99 (1959).
- M8. Mazyukovich, I. V., *Kholodil'n. Tekhn., Tr. Leningr. Tekhnol. Inst. Kholodil'n. Prom.* **11**, 115 (1956).
- M9. Michalik, E. R., *A.I.Ch.E. (Am. Inst. Chem. Engrs.) J.* **3**, 276 (1957).
- M10. Miles, J. W., *J. Fluid Mech.* **8**, 593 (1960).
- M11. Mirev, D., Elenkov, D., and Balarev, K., *Compt. Rend. Acad. Bulgare Sci.* **14**, 263 (1961).
- M12. Monrad, C. C., and Badger, W. L., *Ind. Eng. Chem.* **22**, 1103 (1930).
- N1. Niebergall, W., *Chem.-Ing.-Tech.* **35**, 555, 627 (1963).
- N1a. Nedderman, R. M., and Shearer, C. J., *Chem. Eng. Sci.* **18**, 661 (1963).
- N2. Nikolaev, A. P., *Zh. Prikl. Khim.* **31**, 711 (1958).
- N3. Norman, W. S., and Binns, D. T., *Trans. Inst. Chem. Engrs. (London)* **38**, 294 (1960).
- N4. Norman, W. S., and McIntyre, V., *Trans. Inst. Chem. Engrs. (London)* **38**, 301 (1960).
- N5. Norman, W. S., and Sammak, F. Y. Y., *Trans. Inst. Chem. Engrs. (London)* **41**, 117 (1963).
- N6. Nusselt, W., *VDI (Ver. Deut. Ingr.) Z.* **60**, 549, 569 (1916).
- N7. Nusselt, W., *VDI (Ver. Deut. Ingr.) Z.* **67**, 206 (1923).
- O1. Owen, W. M., *Trans. Am. Soc. Civil Engrs.* **119**, 1157 (1954).
- P1. Pennie, A. M., and Belanger, J.-Y., *Can. J. Technol.* **30**, 9 (1952).
- P2. Poocha, A., *Chem.-Ing.-Tech.* **30**, 648 (1958).
- P3. Portalski, S., The mechanism of flow in wetted wall columns. Ph.D. thesis, Univ. London, England, 1960.
- P4. Portalski, S., *Chem. Eng. Sci.* **18**, 787 (1963); **19**, 575 (1964).
- P5. Portalski, S., *Ind. Eng. Chem. Fundamentals* **3**, 49 (1964).
- R1. Ratcliff, G. A., and Holdcroft, J. G., *Chem. Eng. Sci.* **15**, 100 (1961).
- R2. Ratcliff, G. A., and Reid, K. J., *Trans. Inst. Chem. Engrs. (London)* **39**, 423 (1961).
- R3. Ratcliff, G. A., and Reid, K. J., *Trans. Inst. Chem. Engrs. (London)* **40**, 69 (1962).
- R4. Reinius, E., "Steady uniform flow in open channels," *Trans. Roy. Inst. Technol. Stockholm* **179** (1961).
- S1. Saveanu, T., Ibanescu, I., and Vasiliu, M., *Rev. Chim. (Bucharest)* **13**, 589 (1962).
- S1a. Saveanu, T., and Tudose, R., *Bul. Inst. Politeh. Iasi* **8**, 141 (1962).
- S2. Schmidt, E., Schurig, W., and Sellschopp, W., *Tech. Mech. Thermodyn.* **1**, 53 (1930).
- S3. Schoklitsch, A., *Sitzber. Akad. Wiss. Wien, Math.-Naturw. Kl. Abt. IIa* **129**, 895 (1920).
- S4. Scott, D. S., *Advan. Chem. Eng.* **4**, 199 (1963).
- S5. Scriven, L. E., and Pigford, R. L., *A.I.Ch.E. (Am. Inst. Chem. Engrs.) J.* **4**, 382 (1958).
- S6. Semenov, P. A., *Zh. Tekhn. Fiz.* **14**, 427 (1944).
- S7. Semenov, P. A., *Zh. Tekhn. Fiz.* **20**, 980 (1950).
- S8. Sexauer, T., *Forsch. Gebiete Ingenieurw.* **10**, 286 (1939).

- S9. Sherwood, T. K., and Pigford, R. L., "Absorption and Extraction," 2nd ed. McGraw-Hill, New York, 1952.
- S10. Shibuya, I., *Rept. Inst. High Speed Mech., Tohoku Univ.* **1**, 17 (1951).
- S11. Shiotsuka, T., Honda, N., and Ohata, Y., *Chem. Eng. (Tokyo)* **21**, 702 (1957).
- S12. Stirba, C., and Hurt, D. M., *A.I.Ch.E. (Am. Inst. Chem. Engrs.) J.* **1**, 178 (1955).
- S13. Strang, L. C., Hunter, T. G., and Nash, A. W., *Ind. Eng. Chem.* **29**, 278 (1937).
- T1. Tadaki, T., and Maeda, S., *Chem. Eng. (Tokyo)*, **27**, 66 (1963).
- T2. Tailby, S. R., and Portalski, S., *Trans. Inst. Chem. Engrs. (London)* **38**, 324 (1960).
- T3. Tailby, S. R., and Portalski, S., *Trans. Inst. Chem. Engrs. (London)* **39**, 328 (1961).
- T4. Tailby, S. R., and Portalski, S., *Trans. Inst. Chem. Engrs. (London)* **40**, 114 (1962).
- T5. Tailby, S. R., and Portalski, S., *Chem. Eng. Sci.* **17**, 283 (1962).
- T6. Taylor, N. H., and Hewitt, G. F., The motion and frequency of large disturbance waves in annular two-phase flow of air-water systems. *At. Energy Res. Estab. (Gt. Brit.) Harwell AERE-R 3952* (1962).
- T7. Taylor, N. H., Hewitt, G. F., and Lacey, P. M. C., *Chem. Eng. Sci.* **18**, 537 (1963).
- T8. Taylor, R. H., and Kennedy, J. F., *Trans. Am. Soc. Civil Engrs.* **126** (Pt. I), 541 (1961).
- T9. Ternovskaya, A. N., and Belopol'skiĭ, A. P., *Zh. Fiz. Khim.* **24**, 43 (1950).
- T10. Ternovskaya, A. N., and Belopol'skiĭ, A. P., *Zh. Fiz. Khim.* **24**, 981 (1950).
- T11. Ternovskaya, A. N., and Belopol'skiĭ, A. P., *Zh. Fiz. Khim.* **26**, 1090 (1952).
- T12. Ternovskaya, A. N., and Belopol'skiĭ, A. P., *Zh. Fiz. Khim.* **26**, 1097 (1952).
- T13. Thomas, H. A., *Iowa Univ., Coll. Eng. Studies, Bull.* **20**, 214-229 (1940).
- T14. Thomas, W. J., and Portalski, S., *Ind. Eng. Chem.* **50**, 1081 (1958).
- T15. Tinney, E. R., and Bassett, D. L., *J. Hydraulics Div. Am. Soc. Civil Engrs.* **87** (HY5), 117 (1961).
- T16. Treybal, R. E., and Work, L. T., *Trans. Am. Inst. Chem. Engrs.* **38**, 203 (1942).
- T17. Tsien, H.-S., *Aeron. Dig.* **60** (3), 120 (1950).
- V1. van Rossum, J. J., *Chem. Eng. Sci.* **11**, 35 (1959).
- V2. Vedernikov, V. V., *Compt. Rend. Acad. Sci. URSS* **52**, 207 (1946).
- V3. Verschoor, H., *Trans. Inst. Chem. Engrs. (London)* **16**, 66 (1938).
- V4. Viparelli, M., *Houille Blanche* **16**, 857 (1961).
- V5. Vivian, J. E., and Peaceman, D. W., *A.I.Ch.E. (Am. Inst. Chem. Engrs.) J.* **2**, 437 (1956).
- V6. von Kármán, T., *Trans. Am. Soc. Mech. Engrs.* **61**, 705 (1939).
- V7. Vouyoucalos, S., Effect of surface roughness and hydrolysis on mass transfer. M.Sc. thesis, Univ. Birmingham, England, 1961.
- V8. Vyazovov, V. V., *Zh. Tekhn. Fiz.* **18**, 1519 (1940).
- V9. Vyazovov, V. V., *Khim. Prom.* No. 12, 14 (1940).
- W1. Warden, C. P., M.S. thesis, Mass. Inst. Technol., Cambridge, Massachusetts, 1930; data given by (C15).
- W2. Wilke, W., *Kaeltechnik* **13**, 339 (1961).
- W3. Wilke, W., Wärmeübergang an Rieselfilme, *VDI (Ver. Deut. Ingr.)-Forschungsh.* **490** (1962).
- W4. Wilkes, J. O., and Nedderman, R. M., *Chem. Eng. Sci.* **17**, 177 (1962).

- W5. Wint, A., *Mass transfer in packed towers*. Ph.D. thesis, Cambridge Univ., Cambridge, England, 1960.
- Y1. Yih, C.-S., *Proc. 2nd U.S. Natl. Congr. Appl. Mech. 1954* pp. 623-628. American Society of Mechanical Engineers. New York (1955).
- Y2. Yih, C.-S., *Phys. Fluids* **6**, 321 (1963).
- Y3. Yuan, S. W., in "Turbulent Flows and Heat Transfer" (C. C. Lin, ed.), Vol. V, pp. 428-429. Oxford Univ. Press, London and New York, 1959.
- Z1. Zaitsev, A. A., *Dokl. Akad. Nauk SSSR* **130**, 1228 (1960).
- Z2. Zhavoronkov, N. M., Malyusov, V. A., and Malafeev, N. A., *Khim. Prom.* No. 8, 240 (1951).
- Z3. Zhivaikin, L. Ya., *Intern. Chem. Eng.* **2**, 337 (1962).
- Z4. Zhivaikin, L. Ya., and Volgin, B. V., *Zh. Prikl. Khim.* **34**, 1236 (1961).
- Z4a. Zhivaikin, L. Ya., and Volgin, B. V., *Intern. Chem. Eng.* **4**, 80 (1964).
- Z5. Zotikov, I. A., and Bronskii, L. N., *Inzh. Fiz. Zh. Akad. Nauk Belorussk.* **5** (4), 10 (1962).
- Z6. Zucrow, M. J., and Sellers, J. P., *A.R.S. (Am. Rocket Soc.) J.* **31**, 668 (1961)

SEGREGATION IN LIQUID-LIQUID DISPERSIONS AND ITS EFFECT ON CHEMICAL REACTIONS

K. Rietema

Department of Chemical Engineering
Technical University
Eindhoven, Netherlands

I. Introduction.....	237
A. Segregation in Homogeneous Systems.....	237
B. Segregation in Dispersed Phase Systems.....	239
C. Interaction in the Dispersed Phase.....	240
D. Influence of Segregation on the Conversion Rate of Chemical Reactions..	242
II. The Effect of Segregation on the Kinetics of a Liquid-Liquid Two-Phase Chemical Reaction.....	243
A. Chemical Reaction in a Continuous Stirred Tank Reactor.....	243
B. Segregation and Mass Transfer Limitation.....	258
C. Effect of Drop Size Distribution.....	265
III. Partial Segregation. Theory of Finite Interaction Rate. Models for Interaction in the Dispersed Phase.....	270
A. Homogeneous Interaction Model.....	271
B. Dead-Corner Interaction Model.....	275
C. Circulation Interaction Model.....	280
D. Harada Interaction Model.....	282
IV. Measurements of the Interaction Rate.....	283
A. Measurements by Means of a Chemical Reaction.....	284
B. Measurements by Pure Physical Means.....	288
V. Discussion about the Interaction Rate.....	291
A. The Church-Shinnar Criterium.....	291
B. The Collision Rate p_0	293
C. The Coalescing Chance P	295
VI. Concluding Remarks.....	299
Nomenclature.....	299
References.....	301

I. Introduction

A. SEGREGATION IN HOMOGENEOUS SYSTEMS

The effect of residence time and residence time distribution on the conversion and selectivity obtained in chemical reactors is well known, as

well as the fact that residence time distribution alone is not enough to calculate the chemical conversion unless the chemical order of reaction is equal to one. This was beautifully shown by Kramers (K1) in his introduction, "Physical Factors in Chemical Reaction Engineering," to the first European symposium on this subject, held at Amsterdam in 1957. Kramers compared three different reactor systems which, however, had the same residence time distribution:

- (a) a system consisting of a great number of parallel streams which do not intermix,
- (b) a piston flow reactor followed by an ideal mixer,
- (c) an ideal mixer followed by a piston flow reactor.

For second-order reactions, the conversion obtained in these systems at the same average residence time decreases in the direction as mentioned. For chemical reactions of an order smaller than one, the conversion would increase in this direction, while for an order equal to unity the conversion is the same in all three cases.

At the same symposium, Danckwerts (D2) drew attention to the effect of incomplete mixing on homogeneous reactions. He introduced the concept of segregation, which indicates that in the same vessel there are clumps of fluid which have different concentrations, caused by incomplete mixing. The effect on the conversion of chemical reactors is again an increase in conversion for reactions of an order greater than 1 and a decrease in conversion when the order is less than 1.

The state of segregation, according to an earlier paper by Danckwerts (D1), is determined by two quantities: (a) the scale of segregation and (b) the degree of segregation. The chemical conversion, however, is only affected by the degree of segregation and not by the scale, as long as the spread in residence time remains the same. This holds true generally when the scale of segregation is small and the total number of separate fluid clumps is high enough to allow a statistical treatment of them. Macroscale segregation effects, such as "dead space," "short circuiting," etc., generally cannot be realized without affecting the residence time distribution. Models for this latter type of imperfect mixing have been treated by Cholette *et al.* (C4, C5), and, more recently by Levenspiel and Bischoff (L3). Here we will deal mainly with "microscale segregation." Macroscale segregation will only be included when it may play a role in the interaction of microscale models (see Section III).

Danckwerts defined a degree of segregation J based on the fluctuations in concentration which occur. He studied a chemical reaction in a binary mixture of two components A and B, in which a is the volume fraction of A at a certain point and $(1 - a)$ the volume fraction of B at this same

point. When \bar{a} is the average volume fraction of A in the whole vessel then¹

$$J = \frac{\langle (\bar{a} - a)^2 \rangle_{av}}{\bar{a}(1 - \bar{a})}$$

J varies from zero when mixing is uniform on the molecular scale to unity when segregation is complete ($a = 1$ or 0 at every point). Zwietering (Z2) introduces the concept of maximum mixedness as opposed to the state of complete segregation introduced by Danckwerts. Zwietering shows that in cases where his concept of maximum mixedness holds, the degree of segregation as defined by Danckwerts is not necessarily equal to zero (but only a minimum), except for the ideal mixer. On the other hand, Zwietering's definition of maximum mixedness also holds for the case of a bundle of parallel piston flow reactors all with the same residence time, when there is no mixing between the separate reactors at all.

B. SEGREGATION IN DISPERSED PHASE SYSTEMS

In two-phase systems, the concept of segregation can be introduced more justifiably. Two-phase systems generally have a continuous phase and a dispersed phase. In continuous flow systems, the dispersion is formed upon entrance of the corresponding phase in the reactor, while after this moment the separate particles may either have their own segregated and isolated life during their stay in the reactor or there may be a more or less strong interaction (exchange of matter) with neighboring particles.

This type of segregation, which may be considered as a microscale segregation, appears to be a state which in itself does not say anything about the concentration in the dispersed particles nor about their age. In a batch reactor, for instance, in which all the dispersed particles have the same size, there may be complete segregation (no interaction) and still all the particles will always have the same concentration.

When, however, an extraction, or an extraction combined with a chemical reaction, is carried out between two phases in a continuous stirred tank reactor in which there is no interaction occurring between the dispersed particles (complete segregation), the dispersed particles will have different concentrations because of the spread in residence time. Any kind of interaction between the dispersed particles (e.g., by diffusion or by continuous coalescing and redispersion) then tends to eliminate these concentration differences.

Also, when such a process is carried out in a piston flow reactor (therefore, without a residence time distribution) in which the dispersed particles have different sizes and the chemical reaction is mass-transfer limited, the

¹ For the case of more or less parallel streams Danckwerts defined the degree of segregation by means of the age of a point.

smaller particles will sooner be converted than larger particles, unless the interaction is strong enough to equalize concentration differences between particles at the same spot in the reactor.

Segregation, therefore, will generally cause a spread in concentration in mass transfer and chemical reaction systems, but only when there is a spread in residence time, a spread in particle size, or in any other type of mass transfer or chemical activity determining factor. Interaction generally will tend to eliminate these concentration differences. The segregation is complete when there is no interaction, while at infinite interaction rate there is no segregation. It will be clear that, when segregation is understood in this way, it has only a qualitative meaning and it is useless to define a degree of segregation based on differences in concentration or age of the particles. The only point which seems to be important is the interaction rate and its ratio to the conversion or chemical reaction rate.

In Table I a comparison is given of the different definitions which deal with segregation and mixing for various kinds of systems.

TABLE I
COMPARISONS OF DIFFERENT DEFINITIONS FOR VARIOUS SYSTEMS

System	Interaction rate	State of segregation (here defined)	Degree of segregation (Danckwerts)	State of mixedness (Zwietering)
All systems	∞	0	Minimum	Maximum
Mixing of two components A and B <i>after</i> start up	Finite	Partly segregated	$0 < J < 1$	Partly mixed
Mixing of two components A and B <i>at</i> start up	Finite	Partly segregated	1	0
Two-phase systems in a continuous stirred tank reactor	0	Complete	$0 < J < 1$	Partly mixed
Bundle of parallel piston flow reactors, all with the same residence time	0	Complete	$0 < J < 1$	Maximum
Two-phase batch reaction, dispersed particles all of the same size	0	Complete	0	Maximum

C. INTERACTION IN THE DISPERSED PHASE

In principle, interaction in dispersed phase systems may occur in two ways.

1. *Interaction by Diffusion through the Continuous Phase between Two or More Adjacent Dispersed Particles*

When indeed the state of segregation is a small-scale segregation, then each particle at a certain point will, on the average, be surrounded by other particles which have an average concentration which is characteristic for the point in consideration. When c is the concentration in a particular particle and \bar{c} is the average concentration in all of the particles at the point of interest, then

$$\frac{dc}{dt} = -i(c - \bar{c})$$

in which t is the time and i is the interaction rate constant measured in sec.^{-1} .

Of course i will depend on the average distance between the dispersed particles, on the size of these particles, on the rate of diffusion through the continuous phase, and on the state of turbulence. In a continuous stirred tank reactor \bar{c} will be the same throughout the tank, while for a piston flow reactor \bar{c} will change with the average age of the concerning point.

Interaction by diffusion will seldom occur in two-phase systems, but may be of importance between gas bubbles in a fluidized bed, especially when the fluidized solid is not a catalyst but only a heat carrier. In homogeneous systems, this type of interaction is the normal kind of interaction.

2. *Interaction by Coalescence and Redispersion*

This is the more general type of interaction which may occur in liquid-liquid two-phase systems and in gas-liquid systems where gas is the dispersed phase.

When two drops or bubbles coalesce, the release of energy is so large that before break-up again occurs the contents of the two dispersed particles may be assumed to be completely mixed. So when two drops, of volumes v_1 and v_2 and concentrations c_1 and c_2 , respectively, coalesce, the concentration after break-up is, for both drops, equal to

$$\frac{v_1 c_1 + v_2 c_2}{v_1 + v_2}$$

when all the drops may be assumed to be of the same size, the final concentration is equal to $\frac{1}{2}(c_1 + c_2)$.

When the drop size distribution is constant, the rate of coalescing must be equal to the rate of redispersion, and, in that case, the rate of interaction can be expressed as the rate of coalescing. When two drops of volumes v_1 and v_2 , respectively, coalesce, the total volume of the dispersed phase which is concerned with this coalescence is equal to $v_1 + v_2$. The rate of coalescing is now defined as the fraction of the total volume of dispersed phase which

in unit time is involved in coalescences. When this rate of coalescence is not too large, the chance that a certain drop volume is concerned with a coalescence more than once during this unit time is negligibly small. If not, the unit time should be chosen smaller.

Let the total number of drops be N and the average volume of each drop be \bar{v} , so that the total volume of dispersed phase is $N\bar{v}$. Then the volume of dispersed phase involved in coalescence is $\omega_i N\bar{v}$ and the number of coalescences per unit time is $\frac{1}{2}\omega_i N$. Here ω_i is the coalescing rate or coalescing frequency measured in sec.^{-1} and the chance of having more than two drops involved in a single coalescence is assumed negligible.

D. INFLUENCE OF SEGREGATION ON THE CONVERSION RATE OF CHEMICAL REACTIONS

Suppose that a chemical reaction takes place in a dispersed system between the two reactants A and B, where A is dissolved in the dispersed phase and B in the continuous phase. Suppose further that at a certain place in the reactor the concentration of B is equal to b , while the dispersed drops at this place have different concentrations a of the reactant A caused by segregation. When the chemical conversion for each isolated drop can be described as being of the n th order in the reactant A, then the amount reacting per second in each drop of volume v equals²

$$-v \frac{da}{dt} = vka^n b$$

in which k is the over-all reaction rate constant.

When there are N drops at the place of interest, the total amount reacting in all these drops is

$$\begin{aligned} -Nv \left(\frac{da}{dt} \right) &= \sum_{\text{all drops}} vka^n b \\ &= Nvkb(\bar{a}^n) \end{aligned}$$

\bar{a} and \bar{a}^n indicate the average values of a and a^n , respectively, for all N drops.

Now, unless $n = 1$, $(\bar{a}^n) \neq (\bar{a})^n$, which means that the average conversion rate for all N drops is affected by the way in which the reactant A is distributed over these drops:

$$(\bar{a}^n) < (\bar{a})^n, \quad \text{for } n < 1$$

and

$$(\bar{a}^n) > (\bar{a})^n, \quad \text{for } n > 1$$

which means that, for reactions of an order higher than one, segregation

² The reaction may be of an order in B different from 1 as well, but since there is no segregation in the continuous phase this does not affect the ultimate result.

increases the over-all conversion rate, and, when this order is smaller than one, segregation decreases this conversion rate.

In the following, the concepts of drop conversion rate and over-all conversion rate are used. In the same way as the chemical reaction rate is used to indicate the change in concentration of a reactant with time in a very small volume of a single phase in which the concentration may be considered to be uniform, the concept of drop conversion rate is used for the change in *average* concentration of a reactant with time where this average is taken over the whole volume of a single drop. Because of mass transfer limitation, this drop conversion rate may be lower than the pure chemical reaction rate (see Section II,B,1).

In the same way, the over-all conversion rate is used to indicate the change with time of the concentration of a reactant averaged over the whole volume of one single phase present in the reactor.

Further, the concepts of order of drop conversion and order of over-all conversion are introduced analogous to the well-known concept of order of chemical reaction. The order of drop conversion thus refers to the way in which the drop conversion rate responds to a change in average concentration of a reactant in that same drop. The order of (over-all) conversion refers to the way in which the over-all conversion rate responds to a change in average concentration of a reactant, where the average is taken over the whole corresponding phase present in the reactor (see further also Section II,A,3).

Because of mass transfer limitation, the order of drop conversion may also be reduced, as will be shown in Section II,B,1.

II. The Effect of Segregation on the Kinetics of a Liquid-Liquid Two-Phase Chemical Reaction

A. CHEMICAL REACTION IN A CONTINUOUS STIRRED TANK REACTOR

In this chapter some effects of segregation on the kinetics of a chemical reaction between two liquid phases carried out in a continuous stirred tank reactor (CSTR) will be discussed. In the derivations of these effects it will be assumed that during the reaction the dispersed phase is maintained (e.g., in the case of extraction combined with chemical reaction) and that all dispersed drops have the same size. This means that when there is segregation it is only the age distribution which causes a concentration distribution in the dispersed phase.

Only the two extreme cases will be compared, viz.: (a) complete segregation (no interaction, the subscript *c* will refer to this situation) and (b) no segregation (infinite interaction, referred to by the subscript *n*).

Most of these calculations have been carried out before by Rietema (R2) and by Rietema and Meyerink (R3, R4).

1. Influence on the Over-All Conversion Rate

When a liquid-liquid two-phase chemical reaction is carried out in a CSTR, it may be assumed that the conditions in the continuous phase are the same anywhere and constant with time (no segregation in this phase). When there is complete segregation in the dispersed phase, each drop can be assigned an age t , during which the drop has stayed in the reactor.

For each drop, therefore,

$$-\frac{da}{dt} = ka^nb$$

First it will be assumed that the order of drop conversion in the reactant A is zero, so that

$$-\frac{da}{dt} = kb$$

or

$$a = a_0 - kbt \quad \text{for } t < \frac{a_0}{kb}$$

and

$$a = 0, \quad \text{for } t \geq \frac{a_0}{kb}$$

Here a_0 is the feed concentration of reactant A and k the drop conversion rate constant. If there is no segregation in the dispersed phase, which means that the rate of interaction is so high that all drops have the same concentration, then also the over-all conversion is a linear function of the average residence time τ_n and given by $f_n = \tau_n(kb/a_0)$ for $\tau_n < a_0/bk$ and $f_n = 1$ for $\tau_n \geq a_0/bk$. If however there is no interaction at all, all drops will have different concentrations—depending on their age in the reactor—and the concentration distribution will correspond with the age distribution.

It will be assumed that the well-known age distribution for an ideal mixer also holds for the age distribution in the dispersed phase, which assumption is allowed if the total number of drops is large enough and there are no "dead" corners or short circuiting in the reactor (only micro-scale segregation).

Then the average concentration of the reactant A in the outlet is $\bar{a} = \int_0^\infty (a/\tau_c)g(t) dt$ in which $g(t)$ is the residence time distribution and τ_c the average residence time. For the ideal mixer $g(t) = e^{-t/\tau_c}$. Further,

$$\begin{aligned} a &= a_0 - bkt & \text{for } 0 < t < a_0/bk \\ &= 0 & \text{for } t > a_0/bk \end{aligned}$$

It follows that

$$\bar{a} = \int_0^{a_0/bk} (a_0 - bkt)e^{-t/\tau_c} \frac{1}{\tau_c} dt \quad (1)$$

from which

$$\bar{a} = a_0 - bk\tau_c(1 - e^{-a_0/bk\tau_c}) \quad (2)$$

If f_c is the conversion obtained in this case, then (see Fig. 1)

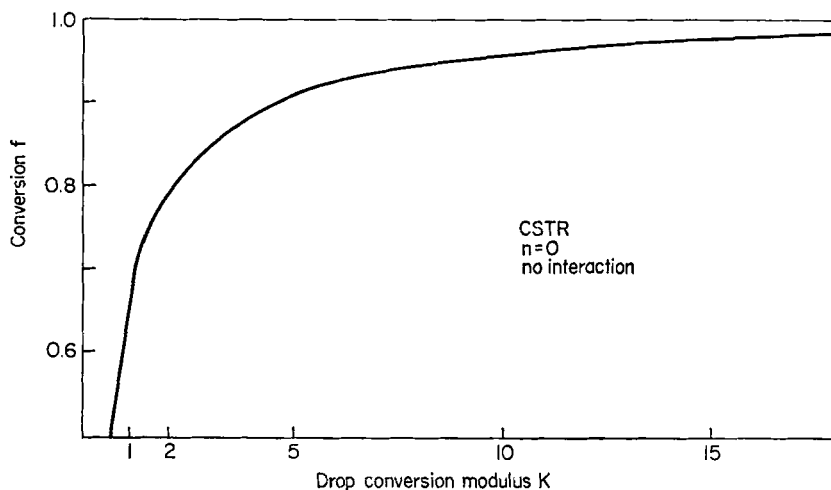


FIG. 1. Conversion f against drop conversion modulus K for a CSTR when $n = 0$ and there is no interaction in the dispersed phase. Drop conversion modulus $K = bk\tau_c/a_0$.

$$\begin{aligned} f_c &= 1 - \frac{\bar{a}}{a_0} = \frac{bk\tau_c}{a_0} (1 - e^{-a_0/bk\tau_c}) \\ &= K(1 - e^{-1/K}) \end{aligned} \quad (3)$$

in which $K = bk\tau_c/a_0$, the drop conversion modulus. Putting $f_n = f_c$ leads to a relation between the residence times τ_n and τ_c for obtaining the same conversion in both cases, viz:

$$\tau_n = \tau_c \left[1 - \exp \left(-\frac{\tau_n}{\tau_c} \frac{1}{f} \right) \right]$$

or

$$\frac{\tau_c}{\tau_n} \ln \left(1 - \frac{\tau_n}{\tau_c} \right) = -\frac{1}{f} \quad (4)$$

In Fig. 2 the ratio τ_c/τ_n is plotted against the conversion f .

When the order of drop conversion in the reactant A is equal to $\frac{1}{2}$, the conversion can be calculated in the same way. When there is no segregation,

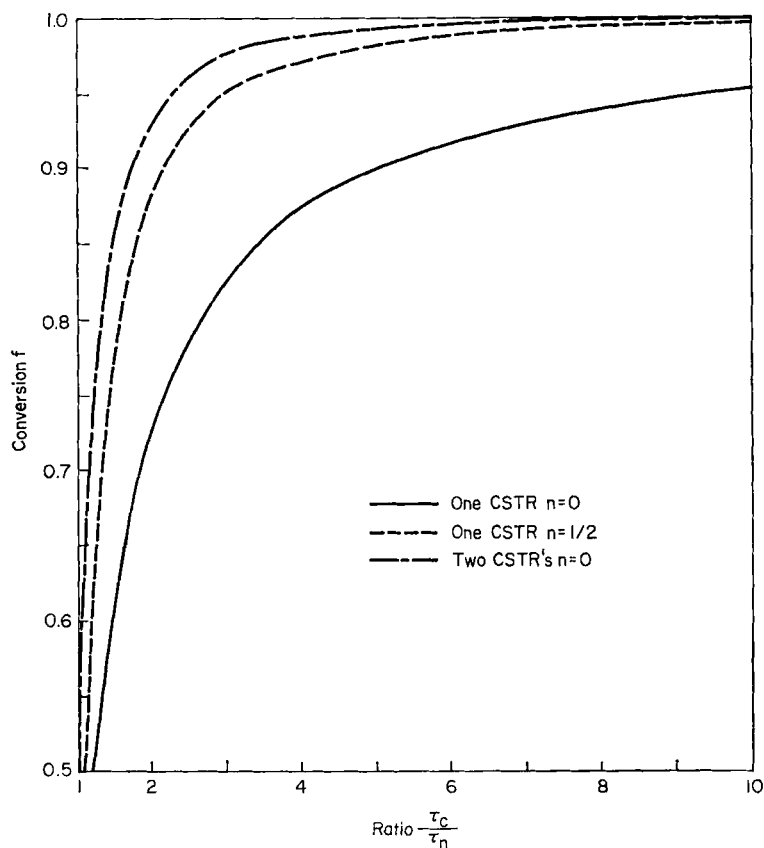


FIG. 2. Plot of τ_c/τ_n against degree of conversion f .

it follows from a simple mass balance that $a_0 = \bar{a} + \tau_n k \bar{a}^{1/2} b$, from which it can be derived that

$$\frac{b k \tau_n}{a_0^{1/2}} = \frac{f_n}{\sqrt{1 - f_n}} \quad (5)$$

When there is complete segregation, the concentration in a drop of age t is given by

$$a = \left(a_0^{1/2} - \frac{b k t}{2} \right)^2 \quad \text{for } 0 < t < \frac{2 a_0^{1/2}}{b k}$$

and

$$a = 0 \quad \text{for } t > \frac{2 a_0^{1/2}}{b k}$$

It follows that

$$\bar{a} = \int_0^{2a_0^{1/2}/bk} \left(a_0^{1/2} - \frac{bkt}{2} \right)^2 e^{-t/\tau_c} \frac{1}{\tau_c} dt$$

from which

$$\bar{a} = a_0 - bk\tau_c a_0^{1/2} + \frac{b^2 k^2 \tau_c^2}{2} \left[1 - \exp \left(\frac{-2a_0^{1/2}}{bk\tau_c} \right) \right]$$

The conversion obtained in this case is

$$f_c = \frac{bk\tau_c}{a_0^{1/2}} - \frac{b^2 k^2 \tau_c^2}{2a_0} \left[1 - \exp \left(\frac{-2a_0^{1/2}}{bk\tau_c} \right) \right] \quad (6)$$

By again letting $f_c = f_n$, for each value of $bk\tau_c/a_0^{1/2}$, the corresponding f_c can be calculated from Eq. (6), and then, from Eq. (5), the corresponding value of $bk\tau_n/a_0^{1/2}$, and so the ratio of τ_c/τ_n can be determined as function of $f_c = f_n$. This result is shown in Fig. 2 with the dotted line.

From Fig. 2 it follows that the effect of segregation for half-order drop conversion is lower than for zero-order drop conversion. For first-order drop conversion the effect will disappear entirely, as has been shown in Section I,D, while for orders of drop conversion greater than one the effect is reversed: segregation increases the over-all conversion rate. This latter case will not be considered further here, as it is very unlikely that in a practical phase system the order of drop conversion is greater than one.

Finally, Fig. 2 also shows (dashed line) the result when two CSTR's of equal volume are operating in cascade with a settler in between, so that in this settler the interaction in the dispersed phase is complete. It further is assumed that no reaction occurs in this settler and that the dispersed phase in both reactors shows either no segregation at all or complete segregation. The result has been calculated for an order of drop conversion equal to zero. Again f has been plotted versus the ratio τ_c/τ_n , where both τ_c and τ_n now mean the total residence time in the two stages. When comparing this result with that for one stage (solid line), it will be clear that the influence of segregation can be markedly reduced when operating in two stages instead of one.

2. Effect of the Fraction of Drops with Zero Concentration

For a good understanding of the mechanism of segregation, especially in the case of zero-order drop conversion, it is necessary to point out the great importance of the fraction of drops with zero concentration.

As shown before, the concentration will be zero when the age of a drop is larger than bk/a_0 .

Therefore, it must be expected that unless the interaction is infinite (no segregation) a certain fraction of the drops will have a concentration equal to zero. In fact this is the case for all processes carried out in a CSTR for which the order of drop conversion is smaller than one.

Furthermore, in the case of zero-order drop conversion, the contribution to the over-all conversion of each drop in which the concentration is not yet equal to zero is the same (independent of its concentration). Therefore, the over-all conversion rate and also the degree of conversion can be calculated from the fraction of drops which have zero concentration.

Suppose that $g(a)$ is the distribution function of the concentration in the drops so that $g(a) \Delta a$ is the fraction of drops with a concentration between a and $a + \Delta a$. Suppose further that G_0 is the fraction of drops with zero concentration. Then

$$\int_0^{a_0} g(a) da = 1 - G_0$$

and

$$\bar{a} = \int_0^{a_0} ag(a) da$$

From the above it follows that the over-all conversion rate is $N_1 = N(1 - G_0)bk$ (where N is the total number of drops), since the drop conversion rate of a drop with concentration greater than zero is equal to bk . Since $N_1 = Nfa_0/\tau$ it follows that $f = (1 - G_0)bk\tau/a_0$. From $f = 1 - \bar{a}/a_0$ it then follows that

$$a_0 - \int_0^{a_0} ag(a) da = bk\tau \int_0^{a_0} g(a) da$$

It must be stressed that this equation holds for every degree of segregation but only when the order of drop conversion is equal to zero.

A more generally valid equation is

$$a_0 - \int_0^{a_0} ag(a) da = bk\tau \int_0^{a_0} a^n g(a) da$$

3. Influence on the Order of Over-All Conversion

When \bar{N}_A is the over-all conversion rate per unit volume which depends on the concentration of the reactants according to $\bar{N}_A = k\bar{a}^n\bar{b}^m$, then the total order of conversion is $n + m$, where n and m are the partial orders of conversion in the reactants A and B, respectively. In a continuous stirred tank reactor the concentration b is constant and the same throughout the reactor, and since we are only interested in the effect on the partial conversion order n we put $k\bar{b}^m = k_1$, so that $\bar{N}_A = k_1\bar{a}^n$ in which \bar{a} is the average concentration of A in the whole reactor.

It follows that

$$d(\ln \bar{N}_A) = n d(\ln \bar{a})$$

or

$$\frac{d\bar{N}_A}{\bar{N}_A} = n \frac{d\bar{a}}{\bar{a}}$$

or

$$n = \frac{\bar{a}}{\bar{N}_A} \frac{d\bar{N}_A}{d\bar{a}} \quad (7)$$

Since $\bar{N}_A = (f/\tau)a_0$ and $\bar{a} = (1 - f)a_0$, in which τ is the average residence time of the dispersed phase, this result can be further elaborated. It has to be kept in mind, however, in which way the average concentration \bar{a} is changed during the experiment: by changing the feed concentration or by changing the average residence time. When a_0 is kept constant,

$$\begin{aligned} n &= \frac{\bar{a}}{a_0} \frac{\tau}{f} \frac{d(f/\tau)}{d(\bar{a}/a_0)} = (1 - f) \frac{\tau}{f} \frac{d(f/\tau)}{d(1 - f)} \\ n &= -\tau \left(\frac{1 - f}{f} \right) \frac{d(f/\tau)}{df} \\ n &= \frac{1 - f}{\tau} \frac{d\tau}{df} - \frac{1 - f}{f} \end{aligned} \quad (7a)$$

When τ is kept constant, the result is

$$\begin{aligned} n &= \frac{\bar{a}}{\bar{N}_A} \frac{d\bar{N}_A}{d\bar{a}} = \frac{\bar{a}}{a_0} \frac{\tau}{f} \frac{1}{\tau} \frac{d(fa_0)}{d\bar{a}} \\ n &= \left(\frac{1 - f}{f} \right) \frac{d(a_0 - \bar{a})}{d\bar{a}} \\ n &= \frac{1 - f}{f} \left(\frac{da_0}{d\bar{a}} - 1 \right) \end{aligned} \quad (7b)$$

For a *homogeneous* chemical reaction of a chemical substance A (without mass transfer limitation and without a segregation effect) carried out in a CSTR the mass balance results in $a_0 = \bar{a} + \tau k_0 \bar{a}^n$ when n is the chemical reaction order. (In this case the chemical reaction order is the same as the over-all conversion order.) It now follows that

$$\begin{aligned} f &= \frac{k_0 \tau}{1 + k_0 \tau}, & \text{for } n &= 1 \\ f &= 1 - \frac{k_0 \tau}{a_0} \frac{k_0 \tau + 2a_0 - \sqrt{k_0^2 \tau^2 + 4k_0 \tau a_0}}{2}, & \text{for } n &= \frac{1}{2} \\ f &= \frac{\tau k_0}{a_0}, & \text{for } n &= 0 \end{aligned}$$

For all these cases it can be easily verified that formulas (7a) and (7b) both give exactly the right order of conversion.

When, however, the over-all conversion rate cannot be represented by a simple equation of the type $\bar{N}_A = k_1 \bar{a}^n$ the order of conversion is not clearly defined, and the application of the two formulas (7a) and (7b) will generally lead to different orders of conversion. For this reason it is always necessary to indicate in which way the average concentration \bar{a} has been changed: by changing the average residence time or by changing the feed

concentration. When this restriction is accepted, formula (7) and its derivatives (7a) and (7b) can be used as *definitions of the order of over-all conversion*. This procedure is followed here.

For cases where the order of drop conversion equals zero and one-half, the order of over-all conversion is calculated as a function of the degree of conversion. The results are shown in Fig. 3. It is remarkable that n increases with the conversion and becomes equal to unity at $f = 1$ when the feed concentration is kept constant.

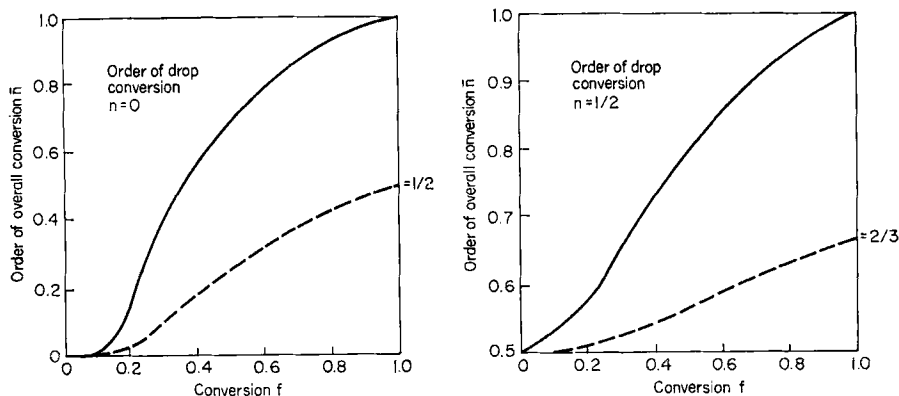
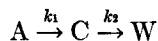


FIG. 3. Order of over-all conversion \bar{n} as function of conversion f in reacting systems where there is no interaction in the dispersed phase: solid lines, a_0 is kept constant; dotted lines, τ is kept constant.

This is interesting especially in those cases where in a reaction between two components one expects mass transfer limitation of at least one of these components and, therefore, an order of conversion in the other component between zero and one-half (see Section II,B,1). When, however, operating at a high degree of conversion, an order of over-all conversion nearly equal to one would be determined experimentally. Therefore, when one finds experimentally an order of conversion equal to one, while also the order of chemical reaction equals one, this is not a good argument to conclude that apparently there is no mass transfer limitation as segregation combined with mass transfer limitation may have caused this effect. To make a conclusion possible the experiment has to be repeated at a low degree of conversion.

4. Influence on Selectivity for Consecutive Reactions

Suppose that a chemical reaction scheme of the type



takes place in the dispersed phase. Of course the reactant B will also take part in these reactions, but, because of reasons already pointed out (see Section II,A,3), this can be accounted for in the reaction constants k_1 and k_2 .

Suppose that C is the desired product and W is an unwanted waste product. Now a selectivity factor S can be defined as the ratio of the total amount of C produced over the total amount of A converted:

$$S = \frac{\bar{c}}{a_0 f} \quad (8)$$

where \bar{c} is the average concentration of C in the outlet.

As selectivity is a factor of importance in commercial production, we will deal here only with reaction schemes which are of practical interest. This means that when a product C is made on a commercial scale according to the reaction $A \rightarrow C$, where a second reaction $C \rightarrow W$ may destroy the product C, this second reaction generally will be of a lower rate than the main reaction. Otherwise this reaction scheme would have no commercial value. This means that we may restrict ourselves to those cases for which the second reaction $C \rightarrow W$ is of an order (order of drop conversion) higher than or the same as that of the first reaction $A \rightarrow C$, since this first reaction is more likely to be limited by mass transfer than the slower second reaction.

It will be shown that under these conditions the selectivity in a completely segregated system generally is lower than in a system where there is no segregation. Of course, for an intermediate degree of segregation the selectivity also will be intermediate. The effect of segregation is calculated for three cases in the accompanying tabulation. The influence of segrega-

Case	Order of drop conversion in	
	First reaction	Second reaction
i	0	0
ii	0	1
iii	$\frac{1}{2}$	1

tion on the selectivity is decreasing in the direction $i \rightarrow ii \rightarrow iii$. For the intermediate cases $(0, \frac{1}{2})$ and $(\frac{1}{2}, \frac{1}{2})$ the effect is difficult to calculate but can be more or less evaluated by interpolation.

For simplicity, the formulas for the degree of conversion of reactant A will be repeated here (the value of b/k being replaced by k_1):

for $n = 0$,

$$f_n = \frac{k_1 \tau_n}{a_0} \quad \text{and} \quad f_c = \frac{k_1 \tau_c}{a_0} \left[1 - \exp \left(\frac{-a_0}{k_1 \tau_c} \right) \right] \quad (3a)$$

for $n = \frac{1}{2}$,

$$f_n = \frac{k_1 \tau_n}{a_0^{1/2}} \left(\bar{a} \right)^{1/2} \quad \text{or} \quad \frac{k_1 \tau_n}{a_0^{1/2}} = \frac{f_n}{\sqrt{1 - f_n}} \quad (5a)$$

and

$$f_c = \frac{k_1 \tau_c}{a_0^{1/2}} - \frac{k_1^2 \tau_c^2}{2a_0} \left[1 - \exp \left(\frac{-2a_0^{1/2}}{k_1 \tau_c} \right) \right] \quad (6a)$$

Case i. *Both Reactions are of Zero Order of Drop Conversion. No segregation.* Mass balances for components A and C result in

$$(a_0 - \bar{a}) = k_1 \tau_n = f_n a_0$$

and

$$\bar{c} = (k_1 - k_2) \tau_n$$

The selectivity, therefore, is

$$S_n = (1 - k_2/k_1) \quad (9)$$

Complete segregation. The concentration of C in each drop changes with time according to

$$c = (k_1 - k_2)t \quad \text{for} \quad 0 < t < \frac{a_0}{k_1}$$

and

$$c = a_0 - k_2 t \quad \text{for} \quad \frac{a_0}{k_1} < t < \frac{a_0}{k_2}$$

At time $t = a_0/k_1$ the concentration of A is zero and at time $t = a_0/k_2$ the concentration of C is zero and all the material has been converted to the waste product W.

It will be assumed again that the well-known residence time distribution for the CSTR also holds for the dispersed phase. Then the average concentration of C is

$$\bar{c} = \int_0^\infty c e^{-t/\tau_c} \frac{1}{\tau_c} dt$$

or

$$\bar{c} = \int_0^{a_0/k_1} (k_1 - k_2)t e^{-t/\tau_c} \frac{1}{\tau_c} dt + \int_{a_0/k_1}^{a_0/k_2} (a_0 - k_2 t) e^{-t/\tau_c} \frac{1}{\tau_c} dt$$

or

$$\bar{c} = k_1 \tau_c (1 - e^{-a_0/k_1 \tau_c}) - k_2 \tau_c (1 - e^{-a_0/k_2 \tau_c}) \quad (10)$$

The selectivity can now be found from Eqs. (3a) (keeping in mind that $b k = k_1$), (8), and (10):

$$S_c = 1 - \frac{k_2}{k_1} \left[\frac{1 - \exp(-a_0/k_2\tau_c)}{1 - \exp(-a_0/k_1\tau_c)} \right] \quad (11)$$

Figure 4 shows both S_n and S_c as functions of conversion for different ratios of the parameter k_1/k_2 . The strong decrease of selectivity, especially at higher conversions, is evident from this figure.

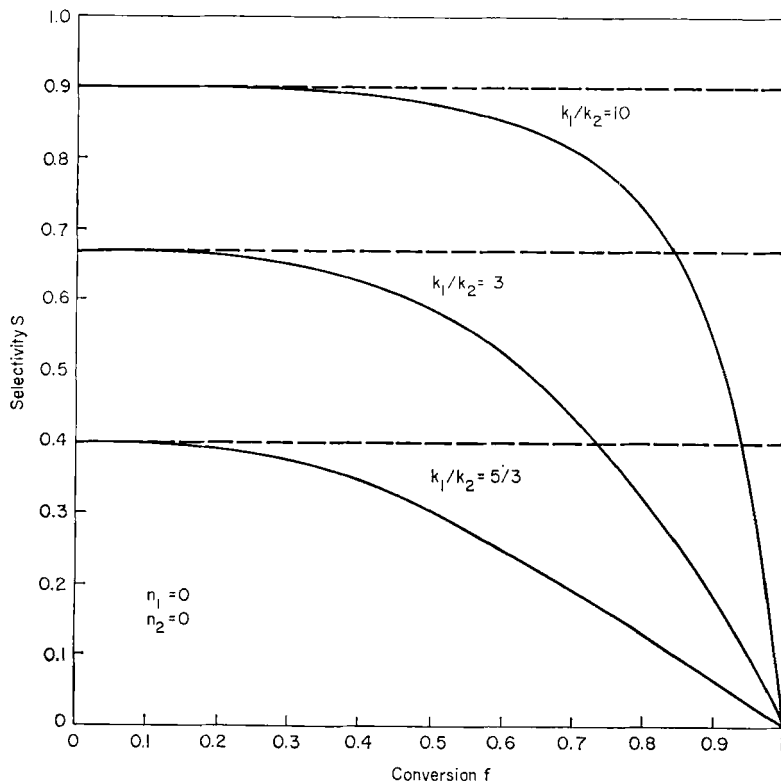


FIG. 4. Selectivity S as function of the conversion f for the case of consecutive reactions, which both are of zero order: solid lines, no interaction; dotted lines, no segregation.

Case ii. *First Reaction of Zero-Order, Second Reaction of First-Order Drop Conversion. No segregation.* Mass balances for components A and C now result in

$$a_0 - \bar{a} = k_1\tau_n = f_n a_0$$

and

$$\bar{c} = \frac{k_1\tau_n}{1 + k_2\tau_n}$$

The selectivity then turns out to be

$$S_n = \frac{1}{1 + k_2\tau_n} \quad (12)$$

Complete segregation. The concentration of C in each drop is given by

$$c = \frac{k_1}{k_2} [1 - \exp(-k_2 t)] \quad \text{for } 0 < t < \frac{a_0}{k_1}$$

and

$$c = \frac{k_1}{k_2} \left[\exp\left(\frac{k_2 a_0}{k_1}\right) - 1 \right] \exp(-k_2 t) \quad \text{for } t > \frac{a_0}{k_1}$$

The average concentration of C in the outlet is calculated in an identical way as before and this results in

$$\bar{c} = \frac{k_1 \tau_c}{1 + k_2 \tau_c} \left[1 - \exp\left(-\frac{a_0}{k_1 \tau_c}\right) \right] \quad (13)$$

The selectivity is found to be

$$S_c = \frac{1}{1 + k_2 \tau_c} \quad (14)$$

This result looks almost identical to that for no segregation [Eq. (12)]. It has to be kept in mind, however, that at the same average residence time the conversion for no segregation is much higher than when there is complete segregation.

The result for both cases has been plotted in Fig. 5 as a function of the conversion with $k_1/k_2 a_0$ as a parameter. Again there is a strong decline in selectivity at higher conversions when there is complete segregation, although this decline is less strong than when both consecutive reactions are of zero order.

The above derived result $S = 1/(1 + k_2 \tau)$ holds always when the second reaction is of first order, no matter what the order of the main reaction is and independently of whether there is segregation or not. This can easily be shown as follows:

For the first order conversion



the total amount of C converted can be calculated straight from the average concentration \bar{c} as already shown in Section I,D and, therefore, is equal to $V k_2 \bar{c}$, in which V is the total volume of the phase in which the reaction occurs. On the other hand, this amount is also equal to the amount of W produced which again is $qv\bar{w}$ (when qv is the throughput of the reacting phase and \bar{w} the average concentration of W). Therefore,

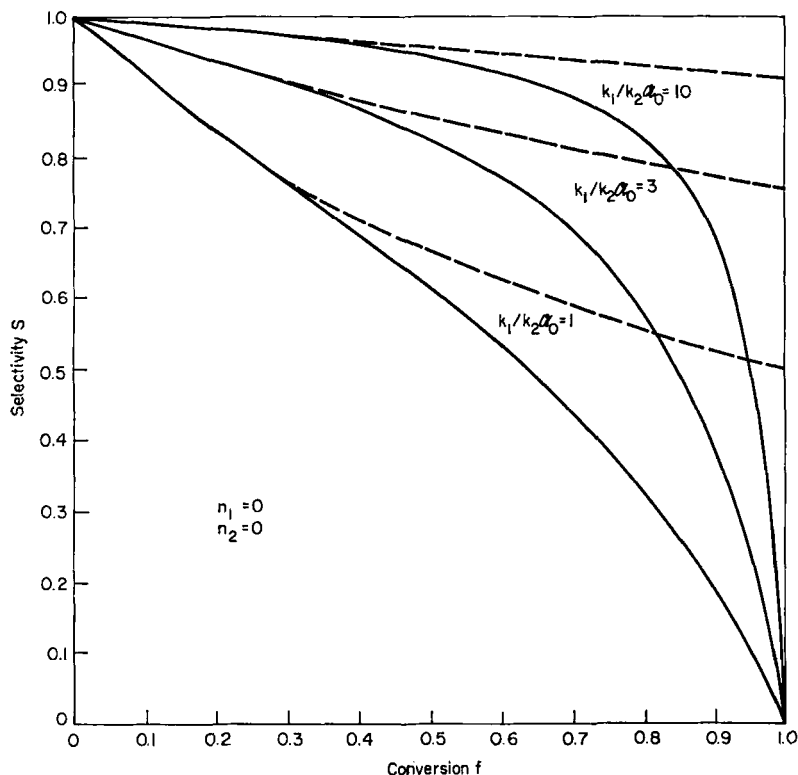


FIG. 5. Selectivity S as function of the conversion f for the case of consecutive reactions of which the first one is of zero order and the second of first order: solid lines, no interaction; dotted lines, no segregation.

$$qv\overline{w} = Vk_2\overline{w}$$

or

$$\overline{w}/\overline{c} = k_2\tau$$

The selectivity S was defined as $S = \overline{c}/fa_0$. But as $fa_0 = \overline{c} + \overline{w}$, it follows that

$$S = \frac{\overline{c}}{\overline{c} + \overline{w}} = \frac{1}{1 + \overline{w}/\overline{c}} = \frac{1}{1 + k_2\tau}$$

Case iii. *First Reaction of Order One-Half, Second Reaction of First-Order Drop Conversion.* By means of the result $S = 1/(1 + k_2\tau)$ the selectivity as function of the conversion can now be easily calculated for the case of complete segregation and no segregation. The result is shown in Fig. 6, where the parameter now is $k_1/k_2a_0^{1/2}$.

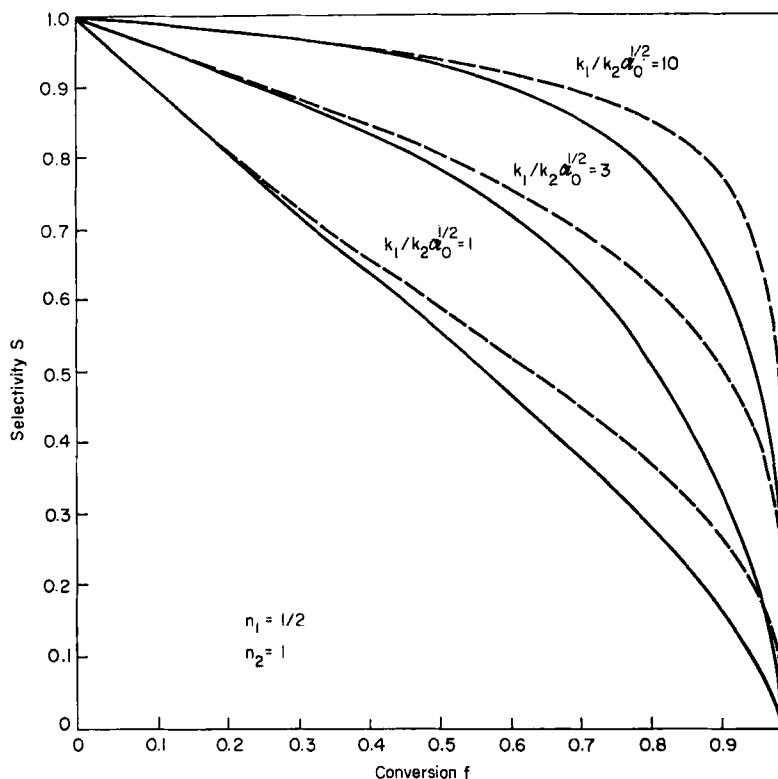
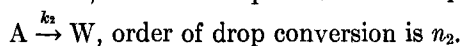
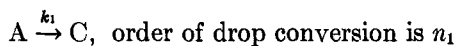


FIG. 6. Selectivity S as function of the conversion f for the case of consecutive reactions of which the first is of half-order and the second of first order: solid lines, no interaction; dotted lines, no segregation.

5. Influence on Selectivity for Simultaneous Reactions

Suppose the two competing reactions are



When both reactions are of the same order ($n_1 = n_2$) the ratio of the amounts of C and W produced is independent of the time in each dispersed drop and equal to the ratio of the reaction constants. Hence, after integration over all drops, this same ratio is found and the selectivity, therefore, is equal to

$$S = \frac{k_1}{k_1 + k_2}$$

This result is the same, whether segregation exists or not. Segregation has no influence on the selectivity when the orders of drop conversion for the two competing reactions are the same. When $n_1 = 1$, the total amount of C produced can be calculated from the average concentration of A: $\bar{c} = k_1\tau\bar{a}$ (see Section I,D). Since, however, \bar{a} also determines the degree of conversion $f = 1 - \bar{a}/a_0$ it follows that

$$S = \frac{\bar{c}}{f\bar{a}_0} = k_1\tau \left(\frac{1-f}{f} \right)$$

Also, this result is independent of the degree of segregation. The same holds true when $n_2 = 1$.

To determine if the effect of segregation on the selectivity for other values of n_1 and n_2 is positive or negative, it is assumed that the second reaction $A \rightarrow W$ is very slow ($k_2a_0^{1/2}/k_1 \ll 1$), so that the degree of conversion can be calculated by assuming that only the first reaction is proceeding. Then the total amount of W produced can be calculated from the average concentration of A (when there is no segregation) and from the distribution of A over all drops (when there is complete segregation). By comparing these amounts of W produced for the two cases, conclusions can be drawn about the effect of segregation.

Example: $n_1 = 0, n_2 = \frac{1}{2}$

Now when $k_2a_0^{1/2}/k_1 \ll 1$, the equation for no segregation is

$$\frac{\bar{w}}{a_0} = \frac{k_2a_0^{1/2}}{k_1} \frac{k_1\tau_n}{a_0} \left(1 - \frac{k_1\tau_n}{a_0} \right)^{1/2}$$

and that for complete segregation is

$$\frac{\bar{w}}{a_0} = \frac{2}{3} \frac{k_2a_0^{1/2}}{k_1} \int_0^{a_0/k_1\tau_c} \left\{ 1 - \left(1 - \frac{k_1t}{a_0} \right)^{3/2} \right\} e^{-t/\tau_c} d \left(\frac{t}{\tau_c} \right)$$

At $f = 0.88$, in which case $k_1\tau_n/a_0 = 0.88$ and $k_1\tau_c/a_0 = 3.0$, the result for no segregation is

$$\frac{\bar{w}}{a_0} = 0.305 \frac{k_2a_0^{1/2}}{k_1}$$

and that for complete segregation is

$$\frac{\bar{w}}{a_0} = 0.107 \frac{k_2a_0^{1/2}}{k_1}$$

which shows that in this case segregation favors a high selectivity.

In Fig. 7, a diagram is given to indicate where segregation favors a high selectivity (+) and where segregation is unfavorable (-). Along the strong lines, segregation has no effect at all on selectivity (always at the same over-all conversion).

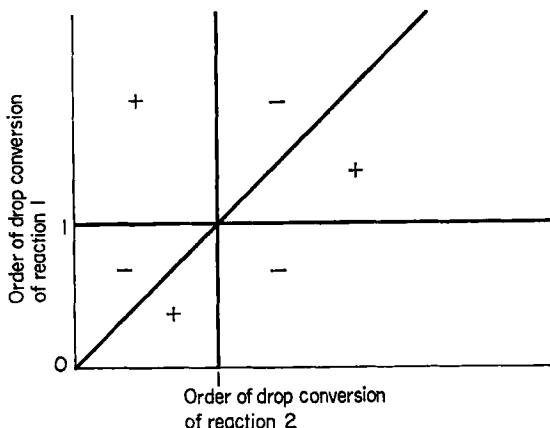


FIG. 7. Influence of segregation on selectivity for simultaneous reactions: along solid lines, no influence; +, segregation favors reaction 1; -, segregation favors reaction 2.

B. SEGREGATION AND MASS TRANSFER LIMITATION

In this section the effect of mass transfer limitation on the drop conversion rate and the order of drop conversion will be treated, and it will be shown that a process for which the real chemical reaction is of first order in the reactant A (which is dissolved in the dispersed phase) can still be influenced by the effect of segregation when the chemical conversion rate is limited by mass transfer of the reactants.

1. Derivation of the Drop Conversion Rate When the Reaction Takes Place in the Dispersed Phase

It will be assumed that the reaction $A + B$ takes place only in the dispersed phase, the reactant A is assumed to be insoluble in the continuous phase, but the reactant B will diffuse into the drops. Further it is assumed that inside the drops there is no mixing but only pure molecular diffusion. The diffusivity of B in the dispersed phase is \mathfrak{D}_B while the mass transfer coefficient outside the drops is m . The partition coefficient of B is H_B and equals the ratio of the concentration of B in the dispersed phase at the interface over the concentration of B in the continuous phase at the interface.

The microkinetics of the chemical reaction that takes place is described by $da/dt = db_a/dt = -k_0 a b_a$ where k_0 is the real chemical reaction rate constant and the index d refers to the dispersed phase. If the components A and B are supplied to the reactor in stoichiometric quantities and

$$h = \frac{\text{volume of the continuous phase}}{\text{volume of the dispersed phase}},$$

then $a_0 = b_0 h$ where a_0 and b_0 are the concentrations of the reactants in the feed.

If now $h/H_B \gg 1$, then in each drop the original concentration of A is much higher than the concentration of dissolved reactant B in the drop. This means that the difference in the concentration of A through the whole cross section of the drop, which is caused by the difference in the chemical reaction rate near the interface and that near the center, may be neglected.

The diffusion rate into the drop of component B, therefore, can be calculated for the apparently stationary state with an over-the-whole-cross-section constant value of $k_0 a = k'$. Then for a spherical drop of radius R , the differential equation becomes

$$\mathfrak{D}_B \left(\frac{d^2 b_d}{dr^2} + \frac{2}{r} \frac{db_d}{dr} \right) - k' b_d = 0 \quad (15)$$

with the boundary conditions

$$(1) \quad \frac{db_d}{dr} = 0 \quad \text{for } r = 0$$

$$(2) \quad b_d = H_B \left(b_c - \frac{N_B}{4\pi R^2 m} \right) \quad \text{for } r = R$$

Here b_c is the equilibrium concentration of B outside the drops and N_B is the consumption rate of B per drop.

The solution of this problem (which is a slightly modified version of the well-known solution by Thiele and Wheeler (T2, W2) for diffusion and chemical reaction in a porous catalyst) runs:

$$\frac{b_d}{b_c} = \frac{H_B}{\sigma b_c} \frac{\sinh \varphi \sigma}{\sinh \varphi} \left(b_c - \frac{N_B}{4\pi R^2 m} \right) \quad (16)$$

where $\sigma = r/R$ and $\varphi = R(k'/\mathfrak{D}_B)^{1/2}$ (Thiele modulus).

Then

$$N_B = 4\pi R^2 \mathfrak{D}_B \left(\frac{db_d}{dr} \right)_{r=R} = 4\pi R^2 m b_c / \left(1 + \frac{mR}{\mathfrak{D}_B H_B} \frac{\tanh \varphi}{(\varphi - \tanh \varphi)} \right) \quad (17)$$

When

$$\frac{mR}{\mathfrak{D}_B H_B} \frac{\tanh \varphi}{(\varphi - \tanh \varphi)} \gg 1,$$

which generally is the case since H_B is small and $m \gg \mathfrak{D}_B/R$, this solution simplifies into

$$N_B = 4\pi R H_B \mathfrak{D}_B b_c \left(\frac{\varphi}{\tanh \varphi} - 1 \right) \quad (18)$$

If also $\varphi > 2$ this can be further simplified to

$$N_B = 4\pi R H_B \mathfrak{D}_B b_c (\varphi - 1) = N_0 (\varphi - 1) \quad (18a)$$

where $N_0 = 4\pi R H_B \mathfrak{D}_B b_c$.

For still larger φ ,

$$N_B \approx 4\pi R H_B \mathfrak{D}_B \mathfrak{b}_c \varphi = 4\pi R^2 H_B \mathfrak{b}_c \sqrt{k_0 a \mathfrak{D}_B}$$

which indicates that in this case the order of drop conversion in the component A is equal to $\frac{1}{2}$. When

$$\frac{mR}{\mathfrak{D}_B H_B} \frac{\tanh \varphi}{(\varphi - \tanh \varphi)} \ll 1,$$

which might be the case when φ is large while $m < \mathfrak{D}_B/R$, the solution becomes $N_B = 4\pi R^2 m \mathfrak{b}_c$, which indicates that in this case the apparent order of the reaction in the component A is zero.

2. Reaction in the Continuous Phase

When the reaction takes place in the continuous phase this means that now $H_B = 0$ and that A is soluble in the continuous phase (partition coefficient is equal to H_A , which means that, at equilibrium and when there is no reaction, $a_c = a_d H_A$).

In general, $h \gg 1$ and this means that when A and B again are supplied in stoichiometric quantities—even if H_A is small—still a_c will be rather large compared with \mathfrak{b} , at least in the direct vicinity of the phase boundary. Therefore, a solution as tried in Section II,B,1, where it was assumed that the concentration of A is constant throughout the cross section of the drops, cannot be obtained now since an equivalent assumption for the component B seems not to be justified. This means that for the real solution it is necessary to solve two simultaneous differential equations: one for component A and one for component B. These equations can only be solved numerically by means of a computer.

With the help of qualitative reasoning, however, it can be shown that when mass transfer is really limiting the conversion rate, the order of drop conversion in the component A is lower than 1 and, occasionally, when the mass transfer *outside* the drop becomes limiting, may even become zero.

In Fig. 8 a schematic course of the concentration profiles near the interface is given. For simplicity H_A is assumed to be 1. Two cases are shown, both with the same bulk concentration of component B but with a bulk concentration of A (α_2), which in case 2 is twice as high as that (α_1) in case 1.

Suppose that in case 2 the conversion rate is twice as high as that in case 1, then in case 2 (compared with case 1):

(a) At any distance r from the interface the concentration of A is twice as high (as is shown in Fig. 8).

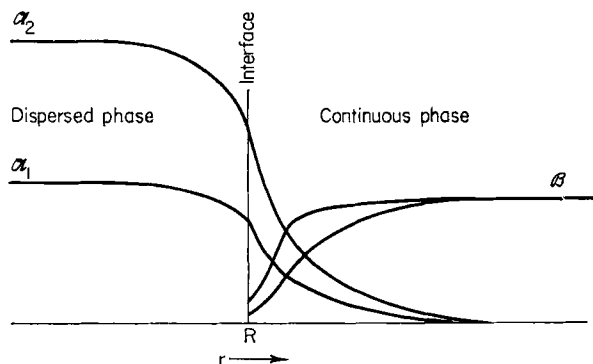


FIG. 8. Schematic course of the concentration profiles for a first-order reaction in the continuous phase with mass transfer limitation.

(b) The consumption rate of B is twice as high, thus the concentration gradient of B is twice as high, and, therefore, at the same bulk concentration of B, the concentration of B must be everywhere lower.

Thus follows that the product $a_c b_c$ must be less than twice as high, perhaps even the same. This means that the conversion rate cannot be twice as high, so there exists a contradiction, which can be avoided only by assuming that the conversion rate is less than twice as high, which means that the order of the drop conversion is less than one.

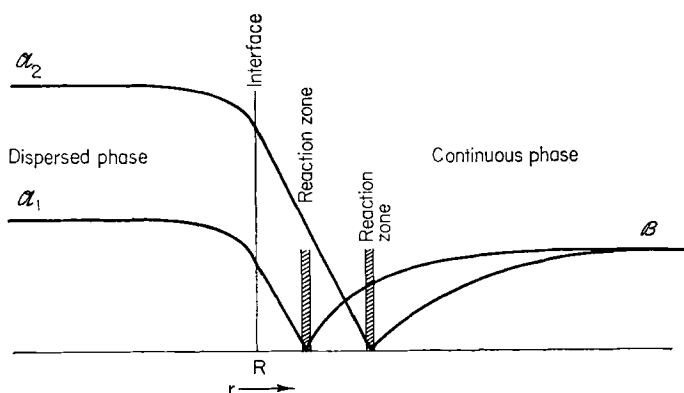


FIG. 9. Schematic course of the concentration profiles for a reaction in the continuous phase, when the mass transfer is entirely limiting.

In Fig. 9, an equivalent situation is designed, but now the mass transfer is entirely limiting, so that when a molecule A meets a molecule B it reacts immediately. Now increasing the concentration of A does not increase the

total reaction rate at all but merely shifts the reaction zone further from the interface. The order of drop conversion in A, therefore, is zero.

3. Effect of Segregation. Derivation of Over-All Conversion Rate for a CSTR

Again it will be assumed here that the continuous coalescing and redispersion of the drops does not influence the mass transfer into the drops. The effect of segregation will be calculated for a CSTR while the reaction takes place in the dispersed phase. For this derivation, use will be made of the equations derived in Section II,B,1. All drops are assumed to have the same diameter.

No segregation. When the interaction rate is infinite compared with the conversion rate, it may be assumed that in all drops the concentration of A is the same and equal to the outlet concentration \bar{a} . When the outside mass transfer is high,

$$N_B = 4\pi H_B R \mathfrak{D}_B b_c \left(\frac{\bar{\varphi}}{\tanh \bar{\varphi}} - 1 \right) \quad (19)$$

in which

$$\bar{\varphi} = R \sqrt{\frac{k_0 \bar{a}}{\mathfrak{D}_B}}$$

When V is the total reactor volume and h the phase ratio, then the total number of drops in the dispersed phase is

$$\frac{V}{1+h} \left(\frac{3}{4\pi R^3} \right)$$

Summation over all drops, therefore, gives

$$\bar{N}_B = \frac{V}{1+h} \left(\frac{3}{4\pi R^3} \right) N_B \quad (20)$$

Also

$$\bar{N}_B = \bar{N}_A = \frac{V}{1+h} \frac{1}{\tau_n} f a_0 = \frac{V}{1+h} \frac{1}{\tau_n} (a_0 - \bar{a})$$

By putting $\varphi_0^2 = R^2 k_0 a_0 / \mathfrak{D}_B$, we obtain

$$(\varphi_0^2 - \bar{\varphi}^2) \left(\frac{\tanh \bar{\varphi}}{\bar{\varphi} - \tanh \bar{\varphi}} \right) = 2E\tau_n \quad (21)$$

in which $E = \frac{3}{4} H_B b_c k_0$. Combined with $f = 1 - (\varphi/\varphi_0)^2$ the conversion f can be calculated for different values of φ_0 and $E\tau_n$. This result is plotted in Fig. 11 by the dotted lines.

Complete segregation. When there is complete segregation, the result for the drop conversion rate has to be integrated over all drops present in the reactor. For each drop the concentration of A is continuously decreasing with respect to its age:

$$N_A = N_B = -\frac{4}{3}\pi R^3 \frac{da}{dt}$$

From

$$\varphi = R \sqrt{\frac{k_0 a}{\mathfrak{D}_B}}$$

it follows that

$$\frac{da}{dt} = \frac{2\mathfrak{D}_B}{R^2 k_0} \varphi \frac{d\varphi}{dt}$$

Substituting this in the result for N_B , as derived in Section II,B,1, gives

$$\frac{\varphi \tanh \varphi}{\varphi - \tanh \varphi} d\varphi = -E dt \quad (22)$$

where again $E = \frac{3}{2}H_B b_c k_0$. The boundary condition of this differential equation is:

$$\varphi = \varphi_0 = R \sqrt{\frac{k_0 a_0}{D_B}} \quad \text{for } t = 0.$$

When $\varphi > 2$ the differential equation can be simplified to

$$\frac{\varphi}{\varphi - 1} d\varphi = -E dt. \quad (23)$$

After integrating, this results in

$$Et = \varphi_0 - \varphi + \ln \frac{\varphi_0 - 1}{\varphi - 1}. \quad (24)$$

For $\varphi < 2$ this integration has to be performed numerically. In Fig. 10, the course of φ as a function of Et is shown for values of φ_0 of 5 and 10.

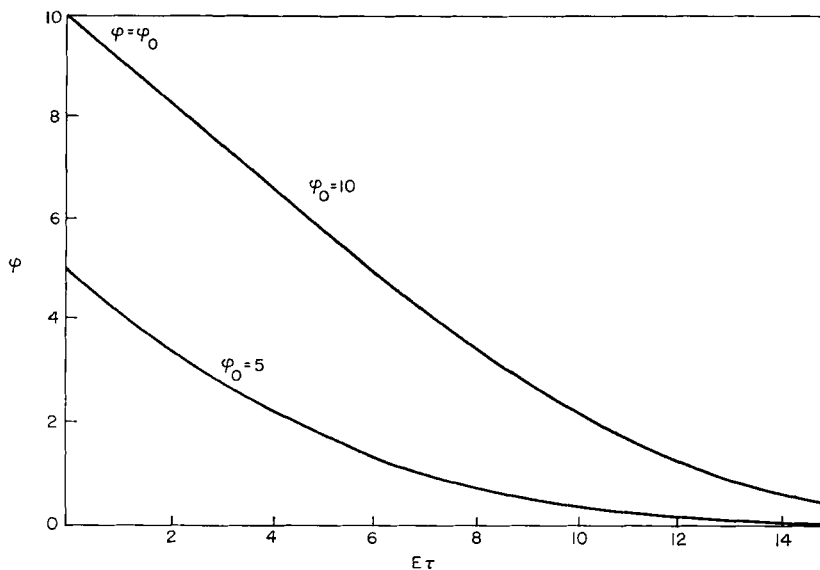


FIG. 10. Plot of φ against Et for two values of φ_0 . First-order reaction with mass transfer limitation.

It must be remarked here that, for very low values of φ , which means for drops which are nearly entirely converted, the assumption that the concentration of A is constant throughout the drop is not justified any longer. We are, however, only interested in large initial values of φ , and in that case the contribution of these nearly converted drops to the over-all reaction rate is very small. No serious error will occur, therefore, by neglecting the difference between the actual contribution of these drops and the above derived result.

Integrating over all drops present gives the total conversion rate \bar{N}_B :

$$\bar{N}_B = \int_0^\infty N_B \frac{V}{1+h} \left(\frac{3}{4\pi R^3} \right) e^{-t/\tau_c} \frac{1}{\tau_c} dt \quad (25)$$

where τ_c is the average residence time in the CSTR, and again the well-known age distribution is assumed to hold. Also,

$$\bar{N}_B = \bar{N}_A = \frac{V}{\tau_c} \frac{1}{1+h} f a_0$$

while from $a = \varphi^2 \mathfrak{D}_B / R^2 k_0$ it follows that

$$N_B = -\frac{4}{3}\pi R^3 \frac{\mathfrak{D}_B}{R^2 k_0} \frac{d\varphi^2}{dt}$$

Finally, we obtain

$$\begin{aligned} f &= \frac{1}{\varphi_0^2} \int_0^\infty \frac{d\varphi^2}{dt} e^{-t/\tau_c} dt \\ &= 1 - \frac{1}{\varphi_0^2} \int_0^\infty \varphi^2 e^{-t/\tau_c} \frac{1}{\tau_c} dt \end{aligned} \quad (26)$$

For different values of φ_0 and $E\tau_c$ the conversion f can now be calculated. In Fig. 11, this result is shown as the solid lines. For a value of $\varphi_0 = 100$, the result coincides exactly with the result derived in Section II,A,1 for half-order drop conversion. For a

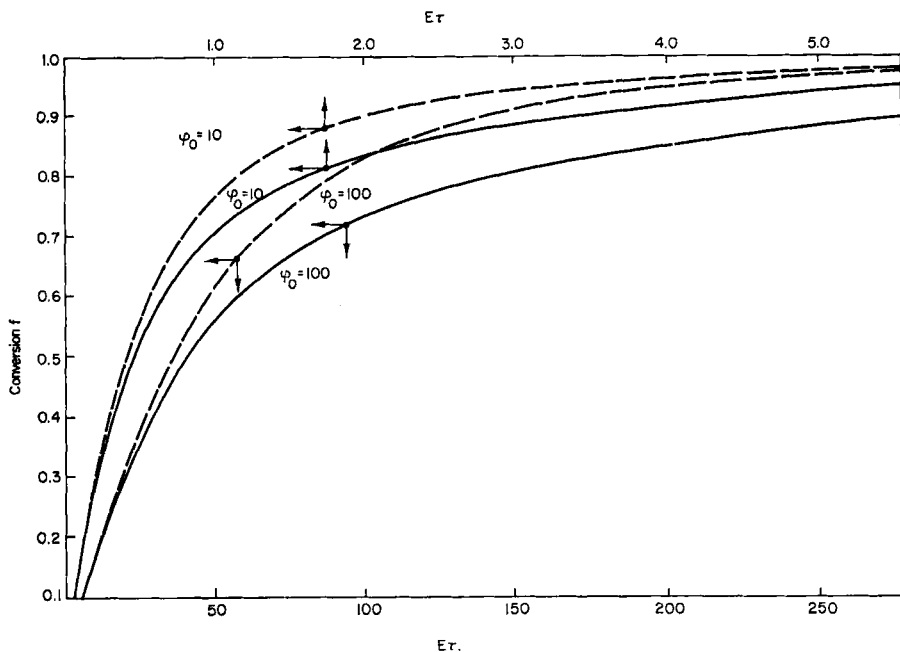


FIG. 11. Conversion f versus $E\tau$ for first-order reaction with mass transfer limitation: solid lines, no interaction; dotted lines, no segregation.

value of $\varphi_0 = 10$, there is still a considerable difference with pure half-order drop conversion.

In Fig. 12, the ratio τ_c/τ_n is plotted versus the conversion for both values of φ_0 .

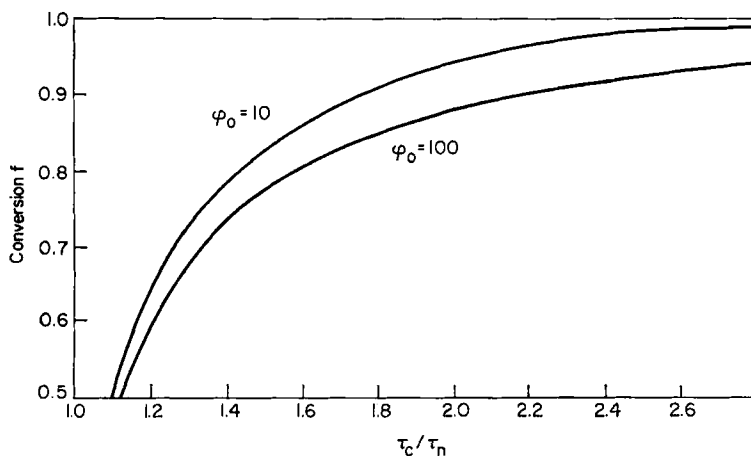


FIG. 12. Ratio of residence times necessary to obtain the same conversion in the two cases of no interaction (τ_c) and no segregation (τ_n) for first-order reaction with mass transfer limitation.

C. EFFECT OF DROP SIZE DISTRIBUTION

In the preceding sections it was always assumed that all drops of the dispersed phase had the same diameter, and that, for the case that there is segregation, a spread in the concentration distribution was only caused by a spread in age distribution. However, as pointed out before, a spread in the drop size distribution may also cause different concentrations in the drops, even when these drops have the same age. Generally this may be expected only when there is mass transfer limitation.

In this section, several cases where there is a spread in drop size distribution will be calculated first for an ideal piston flow reactor in which all liquid parts have the same residence time distribution, and, finally, also the case of a CSTR in which there is a spread in drop size will be calculated, but only for the case of zero-order drop conversion.

As the calculations have to be performed numerically the problem has been simplified in so far as only a very simple drop size distribution function is assumed to hold, namely:

$$\begin{aligned} f(R) &= \frac{1}{R_1(X-1)} & \text{for } R_1 < R < XR_1 \\ f(R) &= 0 & \text{for } R_1 > R > XR_1 \end{aligned} \quad (27)$$

Although, in general, more complicated distribution functions will be encountered, nevertheless, the order of magnitude of the effect of segregation can be estimated from the calculations as they are given here.

1. Piston Flow Reactor

As shown in Section II,B,1, zero-order drop conversion will occur when the drop conversion rate is limited by a relatively low outside mass transfer coefficient. It was derived that then

$$N_B = 4\pi R^2 m \dot{b}$$

as long as there is reactant A available in the drop. Since also $N_B = N_A = -\frac{4}{3}\pi R^3 da/dt$, so that $da/dt = -3m\dot{b}/R$, the course of a can be calculated when the course of b with time is known. However, the course of b with time is determined by all drops together. A direct integration of N_B also leads to nowhere, as the lower integration boundary is determined by the largest drops in which all the reactant A is consumed. For that reason an indirect numerical method has to be carried out.

When

$$\zeta = \frac{3m}{R_1 a_0} \int_0^t \dot{b} dt,$$

then for each segregated drop it is found after integration:

$$\begin{aligned} a/a_0 &= 1 - \zeta R_1/R & \text{for } \zeta < R/R_1 \\ &= 0 & \text{for } \zeta > R/R_1 \end{aligned}$$

After integration over all drops, the average concentration of A is found:

$$\begin{aligned} \bar{a}/a_0 &= 1 - \frac{\zeta}{X-1} \ln X & \text{for } \zeta < 1 \\ &= \frac{X-\zeta}{X-1} - \frac{\zeta}{X-1} (\ln X - \ln \zeta) & \text{for } 1 < \zeta < X \\ &= 0 & \text{for } \zeta > X \end{aligned} \quad (28)$$

For a given value of X , \bar{a}/a_0 can be plotted as function of ζ . From this plot the course of \bar{a}/b_0 with ζ can also be found. Now

$$\frac{d\bar{b}}{d\zeta} = \frac{d\bar{b}}{dt} \frac{dt}{d\zeta} = \frac{d\bar{b}}{dt} \bigg/ \frac{d\zeta}{dt}$$

However,

$$\frac{d\zeta}{dt} = \frac{3m}{R_1 a_0} \dot{b}$$

Therefore,

$$\frac{3m}{R_1 a_0} \dot{b} \frac{d\bar{b}}{d\zeta} = \frac{d\bar{b}}{dt} \quad (29)$$

When now $\bar{b} = \bar{a}/h + z a_0$ in which h is the phase ratio and z is the surplus of reactant B over reactant A, then

$$\frac{3m}{h R_1} \left(\frac{1}{h} \frac{a}{a_0} + z \right) \frac{d(a/a_0)}{d\zeta} = \frac{d(b/a_0)}{dt} \quad (30)$$

Therefore, from the plot of \bar{a}/a_0 versus ζ a plot of $d(b/a_0)/dt$ versus b/a_0 can be derived. From this latter graph b/a_0 as function of t can be calculated by numerical integration.

For the case of $X = 4$, $h = 1$, and $z = 0.1$ the result is given in Fig. 13 where the degree of conversion based on the reactant A is given as function

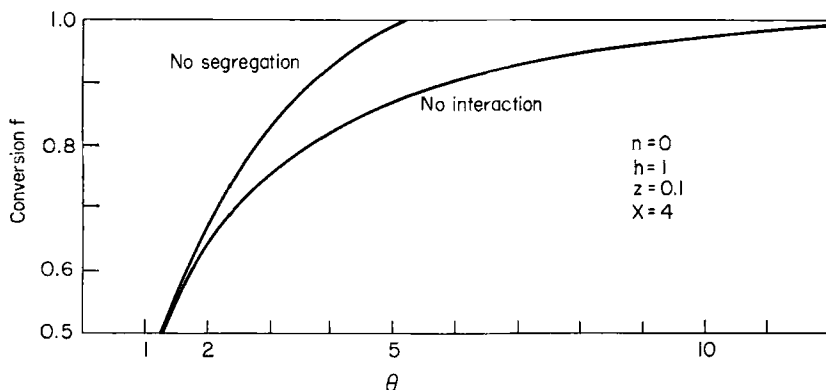


FIG. 13. Conversion f versus dimensionless reaction time θ for piston flow reactor with drop size distribution zero-order drop conversion.

of $\theta = 3mt/hR_1$. Also, the conversion curve for the case of no segregation (infinite interaction, at the same t all drops have the same concentration of reactant A) is shown in this figure. In this latter case,

$$f = 1 - \frac{\bar{a}}{a_0} = (1 - zh) - (1 + zh) \exp\left(-\frac{\ln X}{X - 1} \theta\right) \quad (31)$$

Although the effect of segregation is not as large as in the case of a CSTR with uniform drop size it still cannot be neglected, especially at higher degrees of conversion.

When the surplus of reactant B is so large that it may be assumed to be constant throughout the reactor, the calculations can be performed entirely analytically. If now $\theta' = 3mbt/a_0R_1$, then for the case of no interaction (complete segregation)

$$\begin{aligned} f_c &= \theta'_c \frac{\ln X}{X - 1} & \text{for } \theta'_c < 1 \\ &= \frac{\theta'_c}{X - 1} (\ln X - \ln \theta'_c) + \frac{\theta'_c - 1}{X - 1} & \text{for } 1 < \theta'_c < X \\ &= 1 & \text{for } \theta'_c > X \end{aligned} \quad (32)$$

and for the case of infinite interaction (no segregation)

$$\begin{aligned} f_n &= \theta'_n \frac{\ln X}{X - 1} & \text{when } \theta'_n < \frac{X - 1}{\ln X} \\ &= 1 & \text{when } \theta'_n > \frac{X - 1}{\ln X} \end{aligned} \quad (33)$$

At a degree of conversion 1, the ratio $\theta_c'/\theta_n' = X \ln X/(X - 1)$. This ratio is given for some values of X in the following tabulation:

X	θ_c'/θ_n'
2	1.38
4	1.84
8	2.38
16	2.97

For half-order drop conversion the calculation is somewhat more complicated, of course, but in principle the course of the calculation is the same as for zero-order drop conversion. Based on the formula derived in Section II,B,1

$$N_B = 4\pi R^2 H_B b \sqrt{k_0 a D_B}$$

the calculation has been performed again for the two cases of no interaction and infinite interaction. For the case of $X = 4$, $h = 1$, and $z = 0.1$ the result is shown in Fig. 14, where now

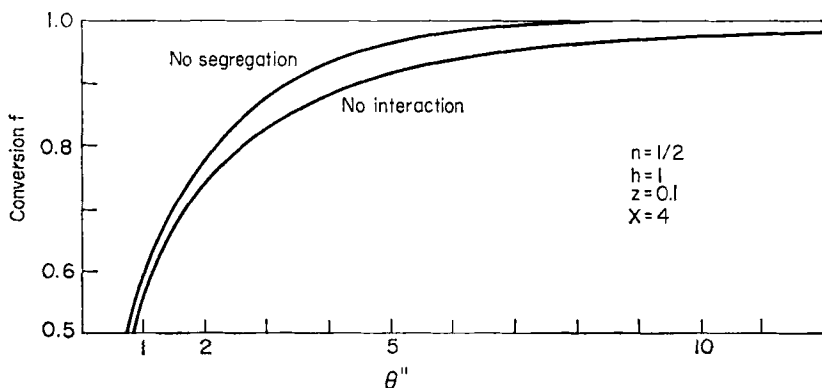


FIG. 14. Conversion f versus dimensionless reaction time θ'' for piston flow reactor with drop size distribution half-order drop conversion.

$$\theta'' = \frac{3H_B a_0^{1/2} \sqrt{k_0 D_B}}{2hR_1} t \quad (34)$$

As could be expected, the effect is even smaller than in the case of zero-order drop conversion.

2. Continuous Stirred Tank Reactor with Nonuniform Drop Size Distribution

In a continuous stirred tank reactor in which the dispersed phase is segregated, a spread in the drop size distribution is present, and there is mass transfer limitation, the spread in the concentration distribution will

be larger than when all drops have the same size. This means that an increased effect of segregation may be expected.

In the case of *complete segregation* the drops may be classified in groups of different particle size ranges. When these size ranges are sufficiently small, each class may be treated as a group of uniform drop size distribution. Since for each class again the normal age distribution for an ideal mixer will hold, the average concentration for each class can be calculated by integration over the age distribution. The average concentration of all classes can, after that, be derived by integration over the drop size distribution. For each drop:

$$N_B = 4\pi R^2 m \bar{b} = -\frac{4}{3}\pi R^3 \frac{da}{dt}$$

or

$$-\frac{da}{dt} = \frac{3m\bar{b}}{R}$$

and

$$\begin{aligned} a/a_0 &= 1 - \frac{3m\bar{b}}{a_0 R} t & \text{when } t < \frac{a_0 R}{3m\bar{b}} \\ &= 0 & \text{when } t > \frac{a_0 R}{3m\bar{b}} \end{aligned}$$

For one class for which the diameter lies between $2R$ and $2R + 2dR$:

$$\begin{aligned} \frac{\bar{a}}{a_0} &= \int_0^{a_0 R / 3m\bar{b}} \left(1 - \frac{3m\bar{b}}{a_0 R} t\right) e^{-t/\tau} \frac{1}{\tau} dt \\ &= 1 - \frac{\theta R_1}{R} (1 - e^{-R/R_1 \theta}) \end{aligned} \quad (35)$$

in which

$$\theta = \frac{3m\bar{b}\tau}{a_0 R_1}$$

This result now has to be integrated over the drop size distribution

$$\frac{\bar{a}}{a_0} = \int_0^\infty \frac{\bar{a}}{a_0} f(R) dR$$

For the same drop size distribution as treated before, this becomes

$$\begin{aligned} \frac{\bar{a}}{a_0} &= \frac{1}{(X-1)R_1} \left[\int_{R_1}^{XR_1} \left\{ 1 - \frac{\theta R_1}{R} (1 - e^{-R/R_1 \theta}) \right\} dR \right] \\ &= 1 - \theta \frac{\ln X}{X-1} + \frac{\theta}{X-1} \int_{1/\theta}^{X/\theta} \frac{1}{p} e^{-p} dp \end{aligned} \quad (36)$$

Since

$$\int \frac{1}{p} e^{-p} dp = \int \frac{dp}{p} - \int dp + \int \left(\frac{p}{2} - \frac{p^2}{6} + \frac{p^3}{24} - \dots \right) dp$$

it follows that

$$\begin{aligned} \frac{\bar{a}}{a_0} &= \frac{1}{\theta(X-1)} \left\{ \frac{X^2-1}{4} - \frac{1}{18\theta} (X^3-1) + \right. \\ &\quad \left. \dots + \frac{(-1)^{n+1}}{(n+1)(n+1)! \theta^{n-1}} (X^{n+1}-1) + \dots \right\} \end{aligned} \quad (37)$$

When again it is assumed that $X = 4$, then

$$\begin{array}{rcl} \bar{a}/a_0 & = & 0.418, \quad \text{for } \theta_c = 2 \\ & = & 0.2095 \quad \quad \quad = 5 \\ & = & 0.114 \quad \quad \quad = 10 \\ & = & 0.0597 \quad \quad \quad = 20 \end{array}$$

No segregation. In this case the average drop conversion rate has to be calculated by direct integration over the drop size distribution. After that, a mass balance gives the average concentration:

$$q(a_0 - \bar{a}) = V(3m\bar{b}) \int \frac{f(R)}{R} dR$$

or

$$\frac{\bar{a}}{a_0} = 1 - \frac{3m\bar{b}\tau}{R_1 a_0} \frac{\ln X}{X - 1} = 1 - \theta \frac{\ln X}{X - 1} \quad (38)$$

For $X = 4$, and the same values for \bar{a}/a_0 as calculated for the case of complete segregation, the corresponding values obtained for θ_n are compared with the values of θ_c in Table II. Also, in Table II, the ratio τ_c/τ_n as

TABLE II
COMPARISON OF θ_c WITH θ_n FOR $X = 4$

\bar{a}/a_0	θ_c	θ_n	θ_c/θ_n	f	τ_c/τ_n
0.418	2	1.26	1.59	0.582	1.43
0.2095	5	1.71	2.9	0.7905	2.58
0.114	10	1.92	5.2	0.886	4.30
0.0597	20	2.04	9.8	0.9403	7.80

calculated before in Section II,A,1 for the case of uniform drop size distribution is given.

By comparing θ_c/θ_n with τ_c/τ_n , it is seen that the effect of segregation is not increased very much if a spread in drop size distribution is also present, and that the greatest effect is caused by the spread in age distribution.

III. Partial Segregation. Theory of Finite Interaction Rate. Models for Interaction in the Dispersed Phase

In the previous section only the two extreme cases (a) no segregation (infinite interaction) and (b) complete segregation (finite interaction) were considered and compared with respect to over-all conversion rate, order of conversion, and selectivity.

Generally one must expect that in practice neither of these extreme cases will hold and that there is a finite interaction rate or partial segregation. This means that dispersed drops may have a certain period during which they keep their own identity, but after a shorter or longer time (which generally is spread statistically) they will coalesce with a neighboring drop, or with another part of the dispersed phase. After exchange of concentrations, new drops will be produced.

This coalescing and redispersion may be either rapid (possibly so rapid that, compared with the reaction rate, the interaction may be considered practically infinite) or it may be slow. The point, however, is: What is rapid and what is slow?

In the next sections, different interaction models will be proposed, two of which have been evaluated, and which make an answer to this question possible.

A. HOMOGENEOUS INTERACTION MODEL

This is the most ideal interaction model which has been accepted by all investigators of interaction to interpret their results of experiments (see Section IV).

In this model the segregation is perfect isotropic microscale segregation. All drops are assumed to have the same size. The chance of coalescing with a neighboring drop is for each drop the same, and independent of time and of the concentration of the drop. Redispersion occurs immediately after coalescing and exchange of concentration. Coalescing and redispersion is assumed to have no effect on mass transfer.

R. L. Curl was the first to work out this model for the case of a chemical process with zero-order drop conversion which is carried out in a continuous stirred tank reactor (C8). His theory, somewhat modified, is given at the end of this section.

The result of the calculations, which have to be carried out by means of a digital computer, is presented in Fig. 15. In this figure, the degree of conversion f is given as a function of the drop conversion modulus k ; the interaction modulus I is a parameter which is twice the ratio of the total number of coalescences that occur per unit time over the total number of drops which are fed to the reactor per unit time ($I = \omega_i \tau$, where ω_i is the coalescing frequency and τ the average residence time). The result of Curl has been confirmed by Veltkamp (V2), who solved the equations of Curl by means of Laplace transformation. Veltkamp and Geurts (V3) also evaluated the case in which the order of drop conversion is $\frac{1}{2}$, the result of which is presented in Fig. 16. Figures 15 and 16 both show that a very high value of the interaction modulus is necessary to obtain a substantial effect on the conversion, especially at higher conversions, and that the case of no

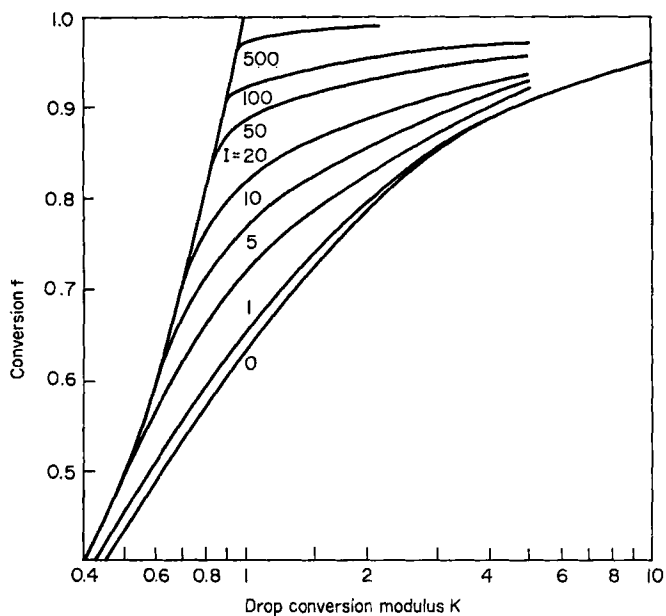


FIG. 15. Effect of *homogeneous interaction* in a CSTR on the conversion. *Zero-order drop conversion.*

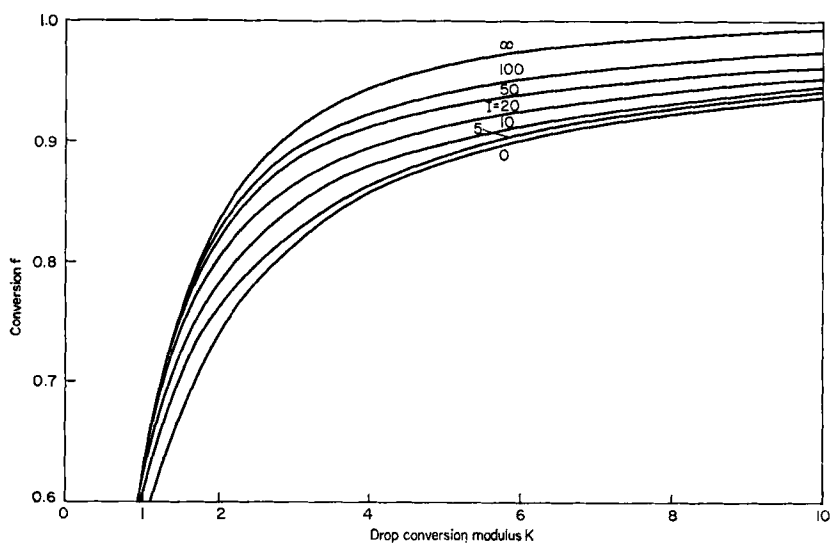


FIG. 16. Effect of *homogeneous interaction* in a CSTR on the conversion *half-order drop conversion.*

segregation (infinite interaction) is very improbable in practice. The concentration distribution which is found in the dispersed phase is very interesting. In Fig. 17 examples for the case of $n = 0$ are given.

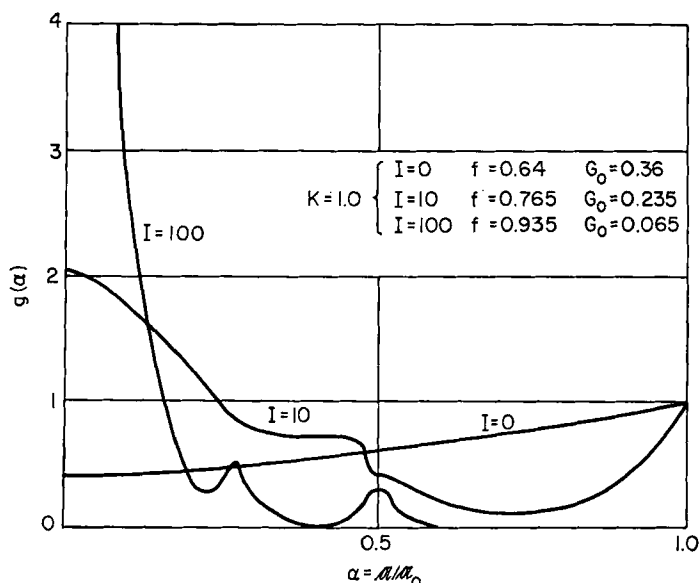


FIG. 17. Three concentration distributions in the dispersed phase for the case of homogeneous interaction when $n = 0$.

As pointed out before (see Section II,A,2), there will always be a fraction of drops with zero concentration while also at the feed concentration there must be a maximum in the concentration distribution. Interaction, therefore, makes sure that subsequent maxima will also occur at $\frac{1}{2}$, $\frac{3}{4}$, $\frac{1}{4}$, etc., times the feed concentration.

Suppose that $g(\alpha)$ is the function describing the concentration distribution in the drops of the dispersed phase, where α is the dimensionless concentration parameter, $\alpha = a/a_0$. When G_0 is the fraction of drops with zero concentration (only for drop conversions less than 1) then

$$\int_0^1 g(\alpha) d\alpha = 1 - G_0 \quad (39)$$

Also, a dimensionless time $\xi = t/\tau$, where τ is the average residence time, will be introduced. The chemical conversion equation $-da/dt = k_1 a^n$ now becomes

$$-\frac{d\alpha}{d\xi} = K\alpha^n,$$

in which the conversion parameter $K = k_1 \tau a_0^{n-1}$.

The change of a fraction of drops in the interval between α and $\alpha + \Delta\alpha$ during a short time $\Delta\xi$ is now caused by

(a) *Chemical reaction*. Drops with a concentration parameter higher than $\alpha + \Delta\alpha$ will move into the interval while other drops will move out of the interval. The ingoing fraction is

$$\Delta g_{1+} = g(\alpha + \Delta\alpha) \Delta'\alpha$$

where

$$\Delta'\alpha = K(\alpha + \Delta\alpha)^n \Delta\xi$$

and the outgoing fraction is

$$\Delta g_{1-} = g(\alpha) \Delta''\alpha$$

where

$$\Delta''\alpha = K(\alpha)^n \Delta\xi$$

Together this gives a total effect:

$$\Delta g_1 = K \frac{d}{d\alpha} \{ \alpha^n g(\alpha) \} \Delta\alpha \Delta\xi$$

(b) *Carry-off with the product stream*. This contribution equals

$$\Delta g_2 = -g(\alpha) \Delta\alpha \Delta\xi$$

(c) *A feed by coalescing*. Drops with a concentration parameter between β and $\beta + d\beta$ will produce twice as many drops in the considered range when coalescing with drops which have a concentration parameter between $(2\alpha - \beta)$ and $(2\alpha + 2\Delta\alpha - \beta - d\beta)$. Therefore,

$$\begin{aligned} \Delta g_3 &= 2I \Delta\xi \int g(\beta)g(2\alpha - \beta)2\alpha d\beta \\ &= 4I \Delta\xi \Delta\alpha \int g(\beta)g(2\alpha - \beta) d\beta \end{aligned}$$

Here I is the interaction modulus. The integration has to be carried out over all possible values of β , that means over the interval

$$2\alpha - 1 < \beta < \alpha \quad \text{when} \quad \alpha > \frac{1}{2}$$

and

$$0 < \beta < \alpha \quad \text{when} \quad \alpha < \frac{1}{2}.$$

In the latter case, however, there is also a contribution of the fraction G_0 of drops with zero concentration. When these drops coalesce with drops in the interval $(2\alpha; 2\alpha + 2\Delta\alpha)$, drops of the desired concentration are also produced:

$$\Delta g_3' = 4IG_0g(2\alpha) \Delta\xi \Delta\alpha$$

(d) *Carry-off by coalescing*. All drops of the considered interval continuously have a chance, by coalescing with drops of other concentrations, to disappear out of the interval. This contribution equals

$$-\Delta g_4 = I g(\alpha) \Delta\alpha \left\{ \int_0^1 g(\beta) d\beta + G_0 \right\} \Delta\xi$$

or

$$\Delta g_4 = -I g(\alpha) \Delta\alpha \Delta\xi$$

Summing up all these contributions the total must be equal to the change with time

$$(\Delta g)_{\text{total}} = \frac{dg}{d\xi} \Delta\alpha \Delta\xi$$

Therefore,

$$\frac{dg}{d\xi} = K \frac{d}{d\alpha} \{\alpha^n g(\alpha)\} - (1 + I)g(\alpha) + 4I \int_{2\alpha-1}^{\alpha} g(\alpha)g(2\alpha - \beta) d\beta \quad \text{for } \alpha > \frac{1}{2}$$

and

$$\frac{dg}{d\xi} = K \frac{d}{d\alpha} \{\alpha^n g(\alpha)\} - (1 + I)g(\alpha) + 4I \int_0^{\alpha} g(\alpha)g(2\alpha - \beta) d\beta + 4IG_0g(2\alpha) \quad (40)$$

for $\alpha < \frac{1}{2}$

In the steady state $dg/d\xi = 0$ for each value of α , while the boundary condition requires that for $\alpha = 1$, $g = 1/K$. When for a certain case all the parameters n , K , I , τ , and C_0 are kept constant the solution of the dynamic equations must evolve to that of the steady state. On a digital computer this procedure has been followed by Curl (C8). He used different numbers of $\Delta\alpha$ intervals (25, 50, and 100), let the transient evolve to the steady state, and then extrapolated the calculated values of $g(\alpha)$ to $\Delta\alpha = 0$. For the procedure followed by Veltkamp to solve these equations, one must be referred to his paper (V2).

Very recently Spielman (S6) calculated the influence of interaction by means of Monte Carlo methods. This very interesting method, which is in fact a direct simulation of the physical process happening, makes it possible to obtain a reasonable accuracy even up to conversions of 99%. His results are in fair agreement with the results obtained by Curl and Veltkamp.

B. DEAD-CORNER INTERACTION MODEL

In this model, and also in the next one, the interaction is no longer homogeneously distributed. As a consequence, the segregation is not pure microscale segregation, but a combination of micro- and macroscale segregation.

Stirred tank reactors are often equipped with baffles in order to obtain an optimal effect of the action of the stirrer and to distribute turbulence as homogeneously as possible. As a consequence, however, this may introduce some dead corners in the wake of these baffles.

Also, when the wall of the stirring vessel is preferentially wetted by the dispersed phase, the wall may be covered with a thin stagnant layer of dispersed phase, which may act, more or less, as a "dead" corner in so far as the chemical reaction is slowed down by poor mass transfer. However, there still may occur a continuous coalescing of dispersed drops with these stagnant layers and corners, while on the other hand these "dead" corners will continuously lose new drops, which are taken up again in the "living" dispersed phase. In this way the "dead" corners act as a medium of interaction.

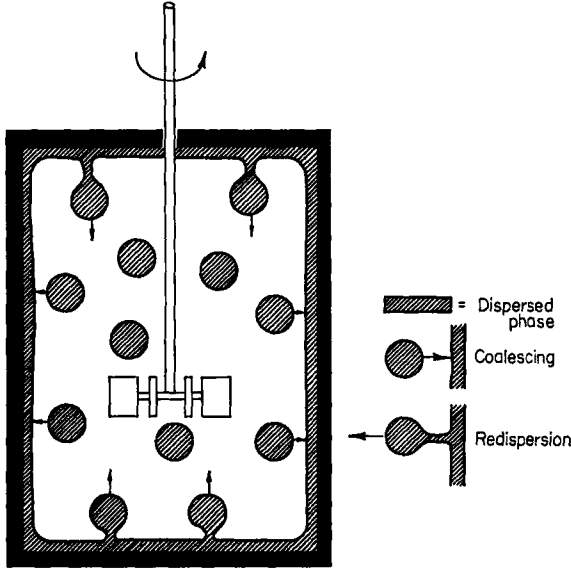


FIG. 18. Principle of *dead corner* interaction.

In the dead-corner interaction model described here, it is assumed that this is the only type of interaction that takes place in the system. This is shown schematically in Fig. 18.

In the stationary state, the total volume contained by the dead corners

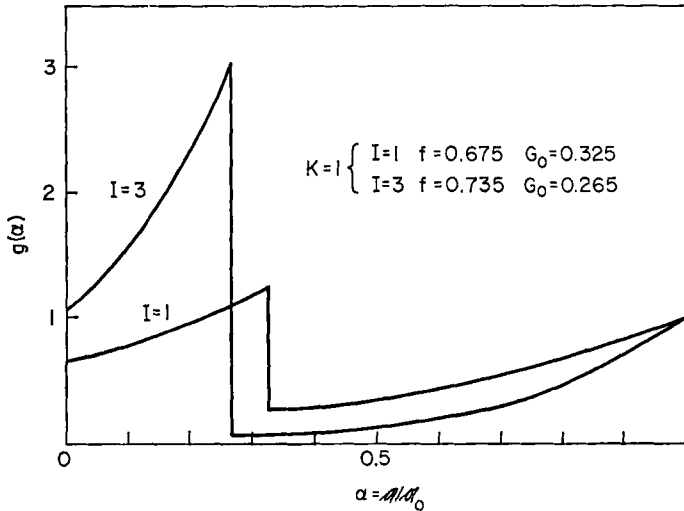


FIG. 19. Two concentration distributions in the dispersed phase for the case of dead corner interaction.

is also constant. When there is no chemical reaction going on in this dead volume, and further, the chance of coalescence with the dead volume is the same for all drops, then the concentration in the dead volume must be equal to the average concentration in the reactor. Then the drops which are produced from the dead volume must also have this average concentration. This means that the concentration distribution of the drops shows a discontinuity at the average concentration in such a way that, when going through the concentration range coming from the feed concentration, the distribution function g falls off; but, at the average concentration, it suddenly jumps to a higher value, only to fall off again when the concentration is decreased further (see Fig. 19). The interaction is described again by a parameter

$$I' = \frac{\text{number of drops coalescing with dead volume in unit time}}{\text{number of drops fed to the reactor in unit time}}$$

This model is simpler to evaluate than the homogeneous interaction model. This evaluation even can be performed without numerical integration. The derivation of the formulas describing this interaction is given below.

The result for zero-order drop conversion is shown in Fig. 20 and for half-order drop conversion in Fig. 21. When compared with the homo-

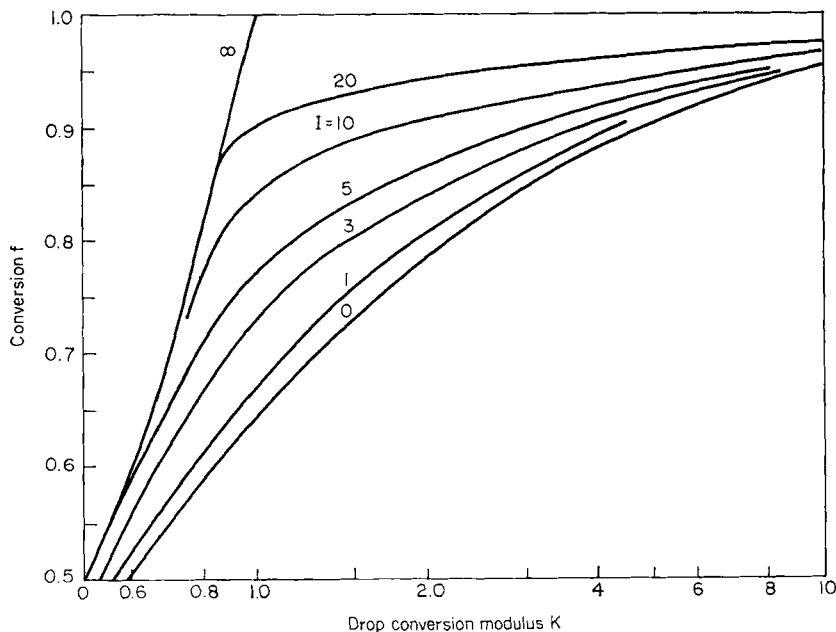


FIG. 20. Effect of dead corner interaction in a CSTR on the conversion. *Zero-order drop conversion.*

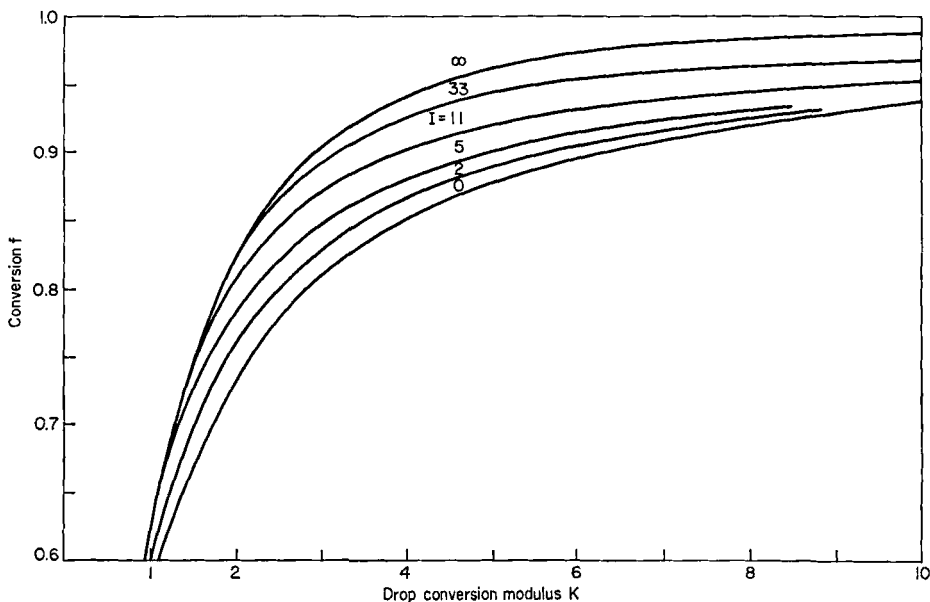


FIG. 21. Effect of dead corner interaction in a CSTR on the conversion. Half-order drop conversion.

geneous interaction model, about the same course of conversion dependence is obtained. The dead corner interaction, however, proves to be more efficient (at the same values of K and I) than the homogeneous interaction. This is not surprising since in homogeneous interaction, especially at higher conversions, many coalescences occur between drops with zero concentration and, therefore, are not effective, while in the case of dead corner interaction every coalescence produces a new drop with the average concentration and so every coalescence is effective.

Suppose the process is a n th-order drop conversion process. As remarked before, the concentration distribution in the dispersed phase consists of three parts:

- (1) a distribution function g_1 running from the feed concentration a_0 to the average concentration \bar{a} ,
- (2) a distribution function g_2 running from \bar{a} to zero,
- (3) a fraction G_0 consisting of all the drops with zero concentration.

A mass balance gives

$$\int_{\bar{a}}^{a_0} g_1(a) da + \int_0^{\bar{a}} g_2(a) da = 1 - G_0 \quad (41)$$

Let us consider a small fraction of drops with concentration between a and $a + \Delta a$. In this fraction drops continuously arrive by chemical reaction from higher concentration, but also drops are lost by chemical reaction to fractions of smaller concentration.

Furthermore drops are lost through the outlet and by coalescence with the dead corners.

When the total number of drops present in the reactor is N , while q drops are lost per unit time through the outlet and p drops are coalescing with the dead corner, then during a time dt :

$$N\{g(a + \Delta a) da' - g(a) da''\} - qg(a + \frac{1}{2} \Delta a) da dt - pg(a + \frac{1}{2} \Delta a) da dt = 0$$

in which

$$da' = -k(a + \Delta a)^n dt$$

and

$$da'' = -ka^n dt.$$

When $\tau = N/q$ = the average residence time, $\tau_1 = N/p$ = the reverse of the coalescing frequency, and $I = \tau/\tau_1$ = the interaction modulus, then

$$\frac{d[a^n g(a)]}{a^n g(a)} = -\frac{da}{ka^n} \left(\frac{1}{\tau} + \frac{1}{\tau_1} \right) \quad (42)$$

or

$$g(a) = \frac{A_0}{a^n} \exp \left[\frac{a^{1-n}}{(1-n)k} \left(\frac{1}{\tau} + \frac{1}{\tau_1} \right) \right]$$

in which A_0 is a constant determined by the boundary conditions. This result holds for both functions g_1 and g_2 . Only the boundary conditions are different:

$$g_1(a) = \frac{1}{k\tau a^n} \quad \text{at } a = a_0$$

$$g_2(a) = g_1(a) + \frac{1}{k\tau_1 a^n} \quad \text{at } a = \bar{a}$$

This finally results in

$$g_1(a) = \frac{1}{k\tau a^n} \exp \left[\frac{a^{1-n} - a_0^{1-n}}{(1-n)k\tau} (1 + I) \right]$$

and

$$g_2(a) = \frac{1}{k\tau a^n} \exp \left[\frac{a^{1-n} - a_0^{1-n}}{(1-n)k\tau} (1 + I) \right] + \frac{1}{k\tau_1 a^n} \exp \left[\frac{a^{1-n} - \bar{a}^{1-n}}{(1-n)k\tau} (1 + I) \right] \quad (43)$$

By introducing

$$\gamma = \frac{a^{1-n}}{(1-n)k\tau} \quad \text{and} \quad \gamma_0 = \frac{a_0^{1-n}}{(1-n)k\tau}$$

and remembering that $g(\gamma) = g(a) da/d\gamma$ we find

$$g_1(\gamma) = \exp [(\gamma - \gamma_0)(1 + I)]$$

and

$$g_2(\gamma) = \exp [(\gamma - \gamma_0)(1 + I)] + I \exp [(\gamma - \gamma_x)(1 + I)] \quad (44)$$

In this latter equation

$$\gamma_x = \frac{\bar{a}^{1-n}}{(1-n)k\tau}$$

where $s = 1/(1 - n)$. The degree of conversion f is now given by the equation

$$f = 1 - \bar{\gamma}^s / \gamma_0^s$$

Therefore, it is necessary to solve $\bar{\gamma}^*$.

For $n = 0$:

$$\bar{\gamma}^* = \bar{\gamma} = \gamma_x$$

$$\begin{aligned}\bar{\gamma} &= \int_{\bar{\gamma}}^{\gamma_0} \gamma g_1(\gamma) d\gamma + \int_0^{\bar{\gamma}} \gamma g_2(\gamma) d\gamma \\ &= \int_0^{\gamma_0} \gamma \exp [(\gamma - \gamma_0)(1 + I)] d\gamma + I \int_0^{\bar{\gamma}} \gamma \exp [(\gamma - \bar{\gamma})(1 + I)] d\gamma\end{aligned}$$

This results in

$$(1 + I)(\gamma_0 - \bar{\gamma}) = 1 - \exp [-(1 + I)\gamma_0] + I\{1 - \exp [-(1 + I)\bar{\gamma}]\} \quad (45)$$

When $(1 + I)\gamma_0 = b$ and $(1 + I)\bar{\gamma} = c$, then

$$I = \frac{b - c - 1 - e^{-b}}{1 - e^{-c}}, \quad (46)$$

while $f = 1 - c/b$. For different combinations of b and c we now can calculate f and I and then also γ_0 . In Fig. 20, the conversion f has been plotted against $K = 1/\gamma_0(1 - n)$ for different values of I .

For $n = \frac{1}{2}$:

$$\bar{\gamma}^* = \bar{\gamma}^2 = \gamma_x^2$$

$$\gamma_x^2 = \int_0^{\gamma_0} \gamma^2 \exp [(\gamma - \gamma_0)(1 + I)] d\gamma + I \int_0^{\gamma_x} \gamma^2 \exp [(\gamma - \gamma_x)(1 + I)] d\gamma$$

and

$$\begin{aligned}(1 + I)^2 \gamma_x^2 &= (1 + I)^2 \gamma_0^2 - 2\{(1 + I)\gamma_0 - 1 + \exp [\gamma_0(1 + I)]\} \\ &\quad - 2I\{(1 + I)\gamma_x - 1 + \exp [\gamma_x(1 + I)]\}\end{aligned} \quad (47)$$

When again $(1 + I)\gamma_0 = b$ and $(1 + I)\gamma_x = c$, then

$$I = \frac{b^2 - c^2 - 2b + 2 - 2e^{-b}}{2(c - 1 + e^{-c})} \quad \text{and} \quad f = 1 - \frac{c^2}{b^2} \quad (48)$$

Figure 21 presents the result of this equation, again as a plot of f versus K for different values of I .

It may be remarked that when, in the above equations, we let $I \rightarrow 0$ or $I \rightarrow \infty$ indeed the same equations as already derived in Section II,A,1 are obtained.

C. CIRCULATION INTERACTION MODEL

A study carried out at the Lawrence Radiation Laboratory of the University of California by Vanderveen (V1) strongly suggests another type of interaction model; see also Vermeulen (V5). Vanderveen measured the drop size at different distances from the impeller of a baffled, stirred tank reactor in which two immiscible liquid phases were contacted, and found that a very substantial increase in drop size occurs at remote distances. The increase, which was attributed to coalescence, appeared to be dependent on the physical properties of the phase system.

As is well known, in baffled, stirred tank reactors there is a strong circulation pattern, as shown in Fig. 22. The dispersed drops will move with this

circulation, break up into small drops in the vicinity of the impeller, and then coalesce to form larger drops further on in the circulation path, while there is little redispersion on this path because of the decay in turbulence along this path. When returning to the impeller the larger drops are broken

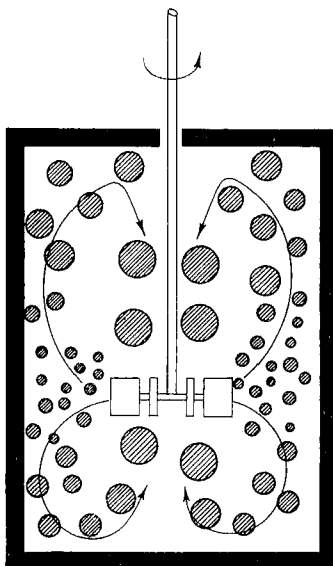


FIG. 22. Circulation of dispersed phase in a baffled two-phase mixing vessel.

up and the whole cycle starts again. Schematically this process is shown in Fig. 23. Of course, this continuous breakup produces a very strong interaction as the small drops, into which one big drop is broken up after passing the impeller, certainly will not unite again to form the same big drop, but will be statistically distributed over many larger drops during coalescing. Two things happen during one circulation:

(a) Because the drops are continuously coalescing without redispersing, mass transfer limitation will increase. Since orders of drop conversion of less than 1 are nearly always caused by mass transfer limitation; this means that the drop conversion rate constant will decrease along a circulation path.

(b) When close to the impeller, there is a more or less pronounced concentration distribution in the small drops; this concentration distribution will be reduced by the continuous coalescing of arbitrary drops to larger drops.

The mechanism of interaction can, therefore, no longer be described by one

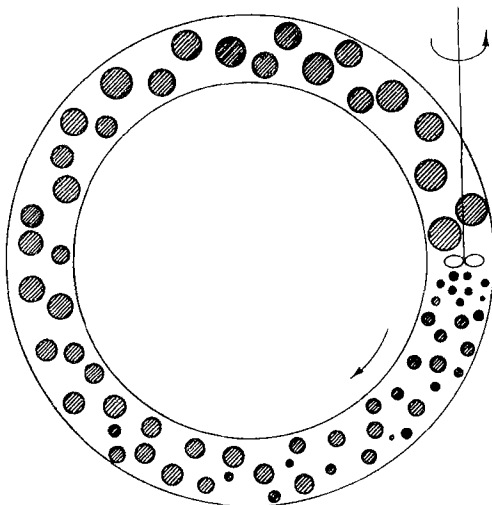


FIG. 23. Principle of circulation interaction.

parameter, but at least two parameters are necessary. The first parameter which is proposed is

$$\lambda = \left(\frac{\text{maximum drop size}}{\text{minimum drop size}} \right)^3$$

λ indicates the total number of small drops which, during one circulation, unite to one large drop. The second parameter then must be

$$\nu = \frac{\text{average residence time}}{\text{time necessary for one circulation}}$$

ν indicates the average number of circulations which a molecule of the dispersed phase goes through during its stay in the reactor. It will be clear that this model is extremely complicated and difficult to evaluate. Only when λ is small (say less than 3) (so that the effect of increased mass transfer limitation can be neglected) and when, at the same time, ν is large (so that pure statistical methods can be applied) can the two parameters be united into a single parameter, $I = \lambda\nu$, which is exactly equal to the parameter used in the homogeneous interaction model. Also, the two models then become nearly identical.

As yet no solution of this model is known.

D. HARADA INTERACTION MODEL

Harada *et al.* (H1) proposed a model in which each drop of the dispersed phase shows an interaction process at regular time intervals t_e . During such an interaction the drop exchanges matter with an imaginary drop of the

same size, but with the average concentration. After this interaction, the original drop starts to react again during a time t_c , after which the process is repeated. Each drop, therefore, more or less keeps its own identity and only gets a "revival" after each time t_c . The physical meaning of this model is shown in Fig. 24.

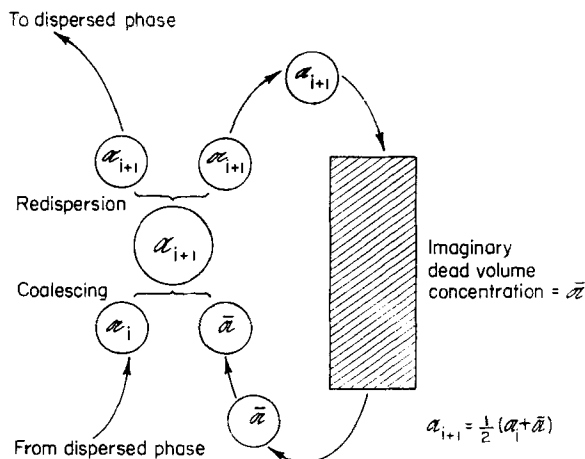


FIG. 24. Harada interaction model.

An imaginary dead volume of the dispersed phase, which by frequent interactions keeps its own concentration equal to the average concentration, continuously produces drops of the average concentration which coalesce with drops of the "living" dispersed phase and exchanges matter with these drops by coalescing and redispersion. After redispersion, however, only one of the two "product" drops stays in the "living" dispersed phase while the other "product" drop returns to the imaginary dead volume. It is especially this latter phenomenon which is quite incomprehensible.

Some resemblance with the diffusion interaction, discussed in Section I,C cannot be denied. At diffusion interaction, however, the interaction occurs continuously and not only at regular intervals. Also, in the diffusion interaction model the interaction is never complete but only tends to reduce the driving force.

As the Harada model, therefore, seems to be very unsatisfactory, the solution of this model will not be further discussed here.

IV. Measurements of the Interaction Rate

Experiments to measure the interaction rate in a dispersed phase system have been carried out by Madden and Damerell (M2), Miller *et al.* (M4),

Groothuis and Zuiderweg (G3), and by Kramers and co-workers (K2), while qualitative experiments were carried out by Matsuzawa and Miyauchi (M3). All these methods use the homogeneous interaction model to interpret the results obtained, while generally care is taken to prevent wetting of the wall by the dispersed phase in order to avoid dead corners.

The methods which have been used so far can be classified into two categories:

(I) Methods in which the course of coalescing is measured by means of a chemical reaction as tracer.

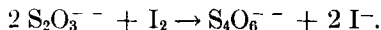
(II) Methods in which the course of coalescing is measured with pure physical means.

A. MEASUREMENTS BY MEANS OF A CHEMICAL REACTION

When the interaction rate is measured in this way one studies the course of a chemical reaction which occurs in the dispersed phase between two components. One component (C) is present in the reactor before the experiment starts and either is dissolved in the continuous phase or homogeneously distributed in the dispersed phase. The other component (A) is added at the beginning of the experiment in a highly concentrated form in a very small extra volume of the dispersed phase. The total amount of A must at least be the stoichiometric equivalent of the total amount of component C already present in the reactor.

When component C is added to the continuous phase this component is extracted to the dispersed phase, but chemical reaction can take place only in drops containing component A. By continuously coalescing and redispersing, the number of drops containing component A is increasing, however, and therefore, the over-all conversion rate will increase. It is required in this method that the order of drop conversion in component A be equal to zero, so that the drop conversion rate be independent of the concentration in the drop.

In this way Madden and Damerell (M2) used the chemical reaction:



In their experiments water was the dispersed phase and toluene the continuous phase. Iodine was dissolved in the toluene, while a concentrated sodium thiosulfate solution was introduced into the reactor at the beginning of the experiment. The free iodine was extracted from the continuous phase to the sodium thiosulfate-containing drops, the number of which was continuously increasing by coalescence and redispersion. The progress of the extraction process was followed by withdrawing samples of the continuous phase and analyzing the iodine content by light absorption. When M is the number of drops which contain thiosulfate, N the total number of drops,

and ω_i the coalescing frequency, it follows from the homogeneous interaction model (see Section III,A) that

$$M = N \frac{Y + e^{-\omega_i t}}{Y} \quad (49)$$

where $Y = M_0/(N - M_0)$ and M_0 is the number of thiosulfate-containing drops at time $t = 0$. When c is the concentration of the iodine in toluene (c_0 being its initial value) and V_c is the total volume of the continuous phase, then

$$-V_c \frac{dc}{dt} = 4\pi R^2 m_0 M c$$

in which m_0 is the mass transfer coefficient and R the radius of a drop. It now follows that

$$\ln \frac{c_0}{c} = \frac{4\pi R^2 m_0 N}{V_c \omega_i} \ln \frac{1 + Y e^{\omega_i t}}{1 + Y} \quad (50)$$

Madden and Damerell carried out their study in a 1.5-liter vessel of stainless steel internally coated with Teflon to prevent wetting by the aqueous dispersed phase. This reactor was stirred by means of a turbine and equipped with wall baffles. They investigated the effect of stirring rate (corresponding with a power input from 0.25 to 2 hp./m.³) and the effect of dispersed phase fraction from 0.0014 to 0.011. The interaction rate ω_i they found varied from 0.04 to 0.5 sec.⁻¹ (see Fig. 25).

Kramers and co-workers used a different method. In their set-up, component 1 is dissolved in the dispersed phase and distributed evenly over this phase before component 2 (dissolved in an extra, but small, volume of dispersed phase) is added. Now the reaction can proceed only when a coalescence occurs between a drop containing component 1 and a drop containing component 2. Because of the high concentration of component 2, the total amount of component 1 contained in the coalesced drops will be entirely consumed, and after redispersion two drops containing only component 2 will result. Also in this case, therefore, the over-all conversion rate is increasing when the interaction proceeds. The only requirement of the reaction is that it be very rapid and that the components do not dissolve in the continuous phase.

In the experiments of Kramers and co-workers, water was the dispersed phase and a mixture of toluene and carbon tetrachloride (density = 965 kg./m.³) the continuous phase. Two types of tracer reactions (I and II) were used:

Reaction I: $5 \text{ I}^- + 6 \text{ H}^+ + \text{IO}_3^- \rightarrow 3 \text{ I}_2 + 3 \text{ H}_2\text{O}$. The dispersed phase contained 4 N sulfuric acid and potassium iodate (KIO_3). At the beginning of the experiment a few drops of a potassium iodide (KI) solution was

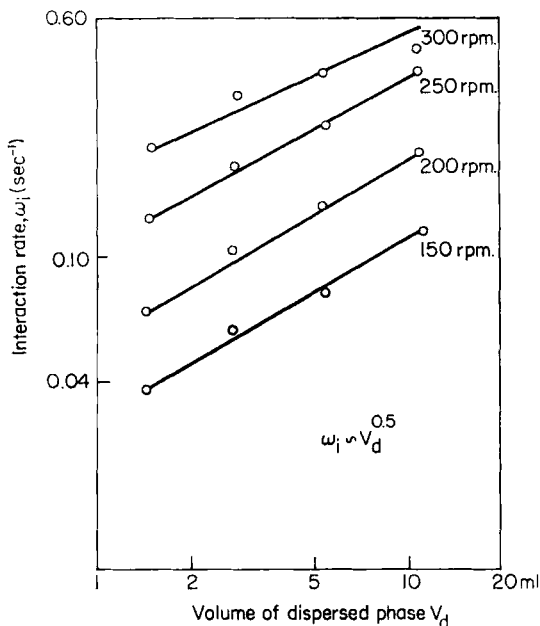


FIG. 25. Results of Madden and Damerell obtained in a 1500-ml. mixing vessel, containing 1000 ml. toluene-iodine solution as continuous phase and water as dispersed phase.

added. The course of the reaction was followed by measuring the light absorption, which increases because the free iodine product was extracted into the continuous toluene phase and then had a bluish-red color.

Reaction II: $4 \text{FeCl}_3 + 3 \text{K}_4\text{Fe}(\text{CN})_6 \rightarrow \text{Fe}_4[\text{Fe}(\text{CN})_6]_3 + 12 \text{KCl}$. The dispersed phase contained the ferrocyanide, and at time $t = 0$ a few drops containing the ferric chloride were added. Because the product $\text{Fe}_4[\text{Fe}(\text{CN})_6]_3$ had a blue color, the course of reaction again could be followed by measuring the light absorption.

Measurements were carried out in a 6-liter brass vessel stirred by means of a flat blade stirrer and equipped with 4 wall baffles. The influence of dispersed phase fraction and of stirring rate was investigated. The dispersed phase fraction was varied from 0.05 to 0.15 while the power input by the stirring was varied from 0.1 to 3 hp./m.³. The interaction rate found was invariably 0.035 sec.⁻¹. Another experiment was carried out by Kramers and de Korver using a short rotary contactor (height = 10 cm., diameter = 9.3 cm., diameter of rotor = 8.0 cm.) which was made entirely of Teflon to prevent wetting of the wall by the aqueous dispersed phase. This reactor

was operated continuously, while reaction II was used to trace the coalescing rate. In this continuous operation it was necessary to feed two dispersed phases, one with the sodium ferrocyanide and the other containing the ferric chloride. Conditions were chosen in such a way that only part of the dispersed drops became colored. The fraction of colored drops was measured by letting the outgoing stream flow over a flat, nearly horizontal, open drain on which all drops could be seen separate from the others. By photographing, and counting the number of blue drops, the interaction rate could be determined. The dispersed phase fraction was always 2.6%. At a rotary speed of 350 min.⁻¹ it was found that $\omega_i = 0.1$ sec.⁻¹, and at a rotary speed of 450 min.⁻¹ $\omega_i = 0.03$ sec.⁻¹.

Matsuzawa and Miyauchi (M3) tried to measure the interaction rate by means of the chemical reaction $2 \text{FeCl}_3 + \text{SnCl}_2 \rightarrow 2 \text{FeCl}_2 + \text{SnCl}_4$ which takes place in the dispersed phase. The two components are mixed before entrance in the reactor, and so the rate of interaction can only be measured indirectly from interpretation of the conversion-mean residence time curve. As follows from the theory for a chemical reaction of which the order of drop conversion is greater than 1, the over-all rate of conversion is higher if there is segregation in the dispersed phase than if the dispersed phase is entirely mixed by means of a high interaction rate. The qualitative conclusion which Matsuzawa and Miyauchi could draw from their experiments was that the conditions in their reactor were very close to complete segregation, which means a negligible interaction rate as compared with the drop conversion rate.

A last possibility, which has not been reported so far, is a method in which one measures the heat of reaction, which is released when drops containing component 1 coalesce with drops containing component 2. This method is only suitable in continuous operation, as otherwise the temperature rise that would occur would affect both the interaction rate and the chemical conversion rate. All other methods mentioned so far are suitable both for batch operation and for continuous operation, with a slight preference for the latter since steady-state operation probably will give more reproducible results. A limitation of all the above methods is that only the interaction rate of an aqueous dispersed phase can be measured, because of the requirement that the chemical reaction be nearly instantaneous. A further disadvantage is that the dispersed phase itself is not of uniform composition, so that the interfacial tension may not be the same for all drops, and therefore the drop size may depend on the amount and type of reactants which the drops contain.

The method used by Madden and Damerell and also the method by means of reaction (I) of Kramers have the disadvantage that mass transfer from the continuous phase to the dispersed phase or vice versa is involved,

which may induce Marangoni effects, and as a consequence the interaction rate may be increased or decreased.

B. MEASUREMENTS BY PURE PHYSICAL MEANS

Miller and associates (M4) measured the interaction rate in a liquid-liquid two-phase *batch* reactor by means of a light transmission technique, which has the advantage that it can be used with the aqueous phase or the organic phase dispersed.

They added a small quantity of highly colored drops to the reactor which otherwise contained only uncolored drops dispersed in the continuous phase. As the color is spread more uniformly about the whole dispersed phase by continuous coalescing and redispersion, the light transmission of the emulsion is decreased according to

$$\frac{\log T_0 - \log T_t}{\log T_0 - \log T_\infty} = 1 - Fe^{-1/2\omega_i t} \quad (51)$$

In this equation T_0 is the light transmission before the dye is added, T_∞ is the light transmission when the dye has spread uniformly over all the drops of the dispersed phase, T_t is the light transmission at a time t after the dye has been added, ω_i is the interaction rate constant, and F is a constant which can be determined experimentally. For the derivation of this formula, one is referred to the paper by Miller *et al.*

Experiments which were essentially batch experiments were performed in reactors of three different sizes, which could be equipped with different kinds of stirring impellers. Special attention was devoted to the injection of the dye; also, the dye itself was carefully selected in relation to the requirement of nonsurface activity. Some of their results are shown in Fig. 26.

Finally, very recently, a method was published by Groothuis and Zuiderweg (G3). Their method can in principle be used also with both phases dispersed, although their results are obtained with an organic phase dispersed. Where the method by Miller *et al.* is essentially a batch mixing experiment, the method of Groothuis and Zuiderweg is essentially a continuous-flow experiment. To a system in which water is the continuous phase they feed continuously two dispersed organic phases, both consisting of a mixture of benzene and carbon tetrachloride but of slightly different composition so that one dispersed phase had a slightly higher density (1.03 g./ml.) than the continuous phase, while the density of the other dispersed phase (0.990 g./ml.) was a little lower than that of the continuous phase. The emulsion was separated in a settler. Through the upper outlet, part of the continuous phase together with "light" dispersed phase was removed, while through the lower outlet the remaining part of the continu-

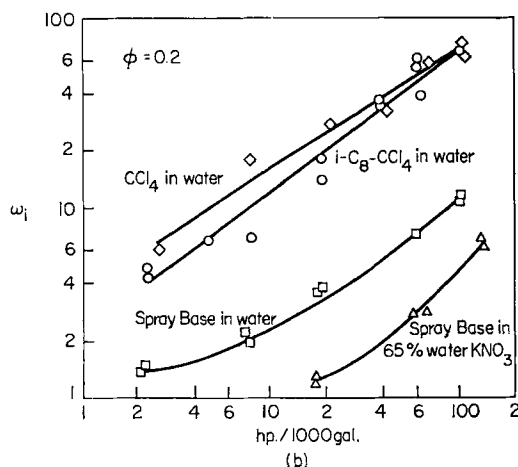
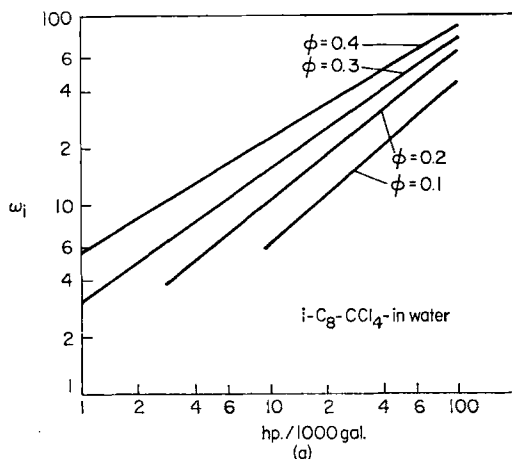


FIG. 26. Results obtained by Miller *et al.* in a 0.30-gal. vessel, propellor in draft tube. (a) Effect of power input and dispersed fraction. (b) Effect of system on interaction rate at $\phi = 0.20$.

ous phase together with the heavy dispersed phase was discharged. This heavy phase also contained that part of the "light" dispersed phase which had interacted with the heavy dispersed phase. This interaction resulted, however, in a dispersed phase which, because of the choice of the original densities, was still of a higher density than the continuous phase. Thus, by measuring the increase of the amount of the heavy phase in the outlet, the interaction rate could be determined.

Groothuis and Zuideweg also measured the influence of mass transfer on the interaction rate and found that when 1.37% acetic acid was added

to the dispersed phase, a twenty-fold increase in the interaction rate resulted. Their results are presented in Fig. 27, in which results obtained by the other investigators are also compared. The data of Madden and Damerell are also extrapolated for a phase ratio $\phi = 0.1$ by means of the correlation $\omega_i \propto \phi^{0.5}$, which was found both by Madden and Damerell, and by Miller *et al.*

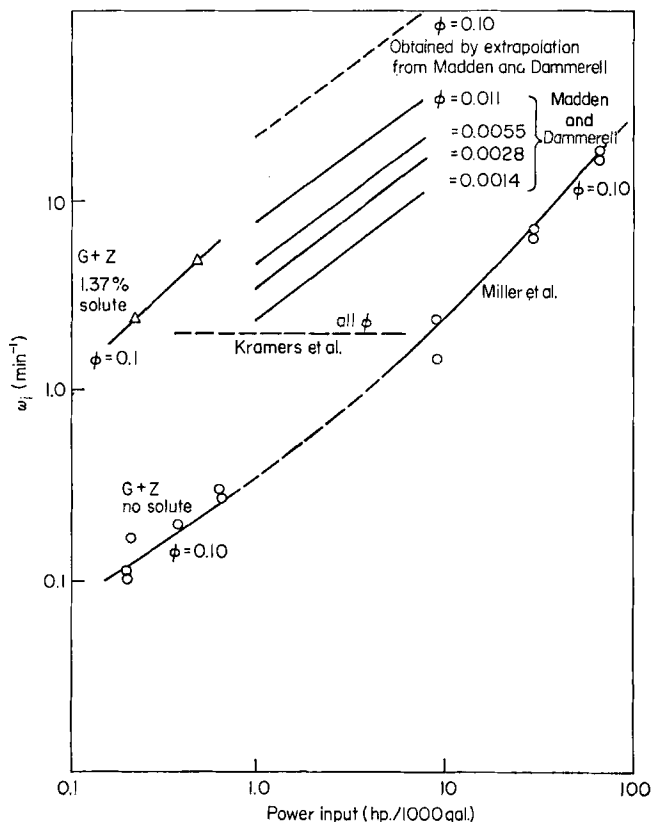


FIG. 27. Experiments of Groothuis and Zuiderweg compared with results of others.

Although the results obtained by Miller *et al.* and those of Groothuis and Zuiderweg for the case of no solute seem to fit remarkably well on one correlating curve, the total picture is so complicated that it must be concluded that quite a lot of work has still to be done before an interaction rate can be predicted with reasonable accuracy for a given phase system at given operating conditions. Nevertheless, the following general conclusions may be drawn with some caution:

- (a) ω_i increases with power input and with the phase ratio ϕ .
- (b) Mass transfer from the drops to the continuous phase seems to increase ω_i strongly.
- (c) When the dispersed phase is an organic liquid, the interaction rate is much lower than when the dispersed phase is an aqueous liquid.
- (d) Both Madden and Damerell, as well as Miller *et al.*, found that addition of inorganic salts to the aqueous phase gives more reproducible results.
- (e) When, for commercial processes (in which the average residence time τ generally falls between several minutes and several hours), the interaction modulus, $I = \omega_i \tau$, is evaluated, a comparison with the graphs of Figs. 15, 16, 20, and 21 leads to the conclusion that in most cases segregation will neither be complete nor zero, and that the interaction rate is a factor which is of high importance in reactor design both to obtain a high degree of conversion and a good selectivity.

V. Discussion about the Interaction Rate

In this section some general aspects of the interaction rate ω_i will be discussed, in particular, the influence of physical and physico-chemical factors. Since we will be considering only those systems that are in a stationary state, the interaction rate can be put equal to the coalescing rate, which is equal to the total volume fraction of the dispersed phase which during unit time is involved in coalescence. Under these circumstances it will be clear that the equilibrium average drop size is determined both by the rate of dispersion, which continuously creates new interfacial area, and by the coalescing rate, which continuously destroys interfacial area. This was already realized by several investigators in the field of liquid-liquid dispersions (C1, R5, V4) and more recently has led to at least a qualitative explanation of the different results obtained for the dependence of average drop size on power input by these investigators (S1).

A. THE CHURCH-SHINNAR CRITERIUM

An interesting theory has been put forward recently by Church and Shinnar (C6, S1, S2). They suppose that very small drops may adhere to each other to form coagulates of still small size, in which the energy of adhesion is larger than the kinetic energy of the turbulent eddies, with a scale comparable to the size of the coagulate, and which tends to remove the separate small drops in the coagulate. In these more or less stable coagulates, coalescing will occur, which ultimately will result in larger drops. There is a critical drop size below which coagulation and, therefore,

coalescing is possible and above which the drops are continuously separated from each other by turbulence before coalescing might occur.

Accepting Kolmogoroff's theory of local isotropy, they find for the critical drop size the relation

$$c_1 \rho \epsilon^{2/3} d^{8/3} / A(h_0) = \text{constant} \quad (52)$$

in which ϵ is the local rate of turbulent energy dissipation per unit mass of fluid, ρ is the density of the continuous phase, and $A(h_0)$ is the energy needed to separate two drops of unit radius from an initial minimum distance h_0 to infinity. Whence, granting the equation for breakup of drops as derived by Hinze (H_2):

$$We(\text{crit}) = \frac{\rho c_2 \epsilon^{2/3} d^{5/3}}{\sigma} = \text{constant} \quad (53)$$

in which σ is the interfacial tension and, assuming that ϵ is proportional with the stirrer speed to the third power, Church and Shinnar are able to make a plot of the drop diameter against the stirrer speed in which there must be a region in which neither breakup nor coalescence occurs (see

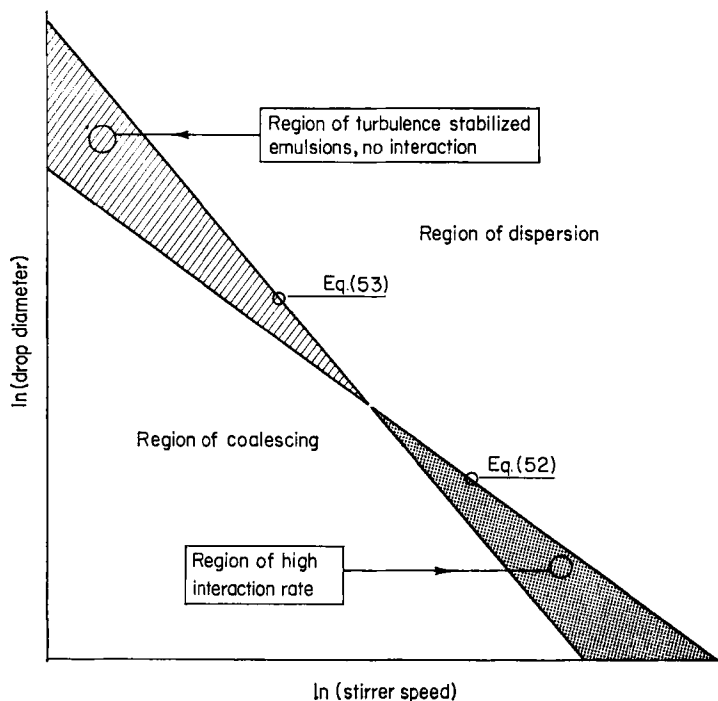


FIG. 28. Church-Shinnar graph.

Fig. 28). Dispersions which fall in this region are called by Church and Shinnar "turbulence-stabilized" dispersions. As pointed out by them, the function $A(h_0)$ depends strongly on the phase system and on whether stabilizing colloids are present or not.

This theory of Church and Shinnar certainly will prove its value, although it has its limitations as well. One of these limitations is that they assume that the turbulence is homogeneously distributed throughout the vessel containing the emulsion. The studies of Vanderveen (V1) and also of Weiss *et al.* (W1) have clearly shown that this generally is not the case and that dispersion occurs in the vicinity of the stirrer while coalescing occurs away from the stirrer (see also the circulation interaction model, Section III,C). Finally the theory only gives an answer to the question of whether or not coalescence is possible but not to the question of how strong the coalescing rate is.

B. THE COLLISION RATE p_0

In the stationary state we may write

$$\begin{aligned}\omega_i &= \left(\frac{\text{total number of effective}}{\text{collision between drops}} \right) \cdot n_c \cdot \left(\frac{\text{average volume of one drop}}{\text{total volume of dispersed phase}} \right) \\ &= (p_{\text{eff}}) \left(\frac{\pi d^3}{6\phi V} \right) (n_c)\end{aligned}$$

where d is the average drop diameter, ϕ the volume fraction of dispersed phase $[= 1/(1+h)]$, V the total reactor volume, and n_c the number of drops involved in one coalescence. Furthermore, the total number of effective collisions p_{eff} is equal to the product of the number of all collisions p_0 times the chance P that a collision will prove to be effective, i.e., will be followed by a coalescing.

$$p_{\text{eff}} = p_0 P \quad \text{and} \quad \omega_i = p_0 P \frac{\pi d^3}{6\phi V} n_c$$

1. Homogeneous Interaction

In the case of homogeneous interaction the mechanism of collisions between separate drops will show some resemblance to the collision mechanism between separate molecules, as assumed in the kinetic gas theory. In accordance with this theory, the collision rate p_0 can be put equal to

$$p_0 = \pi \frac{\sqrt{2}}{2} \bar{u} d^2 \frac{N^2}{V} \quad (55)$$

in which \bar{u} is the average turbulent fluctuation at the scale of the average distance between the drops. Since $\phi = N\pi d^3/6V$ and, in this case, $n_c = 2$, it follows that

$$\omega_i = \left(\frac{12\bar{u}}{\sqrt{2}} \frac{\phi}{d} \right) P \quad (56)$$

From Kolmogoroff's theory of local isotropic turbulence [see Batchelor (B1)] it follows that $\bar{u} \propto \epsilon^{1/3} d^{1/3}$ where ϵ is the turbulent energy dissipation per unit time per unit volume. Therefore,

$$\omega_i \propto \left(\frac{\epsilon^{1/3} \phi}{d^{2/3}} \right) P \quad (57)$$

One must be warned here not to infer the dependence of ω_i on ϵ from this relation, because P will depend on ϵ in an as yet unknown fashion.

Recently, Howarth (H3) gave a derivation of the coalescing rate in a stirred system. He derived the collision rate starting from Smoluchowski's well-known equation for the rapid coagulation in an unstable dispersed system and introduced the time-dependent diffusion of fluid elements proposed by Taylor for the case when the diffusion time is short compared with the Lagrangian integral time scale. The derivation of Howarth is believed to be incorrect because the equation of Smoluchowski was derived with the assumptions that (a) every collision results in coagulation, which is certainly not the case in stirred emulsions, and (b) the diffusion coefficient is constant, therefore it is not allowable to introduce afterwards a time-dependent diffusion coefficient. Although by fitting two empirical constants in his final equation Howarth is able to bring his formula into agreement with the experimental data of Madden and Damerell, the values found for these constants imply that (a) nearly every collision results in coalescence, which means that there can be no room for mass transfer to have any promoting effect on the coalescing rate (see Section V,C,3), and (b) the total number of collisions is so small that the assumption of the diffusion time being short compared with the Lagrangian integral time scale can no longer be correct.

Where most dispersed systems will not have a uniform size distribution it must be expected that this size distribution will also have an effect on the total collision rate. A method of calculating this influence has been indicated by Gillespie (G1a).

2. *Dead Corner Interaction*

The total number of collisions with the dead corners is proportional to the total number of drops in the surface layer opposite the dead corners and—when the theory of local isotropic turbulence holds here also—proportional to the turbulent fluctuation frequency \bar{u}/d . Near the wall, however, the theory of local isotropic turbulence certainly will not hold and—more or less—stationary large scale eddies will occur. Therefore, centrifugal effects will strongly increase the collision rate when the dispersed phase

is of a higher density than the continuous phase and will decrease the collision rate when the dispersed phase is of a lower density. This effect can best be accounted for by another frequency

$$\frac{v}{d} \propto \frac{d \Delta \rho}{\eta} a \quad (58)$$

in which $\Delta \rho$ is the density difference between dispersed phase and continuous phase (positive when the dispersed phase is of higher density, negative when the dispersed phase is of lower density), η is the viscosity of the continuous phase, and a is the average value of the centrifugal acceleration, which strongly depends on the design of the vessel and the stirrer and also on the Reynolds number. This gives, for the collision rate p_0 ,

$$p_0 = c_1 \left(\frac{\bar{u}}{d} + c_2 \frac{d \Delta \rho}{\eta} a \right) \frac{A d N}{V} \quad (59)$$

in which c_1 and c_2 are dimensionless constants and A is the effective surface area of all dead corners in the reactor. The ultimate result for ω_i is (keeping in mind that in this case at each coalescence only one drop is involved, or $n_c = 1$):

$$\omega_i = P c_1 \left(\frac{\bar{u}}{d} + c_2 \frac{d \Delta \rho}{\eta} a \right) \frac{A d}{V} \quad (60)$$

Of course the same warning as in the foregoing section has to be kept in mind here, viz., that P may also depend on ϵ .

C. THE COALESCING CHANCE P

What is necessary for a collision to be followed by a coalescence? What is the mechanism of coalescing? These are questions that have fascinated many scientists and engineers both in the field of the physical chemistry of emulsions and foams and in the engineering field of agitated dispersions.

1. *The Coalescence of Drops with Flat Interfaces*

Cockbain and McRoberts (C7) were the first to study the coalescence of a drop with a flat interface, to be followed by Gillespie and Rideal (G1), Elton and Picknett (E1), the school of Mason (C2, C3, M1), while recently an extensive study has been made by Lang (L1). The general picture of these studies is that when a drop approaches a flat liquid-liquid interface some deformation of the drop and the interface occurs, which deformation depends on the force with which the two are pressed together. As long as no coalescence has occurred the two are separated by a film of the other liquid, which film is continuously thinning with time. Observations of the thinning of this film have been made by Mackay and Mason (M1), who observed film thicknesses as low as 500 Å. After some time the thinning

film breaks at some place, and the content of the drop flows into the continuous phase. In most cases, however, a part of the drop is left behind as a smaller drop, which after some time coalesces again, and the whole process is repeated, for some systems even 5 or 6 times, as observed by Charles and Mason (C2) who call this process "partial coalescence." The different stadia of the whole coalescing process have been illustrated in Fig. 29.

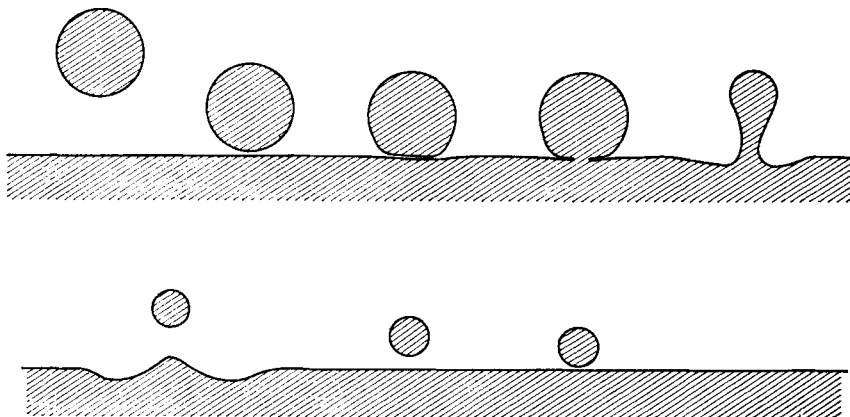


FIG. 29. Different stadia in the process of partial coalescing.

Earlier, the first studies by Cockbain and McRoberts (C7) indicated that the time necessary for coalescing, measured from the point that the drop apparently has come to rest on the flat interface till the moment the first coalescence sets in, is spread statistically around an average value. Both the standard deviation and the mean value depend on the phase system and decrease with increasing temperature and with decreasing drop size, while surface active agents and small impurities that collect at the interface have a strong retarding effect.

In the related field of foam stability, De Vries (D3) has performed some very interesting studies. He suggests that the formation of a hole in the separating film and also the first expansion of this hole requires an increase of free energy. This activation energy, which must be supplied in order to make expansion possible, is proportional to the square of the film thickness and to the interfacial tension. The chance that this activation energy is indeed supplied is then described by a Boltzmann distribution function.

Although this theory certainly explains many of the above-mentioned phenomena it does not account for the observed difference in coalescing rate when the dispersed drops are of an aqueous or of an organic phase, respectively (see Section IV,B).

2. *Studies on Coalescence in Nonstirred Emulsions*

Studies on coalescence in nonstirred emulsions have been made by Smoluchowski (S4), Ravdel (R1), Lawrence and Mills (L2), van den Tempel (T1), and Elton (E2). In these studies it is generally assumed that the coalescing process occurs in two steps: first coagulation between drops and finally breakage of the separating film followed by coalescence. The coagulation is assumed to occur because of Brownian motion or diffusion. When two drops approach each other, two kinds of interacting forces arise: attractive forces (London-van der Waals forces), which act only on a very short range, and repelling forces because of the interaction of the presence of electrokinetic double layers around the particles. Generally these two forces result in the presence of a potential barrier between the two particles [see "Theory of the Stability of Lyophobic Colloids" by Verwey and Overbeek (V6)]. Coagulation is possible only when the kinetic energy of the drops is large enough to overcome this potential barrier. The height of the potential barrier is strongly determined by the ionic strength of the continuous phase, by the valency of the ions present, and by the absorption of ions from the solution.

The influence of the electric potential of the surface of the drops was shown by Watanabe and Gotoh (W3) for the case of mercury droplets in aqueous solutions. In the case of oil drops in water the electric double layer is in the water phase, which makes possible a real interaction between the double layers of the two drops that approach each other. In the case of water drops in an oil phase, however, the electric double layers are on the inside of the drops, so that the interaction of these layers when two drops approach each other is much smaller [see Sonntag and Klare (S5)], which means that the potential barrier is much smaller or may even be absent, and the attraction by London-van der Waals forces predominates. This at least is a first explanation of why systems in which water is the dispersed phase show much higher interaction rates than systems in which oil is the dispersed phase.

In the field of nonstirred emulsions it is generally accepted, unlike the theory of Church and Shinnar, that once coagulation has occurred Brownian movement is not strong enough to break the bond, so that, finally, every coagulation results in a coalescence. Although some of the stabilizing factors in nonstirred emulsions will also be present in stirred emulsions one must be careful to transpose the theories of nonstirred emulsions into the field of stirred emulsions, since the kinetic energy of the drops is so much higher and the drops themselves generally are so much larger than in the case of nonstirred emulsions.

3. Influence of Mass Transfer on the Coalescing Rate

In the foregoing sections the coalescence in pure two-component systems was discussed. As soon as a third component is present in the two-liquid phase system the coalescing rate may be increased or decreased. This might be due to an effect on the thinning of the separating films, for example, in the case that by an action of electrical double layers the approaching drops are repelling each other at short distances. Also the mechanism of film rupture may be affected as, for example, in the case that the third component decreases the interfacial tension. The transfer of the third component from one phase to the other phase might affect the coalescing rate also, as clearly shown by Groothuis and Zuiderweg (G2, G3). They showed that when mass transfer takes place from the dispersed phase to the continuous phase an increased coalescing rate is observed: The explanation which they give is the same as indicated by Zuiderweg and Harmens (Z1) for the stabilization or breakage of foams in distillation columns: The separating film between the drops more rapidly approaches equilibrium than the remaining part of the continuous phase. This means that when mass transfer takes place from the drops to the surrounding phase this separating film will have a higher concentration of the third component. Because, in three-component systems, the interfacial tension between the two phases in equilibrium generally decreases at higher concentrations of the mutual soluble third component, the interfacial tension in the separating film will be smaller than in the remaining part of the drop interface. The gradient of interfacial tension which thus arises induces a liquid flow in the direction of the gradient, and liquid is drawn away from the separating film (Marangoni effect). The separating film, therefore, is more rapidly thinning, which ultimately results in an increased coalescing rate. When mass transfer takes place from the continuous phase to the dispersed phase the opposite occurs, and the coalescing rate will be decreased.

This theory ought to be combined with the theory of stability of lyophobic colloids (see Section V,C,2) in that the energy potential between two approaching drops is now not only determined by the London-van der Waals forces and the interaction of the electric double layer but also by the Marangoni effect induced by mass transfer. At this moment a quantitative treatment of the latter effect is still missing, however, although it could be set up along lines similar to those used by Sternling and Scriven in treating the effect of spontaneous turbulence created by mass transfer (S7).

The theory of Groothuis and Zuiderweg is confirmed for drops coalescing on a flat interface by MacKay and Mason (M1a) and for pairs of drops rising in an extraction column by Smith *et al.* (S3). Dora Thiessen (T3)

showed that in the case of inorganic solutes transferring from a watery phase to an oil phase or vice versa the effect was just reversed: extraction from droplets to the continuous phase retards the coalescing and extraction from the continuous phase to the dispersed phase promotes the coalescing. Since inorganic solutes have the effect of increasing the interfacial tension, these phenomena are still entirely in agreement with the theory of Groot-huis and Zuiderweg as was concluded also by Thiessen.

VI. Concluding Remarks

Although on a theoretical basis we know at this moment that segregation and interaction in two-phase reacting systems is very important both for the over-all conversion rate and for the selectivity, direct confirmation of this theory in reacting systems is missing so far. This is not surprising since experiments in this direction are extremely difficult because both the interaction rate and the conversion rate have to be measured at the same time in the same system. Furthermore, of most heterogeneous reactions sufficient knowledge about the pure chemical kinetics is not available. It cannot be emphasized enough, therefore, that at this moment there is a strong need for clear and convincing experiments in this direction. Although this treatise mainly deals with the effect of segregation in liquid-liquid two-phase reaction systems, in principle it may be of influence in other heterogeneous reaction systems.

The conditions that must be satisfied by a heterogeneous reaction system in order to be sensitive for segregation and interaction are:

- (a) The dispersed phase must be a fluid phase: a liquid or a gas.
- (b) At complete segregation there must occur in the dispersed phase a decrease in concentration with time.
- (c) The order of drop conversion (or "bubble" conversion) in the reactant dissolved in the dispersed phase must be different from unity.

The first two conditions seem to be fulfilled only for (a) liquid-liquid systems; (b) liquid-gas systems: spray towers and bubble columns; and (c) gas fluidized systems in an aggregative fluidization state. To what extent the third condition is fulfilled depends, in most cases, on mass transfer limitation of reactions between two or more components.

Nomenclature

a	Concentration of component A in the dispersed phase	b_c	Concentration of component B in continuous phase
a_0	Initial value of a , or value of a in the feed	b_d	Concentration of component B in dispersed phase

c	Concentration of product C	k'	$= k_0a$
w	Concentration of product W	m	Mass transfer coefficient outside drops
\mathfrak{D}_B	Diffusivity of component B in dispersed phase	n	Order of drop conversion in reactant A
E	$= \frac{3}{2}H_B b_c k_0$	n_c	Number of drops involved in one coalescence
G_0	Fraction of drops with zero concentration	p	Number of drops which coalesce per unit time
H_B	Partition coefficient of component B	p_0	Number of drop collisions per unit time
I	Interaction modulus $= \omega_i \tau = \tau/\tau_1$	q	Number of drops which leave the reactor per unit time
J	Degree of segregation (Danckwerts)	r	Radial coordinate
K	Drop conversion modulus $= k_1 \tau a_0^{n-1}$	s	$= 1/(1 - n)$
M	Number of drops which contain thiosulfate	t	Reaction time
M_0	Initial value of M	\bar{u}	Average velocity fluctuation at scale of average distance between two drops
N	Total number of drops in reactor	v	Volume of one drop
N_B	Total amount of component B which reacts per unit time in one drop	y	$= M_0/N - M_0$
\bar{N}_B	Total amount of component B which is converted per unit time in whole reactor	z	Surplus of reactant B over reactant A
N_0	$= 4\pi R H_B \mathfrak{D}_B b_c$	GREEK LETTERS	
P	Coalescing chance	α, β	a/a_0
R	Radius of drops	γ	$= a^{1-n}/[(1 - n)k\tau]$
S	Selectivity factor	ϵ	Turbulent energy dissipation per unit volume per unit time
T	Light transmission	ζ	$= \frac{3m}{R_1 a_0} \int^t b \, dt$
V	Total reactor volume or total volume of dispersed phase	θ	$= 3mt/hR_1$
X	Ratio of maximum diameter to minimum diameter in dispersion	θ'	$= 3mtb/hR_1 a_0$
a	Volume fraction of component A in a two-component system	θ''	$= \frac{3H_B a_0^{1/2} t (k_0 \mathfrak{D}_B)^{1/2}}{2hR_1}$
b	$= (1 + I)\gamma_0$	λ	$= \left(\frac{\text{maximum drop size}}{\text{minimum drop size}} \right)^3$
c	$= (1 + I)\bar{\gamma}$	ν	$= \frac{\text{average residence time}}{\text{time of one circulation}}$
d	Diameter of drop	ξ	$= t/\tau$
f	Degree of conversion	ρ	Density
$g(\alpha), g(\alpha)$	Concentration distribution functions	$\Delta\rho$	Density of dispersed phase minus density of continuous phase
h	Phase ratio $= \frac{\text{volume continuous phase}}{\text{volume dispersed phase}}$	σ	$= r/R$, or interfacial tension
i	Interaction rate	τ	Average residence time $= N/q$
k_0	Chemical reaction rate constant	τ_1	$= N/p$
k	Drop conversion rate constant	φ	$= R(k_0 a/\mathfrak{D}_B)^{1/2}$
k_1	$= kb$		

ϕ	Volume fraction of dispersed phase	ω_i	Interaction frequency, coalescing frequency = pn_c/N
--------	------------------------------------	------------	--

REFERENCES

- B1. Batchelor, G. K., "The Theory of Homogeneous Turbulence." Cambridge Univ. Press, London and New York, 1953.
- C1. Calderbank, P. H., *Trans. Inst. Chem. Engrs. (London)* **36**, 443 (1958).
- C2. Charles, G. E., and Mason, S. G., *J. Colloid Sci.* **15**, 105 (1960).
- C3. Charles, G. E., and Mason, S. G., *J. Colloid Sci.* **15**, 235 (1960).
- C4. Cholette, A., and Cloutier, L., *Can. J. Chem. Eng.* **37**, 105 (1959).
- C5. Cholette, A., Cloutier, L., and Blanchet, J., *Can. J. Chem. Eng.* **38**, 1 (1960).
- C6. Church, J. M., and Shinnar, R., *Ind. Eng. Chem.* **53**, 479 (1961).
- C7. Cockbain, E. G., and McRoberts, T. S., *J. Colloid Sci.* **8**, 440 (1953).
- C8. Curl, R. L., *A.I.Ch.E. (Am. Inst. Chem. Engrs.) J.* **9**, 175 (1963).
- D1. Danckwerts, P. V., *Appl. Sci. Res.* **A3**, 279 (1953).
- D2. Danckwerts, P. V., *Chem. Eng. Sci.* **8**, 93 (1958).
- D3. De Vries, A. J., *Rec. Trav. Chim.* **77**, 383, 441 (1958).
- E1. Elton, G. A. H., and Picknett, R. G., *Proc. Intern. Congr. Surface Activity, 2nd, London, 1957*, Vol. 1, p. 288. Butterworth, London (1957).
- E2. Elton, G. A. H., *Trans. Faraday Soc.* **54**, 1724 (1958).
- G1. Gillespie, T., and Rideal, E. K., *Trans. Faraday Soc.* **52**, 173 (1956).
- G1a. T. Gillespie, *J. Colloid Sci.* **18**, 562 (1963).
- G2. Groothuis, H., and Zuiderweg, F. J., *Chem. Eng. Sci.* **12**, 288 (1960).
- G3. Groothuis, H., and Zuiderweg, F. J., *Chem. Eng. Sci.* **19**, 63 (1964).
- H1. Harada, M., Arima, K., Eguchi, W., and Nagata, S., *Mem. Fac. Eng. Kyoto Univ.* **24**(4), 431 (1962).
- H2. Hinze, J. O., *A.I.Ch.E. (Am. Inst. Chem. Engrs.) J.* **1**, 289 (1955).
- H3. Howarth, W. J., *Chem. Eng. Sci.* **19**, 33 (1964).
- K1. Kramers, H., *Chem. Eng. Sci.* **8**, 45 (1958).
- K2. Kramers, H., Geerling, P. D. W., de Korver, H., and Voncken, R. M., private communication (1960-1962).
- L1. Lang, S. B., Thesis, Lawrence Radiation Lab. UCRL 10097, Univ. Calif., Berkeley, California, 1962.
- L2. Lawrence, A. S. C., and Mills, O. S., *Discussions Faraday Soc.* **18**, 98 (1954).
- L3. Levenspiel, O., and Bischoff, K. B., *Advan. Chem. Eng.* **4**, 95 (1963).
- M1. MacKay, G. D. M., and Mason, S. G., *Nature* **191**, 488 (1961).
- M1a. Mackay, G. D. M., and Mason, S. G., *J. Colloid Sci.* **18**, 674 (1963).
- M2. Madden, A. J., and Damerell, G. L., *A.I.Ch.E. (Am. Inst. Chem. Engrs.) J.* **8**, 233 (1962).
- M3. Matsuzawa, H., and Miyauchi, T., *Chem. Eng. (Tokyo)* **25**, 582 (1961).
- M4. Miller, R. S., Ralph, J. L., Curl, R. L., and Towell, G. D., *A.I.Ch.E. (Am. Inst. Chem. Engrs.) J.* **9**, 196 (1963).
- R1. Ravdel, A. A., *Dokl. Akad. Nauk SSSR* **90**, 599 (1953).
- R2. Rietema, K., *Chem. Eng. Sci.* **8**, 103 (1958).
- R3. Rietema, K., and Meyerink, E. S. C., in "Alta Tecnologia Chimica, Reazioni E. Reattori," VI^o Corso Estivo di Chimica. Accad. Nazl. Lincei, Rome, 1962.
- R4. Rietema, K., and Meyerink, E. S. C., *Proc. 25th Anniv. Congr. Soc. Chem. Engrs. Japan 1961*, to be published in New York.

- R5. Rodger, W. A., Trice, V. G., and Rushton, J. H., *Chem. Eng. Progr.* **52**, 515 (1956).
S1. Shinnar, R., and Church, J. M., *Ind. Eng. Chem.* **52**, 253 (1960).
S2. Shinnar, R., *J. Fluid Mech.* **10**, 259 (1961).
S3. Smith, A. R., Caswell, J. E., Larson, P. P., Cavers, S. D., *Can. J. Chem. Eng.* **41**, 150 (1963).
S4. Smoluchowski, M. von, *Z. Physik. Chem.* **92**, 129 (1916).
S5. Sonntag, H., and Klare, H., *Z. Physik. Chem.* **223**, 8 (1963).
S6. Spielman, L. A., Masters thesis, Illinois Institute of Technology, 1963.
S7. Sternling, C. V., and Scriven, L. E., *A.I.Ch.E. (Am. Inst. Chem. Engrs.) J.* **5**, 514 (1959).
T1. Tempel, M. van den, *J. Colloid Sci.* **13**, 125 (1958).
T2. Thiele, E. W., *Ind. Eng. Chem.* **31**, 916 (1939).
T3. Thiessen, D., *Z. Physik. Chem.* **223**, 218 (1963).
V1. Vanderveen, J. H., Lawrence Radiation Lab. Rept. UCRL 8733, Univ. Calif., Berkeley, California, 1960.
V2. Veltkamp, G. W., (letter to the editor) to be published in *Chem. Eng. Sci. J.*
V3. Veltkamp, G. W., and Geurts, A. J., to be published in *Appl. Sci. Research-1965*.
V4. Vermeulen, T., Williams, G. M., and Langlois, F. E., *Chem. Eng. Progr.* **51**, 85F (1955).
V5. Vermeulen, T., *Proc. 25th Anniv. Congr. Soc. Chem. Engrs. Japan 1961*, to be published in New York.
V6. Verwey, E. V. W., and Overbeek, J. Th. G., "Theory of the Stability of Lyophobic Colloids." Elsevier, Amsterdam, 1948.
W1. Weiss, L. H., Fick, J. L., Houston, R. H., Vermeulen, T., Lawrence Radiation Lab. UCRL 9787, Univ. Calif., Berkeley 1962.
W2. Wheeler, A. W., *Advan. Catalysis* **3**, 297 (1951).
W3. Watanabe, A., and Gotoh, R., *Kolloid-Z.* **191**, 36 (1963).
Z1. Zuiderweg, F. J., and Harmens, A., *Chem. Eng. Sci.* **9**, 89 (1958).
Z2. Zwietering, T. N., *Chem. Eng. Sci.* **11**, 1 (1959).

AUTHOR INDEX

Numbers in parentheses are reference numbers, and are inserted to enable the reader to locate a reference when the authors' names are not cited in the text. Numbers in *italic* indicate the page on which the full reference is cited.

A

Ablow, C. M., 21 (E2), 22 (E2), *33*
 Adair, G. S., 82, *146*
 Adams, II, E. N., 10, *33*
 Adams, K. A., 92, *146*
 Adler, S. F., 38 (K1), 39, *73*
 Adorni, N., 177 (A1), 222, 227, 229, *228*,
229
 Alimov, R. Z., 189 (A2), 217, *229*
 Allen, D. N. de G., 130, 135, *146*
 Allen, J. M., 189 (A3), 193 (A3), 194, 198,
 199, 225, *229*
 Ambrosio, A., 101, *146*
 Anderson, G. H., 172, 183 (A5), 184, 205
 (A5), 221, 222, *229*
 Anderson, J. R., 52 (A1), 55 (A1), *73*
 Anderson, W. H., 26 (A2), 27 (A2), *33*
 Andreev, A. F., 164, 227, *229*
 Arima, K., 282 (H1), *301*
 Arnett, R. L., *74*
 Arnold, J. H., 90, *146*
 Arthur, J. R., 32 (A5), *33*
 Asai, S., 220 (H14), *232*
 Asbjørnsen, O. A., 203, 222, *229*
 Atkinson, B., 200 (A7), 227, *229*
 Avery, W. H., 12 (P11), *36*

B

Badger, W. L., 186, *234*
 Baeder, D. L., 48 (B1), *73*
 Baer, D., 101, *146*
 Baker, Jr., L. L., 19 (K2), *34*
 Baker, R. W., 37 (C6), 39 (C6), 43 (C6),
 45 (C6), *73*
 Balandin, A. A., 54, *73*
 Balarev, K., 192 (M11), 224 (M11), *234*
 Bankoff, S. G., 80, 93 (H5), 100, 102 (H2),

104 (H2, H3), 123 (H4), 126 (H3), *148*,
150
 Barnes, M. D., 111 (B2, L2), *146*, *149*
 Barnett, L. G., 50, *73*
 Bassett, D. L., 204, *235*
 Batchelor, G. K., 294, *301*
 Bauer, W. J., 152 (B1), 190, 221, *229*
 Baxter, D. C., 134, *146*
 Bays, G. S., 212, *229*, *233*
 Becker, R., 107, *146*
 Beda, G. A., 223, *229*
 Belanger, J.-Y., 177 (P1), 215, *234*
 Belkin, H. H., 177 (B4), 186, 188, 198,
 220, *229*
 Belles, F. M., 17 (B1), 19 (B1), *33*
 Belo pol'skii, A. P., 152 (T9, T12), 192
 (T9, T10, T11, T12), 198, 214, 215, *235*
 Benesi, H., 40 (B3, B4), *73*
 Benjamin, T. B., 163, 165, 167, 187, 189,
 194, 216, 223, *229*
 Bennett, J. A. R., 177 (B8), 205, 223, *229*
 Bergelin, O. P., 171, 177 (D16), 186, 190,
 194 (D16), 198, 215, *230*
 Berl, W. G., 31 (B2), *33*
 Bertolacini, R. J., 39 (M1), 49 (M1), *73*
 Betts, R. A., 152, *231*
 Bick, J. H., 116, *146*
 Bills, K. W., 26 (A2), 27 (A2), *33*
 Binnie, A. M., 160 (B10), 161 (B10), 164
 (B6, B10), 188 (B9, B10), 189 (B9, B10),
 193 (B10), 218, 220, *229*
 Binns, D. T., 222, *234*
 Biot, M. A., 127, *146*
 Bird, R. B., 221, *229*
 Birkhoff, G., 85, *146*
 Bischoff, K. B., 238, *301*
 Black, R. H., 152 (B12), 177 (B12), 178,
 223, *229*
 Blanchet, J., *301*

Boley, B. A., 120, 122, 146
 Boltzman, L., 78, 146
 Bonchkovskaya, T. V., 199, 230
 Booth, F., 91, 146
 Botha, J. P., 17, 33
 Boudart, M., 38 (S7), 39, 48 (B1), 52 (P1), 73, 74
 Boyarchuk, P. G., 225, 229
 Boyer, R. H., 84, 146
 Boys, S. F., 10, 33
 Brauer, H., 155 (B14), 170 (B14), 171 (B14), 173, 177 (B14), 178, 181, 186, 188 (B14), 189 (B14, B15, B16), 190, 196, 197, 198, 199, 201, 203, 206 (B14), 207, 208 (B14), 217, 218, 219, 229
 Braun, R. M., 74
 Brennan, H. M., 39 (M1), 49 (M1), 73
 Brenner, H., 111, 146
 Bressler, R., 153 (B20), 189 (B20), 190, 201, 219, 221, 229
 Brinkley, Jr., S. R., 22 (B5), 23 (B5), 33
 Brötz, W., 177 (B21), 181, 186, 192, 215, 229
 Bronskiĭ, L. N., 152 (Z5), 199, 236
 Brunauer, S., 38, 73
 Brunner, R. K., 206 (L4), 226 (L4), 233
 Buikov, M. V., 109, 147
 Bulewicz, E. M., 10 (B6), 12 (B6), 33
 Bungenberg de Jong, H. G., 82, 147
 Bushmanov, V. K., 166, 229

C

Cahn, J. W., 79, 148
 Calcote, H. F., 16 (C1, C2), 33
 Calderbank, P. H., 291 (C1), 301
 Calvert, S., 172, 184, 205, 214, 216, 229
 Campbell, D. E., 5 (H3), 16 (H3), 25 (H3), 34
 Campbell, E. S., 6 (C3), 6 (C4), 9 (C4), 33
 Carpenter, E. F., 214, 229
 Carslaw, H. S., 78, 132, 147
 Casagrande, I., 177 (A1), 222 (A1), 229 (A1), 228
 Caswell, J. E., 298 (S3), 302
 Cavers, S. D., 298 (S3), 302
 Ceaglske, N. H., 203 (J2), 205 (J2), 214 (J2), 232
 Cf. Frank, P., 78 (N1), 149

Chaiken, R. F., 26 (C5), 33
 Chambré, P. L., 84, 147
 Charles, G. E., 295 (C2, C3), 296, 301
 Charlesworth, D. H., 109, 147
 Charvonina, D. A., 172, 177 (C4), 183 (C4), 184, 189 (C4), 190 (C4), 193 (C4), 197, 204, 220, 229
 Chawla, M. J., 152 (C5), 229
 Chew, J.-N., 177 (C6), 190 (C6), 191 (C6), 193 (C6), 203, 215, 230
 Chien, S.-F., 190, 191 (C7), 197, 204, 223, 230
 Cholette, A., 301
 Chow, V. T., 152 (C8), 230
 Church, J. M., 291, 301, 302
 Chwang, C. T., 177 (C9), 211, 230
 Ciapetta, F. G., 37, 39 (C6), 43, 45 (C6), 46, 70 (M4), 73, 74
 Citron, S. J., 99, 100, 127 (C5), 147
 Clapeyron, B. P. E., 76, 149
 Clark, A., 71 (C7), 73
 Clark, A. H., 31 (V1), 36
 Classen, H., 152 (C10), 177 (C10), 200, 211, 230
 Clayton, C. G. A., 177 (C11), 202, 205, 219, 230
 Cloutier, L., 301
 Cochran, D. L., 133, 147
 Cockbain, E. G., 295, 296, 301
 Cohen, H., 76 (C9), 147
 Colburn, A. P., 207, 214, 229, 230
 Collier, J. G., 177 (C13), 184, 200 (C13), 223, 230
 Collins, D. E., 177 (C14), 183 (C14), 219, 230
 Collins, F. C., 109, 110, 111, 147, 148
 Condon, F. E., 58 (C8), 73
 Connor, J. E., 69 (P7), 74
 Cooper, C. M., 177 (C15), 178 (C15), 186, 211, 212, 230
 Corner, J., 10, 33
 Cornish, R. J., 159 (C16), 211, 230
 Courant, R., 21 (C6), 22 (C6), 33
 Courtney, W. G., 32 (C7), 33
 Crank, J., 78, 136, 138, 147
 Cravarolo, L., 177 (A1), 222 (A1), 227 (A1a), 229 (A1), 228, 229
 Craya, A., 165 (C17), 214, 230
 Csaba, J., 31 (E1), 33
 Cullen, E. J., 218, 220 (D2), 230

Curl, R. L., 271, 275, 283 (M4), 288 (M4), 301
 Curle, N., 130 (C17), 147
 Curtiss, C. F., 2 (H1), 4 (H1), 5 (H3), 6 (H1), 16 (H3), 22 (H1), 25 (H3), 34
 Cyphers, J. A., 12, 34

D

Damerell, G. L., 283, 284, 301
 Danckwerts, P. V., 86, 90 (D1), 91 (D1), 119, 147, 238, 301
 Daughaday, H., 127 (B6), 146
 Davidson, J. F., 183 (H20), 192 (H20), 218, 219, 220, 230, 232
 Davies, J. T., 199, 221, 230
 Deissler, R. G., 172, 176, 230
 De Korver, H., 284 (K2), 301
 Dennis, W. L., 109, 147
 Derbentsev, Y. I., 54 (D1), 73
 de Sendagorta, J. M., 10, 33
 De Vries, A. J., 296, 301
 Dewey, C. F., Jr., 137, 147
 Diagula, A. J., 184 (E1), 231
 Dixon-Lewis, G., 13, 33
 Dmitriev, A. A., 199, 230
 Dobres, R. M., 37 (C6), 39 (C6), 43 (C6), 45 (C6), 73
 Donaldson, G. R., 43, 73
 Donoughe, P. L., 184 (E1), 231
 Doring, W., 107, 146
 Douglass, J., Jr., 136, 147
 Dressler, R. F., 165 (D9, D10, D11), 170, 190 (D9), 214, 215, 230
 Drew, T. B., 177 (C15), 178 (C15), 186 (C15), 211 (C15), 212 (C15, M1), 230, 233
 Dukhin, S. S., 109, 147
 Dukler, A. E., 153, 154 (D12), 171, 172, 176, 177 (D16), 184, 185, 186, 189 (D17), 190, 194 (D16), 198, 205, 215, 220, 221, 223, 227, 230
 Dusinberre, G. M., 134, 147
 Dzhililov, K. N., 130, 149

E

Eckert, E. R. G., 184, 231
 Eguchi, W., 282 (H1), 301
 Ehrlich, L. W., 136, 147

Elenkov, D., 192 (M11), 224 (M11), 234
 Ellis, S. R. M., 152 (E2), 220, 231
 Elton, G. A. H., 295, 297, 301
 Emmert, R. E., 186, 189 (E4), 192 (E4), 215, 231
 Emmett, P. H., 38 (B5), 73
 Escoffier, F. F., 223, 231
 Essenhigh, R. H., 31 (E1), 33
 Evans, G. W., 77, 125, 147
 Evans, M. W., 21 (E2), 22 (E2), 33
 Eyres, N. R., 98 (E4), 134, 147

F

Fallah, A., 177 (F1), 178 (F1), 186 (F1), 212, 231
 Farkas, A., 52 (F1), 73
 Farkas, L., 52 (F1), 73
 Favin, S., 13 (F14), 17 (F14), 31 (F14), 34
 Fehrer, H., 65 (T2), 74
 Feind, K., 172 (F2), 174, 177 (F2), 180 (F2), 181 (F2), 183, 185, 186, 189 (F2), 190 (F2), 191 (F2), 204, 205, 206, 221, 231
 Feldman, S., 165 (F3), 218, 231
 Fenimore, C. P., 10 (F3), 12, 13, 15 (F2), 16 (F3), 33
 Ferguson, F. A., 6 (F1), 33
 Feshbach, H., 113 (M12), 149
 Fick, J. L., 293 (W1), 302
 Fisher, J. C., 86, 147
 Foner, S., 12 (P11), 36
 Forshay, D. R., 22 (L13), 24 (L13), 35
 Fowler, C. M., 98 (F2), 147
 Fox, M. D., 3 (F4), 33
 Fradkov, A. B., 175 (F4), 183 (F4), 213, 231
 Frank, F. C., 81, 147
 Frank-Kamenetski, D. A., 20, 34
 Frazier, G. C., 5 (F6), 6 (F6), 34
 Friezainov, I. V., 132, 147
 Friedman, A., 77, 147, 148
 Friedman, R., 2 (F9), 12, 24 (F10), 25 (L4), 26 (L4), 32 (F10), 34, 35
 Friedman, S. J., 177 (F5), 203, 212, 231
 Friedrichs, K. O., 21 (C6), 22 (C6), 33
 Frisch, H. L., 109, 110, 148
 Fristrom, R. M., 5 (F6), 6 (F6), 12, 13, 15 (F11), 16 (F11, F12), 17 (F14), 19 (F11), 31 (F14), 34, 36

Fuchs, N. A., 109, *148*
 Fulford, G. D., 154 (F7), 155 (F7), 159 (F7), 160 (F7), 161 (F7), 172 (F7), 177 (F7), 180 (F7), 181 (F7), 183 (F7), 186, 188 (F7), 189 (F7), 190 (F7), 191 (F7), 193 (F7), 194 (F7), 195 (F7), 196 (F7), 200 (F7), 204 (F7), 205 (F7), 206 (F7), 207 (F7), 221, 225, *231*

G

Gadazhieva, M. G., 130, *148*
 Gallie, T. N., 136, *147*
 Galwey, A. K., 63 (G1), *73*
 Garwin, L., 216, *231*
 Gay, B., 206 (G2), 219, 220, *231*
 Gaydon, A. G., 12 (G1, G2), 16 (G1), *34*
 Geckler, R. D., 25, 26, *34*
 Geerling, P. D. W., 284 (K2), *301*
 Geurts, A. J., 271, 291 (V4), *302*
 Gibson, R. E., 132, *148*
 Gilkeson, M. M., 50 (B2), *73*
 Gill, L. E., 197 (G3), 205 (G3), 206, 227, *231*
 Gillespie, T., 294, 295, *301*
 Glaser, H., 223, *231*
 Goble, A. G., 63 (P5), *74*
 Goldstein, S., 130, *148*
 Goodman, T. R., 128, 130 (G7), *148*
 Gossage, W., 152 (G5), *231*
 Gotoh, R., 297, *302*
 Graebel, W. P., 165 (G6), 222, *231*
 Green, Jr., L., 26 (S7), *36*
 Greenberg, A. B., 177 (G7), 193 (G7), 217, *231*
 Griffin, J. R., 82, 85, *148*
 Grigull, U., 186, 213, 215, *231*
 Grimley, S. S., 159, 172, 177 (G11), 183 (G10), 189, 190, 193 (G11), 202, 203, 213, *231*
 Grinberg, G. A., 132, *148*
 Gring, J. L., 43 (H7), 67 (H7), 68 (H7), *73*
 Groothuis, H., 284, 288, 298, *301*
 Grosh, R. J., 137, *150*
 Gross, R. A., 21 (G4), 30, *34*
 Grosse, A. V., *34*
 Grover, J. H., 2 (F9), *34*
 Gruber, H. L., 39, *73*

Grunfelder, C., 13 (F14), 17 (F14), 31 (F14), *34*
 Gunn, R., 109, *148*
 Gutowski, R., 126, *148*

H

Haag, W. O., 38 (P3), *74*
 Haensel, V., 37, 43, *73*
 Ham, F. S., 108, *148*
 Hama, F. R., 200, *231*
 Hamill, T. D., 93 (H5), 100, 102 (H2), 104 (H2, H3), 123 (H4), 126 (H3), *148*
 Hannan, R. B., 42 (P2), *74*
 Hanratty, T. J., 164, 167, 169 (H2), 177 (L13), 187, 189 (H2, L12, L13), 192 (H2), 194, 196, 197 (L12), 206 (L12, L13), 208 (L13), 223, 224, *231, 233*
 Hanson, D., 220 (D2), *230*
 Harada, M., 282, *301*
 Harmens, A., 298, *302*
 Hartree, D. R., 96, 98 (E4), 134 (E4), *147, 148*
 Haselden, G. G., 172 (A4), 222 (A4), *229*
 Hassid, A., 177 (A1), 222 (A1), 227 (A1a), 229 (A1), *228, 229*
 Hatta, S., 201, 211, *231*
 Hattman, J. B., 43 (H3), *73*
 Haughton, K. E., 206 (L4), 226 (L4), *233*
 Hay, M. H., 22 (L13), 24 (L13), *35*
 Heartinger, D. J., 199, 222, *231*
 Heinemann, H., 43, 46 (M2), 47 (M2), *73, 74*
 Heinen, F. J., 6 (C4), 9 (C4), *33*
 Heiser, H. W., 38 (N1), *74*
 Herington, E. F. G., 53, 64 (H4, H5), 66, *73*
 Hermans, J. J., 81, 141 (H7), *148*
 Hershman, A., 164, 167, 169 (H2), 187, 189 (H2), 192 (H2), 194, 205 (H6), 206 (H6), 223, *231*
 Hettinger, W. P., Jr., 43, 67, 68 (H7), *73*
 Hewitt, G. F., 161 (H9), 176, 177 (C13, H9, H11), 178, 183 (H9, H10), 184, 189 (T7), 190 (T7), 191 (T7), 193 (T7), 194 (H9, T6, T7), 197, 205, 206 (G3), 208 (H9), 223, 224, 225, 226, 227, 228 (T7), *230, 231, 232, 235*
 Hikita, H., 192 (H13), 199, 220, 221, *232*
 Hindin, S. G., 48, *73*

Hinze, J. O., 292, 301
 Hirschfelder, J. O., 2 (H1), 4 (H1), 5 (H3),
 6 (H1), 10, 16 (H3), 22 (H1), 25 (H3),
 34
 Hitchon, J. W., 197 (G3), 205 (G3), 206
 (G3), 227 (G3), 231
 Hlinka, J. W., 133, 148
 Holdercroft, J. G., 192 (R1), 225, 226, 234
 Holmes, W. H., 189 (H16), 212, 232
 Holmgren, E., 116, 148
 Honda, N., 177 (S11), 183 (S11), 189
 (S11), 192 (S11), 194 (S11), 196 (S11),
 198 (S11), 208 (S11), 219 (S11), 235
 Hoog, H., 66 (H9), 67, 73
 Hoogendoorn, C. J., 152 (H17), 232
 Hopf, L., 156, 159 (H18), 160 (H18), 177
 (H18), 178, 186, 200, 210, 232
 Horning, W. A., 85 (B7), 146
 Horton, R. E., 160 (H19), 186, 189 (H19),
 203, 211, 232
 Horvay, G., 79, 85, 133, 148
 Houston, R. H., 293 (W1), 302
 Houston, R. J., 39 (H10), 40, 73
 Howarth, E. J., 294, 301
 Howkins, J. E., 183 (H20), 192 (H20),
 218, 219, 230, 232
 Hrycak, P., 130, 148
 Hudson, R., 12 (P11), 36
 Hughes, T. R., 39, 73
 Hunter, J. B., 43, 73
 Hunter, T. G., 177 (F1), 178 (F1, S13),
 185 (S13), 186 (F1), 212 (F1, S13), 231,
 235
 Hurt, D. M., 186, 192 (S12), 199, 217, 235
 Hurwitz, H., 51 (S6), 55 (S4, S6), 56 (S4),
 58 (S4, S5), 59 (S4), 61 (R3), 68 (R3), 74

I

Ibanescu, I., 186 (S1), 201 (S1), 226 (S1),
 234
 Iijima, H., 183 (K5), 216 (K5), 232
 Ingham, J., 98 (E4), 134 (E4), 147
 Isaacson, E., 125 (E3), 147
 Isagulyants, G. V., 54 (D1), 73
 Ishihara, T., 152 (I1), 165, 170, 186, 189
 (I2), 192 (I2), 193 (I2), 194, 199, 215,
 224, 232
 Ishihara, Y., 152 (I1), 170 (I1), 199 (I1),
 215 (I1), 232

Itoi, M., 183 (K5), 216 (K5), 232
 Ivantsov, G. P., 79, 148
 Iwagaki, Y., 152 (I1, I3), 165 (I2), 170
 (I1), 187 (I2), 189 (I2), 192 (I2), 193
 (I2), 194 (I2), 199 (I1), 215 (I1), 224
 (I2), 232
 Iwasa, Y., 165 (I2, I4), 186 (I2), 189 (I2),
 192 (I2), 193 (I2), 194 (I2), 224 (I2),
 232

J

Jackson, M. L., 158, 177 (J1), 188, 190
 (J1), 192 (J1), 199, 203, 205, 214, 216,
 232
 Jackson, R., 98 (E4), 134 (E4), 147
 Jacobs, T. A., 2 (P6), 35
 Jaeger, J. C., 78, 132, 147
 James, C. G., 10 (B6), 12 (B6), 33
 Jaymond, M., 177 (J3), 203, 224, 232
 Jeffreys, H., 165 (J4), 177 (J4), 186, 189
 (J4), 203, 211, 232
 Jenkins, Jr., H. P., 19 (M1), 35
 Johnson, I., 111 (J1), 148
 Johnson, R. T., 203 (J2), 205 (J2), 214
 (J2), 232
 Johnson, W. E., 7 (J1, J3), 26, 34
 Jones, G. W., 10 (F3), 12, 13, 15 (F2),
 16 (F3), 33
 Jones, H., 22 (J4), 34
 Jost, W., 2, 34

K

Kaiser, L., 189 (K1), 224, 232
 Kamei, S., 158, 177 (K4), 181, 183 (K4,
 K5), 186, 199, 205, 216, 217, 232
 Kapitsa, P. L., 163, 166, 168, 169, 175,
 177 (K10), 181, 183 (K10), 189 (K10),
 192, 193 (K10), 194, 195, 199, 213, 214,
 232
 Kapitsa, S. P., 169, 177 (K10), 189 (K10),
 193 (K10), 194, 195, 214, 232
 Kasimov, B. S., 161 (K11), 169, 226, 227,
 232
 Kaskan, W. E., 16 (K1), 34
 Kataoka, T., 221 (H15), 232
 Katori, M., 211, 231
 Kawamura, M., 183 (K5), 216 (K5), 232
 Keavney, J. J., 38 (K1), 39, 73
 Keith, C. D., 43 (H7), 67 (H7), 68 (H7), 73

- Keller, J. B., 77, 149
 Kelly, E. W., 216, 231
 Kemball, C., 52 (A1), 55 (A1), 63 (G1), 73
 Kennedy, J. F., 225, 235
 Kenyon, A. S., 111 (B2, L3), 146, 149
 Keulegan, G. H., 155, 165 (K16), 170, 193, 212, 232, 233
 Keulemans, A. I. M., 38 (K2), 56 (K3), 58, 59, 73
 Kilpatrick, M., 19 (K2), 34
 Kimball, G. E., 109, 147
 King, I., 205 (H8, H9, H10), 224 (H8), 231
 King, R. D., 161 (H9), 177 (H9), 183 (H9, H10), 184 (H10), 194 (H9), 197 (H9), 208 (H9), 225 (H9), 227 (H10), 232
 Kinzer, G. D., 109, 148
 Kirkaldy, J. J., 84, 106, 148
 Kirkbride, C. G., 177 (K17), 186, 204, 211, 233
 Kirsch, F. W., 43 (H3), 73
 Kistiakowski, G. B., 30 (K3), 34
 Kläukens, H., 12, 34
 Klare, H., 297, 302
 Klein, G., 12 (K5), 34
 Kluksdahl, H. E., 40, 73
 Knuth, E. L., 92, 148, 152 (K18), 189 (K18), 233
 Koh, J. C. Y., 130, 148
 Kolodner, I., 116, 148
 Konobeev, B. I., 169 (K20, K21), 175, 177 (K21), 183 (K19, K20, K21), 193 (K20, K21), 194 (K20, K21), 197, 206, 218, 224, 226, 233
 Kosterin, S. I., 152 (K23), 233
 Kramers, H., 192 (L15), 216 (L15, L16, L17), 217, 233, 238, 284, 301
 Kreith, F., 131, 133, 148
 Kreyger, P. J., 217, 233
 Kuczynski, G. C., 107, 148
 Kutateladze, S. S., 153, 172, 186, 219, 233
 Kyner, W. T., 77, 149
- L**
- Labuntsov, D. A., 172, 199, 217, 218, 233
 Lacey, P. M. C., 189 (T7), 190 (T7), 191 (T7), 193 (T7), 194 (T7), 197 (G3), 206 (G3), 227 (G3), 228 (T7), 231, 235
 Laderman, A. J., 19 (L1), 22 (L1, L2), 23, 24 (L1), 34, 35
 Laird, A. D. K., 205, 206, 216, 226, 233
 Lamb, H., 233
 Lamé, G., 76, 149
 La Mer, V. K., 107, 111, 146, 148, 149, 150
 Landau, H. G., 94, 99 (L4), 133, 149
 Landauer, R., 107, 148
 Landis, F., 137, 149
 Lang, S. B., 295, 301
 Langleben, M. P., 105 (H3)
 Langlois, F. E., 302
 Larson, P. P., 298 (S3), 302
 Lask, G., 3 (L3), 35
 Lawrence, A. S. C., 297, 301
 Leach, H. R., 160 (H19), 186 (H19), 189 (H19), 203 (H19), 211 (H19), 232
 Le Chatelier, H., 4 (M3), 35
 Leinweber, J. P., 111, 147
 Leum, L. N., 69 (P7), 74
 Levenspiel, O., 238, 301
 Levich, V. G., 166, 168, 170, 182, 192, 198, 212, 213, 221, 233
 Levy, J. B., 25 (L4), 26 (L4), 35
 Lewis, B., 2 (L6), 4, 6 (L11), 18 (L8), 19, 21 (L10), 22 (B5), 23 (B5), 33, 35
 Lewis, G. N., 40, 73
 Lightfoot, E. N., 221 (B11), 229
 Lightfoot, N. H. M., 94, 112, 149
 Lighthill, M. J., 167, 170, 189 (L10, L11), 191, 233
 Lilleleht, L. U., 177 (L13), 189 (L12, L13), 196, 197 (L12), 206 (L12, L13), 208 (L13), 224, 233
 Linnett, J. W., 18 (L12), 35
 Litchfield, E. L., 22 (L13), 24 (L13), 35
 London, A. L., 132, 149
 Longwell, P. A., 135, 149
 Lotkin, M., 137, 149
 Lovegrove, P. C., 161 (H9), 177 (H9, H11), 178, 183 (H9, H10), 184 (H10), 194 (H9), 197 (H9, H11), 205 (H8, H9, H10), 208 (H9), 224 (H8), 225 (H9, H11), 227 (H10, H11a), 231, 232
 Luder, W. F., 41 (L2), 73
 Lynn, S., 191 (L14), 192 (L15, L16, L17), 216, 222, 233
- M**
- McAdams, W. H., 177 (C15), 178 (C15), 186 (C15), 211 (C15), 212, 229, 230, 233

- McCone, Jr., A., 34
 McCullough, Jr., F., 19 (M1), 35
 MacDonald, J. K. L., 125 (E3), 147
 Maček, A., 22 (M2), 24 (F10, M2), 32 (F10), 34, 35
 McHenry, K. W., 39, 49 (M1), 73
 McIntyre, V., 222, 234
 MacKay, G. D. M., 295 (M1), 298, 301
 MacLeod, A. A., 177 (B4), 186 (B4), 188 (B4), 190 (M2), 191, 198 (B4), 220 (B4), 229, 233
 McManus, H. N., 184, 196, 205 (M3), 233
 McRoberts, T. S., 295, 296, 301
 Madden, A. J., 283, 284, 301
 Mahrenholtz, O., 183 (M5), 205, 219, 234
 Malafeev, N. A., 199 (Z2), 214 (Z2), 236
 Mallard, E., 4 (M3), 35
 Malyusov, V. A., 169 (K20, K21), 175 (K20, K21), 177 (K21), 183 (K19, K20, K21), 193 (K20, K21), 194 (K20, K21), 197 (K20, K21), 199 (Z2), 214 (Z2), 217, 218 (K19, K20), 224 (K21), 233, 236
 Mancini, O. J., 135, 149
 Mantzouranis, B. G., 172 (A4, A5), 183 (A5), 184, 205, 221, 222 (A4), 229
 Margenau, H., 113 (M2), 149
 Margulies, R. S., 85 (B7), 146
 Marshall, J. S., 105 (M3), 149
 Marshall, W. R. Jr., 109, 147
 Mason, B. J., 105 (H4), 107 (M5), 109, 149
 Mason, S. G., 295, 296, 298, 301
 Matsuzawa, H., 284, 287, 301
 Maxwell, J. C., 109, 149
 Mayer, E., 17, 20, 35
 Mayer, P. G., 152 (M7), 170, 177 (M7), 189 (M7), 190 (M7), 191 (M7), 192 (M7), 193 (M7), 194 (M7), 196, 199, 224, 234
 Mazyukevich, I. V., 172, 205 (M8), 218, 234
 Meksyn, D., 130 (M7), 149
 Mertens, J., 31 (M5), 35
 Meyerink, E. S. C., 244, 301
 Michalik, E. R., 218, 234
 Mikhelson, V. A., 4 (M6), 35
 Miles, J. W., 165 (M10), 222, 234
 Miller, C. O., 177 (F5), 203, 212, 231
 Miller, R. S., 283, 288, 301
 Millikan, R. C., 32 (M7), 35
 Milliken, T. H., 40 (O1), 46 (M2), 47 (M2), 74
 Mills, G. A., 40 (O1), 43 (H3), 46 (M2), 47, 48 (H8), 73, 74
 Mills, O. S., 297, 301
 Minkoff, G. J., 12 (M8), 35
 Miranker, W. L., 76 (C9), 77, 147, 149
 Mirev, D., 192 (M11), 224, 234
 Mirzadzhanzade, A. K., 130, 149
 Mishuck, E., 26 (A2), 27 (A2), 33
 Miyauchi, T., 284, 287, 301
 Moe, G., 26 (A2), 27 (A2), 33
 Monrad, C. C., 177 (B4), 186, 188 (B4), 198 (B4), 220 (B4), 229, 234
 Morin, F. S., 111, 149
 Morse, P. M., 113 (M12), 149
 Mullins, B. P., 19 (P7), 35
 Munns, G. W., Jr., 42 (M3), 48 (M3), 74
 Murphy, G. M., 113 (M2), 149
 Murray, W. D., 137, 149
 Myers, C. G., 42 (M3), 48 (M3), 70, 74
- N
- Nachbar, W., 7 (J3), 26, 34
 Nagata, S., 282 (H1), 301
 Nakanishi, K., 192 (H13), 220, 221 (H15), 232
 Napier, D. H., 32 (A5), 33
 Nash, A. W., 177 (F1), 178 (F1, S13), 185 (S13), 186 (F1), 212 (F1, S13), 231, 235
 Nedderman, R. M., 177 (W4), 191 (W4), 196, 202, 208 (W4), 226, 227, 234, 235
 Neumann, F., 78, 149
 Newsome, J. W., 38 (N1), 74
 Nicholson, P., 136, 147
 Niebergall, W., 228, 234
 Nielsen, A. E., 108, 149
 Nikolaev, A. P., 183 (N2), 219, 234
 Norman, W. S., 222, 228, 234
 Nusselt, W., 152 (N6, N7), 156, 183, 234
- O
- Oblad, A. G., 40 (O1), 46 (M2), 47 (M2), 74
 Ohata, Y., 177 (S11), 183 (S11), 189 (S11), 194 (S11), 196 (S11), 198 (S11), 208 (S11), 219 (S11), 235

Oishi, J., 158, 177 (K4), 181, 183 (K4, K5),
186, 199, 205, 216, 217, 232
Okane, T., 216 (K6), 232
Olsen, W. T., 30 (O1), 35
Oppenheim, A. K., 19 (L1), 21 (G4), 22
(L1, L2, O2), 23 (L2, O2), 24 (L1), 34,
35
Otis, D. R., 133, 149
Overbeek, J. Th. G., 297, 302
Owen, W. M., 159, 216, 234

P

Parker, W. G., 28 (P1, P2), 31 (P2), 35
Parravano, G., 52 (P1), 74
Paschkis, V., 133, 148
Patterson, G. W., 165 (K16), 212, 233
Pattle, R. E., 82, 149
Peaceman, D. W., 218, 235
Pedrocchi, E., 227 (A1a), 229
Pekeris, C. L., 131, 149
Penner, S. S., 2 (P6), 4, 6 (P5), 10, 19 (P7),
26 (S7), 32 (P4), 35, 36
Pennie, A. M., 177 (P1), 215, 234
Peri, J. B., 42 (P2), 74
Phillips, R. C., 6 (F1), 33
Picknett, R. G., 295, 301
Picone, M., 122, 149
Pigford, R. L., 186, 189 (E4), 191 (S5),
192 (E4), 199, 215, 219, 231, 234, 235
Pimentel, G. C., 74
Pines, H., 38 (P3), 69, 74
Pitkethly, R. C., 63 (P5), 64 (P6), 65, 74
Pitts, P. M., 69, 74
Pitzer, K. S., 74
Planovskii, A. N., 225, 229
Plate, A. F., 66 (P8), 74
Pleshanov, A. S., 131, 149
Pohle, F. V., 165 (D11), 215, 230
Pocza, A., 219, 234
Poots, G., 130, 149
Portalski, S., 165 (P4), 166, 168, 171, 172,
177 (P3, T14), 178, 180 (P3), 181, 186,
189 (T3, T5, T14), 190, 191, 192 (T3),
193 (T4), 195, 197, 198, 200, 203, 205,
220, 222, 225, 226, 228, 234, 235
Potter, Jr., A. E., 19, 36
Potter, R. L., 31 (M5), 35
Powling, J., 19 (P10), 36

Prater, C. D., 48, 70, 74
Prescott, R., 12, 36

R

Ralph, J. L., 283 (M4), 288 (M4), 301
Ratcliff, G. A., 177 (R3), 189 (R2), 192
(R1), 200 (R3), 224, 225, 226, 234
Ravdel, A. A., 297, 301
Redozubov, D. B., 132, 150
Reid, K. J., 177 (R3), 189 (R2), 200 (R3),
224, 234
Reinius, E., 152 (R4), 177 (R4), 182, 186,
200, 225, 234
Reiss, H., 107, 111, 149, 150
Riazantsev, I. S., 92, 150
Rideal, E. K., 53, 64 (H4, H5), 66, 73,
199 (D6), 230
Rideal, E. K., 295, 301
Rieck, R., 78, 150
Rietema, K., 244, 301
Roberts, D., 220 (D2), 230
Rodger, W. A., 291 (R5), 302
Rohrer, J. C., 42 (R2, S3), 48 (S2, S3),
55 (S4), 56 (S4), 58 (S4, S5), 59 (S4),
61 (R3, S1), 62 (S1), 63 (R2, S1), 68
(R3), 69, 74
Romie, F. E., 131, 133, 148
Rosen, G., 10, 36
Rosenhead, L., 130, 148
Rossini, F. D., 74
Rothfus, R. R., 177 (B4), 229
Rubinstein, L. I., 77, 150
Ruddle, R. W., 78, 135, 150
Ruoff, A. L., 78, 150
Rushton, J. H., 291 (R5), 302
Russell, A. S., 38 (N1), 74
Ryland, L. B., 40 (R5), 74

S

Salamandra, G., 36 (S1), 36
Sammak, F. Y. Y., 228, 234
Sanders, R. W., 100, 150
Sarjant, R. J., 98 (E4), 134 (E4), 135,
147, 150
Sashkin, L., 137 (D3), 147
Saveanu, T., 186, 201, 226, 234
Schlesinger, S. I., 137 (O3), 147
Schmidt, E., 135, 150, 186, 234

- Schoklitsch, A., 185, 186, 211, 234
 Schuit, G. C. A., 38 (K2), 58, 73
 Schultz, R. D., 26 (A2, S7), 27 (A2), 33, 36
 Schurig, W., 186 (S2), 234
 Scott, D. S., 153, 228, 234
 Scriven, L. E., 85, 150, 191 (S5), 219, 234, 298, 302
 Seban, R. A., 132, 149
 Seelig, H. S., 39 (M1), 49 (M1), 73
 Seizew, M. R., 92, 146
 Sellers, J. P., 225, 236
 Sellschopp, W., 186 (S2), 234
 Semenov, P. A., 169, 173, 175, 183, 189 (S7), 193 (S7), 213, 214, 234
 Sestini, G., 77, 150
 Setze, P. C., 30 (O1), 35
 Sevastyanova, I. K., 36 (S1), 36
 Severn, R. T., 130, 135, 146
 Sexauer, T., 212, 234
 Shalit, L., 6 (C4), 9 (C4), 33
 Shaw, A. W., 69, 74
 Shea, J. J., 130 (G7), 148
 Shearer, C. J., 196, 227, 234
 Sherwood, T. K., 199 (S9), 215, 235
 Shetnin, B. I., 152 (K23), 233
 Shibuya, I., 163, 214, 235
 Shinnar, R., 291, 301, 302
 Shirosuka, T., 177 (S11), 183 (S11), 189 (S11), 192 (S11), 194 (S11), 196, 198, 208 (S11), 219, 235
 Shulman, R. A., 51 (S6), 55 (S6), 74
 Sibbett, D. J., 70 (M4), 74
 Sieg, R. P., 39 (H10), 73
 Silvestri, M., 177 (A1), 222 (A1), 227 (A1a), 229 (A1), 228, 229
 Simon, D. M., 2 (S2), 36
 Simpson, J. S. M., 18 (L12), 35
 Sinfelt, J. H., 42 (R2, S3), 48 (S2, S3), 51, 55, 56 (S4), 58 (S4, S5), 59, 61 (R3, S1), 62 (S1), 63 (R2, S1), 68 (R3), 69, 74
 Skinner, L. A., 80, 150
 Slack, M. R., 135, 150
 Slichter, L. B., 131, 149
 Smith, A. R., 298, 302
 Smoluchowski, M. von, 297, 302
 Smoluchowski, M. V., 109, 150
 Sneddon, I. N., 22 (S3), 36
 Somorjai, G. M., 80, 150
 Sonntag, H., 297, 302
 Soodak, H., 97, 150
 Spalding, D. B., 10, 17, 20, 26, 33, 36
 Spenadel, L., 38 (S7), 39, 74
 Spielman, L. A., 275, 302
 Starnes, W. C., 58, 74
 Stefan, J., 76, 150
 Steiner, H., 64 (P6, S9), 65, 74
 Stern, R. A., 22 (O2), 23 (O2), 35
 Sternling, C. V., 298, 302
 Stewart, W. E., 221 (B11), 229
 Stirba, C., 186, 192 (S12), 199, 217, 235
 Straatemeier, J. R., 192 (L15, L16, L17), 216 (L15, L16, L17), 233
 Strang, L. C., 178 (S13), 185, 212, 235
 Stumph, H. C., 38 (N1), 74
 Styrikovich, M. A., 153, 172, 186, 219, 233
 Sugden, T. M., 10 (B6), 12, 33
 Summerfield, M., 26 (S8), 28, 32 (S9), 36
 Sunderland, J. W., 137, 150
 Swegler, E. W., 48, 49 (W5), 74
 Swett, C. C., 17 (B1), 19 (B1), 33
- T
- Tadaki, T., 228, 235
 Tailby, S. R., 168, 189 (T3, T5), 190, 191, 192 (T3), 193 (T4), 197 (T2), 198 (T2), 222, 225, 226, 235
 Tamele, M. W., 40 (R5, T1), 74
 Tani, I., 130, 150
 Tarasova, G. A., 66 (P8), 74
 Taylor, B. N., 200 (A7), 227, 229
 Taylor, H. S., 65 (T2), 74
 Taylor, N. H., 189 (T7), 190 (T7), 191 (T7), 193 (T7), 194, 196, 226, 228, 235
 Taylor, R. H., 225, 235
 Teller, E., 38 (B5), 73
 Tempel, M. van den, 297, 302
 Ternovskaya, A. N., 152 (T9, T12), 192 (T9, T10, T11, T12), 198, 214, 215, 235
 Teter, J. W., 43 (H7), 73
 Thiele, E. W., 259, 302
 Thiessen, D., 298, 302
 Thomas, D. G., 111, 150
 Thomas, H. A., 189 (T13), 212, 235
 Thomas, W. J., 172, 177 (T14), 183 (T14), 186, 189 (T14), 205, 220, 235
 Thornton, J. D., 177 (B8), 205, 223, 229

Tinney, E. R., 204, 235
 Tipper, C. F. H., 12 (M8), 35
 Tirkii, G. A., 94, 150
 Towell, G. D., 283 (M4), 288 (M4), 301
 Trapnell, B. M., 54 (T3), 55 (T3), 74
 Treybal, R. E., 185, 213, 235
 Trice, V. G., 291 (R5), 302
 Tsien, H.-S., 152 (T17), 214, 235
 Tudose, R., 226, 234
 Turnbull, D., 107 (T5), 111, 150
 Tweet, A. G., 111, 150
 Twigg, G. H., 66, 74

U

Umnik, N. N., 217 (M6), 234
 Urtiew, P. A., 22 (L2), 23 (L2), 35

V

Vanderveen, J. H., 280, 293, 302
 Vanpee, M. W., 31 (V1), 36
 van Rossum, J. J., 177 (V1), 189 (V1), 221, 235
 van Vliet, R., 160 (H19), 186 (H19), 189 (H19), 203 (H19), 211 (H19), 232
 Vasilio, M., 186 (S1), 201 (S1), 226 (S1), 234
 Vedernikov, V. V., 165 (V2), 213, 235
 Veinik, A. L., 78, 150
 Veltkamp, G. W., 271, 275, 291 (V4), 302
 Verheus, J., 66 (H9), 67 (H9), 73
 Vermeulen, T., 280, 293 (W1), 302
 Verschoor, H., 212, 235
 Verwey, E. V. W., 297, 302
 Viparelli, M., 152 (V4), 189 (V4), 235
 Vivian, J. E., 218, 235
 Voge, H. H., 56 (K3), 59, 73
 Volgin, B. V., 175, 181, 185, 186 (Z4), 204, 205 (Z4a), 225, 228, 236
 Voncken, R. M., 284 (K2), 301
 von Elbe, G., 2 (L6), 4, 6 (L11), 18 (L8), 19, 21 (L10), 35
 von Kármán, T., 4, 10, 11 (V2), 36, 176, 235
 von Mises, R., 78 (N1), 149
 Vouyoucalos, S., 198, 200, 201, 225, 235
 Vyazovov, V. V., 199, 201, 212, 235

W

Wagner, H. G., 3 (L3), 35

Wagstaff, B., 98 (E4), 134 (E4), 147
 Waite, T. R., 110, 150
 Warden, C. P., 177 (W1), 211, 235
 Watanabe, A., 297, 302
 Weaver, R. E. C., 50 (B2), 73
 Webb, A. N., 42, 74
 Webster, A. G., 85 (W2), 150
 Wehner, J. F., 5 (F6), 6 (F6), 9 (W1), 18 (W1), 34, 36
 Weinberg, F. J., 3 (F4), 12, 33, 36
 Weisenberg, I. J., 32 (W3), 36
 Weiss, L. H., 293, 302
 Weisz, P. B., 49 (W2, W5), 69 (W3), 70, 71, 74
 Weller, S. W., 48 (H8), 73
 Wert, C., 108, 150
 Westenberg, A. A., 12, 13, 34, 36
 Wheeler, A. W., 259, 302
 Whitham, G. B., 167, 189 (L11), 233
 Wicks, M., 153, 189 (D17), 205, 227, 230
 Wilde, K. A., 10, 36
 Wilke, W., 186, 189 (W2, W3), 202, 203 (W3), 225, 226, 235
 Wilkes, J. O., 177 (W4), 191 (W4), 202, 208 (W4), 226, 235
 Williams, A., 13, 33
 Williams, B., 172, 184, 205, 216, 229
 Williams, F. A., 10, 36
 Williams, G. M., 302
 Wilson, J. L., 39 (M1), 49 (M1), 73
 Wilson, J. N., 40 (R5), 74
 Wilson, W. E., 31 (B2), 33
 Wint, A., 200 (W5), 236
 Winternitz, P. F., 32 (W3), 36
 Wolfhard, H. G., 12, 28 (P2), 31 (P2, V1), 34, 35, 36
 Work, L. T., 185, 213, 235

Y

Yang, C. H., 21, 36
 Yang, K. T., 130, 150
 Yang, W. J., 94, 150
 Yih, C.-S., 163, 165, 216, 228, 236
 Yuan, S. W., 152 (Y3), 236

Z

Zabor, R. C., 58, 74
 Zaiser, E., 107, 111 (B2), 146, 150

- Zaitsev, A. A., 165 (Z1), 222, 236
Zeldovich, Y. B., 4, 36
Zener, C., 79, 93, 102, 108, 133, 150
Zhavoronkov, N. M., 169 (K20, K21),
175 (K20, K21), 177 (K21), 183 (K19,
K20, K21), 193 (K20, K21), 194 (K20,
K21), 197 (K20, K21), 199, 206, 214,
217 (M6), 218 (K19, K20), 224 (K21),
226, 233, 234, 236
Zhivatkin, L. Ya., 175, 178 (Z3), 181, 183
(Z3), 184, 185, 186 (Z4), 204, 205 (Z4a),
225, 227, 228, 236
Zigmund, F. F., 161 (K11), 169, 226, 227,
232
Zotikov, I. A., 152 (Z5), 199, 236
Zuerow, M. J., 225, 236
Zuffanti, S., 41 (L2), 73
Zuiderweg, F. J., 66 (H9), 67 (H9), 73,
284, 288, 298, 301, 302
Zwietering, T. N., 239, 302

SUBJECT INDEX

A

- Ablation
 - of an annulus, 137-138
 - of a slab, 120-122
- Adsorption
 - aromatics, 51-53
 - liquid, from gases, 89-90
 - methyleyclohexane, 51-53
 - paraffin on platinum site, 58
- Ammonium perchlorate flames, 27-28

B

- Boley's method, 120-122
- Borane flames, 30-31
- Boundary temperatures, fictitious, 120
- Burning, solid propellant, 24-28
 - composite, 25-28
 - crystalline inorganic, 26
 - monopropellants, 24-26

C

- Catalysts, bifunctional reforming, 37-72
 - acidic, 69-70
 - component, 40-42
 - chromia alumina, 53-54
 - chromium oxide, 54
 - conversion of cumene, 70-71
 - exchange reactions, 70
 - hydrocarbon reactions, 49-71
 - metal component, 39-40
 - oxide, 64-66
 - platinum, 38-39, 50-54
 - alumina, 50-51, 55
 - alumina-halogen, 58-60
 - reactions occurring over, 42-49
 - catalytic reforming, 42-44
 - mechanisms, 46-48
 - metal, acidic centers, 48-49
 - thermodynamics, 44-45
 - rhenium, supported, 54
- Coalescing chance P, 295-299
 - drops, flat interfaces, 295-296
 - emulsions, 297
 - mass transfer influence, 298-299
- Column, wetted wall, 173-174, 197
 - static pressure drop, 204-206

Combustion

- gaseous, 24-25
 - velocity, 25
- metals, 30-31

Condensation

- film, 207
- vapor, at liquid surface, 91-92

Conduction, heat

- analytic approximation, 105-132
 - boundary-layer methods, 128-131
 - expansions, small times, 131-132
 - integral equations, 112-127
 - linear methods, 132
 - quasi-stationary, 105-112
 - quasi-steady-state, 105-112
- computer solutions, 132-142
 - numerical schemes, 135-142
- passive and active analog, 132-135
- or diffusion with change of phase, 75-150

equation

- Gauss's theorem, 95-96
- numerical integration, 137
- relaxation methods, 135-136

exact solutions, 78-105

film, 153

problem, variational formulation, 127-128

transient in finite slab, 100-102

Conservation equations

- analytical solutions, 10-12
- boundary conditions, 6-7
- numerical method, 7-10

Cyclization, 66-67

Twigg's mechanism, 66

Cyclohexanes, dehydrogenation, 50-61

Cyclopentanes, 60

D

Deflagration, 21-22

Dehydrocyclization, paraffins, 64-69

- aromatic yields, 67
- catalysts, 64-69
 - oxide, 64-66
 - reforming, 67-69
- cyclization, 66-67

- Dehydrogenation
 cyclohexanes, 50-61
 to aromatics, 50-54
 rate data summary, 50
 sextet theory, 54-55
 methylcyclohexanes
 kinetic rate data, 51
 to toluene, 50-51
- Desorption
 aromatics, 51-52
 toluene, 51-53
- Detonation, 21-24
 gaseous, initiation, 22
- Diffusion with change of phase, 75-150
 equation, 79, 82-83
 neglecting convective term, 107, 109, 142-143
 integral methods, 112-127
 no relative phase motion, 78-84
 concentration-dependent, 82-84
 constant, 78-82
 in one phase only, 78-86
 plane-free boundary, 86-94
 relative motion between phases, 84-94
 constant, 84-86
 three region problems, 94
 in two regions, 86-94
 constant, 86-92
- Dispersion, liquid-liquid, 237-302
- Distributions, source and doublet, 116-120
- Drop(s)
 conversion
 first order, 255-256
 half order, 255-256, 272, 278
 mass transfer limitation, 258-265
 order of, 248-250
 over-all, 244-247
 selectivity, 251-258
 zero order, 246-248, 252-253, 265-266, 272-273, 277
 zero and one half order, 250
 evaporation or growth, 109-110
 size distribution, 265-270
- E**
- Ethylcyclopentane, 60-61
- Evaporation, stationary drops, 109-110
- Expansions, small times, 131-132
- F**
- Film(s)
 flow, liquid, 151-236
 experiments, 208
 macroscopic aspects, 207-208
 theory, 208
 heat and mass transfer, 153
 experiments, 177-179
 friction factor correlation, 178
 gas stream absent, 179-182
 gas stream present, 183-185
 mean thickness, 177-185
 surface waves, 189-200
 vapor, growth, 102-105
 velocity and profiles, 201-206
 chronophotographic method, 202
 by traversing scoop, 202-203
 ultramicroscope, 202
- Filter cake accumulation, 111-112
- Finite-difference methods, 136-142
 melting, ablation, 136-138
 penetration, finite slab, 138-142
 iteration, 141
 Lagrangian interpolation, 142
- Flame(s)
 laminar, one-dimensional, 3-16
 composition profiles, 12-16
 structure, uncertainties, 16
 temperature measurements, 12-16
 theory, 4-12
 optics, 12
 ozone decomposition, 11
 processes, 1-36
 chemical synthesis, 28-32
 as reactor, 31-32
 stabilization, 16-24
 flammability limits, 16-18
 ignition, 19-21
 spatial aspects, 18-19
 transition to detonation, 21-24
 stable, 28-31
 steady-state profile, 20-21
 velocity, 2-3, 17-19
- Flow, liquids in thin films, 151-236
 adjoining stream present, 172-176
 gas, 175-176
 interfacial shear, 173-175
 liquid phase, 172-173
 applications, 152-153
 description, 153-155
 regimes, 154
 types, 153
 experiment results, 176-207
 comparison with theory, 176-207
 surface waves, 189-200
 laminar, 156-162
 axisymmetric, smooth, 158-159
 general equations, 156
 inertia, 161-162
 interfacial shear, 173-175
 three-dimensional, 159-161

- two-dimensional, 156-158
 - thicknesses, 180-181
- papers, 210-228
- theory, 155-176
- turbulent, 170-172, 176
 - thicknesses, 181-184
 - velocity profile equations, 171
- wall roughness, 200-201
- wavy, 166-170
 - theoretical stability, 163-165, 175-176
- Freezing
 - growing liquid column, 133
 - melting
 - computer solutions, 132-133
 - plane, 92-94
 - problems, 130-131
 - progressive, 92
 - semi-infinite region, 115-116
- G**
- Green's functions, 112-117
 - boundary conditions, 113-115
 - heat diffusion equation, 113
- H**
- Heat equation
 - heat-balance integral, 128-130
 - one-dimensional, 120
- Hydrocarbon reactions, 49-71
 - cyclohexane dehydrogenation, 50-55
 - kinetics, isomerization, 61-64
 - paraffins, dehydrocyclization, 64-69
 - reactions, isomerization, 55-61
- Hydrogenolysis, 69-70
- I**
- Ignition, flame system, 19-21
 - minimum energies, 21
 - thermal theory, 20-21
- Interaction
 - Church-Shinnar criterium, 291-293
 - circulation, 280-282
 - collision rate p_c , 293-295
 - dead corner, 275-280
 - dispersed phase, 240-242
 - diffusion through continuous phase, 241
 - coalescence and redispersion, 241-242
- Harada, 282-283
- homogeneous, 271-275
- rate measurements, 283-291
 - chemical, 284-288
 - physical, 288-291
- Isomerization
 - hydrogen and kinetics, 61-64
 - at low pressure, 63-64
 - methylcyclopentane, 62
 - n*-heptane, 61
 - reactions
 - n*-pentane, 55-58
 - 1-pentane, 57-58
 - one-site mechanism, 58-59
 - 2-pentane, 58
 - xylene, 69
- Isopentanes, 56
- K**
- Kapitsa theory, 180-181, 187-188, 193-194, 208
 - interfacial area increase, 197-198
 - wavy flow, 163, 166, 168-169
- Kinetics
 - flame system, 2-3, 12-16
 - segregation effect, 243-270
 - in CSTR, 243-258
 - drop size distribution, 265-270
 - mass transfer limitation, 258-265
- Kolodner's method, 116-120
 - accuracy, 120
- L**
- Landau's transformation, 94-100, 133
 - numerical scheme, 137
- Laplace equation, 105-106, 108
- Liquid, flow in thin films, 151-236
- M**
- Measurements
 - interaction rate, 283-291
 - batch mixing, 288-289
 - continuous flow, 288-290
 - suitability, 287
 - tracer reaction types, 285-287
 - temperature within flame zone, 12-16
- Melt thickness, 123-127
 - boundary conditions, 123-126
 - Gutowski method, 126-127
- Melting-freezing problems, 130-131
 - computer solutions, 132-133
- Methylcyclopentane, 60-61
- Monopropellants, 28
- N**
- Napthas, petroleum, 37-38
- Nucleation, 111
- Nusselt
 - heat transfer equations, 199
 - line, 179-181

P

- Particle, small
 - colloidal, 107
 - growth in condensed phase, 105-111
- Pohlhausen method
 - Karman-, 128-131
 - Goodman's application, 128-130
- Pressure drop, static, 204-206

R

- Reactor
 - continuous stirred tank
 - conversion rate, 262-265
 - drop size distribution, 268-270
 - homogeneous reaction, 272
 - piston flow, 266-268
- Reynolds number, 182, 185, 194-195
 - critical, 172, 179
 - onset of rippling, 186-188
 - turbulence in films, 185-186
- film, 157
 - velocity, 203-204
- for instability, 157, 163
- and interfacial area increase, 197-198
- wall roughness, 200-201

Rippling, 186-189

S

- Segregation, liquid-liquid dispersions, 237-302
 - and chemical reactions, 237-302
 - conversion rate, 242-243
 - in CSTR, 243-258
 - drop size distribution, 265-270
 - mass transfer limitation, 258-265
 - dispersed-phase systems, 239-240
 - interaction, 240-242
 - homogeneous systems, 237-239, 249
 - interaction rate, 291-299
 - measurements, 283-290
 - kinetics of two-phase reaction, 243-270
 - macroscale, 238-239, 275-280
 - microscale, 238, 244, 275-280
 - perfect isotropic, 271-275
 - partial, 270-283
 - system definitions, 240
- Slabs, ablating, 94-102, 120-122
 - computer solutions, 133-135
 - finite, penetration, 138-142
 - Landau's transformation, 94-99
 - thermal properties, 99-100
 - transient heat conduction, 100-102
- Solid, melting rate vs time, 98-99
- Solidification, liquid between parallel boundaries, 122

T

- Tani method, 130-131
- Tarnishing, 90-91, 105
- Transfer, mass, limiting drop conversion, 258-265
 - continuous phase, 260-262
 - for CSTR, 262-265
 - dispersed phase, 260-262
- Turbulence, in films, 185-186

V

- Vapor film
 - growth on plane surface, 102-105
 - liquid column, 102-105

W

- Wall roughness, 200-201
- Waves, surface on films, 189-200
 - film thicknesses, 196-197
 - flow, 189-190
 - interfacial area, 197-198
 - mixing effect, 198-200
 - smooth entry zone, 190-191
 - surface-active materials, 192-193
 - velocities, 194-196
 - ratio with film velocity, 195
 - wavelengths, 193-194

This Page Intentionally Left Blank